**Mathilda Amélia Gonçalves Larsson Dias Coutinho**

Mestre em Conservação e Restauro

# Biological colonization on majolica glazed tiles: biodeterioration, bioreceptivity and mitigation strategies

Dissertação para obtenção do Grau de Doutor em Conservação e Restauro,

especialidade Ciências da Conservação

Orientador: Doutora Filomena Macedo Dinis,
Professor Auxiliar com Nomeação Definitiva,
DCR, FCT-UNL

Co-orientadores: Professor Doutor Fernando Pina, Professor
Catedrático, FCT-UNL

Doutora Ana Zélia Miller, Instituto de Recursos
Naturales y Agrobiología de Sevilla, CSIC

Júri:

Presidente: Prof. Doutora Maria Rosa Santos de Paiva
Arguentes: Prof. Doutor Piero Tiano

Prof. Doutor António Manuel Santos Carriço Portugal
Vogais: Prof. Doutora Ana Luísa Pinheiro Lomelino Velosa

Prof. Doutor João Paulo Pereira de Freitas Coroado

**FACULDADE DE
CIÊNCIAS E TECNOLOGIA
UNIVERSIDADE NOVA DE LISBOA**

**Abril 2015**

**Biological colonization on majolica glazed tiles: biodeterioration, bioreceptivity and mitigation strategies**

*To my family*

# Acknowledgments

The work developed in a PhD project is always the result of the help and encouragement of many people. Therefore, I wish to express my sincere gratitude to:

- Prof. Dr. Maria Filomena Macedo Dinis (DCR-FCT/UNL) who was supervisor of this work for valuable advices, guidance, patience and for the great effort in the last part of the thesis.
- Dr. Ana Zélia Miller (IRNAS-CSIC) who supervised this work improving it with her inputs, valuable advices and guidance. Also, for the hospitality during my stay in Seville (also extended to Dr. José Maria de la Rosa).
- Prof. Dr. Fernando Pina (DQ-FCT/UNL) for all support during the grant application, valuable advices and especially for the freedom of letting develop work I enjoyed.
- Department of Conservation and Restoration (FCT-UNL), thank you to all members of the DCR.
- Photochemistry group and all its members for all work developed there.
- Vicarte Research Unit and its members for all work developed there.
- Prof. Dr. Márcia Vilarigues (Vicarte) for the great opportunity given to me and the huge patience during this last year.
- Prof. Dr. António Pires de Matos (Vicarte), for sending me to Italy where I got acquaintance with this conservation problem.
- Cremilde Rodrigues (Vicarte) for all the assistance and help.
- Ana Maria Alonso (DCR-FCT) for all the help and good mood during all this years.
- Prof. Dr. Alan Philips (UCIBIO-REQUIMTE, FCT/UNL) for the valuable help with the fungi and also with the article revisions.
- To IRNAS-CSIC, Prof. Dr. Cesareo Saiz Jimenez and all the wonderfull people I met at IRNAS. I would like to thank for all the work developed there and for the very good working experience.
- Dr. Pedro Martinez (IRNAS-CSIC) for the patience and valuable guidance during my stay in Seville.
- Dr. Miguel Rogério-Candelera (IRNAS-CSIC) for the work on digital image analysis.
- Prof. Dr. Antonio Gomez -Bolea (Facultat de Biologia of Universitat de Barcelona) for the lichenological analysis and Prof. Dr. Mariona Hernandez-Marine (Facultat de Farmacia of Univresitat de Barcelona) for the confocal microscopy analysis.
- Dr. Luis Cerqueira Alves and Dr. Victoria Corregidor Berdasco (C2TN, IST/UL) for the PIXE analysis.
- Prof. Dr. José Mirão and Dr. Luis Dias (Laboratório Hercules - UEvora) for the SEM analysis
- Dr. Sílvia Pereira (LNEC) for all help and useful advice with charaterization.

" *Like the freshness of a fountain in a patio burning in the heat of the sun, like a fragment of lápis lazúli on the façade of a palace, tiles are without a doubt the most popular and refined expression of Portuguese art*."

François Mathey

The main results presented in this PhD Dissertation have been published in international journals included in the Science Citation Index (SCI):

P.W. Crous, R.G. Shivas, M.J. Wingfield, B.A. Summerell, A.Y. Rossman, J.L. Alves, G.C. Adams, R.W. Barreto, A. Bell, M.L. Coutinho, S.L. Flory, G. Gates, K.R. Grice, G.E.St.J. Hardy, N.M. Kleczewski, L. Lombard, C.M.O. Longa, G. Louis-Seize, F. Macedo, D.P. Mahoney, G. Maresi, P.M. Martin-Sanchez, L. Marvanová, A.M. Minnis, L.N. Morgado, M.E. Noordeloos, A.J.L. Phillips, W. Quaedvlieg, P.G. Ryan, C. Saiz-Jimenez, K.A. Seifert, W.J. Swart, Y.P. Tan, J.B. Tanney, P.Q. Thu, S.I.R. Videira, D.M. Walker and J.Z. Groenewald, Fungal Planet description sheets: 128-153, Persoonia. 29 (2012) 146–201.

M.L. Coutinho, A.Z. Miller, S. Gutierrez-Patricio, M. Hernandez-Marine, A. Gomez-Bolea, M.A. Rogerio-Candelera, A.J.L. Philips, V. Jurado, C. Saiz-Jimenez, and M.F. Macedo Microbial communities on deteriorated artistic tiles from Pena National Palace (Sintra, Portugal), Int. Biodeterior. Biodegradation. 84 (2013) 322–332.

M.L. Coutinho, A.Z. Miller, M.F. Macedo, Biological colonization and biodeterioration of architectural ceramic materials: An overview, J. Cult. Herit. (2015) doi:10.1016/j.culher.2015.01.006 (*In Press*).

M.L. Coutinho, A.Z. Miller, P.M. Martin-Sanchez, J. Mirão, L. Dias, A. Gomez-Bolea, B. Machado-Moreira, L. Cerqueira-Alves, V. Jurado, C. Saiz-Jimenez, A. Lima, A.J.L. Phillips, F. Pina, M.F. Macedo. An integrated approach to evaluate biocidal treatments on the microbial community colonizing majolica glazed tiles. Environmental Microbiology (*Under revision*)

M.L. Coutinho, A.Z. Miller, M.A. Rogerio-Candelera, J. Mirão, L. Cerqueira Alves, J.P. Veiga, H. Águas, S. Pereira, A. Lyubchyk, M.F. Macedo. Bioreceptivtity and biodeterioration of majolica glazed tiles by phototrophic microorganisms under laboratory conditions. Biofouling (*Under revision*)

# Abstract

The impact of microbial activity on the deterioration of cultural heritage is a well-recognized global problem.

Glazed wall tiles constitute an important part of the worldwide cultural heritage. When exposed outdoors, biological colonization and consequently biodeterioration may occur. Few studies have dealt with this issue, as shown in the literature review on biodiversity, biodeterioration and bioreceptivity of architectural ceramic materials.

Due to the lack of knowledge on the biodeteriogens affecting these assets, the characterization of microbial communities growing on Portuguese majolica glazed tiles, from Pena National Palace (Sintra, Portugal) and another from *Casa da Pesca* (Oeiras, Portugal) was carried out by culture and molecular biology techniques. Microbial communities were composed of microalgae, cyanobacteria, bacteria and fungi, including a new fungal species (*Devriesia imbrexigena*) described for the first time.

Laboratory-based colonization experiments were performed to assess the biodeterioration patterns and bioreceptivity of glazed wall tiles produced in laboratory. Microorganisms previously identified on glazed tiles were inoculated on pristine and artificially aged tile models and incubated under laboratory conditions for 12 months. Phototrophic microorganisms were able to grow into glaze fissures and the tested fungus was able to form oxalates over the glaze. The bioreceptivity of artificially aged tiles was higher for phototrophic microorganisms than pristine tile models.

A preliminary approach on mitigation strategies based on *in situ* application of commercial biocides and titanium dioxide ($TiO_2$) nanoparticles on glazed tiles demonstrated that commercial biocides did not provide long term protection. In contrast, $TiO_2$ treatment caused biofilm detachment. In addition, the use of $TiO_2$ thin films on glazed wall tiles as a protective coating to prevent biological colonization was analysed under laboratorial conditions. Finally, conservation notes on tiles exposed to biological colonization were presented.

**Keywords:** glazed tiles, ceramic, microorganisms, biodeterioration and bioreceptivity

# **Resumo**

A biodeterioração é reconhecida como um problema global para a conservação do património. A localização em exterior impossibilita o controlo das condições ambientais que podem favorecer a colonização biológica. O património azulejar encontra-se frequentemente aplicado em fachadas exteriores tornando-o também suscetível à biodeterioração. No entanto, a biodeterioração de azulejos é um tema muito pouco estudado como revelado na revisão da literatura sobre a biodiversidade, biodeterioração e bioreceptividade de materiais cerâmicos arquitetónicos, efetuada nesta tese.

Nesta tese realizou-se a caracterização da microflora presente nos azulejos do Palácio Nacional da Pena (Sintra, Portugal) e nos azulejos da *Casa da Pesca* (Oeiras, Portugal). Foram usados métodos convencionais de microbiologia juntamente com técnicas de biologia molecular, tendo sido identificadas microalgas, cianobactérias, bactérias e fungos entre os quais uma nova espécie (*Devriesia imbrexigena*). Verificou-se que alguns destes microrganismos se desenvolviam dentro de fissuras causando biodeterioração dos azulejos.

Para o estudo da biodeterioração e bioreceptividade foram realizados ensaios de inoculação em laboratório sobre azulejos com um vidrado de composição semelhante aos históricos estudados. A inoculação foi realizada tanto sobre azulejos modelo no seu estado inalterado como em artificialmente envelhecidos. Foram utilizados microrganismos previamente identificados verificando-se que os microrganismos fototróficos se desenvolviam no interior de fissuras e que o fungo testado produzia oxalatos sobre o vidrado.

No sentido de controlar a biodeterioração dos azulejos realizou-se, *in situ*, um estudo preliminar da eficácia e durabilidade de três biocidas comerciais e de nanopartículas de dióxido de titânio (TiO$_2$), tendo sido verificado que os biocidas mais eficientes tinham um curto tempo de ação e que as nanopartículas promoviam o destacamento do biofilme. Foi ainda testado em laboratório a deposição de filmes finos de TiO$_2$ produzidos pela técnica de sol-gel sobre azulejos históricos para prevenir a biodeterioração. Por fim foram redigidas de forma sintética notas sobre a conservação de azulejos expostos à colonização biológica.

**Palavras-chave:** azulejos, cerâmica, microrganismos, biodeterioração e bioreceptividade

# Table of contents

# Figure List

# Table List

# Abbreviations

| | |
|---|---|
| µ-EDXRF | Micro Energy Dispersive X-ray Spectroscopy |
| µ-PIXE | Micro Particle Induced X-ray Emision |
| µ-Raman | Micro Raman spectroscopy |
| ANOVA | Analysis of variance |
| APS | Ammonium persulfate |
| BLAST | Basic Local Alignment Search Tool |
| Chl*a* | Chlorophyll *a* |
| CLSM | Confocal Laser Scanning Microscopy |
| cps | counts per second |
| DGGE | Denaturing Gradient Gel Electrophoresis |
| DMSO | dimethyl-sulfoxide |
| DNA | Deoxyribonucleic acid |
| EDTA | Ethylene-diamine-tetra-acetic acid |
| FE-SEM | Field Emission Scanning Electron Microscopy |
| NCBI | National Center for Biotechnology Information |
| OTU | Operational taxonomic unit |
| PCA | Principal components analysis |
| PCR | Polymerase Chain Reaction |
| PDA | Potato Dextrose Agar |
| Q | Coeficient of water absoption by cappilary |
| QACs | Quaternary Ammonium Compounds |
| Ra | Roughness average |
| RNA | Ribonucleic acid |
| ROS | Reactive Oxygen Species |
| Rq | Root-mean-squared roughness |
| Ry | Total Roughness Height |
| SEM | Scanning Electron Microscopy |
| SEM-EDS | SEM with Energy Dispersive X-ray Spectroscopy |
| SEM-SE | SEM with Secondary Electrons |
| TAE | Tris-Acetate-EDTA buffer |
| TEMED | N'-tetramethylethylenediamine |
| VP-SEM | Variable Pressure SEM |
| WDXRF | Wavelength Dispersive X-ray Spectroscopy |
| wt. | weight |
| XRD | X-Ray Diffraction |
| δ | Water vapor permeability coeficient |

# General

# Introduction
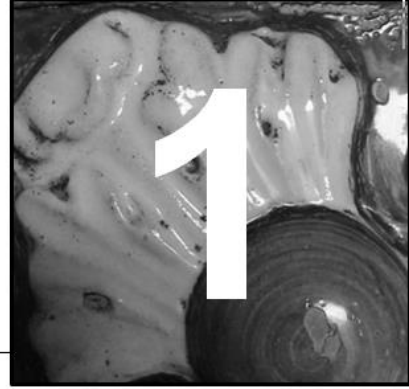
## 1.1. Glazed wall tiles

Glazed wall tiles, in Portuguese designated as "*azulejos*", are ceramic plaques with at least the front face covered by a vitreous coating (glaze). Most of tiles are square-shaped, but they can have a variety of shapes, be flat or decorated with reliefs. Glazed tiles are architectural ceramic materials which are employed as a facing over another building material. The attachment of tiles to a surface is done by the use of a mortar in a process termed cladding and several purposes are associated with the selection of glazed tiles as a building material, such as the increase of impermeability, cleanability and mechanical resistance. In addition, the aesthetic function has particular relevance which explains the artistic and historic value of glazed wall tiles.

The production of traditional ceramic objects involves several steps, starting with the ceramic paste preparation, followed by the forming process, drying, ceramic body firing, glazing and second firing of the glaze.

The ceramic paste preparation consists in the selection, processing and mixture of the raw materials. These are often mixed, purified and grinded to obtain suitable characteristics for the forming process. In traditional ceramics, the paste is mainly composed of clay-based materials (or clay raw materials), which constitute the plastic component of the paste. Clay minerals are the basic components of clay raw materials, which are hydrated aluminosilicates organized in silicates or phyllosilicate sheets formed by tetrahedrons $[SiO_4]^{4-}$ or octahedrons of several types, such as $[AlO_3(OH)_3]^{6-}$ interconnected by $OH^-$ protons. The plasticity of clays is related to the morphology of the plate-like clay mineral particles. When water is added to clays it acts as a lubricant allowing the particles to slide over the others letting the materials to be deformed and be able of retaining the shape. Konta (1995) and Andrade et al. (2011) reviewed in detail the structure, properties and application of clay minerals and clay raw materials.

Coarse grains of different origins (e.g. quartz, fired clay, feldspars, and shells) are often added to the plastic component during the paste preparation in order to control plasticity during the forming process and minimize shrinkage due to water loss during the drying and firing processes. These are designated the non-plastic components of a ceramic paste. Moreover, additives are mixed with the other components of the paste, such as flocculants, plasticizers or colorants.

Forming is the second step in ceramic tile manufacture and involves shaping the ceramic paste. This can be achieved by kneading of the paste with a roll and cutting it into slabs or using molds, particularly for high or low relief decoration of the surface.

After shaping, the tile slabs are air-dried in order to remove the excess of water. During this drying process, water evaporation implies shrinkage of the ceramic paste. Therefore, manufacture defects, such as deformation, cracking and even rupture might occur, influencing the quality of the final product.

For permanent hardening, the ceramic paste needs to be processed by thermal treatment or firing.During firing the ceramic paste suffers transformations, according to its composition and firing conditions (temperature, cycle and atmosphere) (Carter and Norton, 2013). The first reactions during firing are removal of free water (not removed by drying), combustion of organic matter, $\alpha$- to $\beta$-quartz allotropic transformation, loss of $OH^-$ from the clay structure and carbonate decomposition. At temperatures above 800º C, most of the physicochemical transformations occur resulting in the neoformation of minerals phases and formation of grain boundaries through sintering. During the cooling stage, thermal contraction, crystallization and other phase transformations occur on the ceramic body.

Depending on the raw materials and firing conditions a wide variety of ceramic body typologies can be produced. These can be classified according to their porosity, color and composition (Ravaglioli and Krajewski, 1989). According to the literature, the most common tile ceramic bodies are earthenware during the 18-19th century (Borges et al., 1997; Carvalho et al., 2006; Pereira et al., 2011). These type of ceramics are opaque and non-vitrified, being fired at relatively low temperatures, varying between 960˚ and 1050˚ C (Tite, 2009; Dondi et al., 2014). According to Mimoso (2011) firing temperature could range between 800˚ and 1100˚ C, due to the difficulty in controlling temperature. The porosity of earthenware is generally characterized by high values, between 15 and 18%, because it is not vitrified (Ravaglioli and Krajewski, 1989). The porosity in these non-vitrified ceramics depends on voids between the grains and the pores created by gaseous liberation during firing which are not filled by a liquid glassy phase when temperature of glass formation (vitrification) is not achieved. Results of some studies concerning historic Portuguese tiles (16-19th century) have shown slightly high open porosity with values ranging between 22 and 28% (Santos et al., 2012).

In general, the chemical composition of earthenware used to produce Portuguese tiles result from the firing of calcareous rich clays. Pereira et al. (2011) characterized of blue and white majolica tiles from the 17 to 19th centuries being composed of: 40 to 44 wt. % of $SiO_2$, 30-40 wt. % of CaO, 12-15 wt. % of $Al_2O_3$, 1-2 wt. % of $K_2O$ and 5-7 wt. % of $Fe_2O_3$. Several studies described the phases formed by firing of calcareous clays including calcium silicates, calcium aluminosilicates and anorthitic plagioclases (González-García et al., 1990; Trindade et al., 2009). In fact, the mineralogical phases of Portuguese majolica tiles are: quartz ($SiO_2$), gehlenite ($CaAl_2SiO_7$), diopside ($CaMgSi_2O_6$) and calcite ($CaCO_3$) (Carvalho et al., 2006; Pereira et al., 2011). In terms of chromacity, these ceramic bodies are characterized by light colors, from pale pink to yellowish shades due to their content in iron oxide and firing temperature and atmosphere.

After ceramic body completion, a vitreous coating (the glaze) is applied. Thus, glazed tiles are considered to be composite materials, due to the combination of these two materials: ceramic body and glaze (Vendrell-Saz, 2003; Carter and Norton, 2013).

Many glaze compositions have been utilized worldwide (Figueiredo et al., 2005; Coentro et al., 2012, 2014; Gulzar et al., 2012). This Chapter focuses particularly on the description of tin-opacified glazes. These glazes are composed of a lead-silicate glassy matrix with scattered quartz, feldspars and cassiterite ($SnO_2$) crystals. Due to light scattering, these crystals, particularly cassiterite, give opacity and a white color to the glaze (Tite, 2009).

Technically, majolica consists in the application of white opaque glaze over a fired ceramic body, on which the in-glaze pigments are painted before firing. Tite et al., (2015) confirmed recently that Egypt was the birth place of these glazes, circa 8th century A.D. However, in Europe, the continuous production of this type of glazes only started in the 13th century A.D. (Carter and Norton, 2013). The term *Majolica* appears only in this period, long after the beginning of the use of these glazes. This term was introduced to designate the Italian produced white glazed pottery which appeared due to the trade rout through the Spanish island of *Maiorca* (Carter and Norton, 2013). In the Portuguese context, the majolica technique in tile production only started to be used on the second half of the 16th century, probably brought by the Flemish and Italian artists that worked in the country during this period (Berendse et al., 1967). Subsequently, this was the main tile production technique during four centuries in Portugal.

The majolica glazes composition is usually a lead-alkali $SiO_2$–$PbO$–$R_2O$ or high lead silicate ($SiO_2$-$PbO$) glaze (Tite et al., 1998; Doménech-Carbó and Doménech-Carbó, 2005; Tite, 2009). Considering that the composition varied through time the major elements on Portuguese glazed tiles are: 50-70 wt. % of $SiO_2$, 6-10 wt. % of $K_2O$, 1-2 wt. % of $CaO$, 3-10 wt. % of $SnO_2$ and 13- 30 wt. % of $PbO$ (Pereira et al., 2009, 2011; Coentro et al., 2012).

## 1.2. Glazed wall tiles as cultural heritage

Glazed wall tiles are relevant cultural heritage assets due to their historic, artistic, and aesthetic value, as well as their distinguishable feature on the urban landscape. The variety of colors, glosses and iconography of these ceramic elements make their usage associated with an aesthetic intention. Thus, their application in claddings goes far beyond the practical properties, such as mechanical resistance, impermeability, durability and cleanability. Their application is spread worldwide, being particularly used in cultural heritage from the Iberian Peninsula, Italy, France, South America, South Asian and Western Asia countries (Berendse et al., 1967; Lemmen, 1993; Bandini et al., 2002) (see Chapter 2).

The production of glazed tiles can be traced back to the ancient Egypt, around 3000 B.C., spreading later to the Near East and then to Europe (Sabo and Falcato, 1998; El Nouhy, 2013). In southern Europe, due to Islamic influence, glazed wall tiles became part of the culture of Portugal and Spain and afterwards they were also widely applied in Brazil and other latin influenced south American countries (Sabo and Falcato, 1998; Bandini et al., 2002).

After their introduction in the Iberian Peninsula, glazed tiles soon became part of the Portuguese tradition and also an unique vehicle of art expression (Saporiti, 1992). The final decades of the 18th century attest the exceptional architectural integration and quality of paintings achieved by the Portuguese tilework during this period (Correia de Carvalho, 2012). During the 19th century, accompanying the industrial revolution, glaze wall tiles became commonly used on the façades of buildings. Nowadays, contemporary artists, architects and designers use glazed wall tiles as an artistic expression vehicle (Saporiti, 1992; Burlamaqui, 1996). For instance, national artists, such as Julio Resende (1917-2011), Querubim Lapa (1925- ) and Eduardo Nery (1938-2013) are associated to production of artistic glazed tiles (Burlamaqui, 1996). All the aforementioned examples show how the Portuguese tilework reflect the major artistic currents of each historical period. In fact, glazed wall tiles have been used more extensively and consistently in Portugal more than in other European countries. Portuguese tiles are for this reasons mentioned in many international books on tiles history, such as "*Tiles 1,000 years of architectural decoration"* by Lemmen (1993), "*Les Metamorphoses de l´azur, l´art de lázulejos dans le monde latin"* by Bandini et al. (2002) or "*Tiles a general history* "by Berendse et al. (1967).

Recently, in 2009, in the field of conservation and art history, a research unit dedicated to the investigation of tiles named *Rede Temática em Estudos de Azulejaria e Cerâmica João Miguel dos Santos Simões* (RTEACJMSS) (João Miguel dos Santos Simões Thematic Network on the Study of Tiles and Ceramics) at the Institute of the History of Art, Faculty of Letters, University of Lisbon (IHA-FLUL) was created with the aim of promoting the contact between research units dedicated to the investigation of tiles and ceramics (IHA-FLUL, n.d.). Together with the National Tile Museum (*Museu Nacional do Azulejo*) and other institutions several joint actions and projects have lately been conducted in order to explore and value Portuguese glazed tiles heritage.

The project '*SOS Azulejo'* created by the Portuguese Judiciary Police Museum in 2007 to handle the increasing problem of theft, illegal trade and neglect affecting the glazed tile cultural heritage. This project has played a leading role in the creation of municipal legislation for safeguard of this patrimony and in the dissemination and educational actions (Sá, 2014).

Conferences and other dissemination actions regarding tiles as an important part of Portuguese cultural heritage have also arouse during the last years, such as *AzTek - Conservação de azulejos históricos* (2009) held in Lisbon or *AZULEJAR 2012* (2012) held in Aveiro. The rising awareness of the importance to preserve the glazed tiles legacy is proven by the innumerous research projects and networks that were recently created for this purpose.

## 1.3.  Deterioration of glazed wall tiles

Deterioration of glazed wall tiles, like other building materials, can occur due to physical, chemical and biological mechanisms, which can act synergistically (Vendrell-Saz, 2003; Durbin, 2005). The susceptibility of glazed tiles to deterioration is influenced by the intrinsic properties of the ceramic materials, such as mechanical strength, surface hardness and roughness, resistance to temperature fluctuations, porosity, mineralogical composition and chemical stability. These properties depend on the composition of the raw materials, on the ceramic manufacturing

procedures (Raimondo et al., 2009) and also on the tiles conservation state. Production faults, such as surface and structural defects, may play also major role in the ability of ceramics to withstand deterioration processes (Vendrell-Saz, 2003; Kopar and Ducman, 2007; Mimoso et al., 2011; Pereira et al., 2011).

In glazed ceramics, the deterioration of the ceramic-glaze interface is a critical due to its composite nature (Fabbri, 2003; Vendrell-Saz, 2003; Kopar and Ducman, 2007; Mimoso et al., 2011). The characteristics of this interface area are dictated by the composition, compatibility between the two layers and the firing cycles (Kopar and Ducman, 2007; Mimoso et al., 2011).

Deterioration of ceramic tiles is also influenced by extrinsic factors, such as climatic and microclimatic conditions (affected by local urban geometry, building design or adjacent materials), atmospheric pollution and biological colonization (Silvestre and de Brito, 2009, 2011). But there are even more factors contributing to ceramic deterioration: the direct action of Man impelled by the economic situation or lack of knowledge and experience in the conservation field, which may affect material deterioration by direct destructive actions, lack of maintenance and inappropriate conservation interventions (Fabbri, 2003). For instance removal of glazed wall tiles from the wall during conservation and restorations interventions has been considered particularly damaging (Farinha and Tavares, 2003).

Physical deterioration of ceramic materials comprises mechanical damage and water related damage (diffusion, freeze-thaw cycles and soluble salts damage). The main factors causing mechanical damage are impact, scratching, abrasion, shrinking-expantion cycles and structural overload (Buys and Oakley, 1996; Silvestre and de Brito, 2009). Many of these mechanical damage with the exception of overload are caused by the action of external forces applied on the material that will result in its deterioration. Load damage is related to continuous forces, such as those imposed by the structural role of buildings. As a consequence, stress cracks, deformation and structural disintegration of the material may occur (Durbin, 2005; Kopar and Ducman, 2007; Yiu et al., 2007; Silvestre and de Brito, 2009, 2011)

Water related damage are linked to the porous matrix of the ceramic body. Its penetration into the pores hastens the rate of material deterioration, first because water is itself an effective deteriorating agent, dissolving, hydrating and hydrolysing minerals, and, secondly because it holds in solution substances (carbonaceous particles, sulphur compounds, soluble salts) responsible for leaching, pH reduction, efflorescences and subflorescences (Camuffo, 1995; Ordonez et al., 1997; Papida et al., 2000; Linnow et al., 2007; Pereira et al., 2012). In relation to freeze-thaw cycles, water within the pore structure freezes to ice, causing internal pressure. This volume increase combined with repeated freeze-thaw cycles produces micro-fissures, cracks and flaking (Larbi, 2004; Kopar and Ducman, 2007; Figueiredo et al., 2009). Volume changes are also caused by the presence of soluble salts within the porous material combined with cyclic changes in the environmental conditions. Cycles of crystallization, dissolution and re-crystallization of salts causes progressive deterioration, visually denoted through efflorescences on or within the porous material (Larbi, 2004; Bakar et al., 2009; Figueiredo et al., 2009; Mimoso et al., 2011; Pereira et al., 2012). In glazed ceramics, the composite structure, comprising two layers with different hydric properties,

increases the susceptibility to volume fluctuations due to water movement. For instance, in frost or salt crystallization high local tensile forces around the pores generate micro-cracking both in the ceramic body and the glaze (also known as crazing of the glaze)(Borges et al., 1997; Pereira et al., 2012) These forces can be exerted on the ceramic-glaze interface, resulting in fissures and scaling of the glaze, ensuing serious decay and material loss.

Concerning chemical deterioration of glazed wall tiles, the main damage is due to staining and corrosion. Contamination by external substances, such as metal corrosion products, biological colonization, soiling, or other colored substances, can cause the formation of stains. The aesthetic characteristics of the substrate are thus altered and the chemical stability can be affected. Characteristics of the substrate, like higher porosity and roughness, make the material more susceptible to this form of deterioration (Kopar and Ducman, 2007). Corrosion is caused by the chemical reaction of the substrate with any given substance causing its decay. Both the glaze and ceramic body can be chemically deteriorated, which is strongly related to the presence of water and its pH (Eppler, 1992).

Chemical corrosion affects the ceramic body particularly when water is mixed with atmospheric acids, formed from $SO_2$, $NO_x$, and $CO_2$ (Ranogajec et al., 1997; Larbi, 2004). Chemical reactions with the ceramic substrate can produce soluble compounds. This dissolution can result in alterations of the ceramic body, such as an increase in the capillarity porosity (Ranogajec et al., 1997; Larbi, 2004). The solubilization of compounds may weaken the structure and enhance the susceptibility to other types of deterioration. Water can also cause the hydration of mineral compounds resulting in volume fluctuations. Moreover, the remains of solubilized compounds in the ceramic body might act as a contamination by soluble salts as previously described.

Silicate based glazes are specially vulnerable by alkaline environments, since it enables the destruction of the silica network (Eppler, 1992; Hupa et al., 2005; Fröberg et al., 2007; Cannillo et al., 2009). In acidic environments, the reaction with water causes the leaching of ions, particularly alkalis and lead in the case of lead-silicate glazes (Blachere and Procedure, 1976; Wood and Blachere, 1978; Eppler, 1992; Hupa et al., 2005; Fröberg et al., 2007; Cannillo et al., 2009). Although being usually more resistant than the glassy phase, the crystalline phase can also be corroded. The corrosion rate depends on the chemical stability of the crystals (Eppler, 1992; Hupa et al., 2005; Fröberg et al., 2007; Cannillo et al., 2009). Differences in the ability to withstand corrosion of the crystalline and glassy phases of the glaze can lead to selective surface corrosion leading to the formation of pitting (Vandiver, 1992; Fröberg et al., 2007; Cannillo et al., 2009). The corrosion of glazes will cause the alteration of the gloss and can also contribute to mechanical changes of the glaze (Fabbri, 2003; Cannillo et al., 2009).

Despite the globally known relevance of tiles, the number of studies concerning deterioration and conservation methodologies are reduced (Balderrama et al., 2003) compared to other building materials such as stone (Warscheid and Braams, 2000; ICOMOS, 2008; Miller et al., 2012). However, in the last decades many studies and scientific research projects have been performed regarding this issue, specifically on material characterization (Velosa et al., 2001;

Figueiredo et al., 2005; Pereira et al., 2009, 2011; Coentro et al., 2012, 2014; El Nouhy, 2013; Gill et al., 2014), deterioration processes (Figueiredo et al., 2009; Pereira et al., 2012; Silva et al., 2013) and also conservation and treatment methodologies, such as consolidation (Vaz et al., 2008; Prudêncio et al., 2012), soluble salt removal (Borges et al., 1997; Pereira and Mimoso, 2012; Ottosen et al., 2014) and mortars (de Freitas et al., 2014).

The problem of understanding the deterioration of ceramic materials is compounded by the large range of ceramic building typologies, with different textural, compositional and physical characteristics, and by their varying weathering responses under different climatic and environmental conditions. The interactions between the numerous and synergistically acting factors leads to a dynamic and complex process of physical, chemical and biological deterioration. However, little research has been focused on the problem of microorganisms as agents of ceramic biodeterioration.

## 1.4. Biodeterioration of inorganic building materials

Living organisms can interact with the surface of inorganic building materials on which they develop, altering their physical and chemical state (Gadd, 2010). This interaction is more frequent and severe when the materials are exposed outdoors. The process of transformation of a substance into new compounds by biochemical reactions or the action of microorganisms is defined as biodegradation. The term may involve a positive and beneficial connotation of the process (Pinna and Salvadori, 2008). However, transformations are considered harmful when microorganisms colonize anthropogenic materials, such as cultural heritage assets. Thus, the concept of biodeterioration or biological decay was defined as "any undesirable change in the properties of a material caused by living organisms" by Hueck in 1965 (Hueck, 1965). In the field of cultural heritage the decay and deterioration are perceived as damage, which are related the loss of aesthetical, physical, chemical or functional value (ICOMOS, 2008).

Biodeterioration of inorganic materials can result in physical, chemical and aesthetical damage (Kumar and Kumar, 1999; Warscheid and Braams, 2000). The damage is the result of complex mechanical, physical and chemical processes, which often occur simultaneously. The general mechanisms of biodeterioration of some inorganic building materials, such as stone, have been described by several authors (Sand, 1997; Kumar and Kumar, 1999; Warscheid and Braams, 2000; Pinna and Salvadori, 2008; Cuzman et al., 2011). However, little is known about glaze wall tiles biodeterioration (see Chapter 2).

Cultural heritage assets, made of inorganic materials, can be colonized by different organisms which are designated as biodeteriogens when inflicting damage to the material, such as bacteria, fungi, algae, cyanobacteria (or blue-green algae), lichens, mosses (bryophytes) and vascular plants. Generally, microorganisms develop in biological communities, which are an interacting group of various species in a common location. These biological communities present on an inorganic substrate are usually the result of successive colonizations by different organisms through time: starting with the less complex organisms (e.g. bacteria, cyanobacteria, algae, fungi) to the more complex ones (e.g. mosses and vascular plants).

Photoautrophic microorganisms (green microalgae, cyanobacteria and diatoms) use light as energy source and synthesize organic matter from carbon dioxide and mineral components by photosynthesis. These microorganisms are considered the pioneer colonizers of inorganic substrates due to their ability to grow without any presence of organic matter (Ortega-Calvo et al., 1991; Tiano et al., 1995; Tomaselli et al., 2000; Warscheid and Braams, 2000). The strategy of photoautrophic microorganisms and other organisms to settle and develop on hostile environments, such as architectural ceramic materials, is also based on their capacity to form biofilms (Cuzman et al., 2011).

A biofilm is composed of a mono- or multilayer of microbial cells embedded in a hydrated extracellular polymeric matrix (Costerton et al., 1995; Morton et al., 1998; Costerton, 1999; Warscheid and Braams, 2000; Cuzman et al., 2011). These glue-like extracellular polymeric substances (EPS) secreted by the cells enhance the adhesion of microbial cells to the substrate and favour the adherence of nutritive airborne particles (e.g. dust, pollen, spores, oil- and coal-fired carbonaceous particles) from the atmosphere (Saiz-Jimenez, 1995; Koestler et al., 1997; Cecchi et al., 2000; Wimpenny et al., 2000; Tourney and Ngwenya, 2014). EPS may vary in chemical and physical properties, but consist mainly of polysaccharides, fatty acids, proteins and enzymes (Krumbein et al., 1991; Young et al., 2008; Tourney and Ngwenya, 2014). Biofilms also allow the retention of large amounts of water into its structure, protecting the cells from desiccation (Prakash et al., 2003; Gorbushina, 2007). When surface-covering phototrophic biofilms are established, a succession of microorganisms can occur, such as bacteria, fungi, bryophytes and finally vascular plants. This is because of the photosynthetic activity of photoautotrophic microorganisms that converts $CO_2$ into organic compounds that become available for heterotrophic microorganisms, such as fungi and bacteria (Crispim and Gaylarde, 2005; McNamara and Mitchell, 2005; Fernandes, 2006; Roeselers et al., 2006).

Heterotrophic microorganisms need organic matter to grow. Although bacteria are the less complex microorganisms on Earth, they exhibit an extremely wide variety of metabolic types depending on their nutritional categories. For this reason, some bacteria are also considered pioneer colonizers due to their ability to oxidize inorganic substances, while others occur in later phases of colonization (Suihko et al., 2007).

Fungi include microorganisms such as yeasts, moulds and mushrooms. However, the most frequent fungi found on inorganic substrates are moulds (filamentous fungi). Filamentous fungi grow forming long cylindrical structures called hyphae that can penetrate and adhere to the substrate (Jongmans et al., 1997). Fungi also produce a variety of acids and other substances that are highly reactive, being able of interacting with the substrate (Gadd et al., 2014). Therefore, fungi have been recognized as agents of biodeterioration of inorganic materials (Saiz-Jimenez et al., 2012; Sterflinger and Piñar, 2013; Rodrigues et al., 2014).

Several fungal species are able to form symbiotic associations with a green alga or cyanobacterium, forming lichens. Their growth strategy is based on the photosynthetic activity of the green alga (feeds the mycobiont – fungal partner) and the protective action of the fungi (gives protection against radiation and dissection to the photobiont – photoautotrophic partner). Lichens

are able to grow on the most adverse conditions and their growth is often associated with biodeterioration of inorganic substrates (Lisci et al., 2003).

According to their distribution pattern, the microorganisms that inhabit inorganic building materials are classified as epilithic, when growing on the external surface, and endolithic if living in the interior of the substrate and penetrating some millimeters into the pore system (Golubic et al., 1981; Cuzman et al., 2011). This growth strategy, together with the production of biogenic pigments, enable microorganisms to survive in hostile environments (Warscheid and Braams, 2000), such as on the vertical surfaces of monuments and historical buildings.

Bryophyte refers to "non-vascular plants", which are terrestrial plants that do not have true vascular tissue. They include mosses, hornworts and liverworts. Bryophytes and vascular plants are complex organisms that occur at final stages of colonization. Bryophytes are able to grow when moisture and nutrients (e.g. organic deposits) are available. The proliferation of plants is dependent on the presence of a large amount of substrate (available nutrients) that permits the development of roots. The early colonization by bryophytes lead to high moisture and soiling accumulation which allow the development of plants (Warscheid and Braams, 2000).

The occurrence of biodeterioration is dependent on the presence of organisms on the materials. Environmental conditions, like solar radiation, relative humidity, rain exposure and temperature are determinant for biological colonization. However, the susceptibility of a given material to biological colonization is also based on its intrinsic properties (Guillitte, 1995). Bioreceptivity was defined by Guillitte, (1995) as "the aptitude of a material to be colonized by one or several groups of living organisms". This author subdivided this concept in three types: primary bioreceptivity, as the intrinsic potential of a material to suffer biological colonization; secondary bioreceptivity, as the ability of an altered material, changed over time by physical and chemical agents, to be colonized; and tertiary bioreceptivity, as the potential of biological colonization of material altered by human (e.g. after a conservation treatment).

Currently, the main issues to be investigated in the area of biodeterioration of inorganic building materials, that are part of our cultural heritage, can be summarized as (i) characterization of biological community and its interaction with the substrate which is usually based on taxonomic identification of colonizing organisms and analysis of the colonized substrate in field studies or case studies; (ii) laboratory experiments to investigate the susceptibility to biological colonization (bioreceptivity) and biodeterioration, to overcome the complexity of deterioration factors and be able to observe biodeterioration mechanisms; and (iii) research on control of microorganisms and preservation methods to draw effective conservation strategies.

The damaging action of microorganisms makes their mitigation and control essential for the preservation of inorganic built cultural heritage. Microorganism's mitigation strategies have been extensively studied for stone materials (Caneva et al., 1991; Kumar and Kumar, 1999; Speranza et al., 2012). The eradication of microorganisms from inorganic building materials can be achieved by several methods often combining more than one:

- Mechanical methods, which comprise processes based on the physical removal of microorganisms. The complete removal by mechanical methods cannot be achieved

and often results in physical damage to the substrate (Caneva et al., 1991, 2008; Kumar and Kumar, 1999).

- Physical methods, which are based on the direct radiation (ultraviolet light or gamma-radiation), microwaves, thermal treatment on the colonized surface causing microorganisms death (Berti et al., 2008). Also the alteration or suppression of vital elements, like light, or modification of the atmosphere are considered physical methods and will cause the death or inactivation of the cells. Many of these methods are still in an experimental phase, are more complex than the mechanical and chemical methods and have shown some side effects. In fact, some physical methods have been tested on glazed wall tiles. Oliveira et al. (2001) proposed to re-burn the colonized tiles in order to remove the stains and microorganisms from under the glaze. Silva et al. (2011) studied the biodeterioration of glazed tiles from the interior of the National Tiles Museum, in Lisbon (Portugal). Green spots were observed appearing under the glaze as the microorganisms were growing inside the glaze. An approach to eliminate this problem was done using gamma-radiation to inactivate microorganisms, 25% inactivation was achieved on test microorganisms (Gram-positive bacteria). Although proposed as a treatment for biological decay (Silva et al., 2011, 2013), gamma radiation can cause color alterations of the glaze surface (Doğan and Beril Tuğrul, 2001).

- Chemical methods are the most widely used and comprise the use of substances called biocides which have a lethal action on the organisms. They should provide a high biocide efficacy, not interfering with the substrate and having a low environmental and human toxicity (Caneva et al., 2008). Many biocides have been used for stone cultural heritage, such as inorganic compounds, phosphoorganic compounds, alcohols, phenol derivatives, nitroorganic compounds, quaternary ammonium salts, organic metal salts, pyridine and heterocyclic compounds (Caneva et al., 2008; Piñar et al., 2009; de los Ríos et al., 2012). Recently, environmental friendly substances like titanium dioxide ($TiO_2$), essential oils and other substances are being tested for application on cultural heritage (Fonseca et al., 2010; La Russa et al., 2012; Quagliarini et al., 2012; Stupar et al., 2014).

In summary, although recognized as a significant deterioration factor of outdoor ceramic materials, the biodeterioration of ceramic materials has been seldom studied (Oliveira et al., 2001; Lega et al., 2004; Figueiredo et al., 2009; Silva et al., 2013). Thus, biological decay on glazed tiles are not well understood. Regarding glazed wall tiles few field studies have been carried out for identification of biodeteriogens and biodeterioration patterns. In addition, no laboratorial study has been performed with historical tile models to analyse the biodeterioration and bioreceptivity, concepts that will be further discussed in Chapter 2. Compared to the high number of scientific studies conducted for evaluation of mitigation strategies for stone materials, the studies on ceramic materials are still very scarce. Yet, the application of biocides in conservation and restoration interventions of ceramics has been made (Giacomucci et al., 2011; Mandal and Rath, 2013). Some

experimental studies have been performed regarding mitigation strategies specific for glazed wall tiles, like the use of thermal treatment (Oliveira et al., 2001) and gamma radiation (Silva et al., 2011, 2013).

Despite the increasing number of research concerning conservation and preservation of glazed wall tiles, performed in recent years, few studies were made regarding the biodeterioration of glazed wall tiles (Oliveira et al., 2001; Pedi et al., 2009; Giacomucci et al., 2011; Costa et al., 2013).

## 1.5. Aim and objectives

The conservation problem concerning the biodeterioration of glazed ceramic tiles was the motivation for the development of this PhD thesis. The aim of this work was to study the biodeterioration of glazed wall tiles, more precisely majolica glazed tiles. To achieve this goal some methodological/experimental issues ought to be overcome through the following specific objectives:

- To make a review of the literature concerning microbial colonization and biodeterioration of architectural ceramic materials.

- To investigate microbial communities developing on Portuguese majolica glazed wall tiles in outdoor environments and to evaluate the damage inflicted by them on the tiles on real cases.

- To study the biodeterioration and bioreceptivity of glaze wall tiles under laboratory conditions.

- To test the effect of currently used conventional biocides and $TiO_2$ nanoparticles on biofilms colonizing glaze wall tiles.

- To explore a novel treatment based on the application of $TiO_2$ thin films over the glaze to prevent biological colonization and evaluate its applicability on cultural heritage assets.

- To propose conservation measures for glaze wall tiles exposed to biological colonization

## 1.6. Thesis outline

In order to study the biodeterioration of glazed wall tiles the following stages were achieved:

- First, since no general overview on this issue has been performed, an evaluative report of studies found in the literature concerning the identification of organisms colonizing ceramic materials was essential. In this step it was necessary to broaden the scope of this thesis to a larger group of architectural building materials. Therefore, in addition to glazed wall tiles, bricks, roofing tiles and architectural sculpture were analysed. This allowed to survey the biodiversity reported on each ceramic typology (bricks, roofing tiles and wall tiles), and to relate the presence of microorganisms to weathering factors to which each type of ceramics are submitted. Biodeterioration processes occurring on ceramic building materials were described and related to the identified organisms or organism assemblages.  In

addition, the intrinsic properties of ceramic were related with the bioreceptivity and biodeterioration. This overview on microbial colonization and biodeterioration of architectural ceramic materials is presented in Chapter 2.

- Second, due to the lack of knowledge regarding the microorganisms found on glazed wall tiles, it was necessary to perform the analysis of majolica tiles colonized by microorganisms to fill the information gaps in this area. Two cases were selected for this study: the unique nineteenth century glazed wall tiles attributed to Wenceslau Cifka from Pena National Palace (Sintra, Portugal) and the tiles from *Casa da Pesca* (formerly a part of the Marquis de Pombal Palace situated in Oeiras, Portugal), representing a very common typology of Portuguese tiles. Both studies comprised the characterization of the glaze (substrate), the microbial communities and the evaluation of biodeterioration patterns. The characterization of microbial communities found in Pena National Palace tiles was performed using culture and molecular biology approaches. With this microbial characterization a new species of fungus was described. This case study is presented in Chapter 3. The second case study comprises the characterization of the microbial communities from *Casa da Pesca* tiles and was performed using a similar methodological approach as in Pena National Palace. This case study is presented in Chapter 6.

- The third stage consisted in a laboratory biodeterioration and bioreceptivity experiment which was carried out using pristine and artificially aged glaze tile models. The production of the glaze models was based on the characterization of the white ceramic glaze from the Pena National Palace tiles. Complete chemical and physical characterization of the substrate was performed prior to the experiment, followed by their inoculation with a fungus isolated from Pena National Palace tiles. Another set of pristine and artificially aged glaze tiles were inoculated with a photoautotrophic community consisting of microalgae and cyanobacteria from belongs to same genera of those identified on the Pena National Palace tiles. The biodeterioration and bioreceptivity experiment using phototrophic microorganisms is presented in Chapter 4 and the experiment with the fungus is presented in Chapter 5. Both experiments had an incubation time of one year and different techniques were carried out to assess biodeterioration at the end of each experiment.

- Fourth, the colonized majolica tiles from *Casa da Pesca* were selected for testing three commercial biocides and a $TiO_2$ nanoparticles treatment. The effect of the biocides on the microorganisms and on the substrate was monitored and evaluated being described in Chapter 6.

- The fifth stage consisted of the testing of a treatment for glazed wall tiles to inhibit biological colonization based in the application of the $TiO_2$ thin coatings over the glaze. The advantages and limitation of the treatment were analyzed regarding the cultural heritage guidelines for conservation treatments and it is presented in Chapter 7.

- Finally, preliminary notes on conservation measures for colonized glazed tiles based on the observations and case studies analyzed in the previous chapters are presented in Chapter 8.

# Biological colonization and biodeterioration of architectural ceramic materials: An overview

This work presents the first review on biodiversity, biodeterioration and bioreceptivity of architectural ceramics. Literature dating from 1972 to 2014 was compiled and analyzed in order to summarise the current knowledge and to facilitate a better understanding on the subject. Data regarding biodiversity found on architectural ceramic materials was described for three typologies: bricks, roofing tiles and glazed wall tiles. A vast biodiversity has been identified on these ceramic materials, from bacteria to more complex organisms, such as plants. Bricks were the most studied substrate, while literature on glazed wall tiles was scarce as mentioned in Chapter 1.

In the searched literature, different methods had been used to identify and characterize the organisms. This difficults the comparison of the biodiversity found on these substrates. The biodeterioration processes occurring on the different architectural ceramic materials were explained in detail. The relationship between the ceramic intrinsic properties and bioreceptivity was discussed. Porosity and surface roughness seemed to play a major role in bioreceptivity to microbial colonization. Ceramic microstructure has a strong influence on the resistance to biodeterioration. This literature overview demonstrated that there are many gaps in the knowledge concerning biodeterioration of ceramics, especially on glazed ceramics.

## 2.1. Introduction

Architectural ceramics as building materials are used in the construction of architectural work being applied in masonry, roofing, cladding and ornamentation. Buildings and monuments with ceramic elements, whether in the form of bricks, wall and roofing tiles, architectural statuary or floor tiles can be found throughout the world. This work deals with the biological colonization and biodeterioration of architectural ceramic materials, more specifically, traditional ceramics (clay-based) such as, bricks, roofing and wall tiles. Utilitarian ceramic objects and technical ceramics are not considered. A significant number of architectural ceramic materials are part of our cultural heritage and therefore ought to be preserved since they have historical and artistic value. Fig. 2.1 illustrates examples of glazed wall tiles and bricks on historical buildings from Portugal.

**Fig. 2.1** Ceramic building materials in Portuguese assets: (a) wall tile panels illustrating the aesthetical ornamentation of a garden belonging to a historical building, *Casa da Pesca*, in Oeiras; (b) detail of the 18th century glazed tiles with iconographic illustration from *Casa da Pesca*, Oeiras; (c) bullfight arena in Lisbon (in Portuguese: *Praça de Touros do Campo Pequeno*) built with bricks in the last decade of the 19th century.

The use of ceramic as a building material dates back to antiquity and has continued throughout history until nowadays. Their selection for construction purposes has been motivated by questions of durability, availability, workability, cost, speed and appearance. Workability, cost and speed play a crucial role in the use of ceramics when compared to stone, owing much to the ease and economy of forming raw ceramic materials. Sun-dried clay bricks were used for construction, but with the passage of time, these started to be fired to enhance their resistance. The use of these fired ceramic bricks in buildings construction started in Egypt around 5000 B. C. and later spread to Europe during the Roman Empire (Hamilton, 1978; Gerard, 2007). In turn, the use of ceramic tiles as roofing materials started in China around 1500 B.C. (Knapp, 2000). Although glazes can be found on roofing tiles and bricks, they are most common on floor and wall tiles. As mentioned in Chapter 1, their usage began in the ancient Egypt around 3000 B.C., later spreading to the Near East and then to Europe (Sabo and Falcato, 1998; El Nouhy, 2013). Due to Islamic influence, glazed wall tiles gained great importance in Portugal, Spain and later in Brazil and other south American latin countries (Sabo and Falcato, 1998; Bandini et al., 2002).

Traditional ceramics, like described in Chapter 1 are simply made of clay mixed with water, which are then shaped during the forming process. Subsequently, the material is air-dried and fired for permanent hardening. The composition, texture and porosity of the resulting ceramic body depend on the raw materials composition and their granulometry, and affected by the firing temperature and cycle to which they were subjected.

Some ceramics are complemented with a coating: an engobe or a glaze. The engobe is a colored coating of fine grained clay that is applied over the ceramic body to reduce surface roughness. The glaze consists of a vitreous coating, also applied over the surface of the ceramic body, to enhance mechanical strength. It is composed of a crystalline phase embedded in a glassy matrix, formed by the melting of the raw components during firing. This coating is impermeable and is usually very smooth. Glazes, as glass, can have a variety of colors, textures and glosses (Rhodes and Hopper, 2000). For this reason, the use of glazed ceramic elements in architecture has a strong aesthetical intension, and more than just color, wall tiles are often made with illustrations of great artistic and historical value.

A wide range of raw materials and compositions can be used for the production of ceramic bodies, engobes and glazes, such as clay minerals (e.g. kaolinite, illite), quartz, feldspars, carbonates, silicates and oxides (Carter and Norton, 2013). Ceramic production, from forming until the final coating application, can indeed involve a wide variety of methodologies, from traditional methods, such as manual forming, to more complex technologies, such as extrusion or pressure forming, which are nowadays used in industry (Carter and Norton, 2013).

Generallythe deterioration of ceramic materials, like in other building materials, is influenced by the characteristics of the substrate (e.g. mineralogical composition, porosity surface roughness), environmental agents (e.g. wind, sunlight, temperature, rain, and relative humidity), microclimatic conditions (e.g. local urban geometry, building design or adjacent materials), atmospheric pollution and biological colonization. These factors can induce physical, chemical and biological decay on the architectural ceramic materials. Several studies have been performed concerning mineralogical, chemical and physical characteristics of ceramics used in construction, as well as on the factors and mechanisms of physical and chemical deterioration (e.g. (Larsen and Nielsen, 1990; Eppler, 1992; Larbi, 2004; Hupa et al., 2005; Lopez-Arce and Garcia-Guinea, 2005; Kopar and Ducman, 2007; Lynch, 2007; Andrés et al., 2009; Cannillo et al., 2009; Raimondo et al., 2009; Dondi et al., 2014)). Overviews of weathering and pathologies of roofing materials were performed by Berdahl et al. (2008) and Garcez et al. (2012). Likewise, Yiu et al. (2007), Silvestre and de Brito (2009) and Silvestre and de Brito (2011) described the most common decay factors affecting this architectural ceramic typology.

Biodeterioration or biological decay has been reported as a very common phenomenon on outdoor ceramic materials (e.g. (Ravaglioli and Krajewski, 1989; Buys and Oakley, 1996; Sand, 1997; Warren, 1999; Pinna, 2002; Sand et al., 2002; Oakley and Jain, 2002; Lurdes Esteves, 2003; Mazzotti, 2003; Lega et al., 2004; Durbin, 2005; Figueiredo et al., 2009; Mimoso et al., 2011; Baricza et al., 2012; Hassan and Harun, 2013)). However, few studies have been performed focused on the identification of colonizing microorganisms and their damage on ceramic materials, in comparison to studies on other building materials such as stone (Sand, 1997; Warscheid and Braams, 2000; Macedo et al., 2009; Cuzman et al., 2011).

The occurrence of biodeterioration is dependent on the presence of organisms on the materials. The susceptibility of a given material to biological colonization is based on its intrinsic properties and was defined by Guillite (1995) as bioreceptivity. This author subdivided this concept in three types: primary bioreceptivity, as the intrinsic potential of a material to biological colonization; secondary bioreceptivity, as the ability of an altered material, changed over time by physical and chemical agents, to be colonized; and tertiary bioreceptivity, as the potential of material to be colonized due to human interventions(e.g. after a conservation treatment).

The biological communities present on an inorganic substrate are usually the result of successive colonizations by different organisms through time. The colonization process can be described as starting with the less complex organisms to the more complex ones like described in Chapter 1. Ceramic materials can be colonized by different organisms, such as bacteria, fungi, algae, cyanobacteria (or blue-green algae), lichens, mosses (bryophytes) and vascular plants.

Today the important role of organisms in the deterioration of cultural heritage building materials is well established (Ortega-Calvo et al., 1991; Crispim and Gaylarde, 2005; Sterflinger, 2010; Gaylarde et al., 2011; Sterflinger and Piñar, 2013). Nevertheless, control and mitigation methods for these biodeterioration processes are still far from being solved. Yet there is a consensus regarding biodeteriogens identification and knowledge of biodeterioration mechanisms as crucial steps for any conservation and restoration intervention of biologically colonized assets (Otlewska et al., 2014a). Regarding biodeterioration of architectural ceramic materials, there is no literature review on this subject making it a very difficult topic to study. In fact, the data regarding this subject is scattered and difficult to assess. Therefore, it is urgent to make a compilation and a critical overview of the published data. This work aims to give a comprehensive overview of the biological colonization and biodeterioration ofbricks, roofing tiles and glazed wall tiles. In order to achieve this main goal it was necessary:

- to gather all literature concerning the identification of organisms colonizing architectural ceramic materials;

- to divide the architectural ceramic materials in three main typologies: bricks, roofing tiles and wall tiles; in order to make a clear discussion of the results

- to list the microbial diversity found on each ceramic typology;

- to relate the organisms identified on each ceramic typology with the weathering factors to which they were subjected;

- to describe and relate the biodeterioration processes occurring on ceramic building materials;

- to relate the intrinsic properties of ceramic with bioreceptivity and biodeterioration.

## 2.2. Micro- and macroorganisms found on architectural ceramic assets

The geographical distribution of the architectural ceramic assets where biological colonization was reported is shown in Fig. 2.2. Studies were performed in countries from eastern Asia to occidental areas in America. Most studies were carried out in European countries (Fig. 2.2). Assets which are not Cultural Heritage were also considered in this work, for the reason that relevant data regarding this theme was provided through their analysis.

**Fig. 2.2** Geographical distribution of the studies regarding biological colonization of architectural ceramic materials. Sign (▲) indicates countries. Adapted from https://commons.wikimedia.org/wiki/File:World_map_blank_without_borders.svg.

Material characteristics of architectural ceramic materials with biological colonization and respective bibliographic references are listed in Table 2.1. As mentioned before, ceramic building materials exist in a variety of shapes according to their role and typology, which determine their exposure to weathering factors. Therefore, in order to perform a more clear discussion of the results, ceramic building materials were divided according to three ceramic typologies: bricks and architectural sculptures (Table 2.2 and 2.3), roofing tiles (Table 2.4 and 2.5) and glazed wall tiles (Table 2.6).

Fig. 2.3 shows the percentage of the analysed studies according to ceramic typology. Bricks (57%) and roofing tiles (30%) were the most studied typologies; they are indeed the most widespread ceramic building materials being used worldwide and representing a major field in the ceramic industry. The less studied architectural ceramic typology is glazed wall tiles (13%).
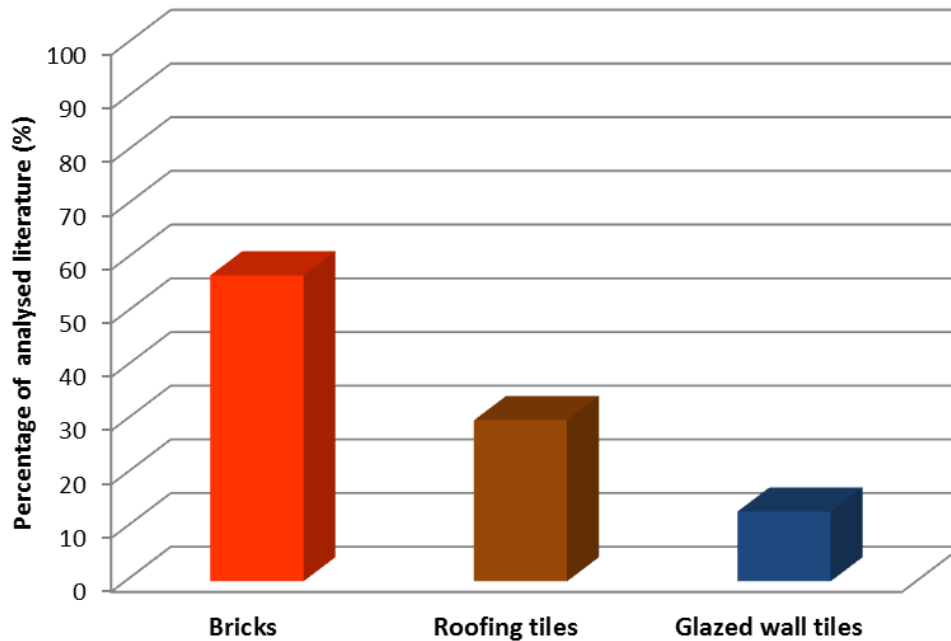
**Fig. 2.3** Percentage (%) of analyzed studies regarding each ceramic building material typology considered in this work: bricks, roofing tiles and glazed wall tiles.

Most of the studies did not provide detailed information regarding ceramic composition and characteristics, with the exception of those devoted to glazed wall tiles (Table 2.1). This may be due to the fact that all of these tiles are classified as cultural heritage and therefore knowledge on the composition is crucial for any conservation intervention.

**Table 2.1** Investigated worldwide architectural assets organized according to the typology of the ceramic building material (brick, roofing tile and glazed wall tile) with corresponding substrate characteristics and bibliographic reference.

| Ref. no. | Architectural assets and/or location | Substrate characteristics | Reference |
|---|---|---|---|
| | **Bricks** | | |
| 1 | Architectural sculptures of the Seville Cathedral (Spain) | Fired clay ceramics | Ortega-Calvo et al., (1991) |
| 1a | Architectural sculptures of the Seville Cathedral (Spain) | Fired clay ceramics (quartz, gehlenite and wollastonite and Illite, quartz, calcite and feldspars) | Pérez-Rodríguez et al., (1998) |
| 2 | Buildings in Auschwitz-Birkenau Memorial Site (Poland) | Fired clay ceramics | Rajkowska et al., (2014) |
| 2a | Buildings in Auschwitz-Birkenau Memorial Site (Poland) | Fired clay ceramics | Nowicka-Krawczyk et al., (2014) |
| 2b | Buildings in Auschwitz-Birkenau Memorial Site (Poland) | Fired clay ceramics | Otlewska et al., (2014b) |
| 3 | Buildings (Singapore) | Fired clay ceramics | Chua et al., (1972) |
| 4 | Buildings and Monuments (Ireland) | Fired clay ceramics | Rindi and Guiry, (2002) |
| 5 | Carmelite Convent in Alcalá de Henares (Spain) | Fired clay ceramics | Gómez-Alarcón and Cilleros (1995) |
| 6 | Guayaquil Bridge in Antioquia (Colombia) | Fired clay ceramics | Jones (2002) |
| 7 | Islamic wall in Alcazar of Toledo (Spain) | Fired clay ceramics (illite, quartz, alkali and plagioclase feldspars and calcite) | López-Arce et al. (2003) |
| 8 | Jorbangla temple in Bishnupur (India) | Fired clay ceramics | Mandal and Rath (2013) |
| 9 | Kalachand temple in Bishnupur (India) | Fired clay ceramics | Mandal and Rath (2013) |

**Table 2.1** Investigated worldwide architectural assets organized according to the typology of the ceramic building material (brick, roofing tile and glazed wall tile) with corresponding substrate characteristics and bibliographic reference.

| Ref. no. | Architectural assets and/or location | Substrate characteristics | Reference |
|---|---|---|---|
| 10 | La Plata Cathedral in Buenos Aires (Argentina) | Fired clay ceramics (Al, Si, K, Ca and Fe) | Videla (2002) |
| 10a | La Plata Cathedral in Buenos Aires (Argentina) | Fired clay ceramics (Al, Si, K, Ca and Fe) | Herrera and Videla (2004) |
| 11 | Lalitgiri excavated sites in Orissa (India) | Fired clay ceramics | Pattanaik and Adhikary, (2002) |
| 12 | Lalji temple in Bishnupur (India) | Fired clay ceramics | Mandal and Rath (2013) |
| 13 | Madan Mohan temple in Bishnupur (India) | Fired clay ceramics | Mandal and Rath (2013) |
| 14 | Medici Fortress in Livorno (Italy) | Fired clay ceramics | Tomaselli et al. (2000) |
| 15 | Medici Fortress in Sienna (Italy) | Fired clay ceramics | Tomaselli et al. (2000) |
| 16 | Monuments in Toledo (Spain) | Fired clay ceramics (illite, calcite, gehlenite, diopside, quartz and feldspar) | Lopez-Arce and Garcia-Guinea (2005) |
| 17 | Monuments Sarat, Mayurbhanj, Orissa (India) | Fired clay ceramics | Samad and Adhikary (2008) |
| 18 | Nanjing Ming city wall (China) | Fired clay ceramics (illite, albite and feldspar) | Qi-Wang et al. (2011) |
| 19 | Capitolium - Ostia Antica in Rome (Italy) | Fired clay ceramics | Lisci et al. (2003) |
| 20 | Piazzetta degli Ariani brick wall in Ravenna (Italy) | Fired clay ceramics | Raimondi et al. (2009) |
| 21 | Private house and cellar in Baumgarten (Austria) | Fired clay ceramics | Ettenauer et al. (2012) |
| 22 | Radha-shyam temple in Bishnupur (India) | Fired clay ceramics | Mandal and Rath (2013) |
| 23 | Rasmancha temple in Bishnupur (India) | Fired clay ceramics | Mandal and Rath (2013) |
| 24 | Sarnath excavated sites in Uttar Pradesh (India) | Fired clay ceramics | Pattanaik and Adhikary (2002) |
| 25 | Schleswig Cathedral (Germany) | Fired clay ceramics | Palmer and Hirsch (1991) |
| 26 | Shyam-rai temple in Bishnupur (India) | Fired clay ceramics | Mandal and Rath (2013) |
| 27 | St. Francis Convent in Mulla (Spain) | Fired clay ceramics | Uher et al. (2005) |
| 28 | Temples in Bishnupur (India) | Fired clay ceramics | Pattanaik and Adhikary (2002) |
| 29 | Udaigiri excavated site in Orissa (India) | Fired clay ceramics | Pattanaik and Adhikary (2002) |
| 30 | Not specified | Fired clay ceramics | John (1988) |
| 31 | Arch of an 18th century gate in Vignano, Siena (Italy) | Fired clay ceramics | Lisci et al. (2003) |
| | **Roofing tiles** | | |
| 32 | 6-10 years aged roofing tiles from Panonia in Vojvodina region (Serbia) | Fired clay ceramics (illite-kaolinite clay material with carbonates and quartz) | Ranogajec et al. (2005) |
| 33 | 6-10 years aged roofing tiles from Panonia in Vojvodina region (Serbia) | Fired clay ceramics (illite-kaolinite clay material with carbonates and quartz) | Kiurski et al. (2005) |
| 34 | 20-30 years ceramic roofing tiles from Kanjiza and near the river Tisa (Serbia) | Fired clay ceramics | Radeka et al. (2007)b |
| 35 | Aged roofing tiles from Novi Becej region (NE Serbia) | Fired clay ceramics | Radeka et al. (2007)a |
| 36 | Buildings (Singapore) | Fired clay ceramics | Chua et al. (1972) |
| 37 | Roofing tiles (India) | Fired clay ceramics | Dan et al. (1981) |
| 38 | Roofing tiles exposed 1,63 years in 7 experimental stations in California State: El Centro, Corona, Colton, Shafter, Richmond, Sacramento, McArthur (USA) | Fired clay ceramics | Cheng et al. (2011) |

**Table 2.1** Investigated worldwide architectural assets organized according to the typology of the ceramic building material (brick, roofing tile and glazed wall tile) with corresponding substrate characteristics and bibliographic reference.

| Ref. no. | Architectural assets and/or location | Substrate characteristics | Reference |
|---|---|---|---|
| 39 | Roofing tiles exposed in experimental stations in 6 locations: Göttingen, Schermbeck, Schönerlinde, Ostrach, Unsleben, and Zingst (Germany) | Fired clay ceramics without coating, black vanished or engobe ceramics | Gladis and Schumann (2011a) |
| 40 | Roofing tiles from Lieblingshof (Germany) | Fired clay ceramics | Görs et al. (2007) |
| 41 | Roofing tiles from Oporto (Portugal) and Vigo (Spain) | Fired clay ceramics | Laiz et al. (2006) |
| 42 | Royal Palace of Portici in Campania (Italy) | Fired clay ceramics (aluminosilicates with sand or siliceous carbonate) | Motti and Stinca (2011) |
| 43 | Salamanca Cathedral (Spain) | Fired clay ceramics | Garcia-Rowe and Saiz-Jimenez (1991) |
| 43a | Salamanca Cathedral (Spain) | Fired clay ceramics | Ortega-Calvo et al. (1993) |
| 44 | Sekishu roofing tile from Higashi-Hiroshima (Japan) | Glazed ceramics (alkali-feldspar glaze) | Watanabe et al. (2006) |
| 44a | Sekishu roofing tile from Higashi-Hiroshima (Japan) | Glazed ceramics (alkali-feldspar glaze) | Watanabe et al. (2009) |
| 45 | Toledo Cathedral (Spain) | Fired clay ceramics | Garcia-Rowe and Saiz-Jimenez (1991) |
| 46 | Terunelli, Tamil Nadu (India) | Fired clay ceramics | Saxena et al. (2004) |
| 47 | Not specified | Fired clay ceramics | John (1988) |
| | **Glazed wall tiles** | | |
| 48 | *Grande Albergo Ausonia & Hungaria* in Venice (Italy) | Glazed ceramics (white and painted immersion silica-lime-lead glazed tiles on soft stoneware ceramic body) | Giacomucci et al. (2011) |
| 49 | *Pena National Palace* in Sintra (Portugal) | Glazed ceramics (majolica, silica-lead tin opacified glaze) | Coutinho et al. (2011) |
| 49a | *Pena National Palace* in Sintra (Portugal) | Glazed ceramics (majolica, silica-lead tin opacified glaze) | Coutinho et al. (2013) |
| 49b | *Pena National Palace* in Sintra (Portugal) | Glazed ceramics (majolica, silica-lead tin opacified glaze) | Crous et al. (2012) |
| 50 | *Pin ho Manson* in Belém (Brazil) | Glazed ceramics (decalcomania glazed tiles with ceramic paste with quartz, mullite, cristobalite, calcite, and anorthite) | Oliveira et al. (2001) |
| 50a | *Pinho Manson* in Belém (Brazil) | Glazed ceramics (german and Portuguese silica-lead glazed tiles) | Costa et al. (2013) |
| 51 | *Santo António Convent in Salvador* (Brazil) | Glazed ceramics (majolica) | Pedi et al. (2009) |
| 52 | *St. Francis Church and Convent in Salvador (Brazil)* | Glazed ceramics (majolica technique silica lead tin opacified glaze) | Oliveira et al. (2001) |

## 2.2.1. Bricks and architectural sculptures

Traditionally, bricks are known to be made of polymineral red clays, such as illite, kaolinite, chlorite, vermiculite or smectites (Konta, 1995). Therefore, after firing a ceramic body rich in silica, with high $Fe_2O_3$ and CaO content and also with alkalis ($K_2O$ and $Na_2O$) is obtained (Konta, 1995). In fact, most of the bricks presented in Table 2.1 consist of fired red-clay bricks. Usually, bricks

have porous and rough surfaces, which provide anchoring sites and micro-refuges for the attachment and settlement of microorganisms. Tables 2.2 and 2.3 list the microorganisms (bacteria, cyanobacteria, algae and fungi) and organisms (lichens, bryophytes and vascular plants) detected on bricks and ceramic ornamental statuary, respectively, together with the identification method. Ceramic ornamental statuary was also considered in the present work being described together with bricks (Table 2.2). However, only two papers were found in the literature regarding this ceramic typology (Ortega-Calvo et al., 1993; Pérez-Rodríguez et al., 1998). Both studies analysed the same cultural heritage asset: the Pardon Gate in the Seville Cathedral (Spain), which is ornamented with terracotta sculptures.

Several bacteria have been identified on brick surfaces (Table 2.2). This group of microorganisms is ubiquitous being able to colonise almost all types of materials. Overall, 43 taxa were identified belonging to seven phyla: Actinobacteria (9%), Bacteroidetes (12%), Chloroflexi (2%), Deinococcus-Thermus (2%), Firmicutes (28%), Proteobacteria (44%) and TM7 (2%) (Table 2.2). Firmicutes and Proteobacteria were the dominant bacterial groups. Firmicutes phylum was represented by the genera *Bacillus*, *Brevibacillus*, *Sarcina* and *Virgibacillus.*
Proteobacteria phylum was represented by a higher number of genera, namely *Achromobacter, Acinetobacter, Halomonas, Massilia, Proteus, Rhizobium, Rubellimicrobium, Saccharophagus, Salinisphaera, Sinorhizobium, Thioalkalivibrio, Thiobacillus, Pseudomonas* and *Xanthomonas.* All these bacteria were identified on bricks from five different assets located in China, Colombia, Spain and Poland (Gómez-Alarcón and Cilleros, 1995; Jones, 2002; Lopez-Arce and Garcia-Guinea, 2005; Qi-Wang et al., 2011; Otlewska et al., 2014b).

Solely *Bacillus* sp. was detected on more than one asset, specifically on bricks from China (Qi-Wang et al., 2011) and Spain (Gómez-Alarcón and Cilleros, 1995). Six different species from this genus (*Bacillus* sp.) were identified on bricks (Table 2.2). However, it is important to notice that the isolation of some of these genera was done by culture methods which have been reported to yield mainly spore-forming bacteria, such as *Bacillus* or *Brevibacillus* (Laiz et al., 2003; Pepe et al., 2010).

Some of the identified bacterial genera, such as *Halomonas* and *Salinisphaera,* are extremophile bacteria; therefore, they were found on ceramics with salt effluorescences due to their capacity to grow on salt-rich environments (Otlewska et al., 2014b). Halophilic bacteria have also been reported on other deteriorated building materials (Saiz-Jiménez and Laiz, 2000).

Photoautotrophic microorganisms (cyanobacteria and microalgae) present the higher number of members of all organisms found on bricks, with a total number of 108 taxa reported, 72 of them being cyanobacteria and 47 algae (Table 2.2). Concerning cyanobacteria, Chroococcales (31%), Nostocales (28%), Oscillatoriales (28%), Pleurocapsales (8%) and Stigonematales (6%) were the identified orders. These microorganisms were found on 20 different assets from Spain, Italy, Poland, India, Singapore and Colombia (Table 2.2). Half of the total cyanobacteria taxa were reported by Mandal and Rath (2013) on bricks from seven different temples of Bishnupur (India). Within cyanobacteria taxa, 51 were found in more than one asset (Table 2.2) with the most widespread species being *Lyngbya corticicola*, *Nostoc microscopicum* and *Scytonema schmidtii.*

These filamentous cyanobacteria are capable of forming specialized structures, called heterocyst, that enable them to fix nitrogen ($N_2$) directly from the air (Fig. 2.4). These structures, together with other survival strategies, such as the production of protective sheaths, allow them to survive in hostile environments (e.g. without nitrogen and dry) by creating a biofilm
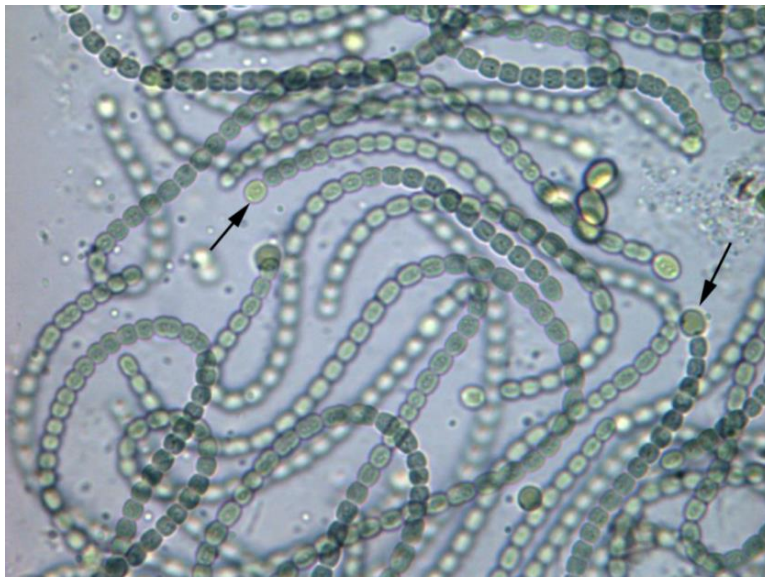


**Fig. 2.4** Micrograph of the cyanobacterium *Nostoc paludosum* (presented in Table 2.6) with heterocyst (arrows), collected from glazed wall tiles from Pena National Palace (x 60).

A biofilm is composed of a mono- or multilayer of microbial cells embedded in a hydrated extracellular polymeric matrix (Costerton et al., 1995; Morton et al., 1998; Warscheid, 2000). These glue-like extracellular polymeric substances (EPS) secreted by the cells enhance the adhesion of microbial cells to the substrate and favour the adherence of nutritive airborne particles (e.g. dust, pollen, spores, oil- and coal-fired carbonaceous particles) from the atmosphere (Saiz-Jimenez, 1995; Koestler et al., 1997; Cecchi et al., 2000; Warscheid and Braams, 2000; Wimpenny et al., 2000). Biofilms also allow the retention of large amounts of water into its structure, protecting the cells from desiccation (Prakash et al., 2003; Gorbushina, 2007).

Regarding algae, 47 taxa were identified, 31 of which belonging to Chlorophyta (green algae), 12 to Bacillariophyta (diatoms), 2 to Xanthophyta (yellow-green alga) and 2 to Streptophyta (charophyte green algae) (Table 2.2). They were identified on 16 different assets from Spain, Italy, Ireland, Poland, Singapore, India and Colombia. Chlorophyta were represented by three main classes: Ulvophyceae (19%), Trebouxiophyceae (32%) and Chlorophyceae (48%) (Table 2.2). *Chlorella*, *Chlorococcum*, *Trentepohlia* and *Bracteacoccus* were the most widespread genera (Table 2.2) The occurrence of *Chlorella* and *Chlorococcum* on inorganic substrates in European, American and Asian countries has been reported by Ortega-Calvo et al. (1995) and was even referred to as the most abundant green algae genera found in stone monuments from the Mediterranean Basin (Macedo et al., 2009). *Trentepohlia* is a filamentous subaerial green alga, which can inhabit on different substrates, such as wood, leaves and rock (Rindi and Guiry, 2002). It can be frequently found as lichen photobiont (John, 1988; Coutinho et al., 2013). *Bracteacoccus* has also been identified on stone monuments in Portugal, Spain and Germany (Macedo et al.,

2009; Hallmann et al., 2013). Diatoms (Bacillariophyta) were much less identified than Chlorophyta (Table 2.2). Their taxonomic classification was performed by four studies: Ortega-Calvo et al. (1995) being the species found on ceramic sculptures from the Seville Cathedral, Mandal and Rath (2013) that identified diatoms on sculpted bricks from monuments in India, and Rajkowska et al. (2014) and Nowicka-Krawczyk et al. (2014) that characterize the biological colonization on historic building from the former Auschwitz II-Birkenau concentration camp in Poland (Table 2.2). Diatoms are mostly confined to aquatic environments (Patrick, 1977). Nevertheless, some species of diatoms grow in communities together with phototrophic microorganisms, such as green algae and cyanobacteria, being able to inhabit soils and humid rocks (Patrick, 1977; Souffreau et al., 2010). These photoautrophic microorganisms (green microalgae, cyanobacteria and diatoms) use light as an energy source and synthesise organic matter from carbon dioxide and mineral components by photosynthesis, and therefore they are considered the pioneer colonizers of inorganic substrates due to their ability to grow without any presence of organic matter (Ortega-Calvo et al., 1991; Tiano et al., 1995; Tomaselli et al., 2000; Warscheid and Braams, 2000). The strategy of photoautrophic microorganisms to settle and develop on hostile environments, such as architectural ceramic materials, is based on their capacity to form biofilms (Costerton et al., 1995; Morton et al., 1998; Warscheid, 2000).

A total of 12 taxa of fungi, represented by the phyla Ascomycota (82%), Basidiomycota (9%) and Zygomycota (9%) were also identified on bricks (Table 2.2). The most widespread genera were *Alternaria*, *Penicillium* and *Aspergillus*, reported on three different assets from Spain, Germany and Colombia (Table 2.2). These are airborne fungi found in various climates worldwide. *Alternaria* is commonly isolated from soils, monuments and indoor environments (Šimonovičová et al., 2004; Sterflinger, 2010) and *Aspergillus* and *Penicillium* have also been reported colonizing several stained glass windows (e.g. Carmona et al., 2006; Rodrigues et al., 2014)). Glass, like glazed ceramics materials, is a limited-nutritional substrate. The presence of these fungi might be explained by the osmophilic and xerophilic nature of some species belonging to these genera(Claudia Schabereiter-Gurtner et al., 2001; Carmona et al., 2006).

**Table 2.2 Microorganisms reported on bricks and architectural sculptures together with the identification method and reference number (Table 2.1 Ref. No.).**

| Bacteria[a] | Met[b] | Ref no. | Cyanobacteria[a] | Met[b] | Ref no. | Algae[a] | Met[b] | Ref no. | Fungi[a] | Met[b] | Ref no. |
|---|---|---|---|---|---|---|---|---|---|---|---|
| Achromobacter piechaudii | CMB | 18 | Aphanothece castagnei | C | 8, 9, 12, 23, 26 | Achnanthes coartata | C | 1 | Alternaria sp. | C | 5, 6 |
| Acinetobacter junii | CMB | 18 | Aphanothece microscopica | C | 8,13, 23, 26 | Achnanthidium minutissimum | C | 2a | Aspergillus sp. | C | 6, 25 |
| Bacillus sp. | C | 5 | Aphanothece pallida | C | 8, 12, 22, 23 | Apatococcus lobatos | C | 2a, 27 | Fusarium sp. | C | 6 |
| Bacillus sp. | CMB | 18 | Aphanothece stagnina | C | 8, 13, 23 | Bracteacoccus minor | C | 1, 8, 9, 12, 26 | Gibberella sp. | C | 6 |
| Bacillus aquimaris | CMB | 18 | Calothrix sp. | C | 3, 30 | Chlorella sp. | C | 2a, 1, 3, 15, 30 | Monilia sp. | C | 6 |
| Bacillus firmus | CMB | 18 | Calothrix clavatoides | C | 12, 23 | Chlorella homosphaera | C | 1 | Mucor sp. | C | 6 |
| Bacillus fusiformis | CMB | 18 | Calothrix marchica | C | 22, 23 | Chlorella vulgaris | C | 1, 27 | Paecilomyces sp. | C | 25 |
| Bacillus megaterium | CMB | 18 | Chlorogloea sp. | C | 3, 30 | Chlorella zoofingensis | C | 1 | Penicillium sp. | C | 6, 25 |
| Bacillus niabensis | CMB | 18 | Chroococcidiopsis sp. | C | 14, 15 | Chlorellidium tetrabotrys | C | 1 | Phoma sp. | C | 5 |
| Bacillus simplex | MB | 18 | Chroococcidiopsis kashayi | C | 23, 26, 27 | Chlorhormidium pseudostichococcus | C | 30 | Rhodotorula sp. | C | 6 |
| [Polyangium] brachysporum | CMB | 18 | Chroococcus sp. | C | 2a, 3, 30 | Chlorococcum sp. | C | 3, 30 | Tricoderma | C | 6 |
| Brevibacillus agri | CMB | 18 | Chroococcus indicus | C | 8, 9, 12, 23 | Chlorococcum infusionum | C | 2a, 12, 23, 26 | Ulocladium sp. | C | 5 |
| Deinococcus maricopensis | MB | 18 | Chroococcus minor | C | 2a, 8, 13, 22, 23 | Chlorosarcinopsis sp. | C | 1, 27 | NI[a] fungi | C | 10, 10a |
| Gracilimonas sp. | MB | 2b | Chroococcus turgidus var. maximus | C | 8, 22, 23, 26 | Chlorosarcinopsis cf. arenicola | C | 27 | NI[a] fungi | SEM | 1a, 7, 16, 25 |
| Gramella sp. | MB | 2b | Chroococcus varius | C | 8, 9, 12, 23, | Coenochloris sp. | C | 2a | NI[a] fungi | MB | 21 |
| Halomonas ventosae | MB | 2b | Cyanosarcina | C | 12, 23, 26 | Denticula kuetzingii | C | 2a | NI[a] Yeasts | C | 10 |

**Table 2.2 (cont.).**

| Bacteria[a] | Met[b] | Ref no. | Cyanobacteria[a] | Met[b] | Ref no. | Algae[a] | Met[b] | Ref no. | Fungi[a] | Met[b] | Ref no. |
|---|---|---|---|---|---|---|---|---|---|---|---|
| Halomonas nitritophilus | MB | 2b | Cyanosarcina parthenonensis | C | 8, 9, 23 | Desmococcus olivaceus | C | 30 | | | |
| Halomonas muralis | MB | 2b | Cyanosarcina spectabilis | C | 8, 12, 17, 26 | Diadesmis contenta | C | 2 | | | |
| Massilia timonae | CMB | 18 | Cyanothece aeruginosa | C | 9, 23 | Draparnaldia sp. | C | 6 | | | |
| Micrococcus sp. | C | 5 | Fischerella tenuis | C | 11 | Ecdysichlamys obliqua | C | 1 | | | |
| Proteus sp. | C | 6 | Gloeocapsa sp. | C | 2a, 3, 30 | Euastrum sp. | C | 2a | | | |
| Rhizobium sp. | C | 6 | Gloeocapsa sanguinea | C | 8, 26 | Gomphonema lanceolatum | C | 12, 23 | | | |
| | | | Gloeothece sp. | C | 2a, 3, 30 | Gomphonema parvulum | C | 2a | | | |
| Rubellimicrobium aerolatum | MB | 2b | Gloeothece palea | C | 18 | Haematococcus pluvialis | C | 1 | | | |
| Rubrobacter sp. | MB | 18 | Gloeothece rupestres | C | 8, 9, 12, 26 | Hantzschia amphioxys | C | 1 | | | |
| Saccharophagus degradens | MB | 2b | Gloeothece rhodochlamys | C | 17, 29 | Klebsormidium flaccidum | C | 1 | | | |
| Salinisphaera shabanensis | MB | 2b | Leptolyngbya sp. | C | 2a, 14, 15 | Muriella terrestris | C | 1, 27 | | | |
| Sarcina sp. | C | 6 | Leptolyngbya boryana | C | 8, 13, 22, 23 | Navicula gracilis | C | 22, 26 | | | |
| Sinorhizobium fredii | MB | 2b | Leptolyngbya fareolarum | C | 2a | Navicula mutica | C | 1 | | | |
| Streptococcus sp. | SEM | 16 | Leptolyngbya polysiphoniae | C | 12, 23, 26 | Neochloris bilobata | C | 1 | | | |
| Streptomyces sp. | MB | 18 | Lyngbya sp. | C | 6 | Nitzschia amphibia | C | 13, 22 | | | |
| Thioalkalivibrio versutus | MB | 2b | Lyngbya arboricola | C | 12, 22, 23, | Nitzschia palea | C | 22, 23 | | | |
| Thiobacillus denitrificans | C | 5 | Lyngbya corticicola | C | 8, 9, 12, 13, 22, 23, 26 | Prasiola crispa | C | 4 | | | |
| Virgibacillus carmonensis | MB | 2b | Lyngbya major | C | 8, 9, 12, 13, 23 | Prasiola calophylla | C | 4 | | | |
| Uncultured Actinobacterium | MB | 18 | Mycrocystis sp. | C | 6 | Protococcus sp. | C | 3 | | | |
| Uncultured bacterium Bacteroidetes | MB | 18 | Microcoleus vaginatus | C | 1 | Printzina effuse | C | 12, 23 | | | |
| Uncultured bacterium Chloroflexi | MB | 18 | Myxosarcina sp. | C | 3, 14, 30 | Pseudendoclonium printzii | C | 1 | | | |
| Uncultured bacterium Deltaproteobacteria | MB | 18 | Myxosarcina concinna | C | 1 | Radiococcus nimbatus | C | 12, 22, 23 | | | |
| Uncultured bacterium TM7 | MB | 18 | Myxosarcina spectabilis | C | 28 | Rosenvingiella polyrhiza | C | 4 | | | |
| Uncultured Flavobacteriales | MB | 18 | | | | | | | | | |

Table 2.2 (cont.).

| Bacteria[a] | Met[b] | Ref no. | Cyanobacteria[a] | Met[b] | Ref no. | Algae[a] | Met[b] | Ref no. | Fungi[a] | Met[b] | Ref no. |
|---|---|---|---|---|---|---|---|---|---|---|---|
| Uncultured Proteobacterium | MB | 18 | Nostoc sp. | C | 3, 30 | Scenedesmus quadricauda | C | 1 | | | |
| Uncultured Pseudomonas sp. | MB | 18 | Nostoc commune | C | 11, 24, 28 | Stichococcus bacillaris | C | 1 | | | |
| Uncultured Sphingobacteria | MB | 18 | Nostoc linckia | C | 12, 26 | Trebouxia | C | 2a | | | |
| Xanthomonas sp. | C | 6 | Nostoc microscopicum | C | 8, 9, 12, 13, 22, 23, 26 | Trentepohlia sp. | C | 2a, 3, 30 | | | |
| NI bactéria | C | 10a, 25 | Nostoc punctiforme | C | 1 | Trentepohlia áurea | C | 23, 26 | | | |
| NI bactéria | C, SEM | 10 | Oscillatoria sp. | C | 3, 30 | Tryblionella hungarica | C | 2a | | | |
| NI bactéria | SEM | 1a, 16 | Oscillatoria amphigranulata | C | 1 | Ulothrix sp. | C | 14 | | | |
| NI bactéria | MB | 21 | Phormidium aerugineo-coeruleum | C | 12, 23 | Xanthonema sp. | C | 2a | | | |
| | | | Phormidium ambiguum | C | 8, 23 | NI Diatoms | SEM | 7, 16 | | | |
| | | | Phormidium autumnale | C | 1 | NI Chlorophyta | SEM | 7, 16 | | | |
| | | | Phormidium retzii | C | 23, 26 | NI Chlorophyta | Chla | 20 | | | |
| | | | Phormidium ténue | C | 1 | NI Chlorophyta | M, SEM, Chla | 25 | | | |
| | | | Phormidium tergestinum | C | 2A | NI Chlorophyta | M | 10, 10a | | | |
| | | | Plectonema sp. | C | 15 | | | | | | |
| | | | Plectonema boryanum | C | 1 | | | | | | |
| | | | Pleurocapsa sp. | C | 15 | | | | | | |
| | | | Porphyrosiphon ceylanicus | C | 12, 23 | | | | | | |
| | | | Scytonema sp. | C | 3, 15, 30 | | | | | | |
| | | | Scytonema bohneri | C | 8, 13, 22, 23, | | | | | | |
| | | | Scytonema drilosiphon | C | 2, 2a | | | | | | |

Table 2.2 (cont.).

| Bacteria[a] | Met[b] | Ref no. | Cyanobacteria[a] | Met[b] | Ref no. | Algae[a] | Met[b] | Ref no. | Fungi[a] | Met[b] | Ref no. |
|---|---|---|---|---|---|---|---|---|---|---|---|
| | | | Scytonema geitleri | C | 8, 9, 23 | | | | | | |
| | | | Scytonema multiramosum | C | 8, 9, 12, 26 | | | | | | |
| | | | Scytonema rivulare | C | 8, 9, 12, 23, 26 | | | | | | |
| | | | Scytonema schmidtii | C | 8, 9, 12, 13, 22, 23, 26 | | | | | | |
| | | | Stigonema tomentosum | C | 22, 26 | | | | | | |
| | | | Synechocytis sp. | C | 1 | | | | | | |
| | | | Synechococcus aeruginosus | C | 22, 23 | | | | | | |
| | | | Tolypothrix arenophila | C | 11 | | | | | | |
| | | | Tolypothrix byssoidea | C | 1 | | | | | | |
| | | | Tolypothrix fragilis | C | 24 | | | | | | |
| | | | Tolypothrix conglutinata | C | 28 | | | | | | |
| | | | Westiellopsis sp. | C | 3, 30 | | | | | | |
| | | | Westiellopsis prolifica | C | 12, 23 | | | | | | |
| | | | NI Cyanobacteria | M | 10, 10a, 25 | | | | | | |

[a] NI: Non-identified
[b] Identification methods (Met): C – Culture methods; Chla – Chrolophyll a quantification; CMB – Molecular biology of cultured isolates; M – Morphological; MB – Molecular biology; SEM – Scanning electron microscope

Lichens have also been reported on brick walls from four different assets (Table 2.3). However, only Lisci et al. (2003) identified species of lichens exposed on the North brick walls of the Capitolium from Ostia Antica (Italy): *Dirina massiliensis*, *Dirina stenhammari*, *Lecidella carpathica* and *Rocella phycopsis*.

**Table 2.3.** Organisms reported on bricks and architectural sculptures together with the identification method and reference number (Table 2.1 Ref. No.).

| Lichens[a] | Met[b] | Ref no. | Bryophytes[a] | Met[b] | Ref no. | Vascular Plants[a] | Met[b] | Ref no. |
|---|---|---|---|---|---|---|---|---|
| *Dirina massiliensis* | M | 19 | *Bryum argenteum* | M | 2 | NI[a] plants | M | 10, 10a |
| *Dirina stenhammari* | M | 19 | *Marchantia polymorpha* | M | 2 | Cypress | M | 34 |
| *Lecidella carpathica* | M | 19 | *Plagiothecium curvifolium* | M | 2 | | | |
| *Rocella phycopsis* | M | 19 | *Tortula muralis* | M | 2 | | | |
| NI[a] Lichen | M | 2, 6, 26 | NI[a] Bryophytes | M | 6,10, 10a | | | |
| NI[a] Lichen | SEM | 7, 16 | | | | | | |

[a] NI: Non-identified
[b] Identification methods (Met): M – Morphological; SEM – Scanning electron microscopy

Most of these lichens have been reported on different substrates and environments, such as stone and wall paintings (Hauck et al., 2007; Zucconi et al., 2012). In fact, the main biodeteriogen found on the wall paintings of the Holy Saviour's cave in Italy was *Dirina massiliensis* (Zucconi et al., 2012). Brick surfaces can also harbour bryophytes and vascular plants as shown in Table 2.3 Rajkowska et al. (2014) identified four different species of bryophytes, on the outer surfaces of brick buildings, from the Auschwitz-Birkenau Memorial Site (Poland). Other authors also found bryophytes on bricks but they were not taxonomically identified (Gómez-Alarcón and Cilleros, 1995; Mandal and Rath, 2013). Bryophytes can inhabit different environments from tropical to artic climates (Pharo and Zartman, 2007). Many bryophytes are poikilohydric which makes their hygric balance dependent on the environmental water (Green and Lange, 1994). This type of organism is frequently tolerant to desiccation, such as the bryophytes *Bryum argenteum* and *Torula muralis* (Akter et al., 2014). These characteristics enable bryophytes to develop on inhospitable substrates like bricks (Table 2.3). The detrimental action of bryophytes on stone has also been reported. For instance, *Torula muralis* has been associated to biophysical damage on stone substrates due to rhizoid penetration (Hughes, 1982).

Vascular plants, namely a Cypress was reported to be growing over a brick structure (Table 2.3) (Lisci et al., 2003). Yet, this is the only work providing vascular plant classification. Nevertheless, one can infer the damage caused by vascular plants on bricks from the several works reporting the biodeterioration effect of plant roots on stone monuments, mainly in tropical environments (e.g. (Kumar and Kumar, 1999; Lisci et al., 2003).

### 2.2.2. Ceramic roofing tiles

Ceramic roofing tiles are fired clay slabs with similar composition to bricks, consisting of illite-kaolinite clay with quartz and carbonates (Kiurski et al., 2005; Ranogajec et al., 2005; Radeka

et al., 2007a, 2007b; Motti and Stinca, 2011). Although roofing tiles are extensively studied, few data are available in the literature regarding their chemical and mineralogical composition (Table 2.1). Nevertheless and similar to bricks, fired clay ceramic roofing tiles are clearly more common than those performed on glazed roofing tiles. These last typologies were the subject of only two studies (Watanabe et al., 2006, 2009) and one on varnished surfaces (Gladis and Schumann, 2011a) (Table 2.1).

Since the main function of roofing tiles is to shelter the interior of the building from rain, wind and solar radiation, they are exposed to harsh weathering factors, including biological agents which may induce biodeterioration phenomena (Berdahl et al., 2008). Unlike bricks, their exposed surfaces are not vertical, being usually applied with a low roof slope (oblique-angled).

Tables 2.4 and 2.5 list the microorganisms (bacteria, cyanobacteria, algae and fungi) and organisms (lichens, bryophytes and vascular plants) identified on ceramic roofing tiles from several studies, respectively, together with the identification method.

A total of 20 bacterial taxa were detected on ceramic roofing tiles, belonging to the phyla Actinobacteria (45%), Proteobacteria (35%), Firmicutes (15%) and Deinococcus-Thermus (5%) (Table 2.4). All these bacteria were found on roofing tiles from USA, Portugal and Spain (Laiz et al., 2006; Cheng et al., 2011) (Table 2.4). Regarding identified bacterial taxa, they were different from those detected on bricks, with the exception of the *Bacillus* genus (Table 2.2 and Table 2.4). Noteworthy is the lower biodiversity of photoautotrophs found on ceramic roofing tiles (Table 2.4) when compared to bricks (Table 2.2). A total of 24 taxa of phototrophic microorganisms were identified, 12 of them belonging to cyanobacteria and 12 to algae. Among cyanobacteria, Chroococcales (42%), Nostocales (25%), Oscillatoriales (17%), Pleurocapsales (8%) and Stigonematales (8%) were the recognized orders (Table 2.4). All cyanobacteria genera identified on roofing tiles (Table 2.4) were also present on bricks (Table 2.2). These cyanobacteria genera were found on tiles from India, Singapore and Spain (Table 2.4). The presence of cyanobacteria was also reported on roofing tiles from USA (Cheng et al., 2011) and Serbia (Radeka et al., 2007a), but no further taxonomic classification was made (Table 2.4). Moreover, cyanobacteria were also detected on other roofing materials, such as fiber cement (Shirakawa et al., 2014) and asbestos–cement roofing material (Favero-Longo et al., 2009).

Algae on roofing tiles were represented by the phyla Chlorophyta and Xanthophyta. Chlorophyta are present with three main classes: Ulvophyceae (9%), Trebouxiophyceae (18%) and Chlorophyceae (73%) (Table 2.4). Microalgae were reported on ceramic roofing tiles from Portugal (Laiz et al., 2006), Spain (Ortega-Calvo et al., 1993; Laiz et al., 2006), Singapore (Chua et al., 1972) and India (Dan et al., 1981), with *Chlorella* being the most widespread genus. As mentioned before, *Chlorella* is commonly found on inorganic building materials, and was also identified on brick surfaces (Table 2.2) and on fiber cement roofing tiles (Shirakawa et al., 2014). Other genera present on roofing tiles *Trebouxia* and *Trentepohlia* occur in approximately 20% of all lichens and has rarely been found free-living (Laiz et al., 2006; Macedo et al., 2009), suggesting that they may be involved in a lichenisation process. Similarly, *Stichococcus* can also be found as a phycobiont of the lichen *Endocarpon pusillum* which was identified in roofing tiles in Serbia (Table 2.5).

The lower biodiversity of phototrophic microorganisms found on ceramic roofing tiles, in comparison with bricks, can be explained by the fact that the former are usually subjected to extreme weather conditions, such as high temperature amplitude, high radiation exposure and fast surface drainage, probably delaying the development of photoautotrophs (John, 1988).

Fungi were detected on ceramic roofing tiles from four different countries, USA (Cheng et al., 2011), Portugal and Spain (Laiz et al., 2006) and Germany (Görs et al., 2007) (Table 2.4). Laiz et al. (2006) using molecular biology techniques identified seven genera belonging to phyla Ascomycota (71%) and Basidiomycota (29%) on ceramic roofing tiles from Oporto (North Portugal) and Vigo (North Spain) (Table 2.4). Three of these genera were also found on bricks: *Fusarium*, *Penicillium* and *Rhodotorula* (Table 2.2). Titze and de Hoog (1990), reported the presence of the fungus *Capnobotryella renispora* on roof tiles, however no description of the substrate was provided. All the fungal genera reported on ceramic roofing tiles have also been identified on stone building materials (Gadd, 2007).

**Table 2.4** Microorganisms reported on roofing tiles together with the identification method and reference number (Table 2.1 Ref. No.).

| Bacteria[a] | Met[b] | Ref no. | Cyanobacteria[a] | Met[b] | Ref no. | Algae[a] | Met[b] | Ref no. | Fungi[a] | Met[b] | Ref no. |
|---|---|---|---|---|---|---|---|---|---|---|---|
| Actinobacteria | PLRQA | 38 | Calothrix sp. | C | 47 | Desmococcus olivaceus | C | 47 | Clathrospora sp. | CMB | 41 |
| Alcaligenes sp. | CMB | 41 | Chroococcus sp. | C | 36, 47 | Chlamydomonas sp. | C | 37 | Fusarium sp. | CMB | 41 |
| Arthrobacter sp. | CMB, MB | 41 | Chlorogloea sp. | C | 36, 47 | Chlorella sp. | C | 36, 47 | Lecythophora sp. | CMB | 41 |
| Azospirillum sp. | CMB | 41 | Gloeocapsa sp. | C | 36, 47 | Chlorella sp. | CMB | 41 | Penicillium sp. | CMB | 41 |
| Bacillus sp. | CMB, MB | 41 | Gloeothece sp. | C | 36, 47 | Chlorella vulgaris | C | 43a | Pleospora sp. | CMB | 41 |
| Blastococcus sp. | CMB | 41 | Microcystis sp. | C | 37, 47 | Chlorococcum sp. | C | 36, 47 | Rhodotorula sp. | CMB | 41 |
| Brevibacterium sp. | CMB | 41 | Myxosarcina sp. | C | 36, 47 | Eudorina sp. | C | 37 | Ustilago sp. | CMB | 41 |
| Brevundimonas sp. | CMB | 41 | Nostoc sp. | C | 36, 47 | Klebsormidium flaccidum | C | 43a | NI[a] Fungi | PLRQA | 38 |
| Cellulomonas sp. | CMB, MB | 41 | Oscillatoria sp. | C | 37, 47 | Stichococcus sp. | CMB | 41 | NI[a] Fungi | Erg | 40 |
| Deinococcus sp. | CMB | 41 | Phormidium autumnale | C | 43a | Trebouxia sp. | CMB | 41 | | | |
| Firmicutes | PLRQA | 38 | Scytonema sp. | C | 36, 47 | Trentepohlia sp. | C | 36, 47 | | | |
| Frigoribacterium sp. | CMB | 41 | Westiellopsis sp. | C | 36, 47 | Volvocales | C | 47 | | | |
| Kocuria sp. | CMB, MB | 41 | NI[a] Cyanobacteria | PLRQA | 38 | NI[a] Chlorophyta | Chla | 39, 40 | | | |
| Methylobacterium sp. | CMB | 41 | NI[a] Cyanobacteria | M | 35 | NI[a] Chlorophyta | M | 35 | | | |
| Microbacterium sp. | CMB, MB | 41 | | | | | | | | | |

**Table 2.4 (cont.).**

| Bacteria[a] | Met[b] | Ref no. | Cyanobacteria[a] | Met[b] | Ref no. | Algae[a] | Met[b] | Ref no. | Fungi[a] | Met[b] | Ref no. |
|---|---|---|---|---|---|---|---|---|---|---|---|
| Myxococcus sp. | CMB | 41 | | | | | | | | | |
| Paenibacillus sp. | CMB, MB | 41 | | | | | | | | | |
| Pseudomonas sp. | CMB, MB | 41 | | | | | | | | | |
| Sphingomonas sp. | CMB, MB | 41 | | | | | | | | | |
| Streptomyces sp. | CMB, MB | 41 | | | | | | | | | |
| NI[a] Bacteria | PLRQA | 38 | | | | | | | | | |

a NI: Non-identified

b Identification methods (Met): C – Culture methods; Chla – Chrolophyll a quantification; CMB – Molecular biology of cultured isolates; Erg. – Ergosterol quantification; M – Morphological; MB – Molecular biology; PLRQA – phospholipid and respiratory quinone analyses; SEM – Scanning electron microscopy.

Roofing tiles can also be colonized by lichens, bryophytes and vascular plants (Table 2.5). Fig. 2.5 shows roofing tiles colonized by a very mature community of organisms that include lichens, bryophytes and vascular plants.



**Fig. 2.5.** Biological colonization of roofing tiles from a house in Alentejo region (south of Portugal).

Several studies provide a comprehensive picture of the role of lichens in the deterioration of glazed and unglazed roofing tiles (Saxena et al., 2004; Kiurski et al., 2005; Ranogajec et al., 2005, 2008; Watanabe et al., 2006, 2009). Five different lichen species were identified in India, Serbia and Japan (Table 2.5). *Verrucaria nigrescens*, which is a crustose epilithic lichen, can commonly be found on stone work (Speranza et al., 2013). Radeka et al. (2007a) reported *V. nigrescens* proliferating on ceramic roofing tiles from Serbia, but it has also been reported in other roofing materials, namely cement-asbestos roofing tiles (Favero-Longo et al., 2009). *Peltula euplaca* and *P. patellata* were identified in clay roofing tiles in India, showing a prominent cortex, as a draught and photo protective layer against intensive solar irradiance (Saxena et al., 2004). *Peltula* and *Endocarpon* are xerophytic lichens and, therefore, they are well adapted to water limited conditions which might explain their proliferation on such harsh environments as roofing tiles (Saxena et al., 2004). *Lecidella asema* was also identified on a different substrate, glazed Japanese *Sekishu* roofing tiles (Table 2.5). All the lichen genera reported on Table 2.5 have been identified on other inorganic building materials (e.g. (Lisci et al., 2003; Carter and Viles, 2004)). Garcia-Rowe and Saiz-Jimenez (1991) found lichens and bryophytes in Salamanca and Toledo Cathedrals (Spain), but did not proceed to their identification (Table 2.5).

**Table 2.5.** Organisms reported on roofing tiles together with the identification method and reference number (Table 2.1 Ref. No.).

| Lichens[a] | Met[b] | Ref no. | Bryophytes[a] | Met[b] | Ref no. | Vascular Plants[a] | Met[b] | Ref no. |
|---|---|---|---|---|---|---|---|---|
| *Endocarpon pusillum* | M | 35 | NI[a] Bryophytes | M | 43, 45 | *Anthriscus caucalis* | M | 45 |
| *Lecidella asema* | M | 44, 44a | | | | *Antirrhinum majus* | M | 45 |
| *Peltula euplaca* | M | 46 | | | | *Antirrhinum siculum* | M | 42 |
| *Pertula patellata* | M | 46 | | | | *Bromus hordeaceus* | M | 43 |
| *Verrucaria nigrescens* | M | 33, 34, 35 | | | | *Bromus madritensis* | M | 43 |
| Verrucariales | M | 32 | | | | *Bromus sterilis* | M | 43 |
| NI[a] Lichen | M | 40, 43, 45 | | | | *Campanula erinus* | M | 45 |
| | | | | | | *Centranthus ruber* | M | 42 |
| | | | | | | *Lactuca virosa* | M | 45 |
| | | | | | | *Lolium rigidum* | M | 43 |
| | | | | | | *Piptatherum miliaceum* | M | 43 |
| | | | | | | *Rostraria cristata* | M | 43 |
| | | | | | | *Sedum sediforme* | M | 42, 45 |
| | | | | | | *Umbilicus rupestris* | M | 45 |
| | | | | | | *Valantia muralis* | M | 42 |
| | | | | | | *Hypochaeris achyrophorus* | M | 42 |
| | | | | | | *Micromeria graeca* | M | 42 |

[a] NI: Non-identified
[b] Identification methods (Met): M – Morphological

A total of 17 plant species were identified on ceramic roofing tiles from Spain and Italy (Table 2.5). Motti & Stinca (2011) identified vascular flora growing on different building materials including ceramic roofing tiles from the Royal Palace of Portici in Italy (Table 2.5). These authors concluded that most of the identified vascular flora was ubiquitous, with the exception of *Sedum sediforme*, which seemed to grow favourably on ceramic roofing tiles. The genera *Antirrhinum* and *Sedum* were found on roofing tiles from Spain (Garcia-Rowe and Saiz-Jimenez, 1991) and Italy (Motti and Stinca, 2011).

On ceramic roofing tiles the higher diversity of microorganisms was detected within the bacteria group (Table 2.4). However, these data were uniquely collected from two studies (Laiz et al., 2006; Cheng et al., 2011). A high diversity of vascular plants was also found on this ceramic material (Table 2.5). Nevertheless, many studies (7) are only dedicated to the presence of lichen on roofing tiles (Table 2.5), suggesting that these organisms have a high importance for authors studying ceramic roofing tiles colonization (Saxena et al., 2004; Kiurski et al., 2005; Watanabe et al., 2006, 2009; Radeka et al., 2007a, 2008).

### 2.2.3. Glazed wall tiles

Glazed ceramic wall tiles are made of a ceramic body covered by a vitreous coating. The glaze composition is highly variable, contrasting to the other ceramic building materials considered in this work (Table 2.1). Wall tiles present a vertical surface, as bricks do; however, their glassy coating presents a smooth and impermeable surface. These characteristics may not favour the development of biological colonization and thus only 8 studies devoted to the biodeterioration of

glazed tiles, from 5 different assets, were found in the literature. This can also be explained by the fact that the use of glazed wall tiles is not as widespread as bricks and roofing tiles.

The studies found on microbial colonization on glazed wall tiles refer only to microorganisms (bacteria, cyanobacteria, algae and fungi) (Table 2.6). Nonetheless, lichens and bryophytes can also be found as it can be seen in Fig. 2.6 on two outdoor glazed wall tiles from the Sintra National Palace (Portugal). Bacterial diversity reported on glazed wall tiles is represented by a total of 18 taxa, belonging to 4 phyla: Proteobacteria (50%), Actinobacteria (33%), Bacteroidetes (11%) and Chloroflexi (6%) (Table 2.6). Bacteria species were identified on tiles from two different Mediterranean cultural heritage assets, one in Italy (Giacomucci et al., 2011) and another in Portugal which is presented in Chapter 3.
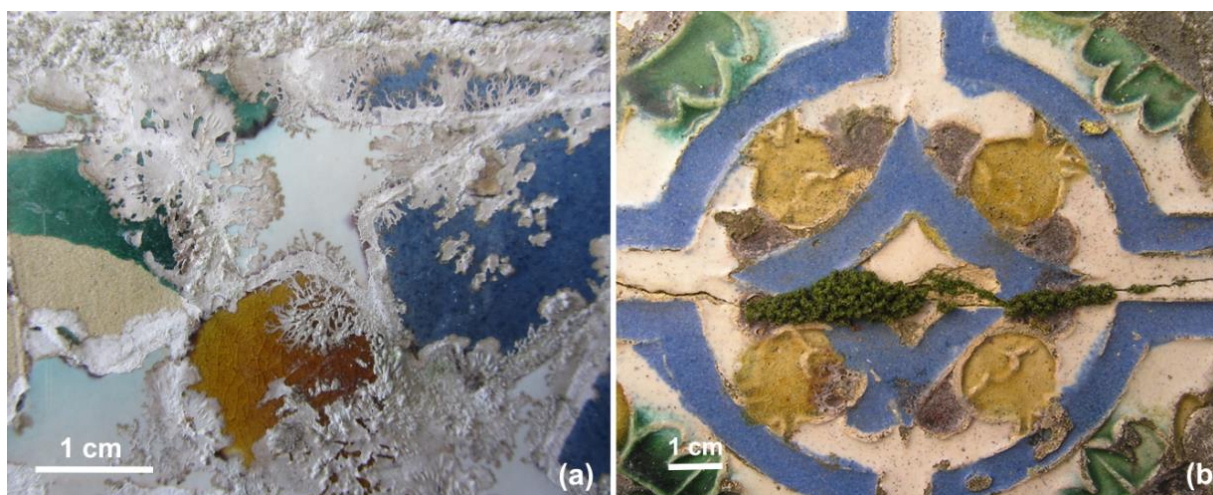


**Fig. 2.6** Biological colonization of glazed wall tiles from the Sintra National Palace (Portugal). (a) Colonization by lichens. (b) Colonization by bryophytes through a fracture of the ceramic body.

Photoautotrophic microorganisms (cyanobacteria and microalgae) were also identified on glazed wall tiles, comprising 35 taxa, 17 of them belonging to cyanobacteria and 18 to algae (Table 2.6). Cyanobacteria consists of four phyla, Chroococcales (35%), Nostocales (47%), Oscillatoriales (12%) and Pleurocapsales (6%) that were studied on 4 different assets from Brazil (Oliveira et al., 2001), Portugal (Coutinho et al., 2013) and Italy (Giacomucci et al., 2011). Members of the genera *Calothrix*, *Chroococcidiopsis*, *Chroococcus*, *Cyanosarcina*, *Gloeocapsa*, *Gloeothece*, *Lyngbya*, *Nostoc*, *Plectonema*, *Scytonema* and *Tolypothrix* were also identified on bricks (Table 2.2 and 2.6). Most of these cyanobacteria were identified by Coutinho et al. 2013 (described in Chapter 3) who found an abundant biodiversity of phototrophic microorganisms on the glazed wall tiles from Pena National Palace, in Sintra (Portugal). These authors also studied the biodeterioration occurring on those tiles. From Table 2.6 we can notice that a total of 18 distinct taxa of microalgae have been reported on glazed wall tiles; of these, 14 belong to the phylum Chlorophyta, 3 to Xanthophyta and 1 to Bacillariophyta (Table 2.6). Three classes represented the Chlorophyta phylum: Ulvophyceae (21%), Trebouxiophyceae (36%) and Chlorophyceae (43%). *Chlorella* and *Navicula* were the only

two genera identified on glazed tiles from two different assets (Table 2.6). Some algae genera were also described on bricks, namely *Apatococcus, Bracteacoccus, Chlorella, Klebsormidium, Navicula* and *Trentepohlia* (Table 2.2 and Table 2.6). The highest biodiversity of microalgae was observed on the glazed wall tiles from Pena National Palace, in Sintra (Portugal) described in detail in Chapter 3 (Coutinho et al., 2013).

A total of 31 taxa of fungi were identified on three different assets from Portugal (Coutinho et al., 2011, 2013), Brazil (Pedi et al., 2009) and Italy (Giacomucci et al., 2011)(Table 2.6). Ascomycota (90%) was the dominant phylum, while Basiodiomycota (10%) represented only a minor part of the fungi. Some of the listed genera were also identified on bricks, such as *Alternaria*, *Aspergillus*, *Fusarium*, *Penicillium* and *Phoma* (Table 2.2 and Table 2.6). The genera *Fusarium* and *Penicillium* were identified on more than one asset, specifically on glazed tiles from Portugal and Brazil (Table 2.6).

**Table 2.6** Microorganisms reported on glazed wall tiles together with the identification method reference number (Table 2.1 Ref. No.).

| Bacteria[a] | Met[b] | Ref no. | Cyanobacteria[a] | Met[b] | Ref no. | Algae[a] | Met[b] | Ref no. | Fungi[a] | Met[b] | Ref no. |
|---|---|---|---|---|---|---|---|---|---|---|---|
| Anaerolinea thermophila | MB | 49a | Aphanocapsa parietina | C | 49a | Apatococcus lobatus | C | 49a | Alternaria sp. | C, MB | 49, 49a |
| Aurantimonas sp. | MB | 49a | Calothrix sp. | C | 49a | Bracteacoccus minutus | C | 49a | Aspergillus flavus | C | 51 |
| Beijerinckia fluminensis | MB | 49a | Cyanosarcina sp. | C | 50,50a, 52 | Chlorella ellipsoidea | MB | 49a | Aspergillus sydowii | C | 51 |
| Methylibium sp. | MB | 48 | Chroococcidiopsis sp. | C, MB | 49a | Chlorella saccharophilum | MB | 48, 49a | Aspergillus versicolor | C | 51 |
| Microcella putealis | MB | 48 | Chroococcus sp. | C | 50, 50a, 52 | Desmococcus olivaceus | C | 49a | Arthrinium sp. | C | 49 |
| Modestobacter sp. | MB | 49a | Gloeothece sp. | C | 49a | Diaphragma radiosum | C | 49a | Aureobasidium pullulans | MB | 48 |
| Oxalicibacterium faecigallinarum | MB | 48 | Gloeocapsa sp. | C | 49a | Dictyochloris pulchra | C | 49a | Capnobotryella sp. | MB | 49a |
| Pseudonocardiaceae | MB | 48 | Lyngbya sp. | C | 52 | Klebsormidium flaccidum var. crissum | C | 49a | Capronia sp. | MB | 49a |
| Rhodovastum atsumiense | MB | 49a | Nostoc sp. | C, MB | 49a | Klebsormidium flaccidum var. nitens | C | 49a | Chrysosporium sp. | C | 49a |
| Sphingomonas sp. | MB | 49a | Nostoc paludosum | C | 49a | Klebsormidium pseudostichococcus | C | 49a | Cladosporium sp. | C | 49a |
| Yonghaparkia alkaliphila | MB | 48 | Nostoc punctiforme | C | 49a | Navicula sp. | C | 49a | Devriesia imbrexigena | C | 50, 50a, 52 |
| Uncultured Actinobacteria | MB | 48 | Nostoc commune | C | 49a | Oocystis solitaria | C | 49a | Epicoccum sp. | C | 49 |
| Uncultured Alphaproteobacteria | MB | 48 | Plectonema edaphicum | C | 49a | Stichococcus bacillaris | C | 49a | Fellomyces sichuanensis | MB | 49a |
| Uncultured Bacteroidetes | MB | 48 | Scytonema sp. | C | 50, 50a, 52 | Trentepohlia sp. | C,MB | 49a | Fusarium sp. | C | 49 |

**Table 2.6** (Cont.)

| Bacteria[a] | Met[b] | Ref no. | Cyanobacteria[a] | Met[b] | Ref no. | Algae[a] | Met[b] | Ref no. | Fungi[a] | Met[b] | Ref no. |
|---|---|---|---|---|---|---|---|---|---|---|---|
| Uncultured Betaproteobacteria | MB | 48 | Synechococcus lividus | C | 48 | Trentepohlia monilia | C | 48 | Fusarium solani | C | 51 |
| Uncutured Flexibacteraceae | MB | 48 | Tolypothrix sp. | MB | 49a | Ulothrix sp. | MB | 49a | Geotrichum candidum | C | 51 |
| Uncultured Methylibium sp. | MB | 48 | Tolypothrix distorta | C | 49a | Rosenvingiella radicans | C | 49a | Gliocladium sp. | C | 49 |
| Uncultured Microcella sp. | MB | 48 | | | | Trebouxia sp. | C | 49a | Hortaea thailandica | MB | 49a |
| | | | | | | | | | Kockovaella schimae | MB | 49a |
| | | | | | | | | | Monodictys levis | C | 51 |
| | | | | | | | | | Neofusicoccum sp. | C | 49 |
| | | | | | | | | | Penicillium sp. | C | 49 |
| | | | | | | | | | Penicillium citrinum | C | 51 |
| | | | | | | | | | Penicillium fellutanum | C | 51 |
| | | | | | | | | | Penicillium waksmanii | C | 51 |
| | | | | | | | | | Pestalotiopsis sp. | C | 49 |
| | | | | | | | | | Phoma herbarum | MB | 48 |
| | | | | | | | | | Saccharata sp. | MB | 49a |
| | | | | | | | | | Sporobolomyces coprosmae | MB | 48 |
| | | | | | | | | | Stigmina sp. | MB | 49a |
| | | | | | | | | | Tricoderma sp. | C | 49 |
| | | | | | | | | | NI Fungi | SEM | 50a |
| | | | | | | | | | NI Yeasts | C | 49 |

a NI: Non-identified.

b Identification methods (Met): C – Culture methods; M – Morphological; MB – Molecular biology; SEM – Scanning electron microscopy

In resume, photoautotrophic microorganisms (cyanobacteria and algae) are widespread on glazed tiles, being many genera coincident with those identified on bricks and roofing tiles (Table 2.2, Table 2.4 and Table 2.6). The highest number of fungal taxa was identified on glazed tiles.

### 2.2.4.  Comparison of all substrates ceramic typologies

The dominant bacterial phylum present on all ceramic typologies and presenting a considerable proportion of the total number of bacterial taxa on all substrates was Proteobacterium. Additionally, members of Actinobacterium were found on all substrates being the second most represented phylum on roofing and glazed wall tiles, and the third on bricks. Firmicutes were the second most represented on the former mentioned typology (Bricks). On the basis of the currently available data, bacteria presented a high biodiversity among the analysed ceramic typologies. No genera were common to the three ceramic typologies and only four were reported on more than one typology: *Bacillus*, *Deinococcus*, *Sphingomonas* and *Streptomyces*.

The majority of cyanobacteria identified on bricks and roofing tiles belonged to Chroococcales, followed by Nostocales and Oscillatoriales orders. Glazed wall tiles were an exception, with Nostocales being the most represented order, followed by Chroococcales and Oscillatoriales. Only four genera were identified in all the studied ceramic typologies: *Gloeocapsa*, *Gloeothece*, *Nostoc* and *Scytonema*. These cyanobacterial genera have been identified on stone monuments and many have a gelatinous sheath that acts as a water reservoir enabling them to grow in water-limited conditions (Macedo et al., 2009).

Concerning algae reported on the three ceramic substrates, most retrieved algae belonged to Chlorophyta, represented by Chlorophyceae, Ulvophyceae and Trebouxiophyceae classes. The Chlorophyta which were common to all ceramic typologies were *Chlorella, Desmococcus*, *Stichococcus*, *Trebouxia* and *Trentepohlia*; all were reported on stone monuments (John, 1988; Macedo et al., 2009). Notable is the fact that roofing tiles showed the lowest diversity of algae for all ceramic typologies and no Bacillariophyta was identified on this substrate. This fact may rely on the weathering conditions to which roofing tiles are exposed, that may constrain the development of such organisms on this ceramic typology.

The fungal diversity of all ceramic typologies had Ascomycota as the dominant phylum. *Fusarium* and *Penicillium* were the only genera common to the three ceramic building material typologies studied in this work. Based on the fact that they are widespread airborne fungi with a large capacity to survive in different environments, their presence in all substrates is not surprising (Suihko et al., 2007).

Lichens, bryophytes and vascular plants taxa identified on bricks and roofing tiles were not coincident. However, the identification of macroorganisms compared with studies presenting identification of microorganisms was less common.

In conclusion, the vast majority of the listed ceramic dwelling organisms had previously been reported on other cultural heritage assets, such as stone or glass, suggesting that biological colonization can occur on a substrate independently of their nature (Sáiz-Jiménez and Laiz, 2000; Carmona et al., 2006; Macedo et al., 2009).

## 2.3. Organisms identification and quantification methods used on architectural ceramic materials

Methods used for the micro- and macroorganism's identification and characterization on architectural ceramic materials were diverse (Tables 2.2 to 2.6). Identification of organisms can be achieved by different methods, from simple visual examination to sophisticated DNA-based analysis. Some authors reported the occurrence of organisms (phototrophic organisms, lichen, bryophytes and vascular plants) by morphological traits obtained only by visual examination (Garcia-Rowe and Saiz-Jimenez, 1991; Videla, 2002; Herrera and Videla, 2004; Radeka et al., 2007a). Therefore, no further taxonomic identification was possible for these cases being listed as Non Identified organisms (NI) (Tables 2.2 to 2.6). Morphological features can also be observed by scanning electron microscopy (SEM), which was used by several researchers to detect the presence of microorganisms on ceramic substrates (Palmer and Hirsch, 1991; Kiurski et al., 2005; Lopez-Arce and Garcia-Guinea, 2005; Ranogajec et al., 2005; Radeka et al., 2007a, 2007b). This technique is useful for the identification of microbial colonization profiles and observation of microbe-mineral interactions, which are important features for understanding the biodeterioration dynamics. Yet, in terms of taxonomic classification SEM is considered a limited technique (Heikkilä et al., 1988).

The taxonomic identification of lichens, bryophytes and vascular plants can be done by the recognition of phenotypic characters by direct visual inspection or under stereomicroscopy by following dichotomous keys (e.g. Smith et al., 1992; Clauzade and Roux, 1985; Nimis et al., 1987; Nimis, 1993; Wirth et al., 2004). All the taxonomically classified lichens, bryophytes and vascular plants listed in Tables 2.3 and 2.5 were identified by morphological analysis following these procedures.

Regarding microorganisms, the identification methods are usually more complex, being divided into culture and culture-independent methods. Common microorganism identification includes culture methods which rely on isolation of microorganisms in culture media and subsequent identification of isolated strains under optical microscope (e.g. Gómez-Alarcón and Cilleros, 1995; Oliveira et al., 2001; Jones, 2002 ) (Table 2.2 and Table 2.6). The limitations of these techniques are well known, particularly regarding bacterial communities, due to the low percentage of cultivable bacteria (ca.1%) (Ward et al., 1990). Few studies present in this work used solely culture based methods for the identification of bacteria (Gómez-Alarcón and Cilleros, 1995; Jones, 2002).

In contrast, culture methods and morphological identification of cyanobacteria and algae, are well established methods and can allow taxonomic classification until the species level. In fact, most phototrophic microorganisms found on ceramic substrates were identified by culture techniques, as can be seen in Table 2.2, Table 2.4 and Table 2.6 (e.g. Gómez-Alarcón and Cilleros, 1995; Oliveira et al., 2001; Pedi et al., 2009; Nowicka-Krawczyk et al., 2014) . Also, most of the fungal taxa reported on bricks and glazed wall tiles were identified by culture dependent methods (e.g. Palmer and Hirsch, 1991; Gómez-Alarcón and Cilleros, 1995; Pedi et al., 2009;

Coutinho et al., 2013). In the recent decades taxonomic identification of fungi has become very controversial; not only culture techniques have been questioned due to selectivity caused by the growth media during the isolation, but also phenotypic classification and correspondent genetic markers, which are considered to be not reliable (Bass and Richards, 2011). Still, the isolation of microbial strains by culturing is an important step for the identification of new species, physiology studies and it also allows the use of microorganisms in laboratory assays.

Molecular biology techniques are today the most widely used methods for the identification of microorganisms in several fields of science including cultural heritage (Otlewska et al., 2014a), consuming less time, requiring lower amount of sample material and identifying both viable and non-viable organisms. However, inherent limitations include high assay costs and a level of technical expertise. Moreover, the fact that DNA-based molecular biology techniques do not allow the separation between the viable (possible biodeteriogens) from non-viable organisms is a major drawback of this technique. Yet, RNA-based molecular techniques allow also the identification of metabolically active non-culturable microorganisms (Portillo et al., 2008).

The phylogenetic characterization of the bacterial communities present on bricks, roofing tiles and wall tiles was mostly based on DNA-based analysis, whether from isolated strains (Laiz et al., 2006; Qi-Wang et al., 2011) or directly on environmental samples (Giacomucci et al., 2011; Qi-Wang et al., 2011; Coutinho et al., 2013; Otlewska et al., 2014b) (Table 2.2, Table 2.4 and Table 2.6). Only few photoautotrophic microorganisms were identified on roofing and glazed wall tiles by molecular methods (Laiz et al., 2006; Giacomucci et al., 2011; Coutinho et al., 2013). Some authors report that the presence of sheaths in photoautotrophic communities or other protective structures can affect the efficiency of DNA extraction (Garcia-Pichel et al., 2001). In opposition to the other ceramic typologies, the taxonomically classified fungi reported on roofing tiles (Table 2.4) were all identified by molecular methods (Laiz et al., 2006) . On glazed wall tiles (Table 2.6), most of the identified fungi were obtained by culture methods, although molecular methods were also used (Giacomucci et al., 2011; Coutinho et al., 2013). Nevertheless, it is noteworthy that many studies have referred to the bias introduced by molecular biology due to limitations of the DNA databases which are still far from complete (McNamara and Mitchell, 2005; del Campo et al., 2014) .

The results of microbial identification obtained by using culturing and molecular methods simultaneously usually provide a more complete information (McNamara and Mitchell, 2005; Qi-Wang et al., 2011; Al-Awadhi et al., 2013; Coutinho et al., 2013). Two studies regarding the identification of the microbial communities on architectural ceramic materials exemplify the difference in results obtained by using both methods (Qi-Wang et al., 2011; Coutinho et al., 2013). Qi-Wang et al. (2011) used an approach comprising molecular and culture-dependent methods in the identification of bacterial communities on bricks from the Nanjing Ming city wall (China) obtaining different results from natural samples or isolated samples (Table 2.2). Similarly, Coutinho et al. (2011,2013) (data presented in Chapter 3) also used a polyphasic approach for the identification of phototrophic and fungal community colonizing glazed wall tiles from Pena National Palace (Portugal) (Table 2.6). Culture techniques allowed the identification of 11 genera of

filamentous fungi and one non-identified yeast (Coutinho et al., 2011), whereas molecular methods allowed the identification of fungi that were not detected by culture techniques (Coutinho et al., 2013, see Chapter 3).

The detection and quantification of biomarkers is another culture-independent identification method, although it is less used in the analysed literature (Table 2.2, 2.4 and 2.6). Chlorophyll *a* and ergosterol analysis allow the detection and biomass quantification of photoautotrophs and fungi, respectively. Chlorophyll *a* was used in all ceramic typologies for the detection and quantification of phototrophic microorganisms (Palmer and Hirsch, 1991; Görs et al., 2007; Raimondi et al., 2009; Gladis and Schumann, 2011b). Ergosterol was only used in the identification of fungi on roofing tiles by Görs et al. (2007) in order to assess the quantification of fungi on several building materials. Another method used for the characterization of microbial communities on roofing materials was phospholipid and respiratory quinone analyses. This allows to estimate biomass and community composition facilitating the differentiation of certain groups of microorganisms (Cheng et al., 2011). All described methods make possible to calculate the amount of organisms present on the substrate, and thus providing information regarding its deteriogenic action and tendency to be colonized (Miller et al., 2012). However, only high taxonomical ranks can be achieved by these methods.

In conclusion, the taxonomic level obtained by the different approaches varies according to the method and organism under study. In addition, the fact that microbiology has drastically changed in the last few decades, difficults the comparison of the biodiversity found on these substrates. So, in order to have a better knowledge on the microbial community colonizing ceramic materials, different identification methods should be used together (e.g. culture, molecular biology and methods based on living biological markers).

## 2.4. Biodeterioration of architectural ceramic materials

Living organisms are capable of interacting with materials causing changes in their properties. In the case of ceramic cultural heritage assets, biodeterioration can be aesthetical, physical and chemical, and most of the times, these three deterioration forms intertwined. The production of organic pigments and development of colored biofilms on surfaces can change the visual appearance of the materials (Alakomi et al., 2004; Gorbushina, 2007; Nowicka-Krawczyk et al., 2014). The production of colored substances is common to many different organisms (e.g. Urzì and Realini, 1998; Alakomi et al., 2004; Gorbushina, 2007). In fact, most of the ceramic colonizing organisms reported in Tables 2.2 to 2.6 produce colored substances and consequently form colored biofilms. As mentioned before, the use of ceramic materials in architecture is also connected with aesthetical purposes (e.g. color, glaze and texture). Aesthetical biodeterioration is clearly the first and most evident impact affecting the ceramic substrate. In the literature, aesthetical biodeterioration is reported (Kiurski et al., 2005; Ranogajec et al., 2005; Watanabe et al., 2006; Radeka et al., 2007a; Mandal and Rath, 2013; Nowicka-Krawczyk et al., 2014). Consequently, this form of deterioration has a very negative impact, particularly in cultural heritage

assets. An example of this was found on glazed wall tiles by Coutinho et al. (2013) in which a green and black patina composed of bacteria, fungi and photoautotrophic microorganisms was growing on historic tiles from the Pena National Palace, in Sintra (Portugal), which compromised its aesthetic appreciation (Fig. 2.7). This figure clearly shows the contrast between a cleaned glazed wall tile, where the biofilm has been removed, and a tile covered by the biofilm (Fig. 2.7). The formation of stains on wall tiles and bricks due to biological activity were also reported by several other authors (Oliveira et al., 2001; Pedi et al., 2009; Silva et al., 2011; Mandal and Rath, 2013).



**Fig. 2.7** Glazed wall tiles from Pena National Palace in Sintra (Portugal) showing a tile after the biofilm removal (on the left) and a tile covered by the green/black biofilm (on the right).

Studies regarding the colonization of ceramic roofing tiles by lichens also emphasized the aesthetic damage caused by the color alteration of red clay bricks into dark surfaces due to the proliferation of the black colored lichen *Verrucaria nigrescens* (Kiurski et al., 2005; Radeka et al., 2007a). Although the gathered literature showed a low biodiversity (Table 2.4 and Table 2.5), the observation of buildings and monuments with discoloration of the ceramic roofing tiles seems to indicate that the colonization of these substrates is a very common phenomenon. Endolithic growth of biofilms has been reported on glazed ceramic building materials, both wall tiles and bricks, also causing visual changes (Palmer and Hirsch, 1991; Oliveira et al., 2001; Pedi et al., 2009; Silva et al., 2011, 2014).

Ceramic surface features, such as roughness, superficial flaws and porosity, make ceramic materials prone to staining (Hupa et al., 2005). Many microbial organic pigments firmly bound to inorganic substrates causing color changes (Roeselers et al., 2006). Mandal and Rath (2013) analysed a black photosynthetic biofilm developing over the carved terracotta bricks, in India (Table 2.1). They suggested that some of the identified cyanobacteria genera (Table 2.2), such as *Lyngbya*, *Gloeocapsa* and *Scytonema*, having thick sheaths with intense colors, could be

responsible for the staining on the ceramic body. In addition, bioprecipitation of metabolic products might cause staining of the substrate. López-Arce et al. (2003) studying the decay of unburied bricks from the archaeological excavation in the Alcázar of Toledo (Spain), reported the deposition of manganese micro-nodules which were probably mediated by cyanobacteria or other microorganisms present in the biofilms developing on the ceramic surface.

Besides the aesthetical function, building materials also have other functional properties, associated to their role in the building, such as structural, thermal and hygric isolation and solar reflectance. These characteristics might be changed due to the development of biofilms and accumulation of microbial biomass on roofs being therefore associated with the loss of functional properties, such as. reflectance, drainage and insulation (Cheng et al., 2011; Shirakawa et al., 2014). The development of biofilms composed of phototrophs and fungi were associated with this type of changes. Lichens have also been considered biodeteriogens of stone substrates(Carter and Viles, 2004). For instance, Carter and Viles (2004) reported that *Verrucaria nigrescens* caused a temperature increase of the underlying substrate where it was hosted. Therefore, this lichen that was reported on ceramic substrates, particularly on roofing tile could cause high thermal gradient cycles promoting the breakdown of the substrate.

Physical deterioration processes have been extensively studied on ceramic building materials (e.g. Larbi, 2004; Kopar and Ducman, 2007; Bakar et al., 2009; Figueiredo et al., 2009; Sánchez de Rojas et al., 2011; Silva et al., 2014). Physical and biophysical damage can be described as the result of the loosening of intergranular bonds caused by volume fluctuations (expansion and shrinkage) that weaken materials (Kühnel, 2004). Microbial volume fluctuations can have a strong effect on the physical state of a ceramic building material. These fluctuations can be due to volume changes of microbial cells during growth or penetration of biological structures into the ceramic material, such as fungal or lichen hyphae (e.g. (Kiurski et al., 2005; Radeka et al., 2008) ). Laboratory assays to evaluate the biophysical deterioration by fungi (*Aspergillus niger* and *Cladosporium* sp.) on ceramic roofing tiles have been performed by some authors (Radeka et al., 2007b; Ranogajec et al., 2008). Fungal colonization was influenced by the pore space structure (e.g. porosity, permeability, capillarity kinetics) and by surface roughness (Radeka et al., 2007a; Ranogajec et al., 2008). The inoculation of microorganisms induced slight porosity alterations, specifically in the size of small pores (<1 um) (Radeka et al., 2007a; Ranogajec et al., 2008).

Extracellular polymeric substances (EPS) may induce volume fluctuations inside the ceramic materials due to their high capacity for water uptake and drainage (Palmer and Hirsch, 1991; Mandal and Rath, 2013). Therefore, biofilms allow the retention of large amounts of water into its structure, protecting the cells from desiccation (Prakash et al., 2003; Gorbushina, 2007; Cuzman et al., 2011) . Diurnal environmental hygric variations lead to extreme volume fluctuations of EPS which exert strong forces on the substrate causing its decay. Some of the cyanobacteria genera compiled in this review (Table 2.2, Table 2.4 and Table 2.6) (e.g. *Gloeocapsa* sp., *Gloeothece* sp., *Chroococcus* sp., *Plectonema* sp. and *Scytonema* sp.) have a gelatinous sheath that acts as a reservoir of water, allowing them to survive even when dry conditions prevail (Ortega-Calvo et al., 1991). When these microorganisms are located in pores or fractures, their sheaths

may undergo dimensional changes, according to the more or less dry climate, and these changes will cause damage on architectural ceramic elements. For instance, Palmer and Hirsch (1991) and Mandal and Rath (2013) demonstrated that the presence of photosynthetic biofilms was related to the biophysical decay observed in glazed bricks in Germany and terracotta bricks in India, respectively (Table 2.2). Indeed in glazed ceramics, which combine two materials with different properties, the ceramic-glaze interface is a critical feature (Kopar and Ducman, 2007; Mimoso et al., 2011). The biological colonization of the ceramic-glaze interface can be devastating. Palmer and Hirsch ( 1991) observed irretrievable losses on glazed bricks from the Schleswig Cathedral (Germany) due to the development of a biofilm underneath the glaze which caused the spalling of the glaze (Table 2.2). Likewise, lichens have been associated with damage in the pore structure of ceramic roofing tiles caused by hyphen penetration into pores, fissures and cracks (Kiurski et al., 2005; Ranogajec et al., 2005; Radeka et al., 2007a, 2007b).

The presence of biofilms can also hasten ceramic physical deterioration by synergetic effect with abiotic physical factors, such as freeze-thaw cycles resulting in fracturing or accentuate changes in moisture circulation due to high temperature fluctuation (Palmer and Hirsch, 1991; Mandal and Rath, 2013). The synergetic effect caused by the colonization of the salt damaged ceramic tiles (Viúva Lamego Factory) can be seen in Fig. 2.8. The colonization of the ceramic interface by a lichen and black biofilms causes the black staining of the interface and promotes the glaze detachment (Fig. 2.8). In summary, most of the microorganisms reported on Tables 2.2 to 2.6, like cyanobacteria, algae, fungi, lichens, bryophytes and vascular plants are able to cause physical decay of ceramic materials.
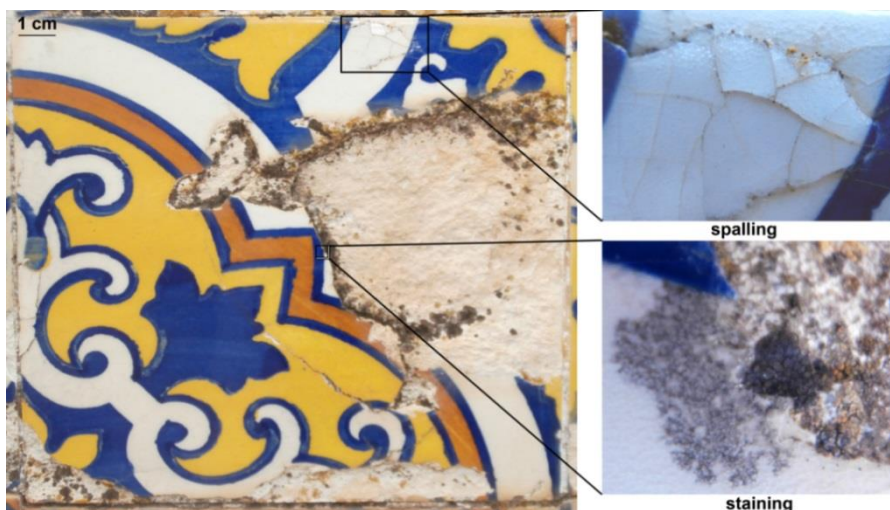


**Fig. 2.8** Biological colonization of glazed wall tiles from private house in the Alentejo district (Portugal) by lichens and a black biofilm with details in macrophotography of the spalling and staining of the glaze.

The direct action of metabolic products exuded by organisms on inorganic substrates is the main cause of chemical biodeterioration. This biodeterioration phenomenon can promote the increase of capillary porosity of the ceramic body and the formation of efflorescences, which may weaken the ceramic material and enhance the susceptibility to other types of deterioration (Ranogajec et al., 1997; Larbi, 2004). The biochemical deterioration of the ceramic body by lichens and fungi has been reported by several authors (Kiurski et al., 2005; Ranogajec et al., 2005, 2008; Radeka et al., 2007b). Some organic acids excreted by microorganisms (e.g. fungi and lichens) act as chelating agents, which sequester metallic cations from the substrate, such as $Ca^{2+}$, $Mg^{2+}$, $Fe^{3+}$ and $Mn^{2+,3+}$, precipitating in the form of salts (Albertano et al., 2000; Fernandes, 2006; Gorbushina, 2007). For instance, lichens and fungi produce oxalic acid that can chelate calcium and form calcium oxalates. The deposition of this bioprecipitated mineral into the ceramic matrix results in mechanical and chemical damage by changes in porosity and formation of soluble salts leading to salt crystallization (Albertano et al., 2000; Gorbushina, 2007; Suihko et al., 2007). In fact, the role of oxalates in the biodeterioration processes has recently been reviewed by Gadd et al. (2014).

The lixiviation of ceramic compounds, enhanced by the presence of bacteria, has been identified on bricks (Qi-Wang et al., 2011). In this study, Qi-Wang et al. (2011) performed laboratory assays on the ability of isolated bacterial strains to enhance silica solubility. More than 20 taxa belonging to Firmicutes and Proteobacteria were proven to enhance ceramic dissolution. Actually, Proteobacterium was one of the most represented bacterial phylum in all ceramic typologies (Table 2.2, Table 2.4 and Table 2.6).

It is also well-known that halophilic bacteria, which were identified on ceramic substrates (Table 2.2), are able to bioprecipitate minerals (Sáiz-Jiménez and Laiz, 2000; Otlewska et al., 2014b). Otlweska et al. (2014b) identified halophilic genera on the deteriorated floor bricks from the former Auschwitz II–Birkenau concentration. Salt crystallization, as previously mentioned seriously damage porous materials.

To our knowledge few studies were performed to investigate the biochemical action of microorganism on glazed substrates and none presented the identification of the microorganism involved in the deterioration process (Tennent et al., 1996; Tennent, 2013) . Nevertheless, their ability to interact with compounds present in glazes has been reported (Jongmans et al., 1997; Hoffland et al., 2003; Brehm et al., 2005; Gadd, 2010). Brehm et al. (2005) reported that biofilm growth significantly increased the breakdown of different silica samples (quartz sand, crystalline quartz and commercial glass). Many mineral requirements of microorganisms are present in the ceramic and glaze compositions. For instance, the colorants of the glaze usually composed of transition metal oxides, such as Mn, Fe, Co, Cu or Ni oxides, are elements that integrate the biogeochemical cycles of some organisms (Gadd, 2010). They can use the substrate in redox reactions, as a donor or acceptor of electrons, causing the oxidation or reduction of an element, such as iron (Uroz et al., 2009). Lead is a major component in historic glazes being used as a fluxing agent. As far as we know, the only reported chemical biodeterioration of glazes is the blackening caused by sulphur reducing bacteria on buried archaeological ceramics with lead-based

glazes. Their metabolic processes cause the formation of black crystalline lead sulphide particles within the glaze (Tennent et al., 1996; Tennent, 2013). The current research has not been able to draw strong conclusions regarding the influence of microorganisms on the chemical biodeterioration of glazes. It is not clear if their main action is simply based on their growth on inorganic substrates by changing the electrochemical equilibrium leading to corrosion, such as in the biocorrosion of metals (Sylvestre et al., 2009), or whether they are dynamically extracting elements to satisfy their mineral requirements, such as on stone (Jongmans et al., 1997; Chen et al., 2000).

## 2.5.    Bioreceptivity of architectural ceramic materials

In the case of ceramic materials the relation between intrinsic properties and bioreceptivity has been appraised by different researchers through laboratory-based bioreceptivity experiments (e.g. Guillitte and Dreesen, 1995; Gazulla et al., 2011; Gladis and Schumann, 2011a; Portillo et al., 2011; Giovannacci et al., 2013; D'Orazio et al., 2014; Radeka et al., 2014). Ceramic bioreceptivity, similar to what occurs on stone, is mainly associated with ceramic physical characteristics, such as porosity and surface roughness (Tiano et al., 1995; Gazulla et al., 2011; Gladis and Schumann, 2011a; Portillo et al., 2011; D'Orazio et al., 2014). Porosity reflects the absorption and movement of water within the pore structure being directly related to water availability for microorganism. For instance, bioreceptivity of stone to photoautrophic colonization was higher on stones with higher values of open porosity and water absorption by capillarity rise (Miller et al., 2010). In fact, capillary rise is reported to be the most common mechanism whereby water penetrates building materials (Karoglou et al., 2005). Adhesion and settlement of organisms are also crucial aspects for biological colonization, therefore the higher number of anchoring sites and micro-refuges which are expressed by means of the surface roughness enhance the bioreceptivity of a material (Koestler et al., 1997; Scardino et al., 2008). For this reason, the smooth and impermeable surface of glazes leads to a higher resistance to microbial colonization (Gazulla et al., 2011; Gladis and Schumann, 2011a; Portillo et al., 2011). Similar to other inorganic materials a weak relationship between chemical composition and bioreceptivity has been established (Guillitte and Dreesen, 1995; Gazulla et al., 2011). However, the pH was been pointed out as a factor causing inhibition of microbial growth on ceramic substrates. Tiano et al. (1995) reported that high pH of a powdered brick suspension was the main factor causing the growth inhibition of photosynthetic microorganisms during the incubation experiment. The corrosion of glass and ceramics occurs through the lixiviation of alkaline oxides into the solution which can cause the rise of the pH in this case the corrosion process is related to the chemical composition of the substrate. Although the materials intrinsic properties might influence their bioreceptivity, it is known that outside laboratorial conditions biological colonization is strongly dependent on environmental conditions, with even the least bioreceptive surfaces being readily colonized.

## 2.6. Conclusions

Regarding the overall biodiversity of ceramic materials, a total of 70 bacterial taxa, 97 cyanobacteria, 65 algae, 49 fungi, 9 lichens, 4 mosses and 18 vascular plants were identified as ceramic-dwelling organisms. Bacteria, cyanobacteria, algae and fungi are reported as colonizers on all the typologies studied (bricks, roofing tiles and glazed wall tiles). Lichens, bryophytes and vascular plants were only reported on bricks and roofing tiles. However, the authors showed that bryophytes and lichens can also occur on glazed wall tiles. The listed organisms cannot be analysed in terms of abundance or biodiversity patterns since many studies are directed by research aims, privileging the identification of a group of organisms. For instance, some studies selectively identified bacteria, phototrophs, fungi and lichens. In addition, the number of case studies found for each ceramic typology is variable (Table 2.1). Therefore, at the current state of knowledge, no statistical analysis was performed with this data and it was not possible to establish any relation between a given organism and a certain ceramic typology. Nevertheless, in this article these preliminary data were organized in a simple and useful way for further research.

The identification of microorganisms was mainly performed by culturing methods, except for bacteria which were mostly identified by DNA-based analysis. Lichens, bryophytes and vascular plants were identified by phenotypic identification. Biodeterioration of ceramic building materials causes cultural and economic problems, since it seriously affects the properties, functionality, durability and resistance of the materials. Aesthetical biodeterioration is also a common factor to the analysed studies. Several studies showed that physical and/or chemical biodeterioration of unglazed ceramics can occur, which is strongly dependent on the porosity and pore structure of the substrate. On glazed ceramics the occurrence of biophysical damage, due to endo- and/or cryptolithic colonization, can provoke the spalling of the glaze.

Biochemical deterioration of unglazed ceramics has been identified as being connected to calcium and silica mobilization, and is associated with fungi and bacteria. The analysed studies focusing on glazed ceramics did not demonstrate any influence of the organisms in the biocorrosion. Thus, the extent of damage that biological agents can cause on this substrate is still unknown.

Bioreceptivity experiments show that porosity and surface roughness are the main factors that influence primary bioreceptivity of ceramic building materials. For this reason, unglazed ceramics present a much higher bioreceptivity compared to glazed ceramic substrates. However, the effect of chemical composition and surface pH on bioreceptivity has been little investigated.

Biodiversity of bricks, roofing and glazed tiles was found in few studies compared to biodiversity of other substrates, like stone. In addition, the reviewed studies were performed in different geographical location, with different climatic conditions influencing biodiversity. At the current state of knowledge it is still too early to draw conclusions on the correlation of organism or assemblages to a typology of ceramic architectural material or a substrate.

The presented overview of worldwide literature on biodiversity, biodeterioration and bioreceptivity of architectural ceramic materials showed that most of the gathered studies were on bricks (almost half of the total number of studies), while a few dealt with glazed wall tiles. Thus, an

urgent need for further studies characterizing the microbial communities growing over glazed wall tiles is urgently needed. Therefore in Chapter 3 and 6 a polyphasic approach was used in order to characterize the microbial communities developing over glazed wall tiles. Future investigations will also focus on a better understanding of the biochemical and biophysical deterioration processes of historical glazed surfaces by phototrophic microorganisms and fungi through laboratorial tests. Moreover, the influence of the conservation condition on the susceptibility to biodeterioration and bioreceptivity of glazed ceramic tiles will also be analysed in Chapter 4 and 5, since the studies investigating biodeterioration focused mainly on unglazed ceramics and the studies on bioreceptivity although using glazed ceramics analysed only modern glazes.

# Microbial communities on deteriorated artistic tiles from Pena National Palace (Sintra, Portugal)
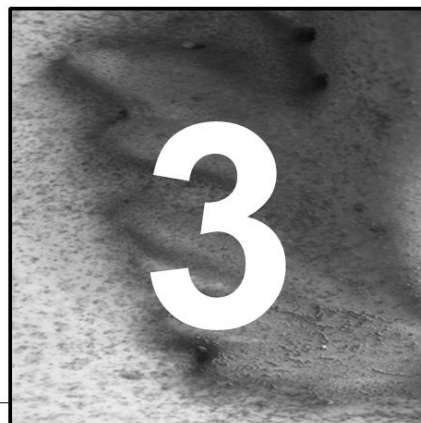
Pena National Palace (Sintra, Portugal) was built in the 19th century and tiles, typical of Portuguese and Oriental art expression, were widely used as decorative elements throughout the outside walls of the palace. This study focuses on a passageway (Triton tunnel) that is covered with distinct tile panels from the second half of the 19th century, attributed to Wenceslau Cifka. These tiles were covered by a green and/or black patina caused by microorganisms, whose identification was carried out by culture and molecular methods, light microscopy, confocal laser scanning microscopy, and scanning electron microscopy. The glaze substrate on which these organisms were growing was also characterized. Our results showed that the biological patina is composed of microalgae, cyanobacteria, bacteria, and some lichenized fungi. Also new fungal specie was identified as part of this biological community. Some of these microorganisms penetrate within fissures and pores, producing tile biodeterioration.

## 3.1    Introduction

Pena National Palace (Sintra, Portugal) was built in the 19th century by Fernando Coburg Gotha (Fernando II) who was influenced by the eclectic and romantic trends of the time. The palace has several outside walls covered with artistic tiles. In this study we focused on a passageway (Triton tunnel) that is covered with distinct tile panels from the second half of the nineteenth century, attributed to Wenceslau Cifka (Carneiro, 2009). As described in Chapter 2, glazed ceramic tiles have been used as an ornamental material, inside or outside and are of great importance, in several countries, particularly in Portuguese, Spanish and Brazilian cultural heritage. The literature review presented in Chapter 2 showed that there are only few studies on the biodeterioration of tiles. Identification of microorganisms involved in biodeterioration is one of the most important steps in the process of preservation and conservation of building materials and should be done before any intervention. This identification enables an understanding of the role played by microorganisms

in the biodeterioration process by correlating the interaction between organism´s activity and the material. Also optimum approaches to mitigation can only be achieved after knowledge of the microbial community and their effects. Therefore, the main objective of this work was the identification of the microorganisms responsible for the black and green patinas covering the Triton tunnel tiles, in Pena National Palace, Sintra, Portugal, and their role on tiles biodeterioration.

## 3.2    Materials and Methods

### 3.2.1    Site description and sampling

This study was focused on a passageway (Triton tunnel), from Pena National Palace, covered with distinct tile panels dating from the second half of the nineteenth century (Fig. 3.1) attributed to Wenceslau Cifka (Carneiro, 2009). This artist was also known for his work as a photographer, a painter and also a ceramist, particularly for his Italian Renaissance Style Faience (Carneiro, 2009). The passageway goes through the building, connecting the front of a courtyard to a backyard patio. The panels were decorated with plant or heraldic motifs, have a high relief decoration and were produced using the majolica technique (Fig. 3.1). The tiles from the Triton tunnel of the Pena National Palace are coated by a lead-alkali glaze with heterogeneous composition due to the variable presence of Si, Sn and Pb oxides.
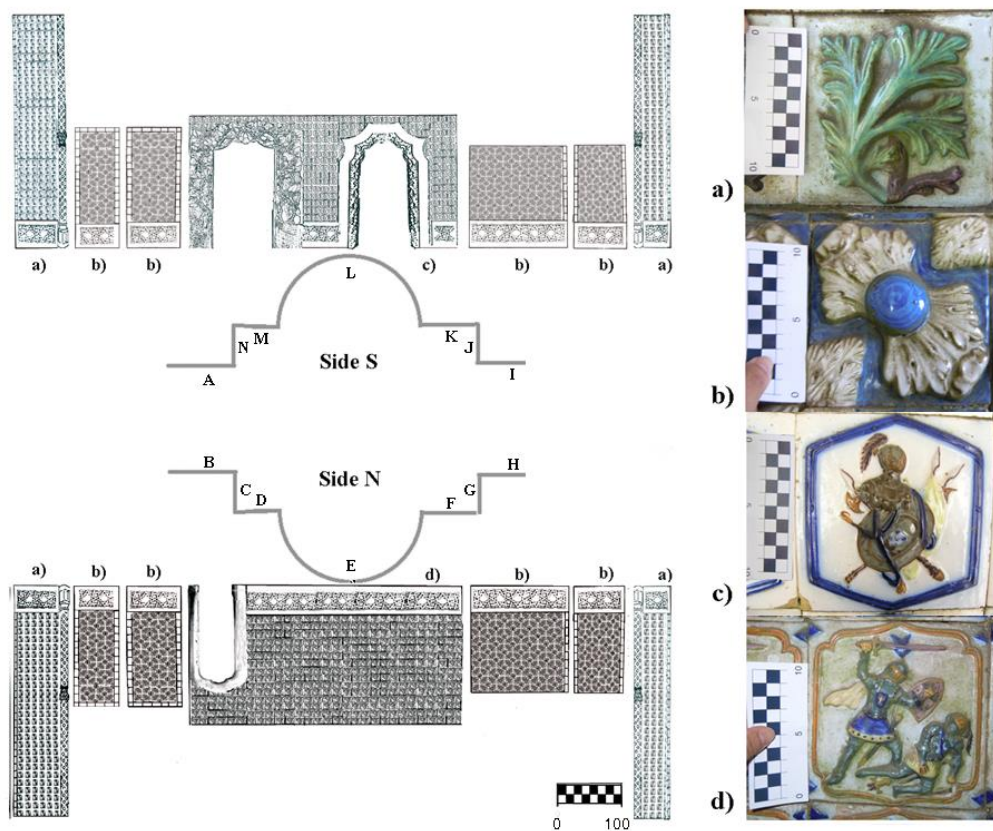


**Fig. 3.1** Scheme of the Triton tunnel passageway with the locations of the panels (A-N) and their tile motifs (a-d). Bar in cm.

Pena National Palace, located on the top of a hill (alt. 470 m) in Serra de Sintra (38°47'N, 9°25'W), is influenced by oceanic conditions (only 8-9 Km from the sea), and surrounded by a vast forested area. Serra de Sintra has a microclimate characterized by mildly cold temperatures, high relative humidity levels and heavy rainfall that enhance biological colonization. Consequently, the tiles produced by W. Cifka were severely colonized by microorganisms, as shown in Fig. 3.2. Flaking of the glaze, especially at the borders (Fig. 3.2a) and in the high relief figures caused large lacunae of the glaze in most extreme cases (Fig. 3.2b).
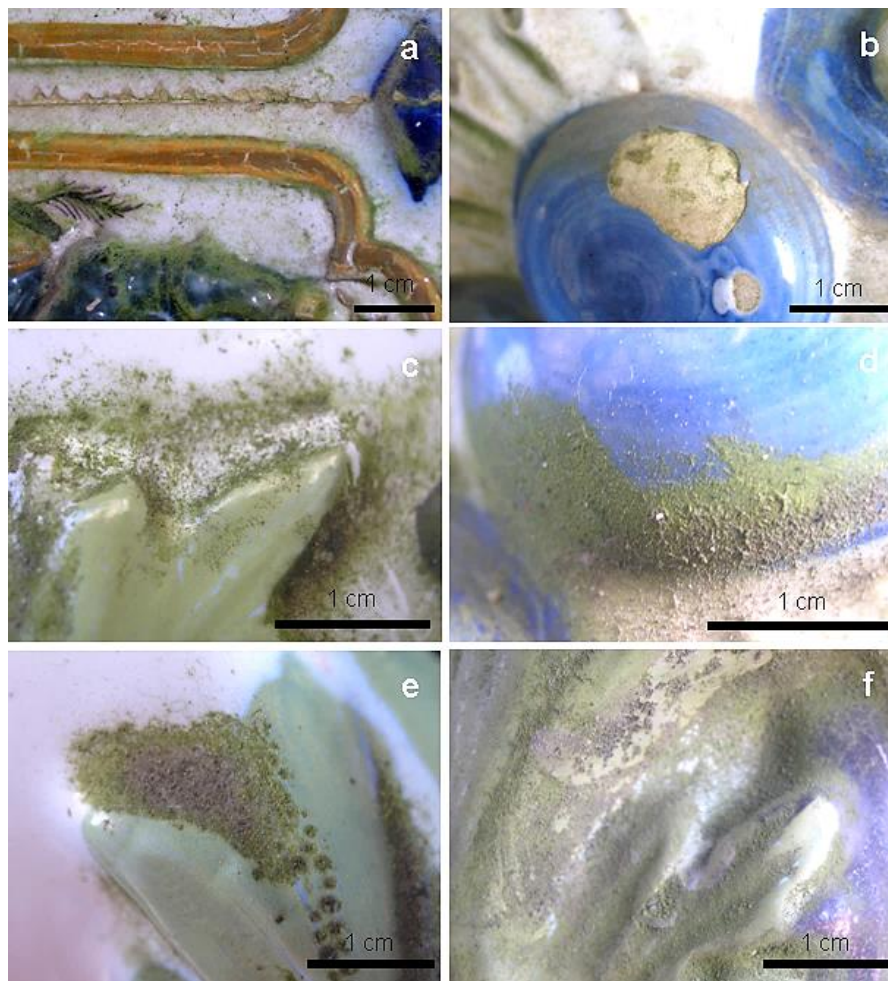


**Fig. 3.2** Detailed image of the decayed tiles. (a) Flaking on the border of a tile. (b) Growth of the biofilm on the ceramic body on a lacuna. (c-f) Preferential growth on the depression areas where green biofilms and airborne particles accumulate.

The flaking seems to be related or at least enhanced by the presence of microorganisms in the interface between the glaze and the ceramic substrate. In addition there is green colonization of the ceramic body below the missing glaze (Fig. 3.2b). Extensive thin green and black biofilms (Fig. 3.2c, d, e, f), which were particularly apparent on the depression of the relief motifs were noticed on the tiles.

Sampling surveys along the tunnel were conducted between October 2009 and January 2011, under the supervision of the Portuguese authorities in charge of the Pena National Palace. In 2009, small glaze fragments were removed using a scalpel from ceramic tiles detached areas for chemical characterization and field emission scanning electronic microscopy (FESEM). Green biofilms were gently scrapped, using a sterilized scalpel, from the top surface layers of the artistic tiles and placed in sterile tubes for molecular biology (samples from panels B, D and E) and identification of photosynthetic microorganisms by culture methods (samples from panels B, E and F). Photosynthetic biomass was also determined by the quantification of chlorophyll *a*. Samples for light and confocal laser scanning microscopy were collected from areas depicting higher photosynthetic biomass.

### 3.2.2 Characterization of the glazed substrate
#### 3.2.2.1 Micro-particle induced x-ray emission (µ-PIXE)

In order to determine the glaze compositions µ-PIXE analysis was performed. Ion beam analysis have been widely explored for the study of art works and archaeological artefacts (Calligaro et al., 2004). PIXE has been used for the characterisation of heterogeneous majolica glazes, since it can detect in a single measurement all the essential components of such vitreous materials (Zucchiatti et al., 2002). The analyses were performed with an Oxford Microbeams OM150 type scanning microprobe for focusing down to $3 \times 4$ µm$^2$ a 1 MeV proton beam. The sample fragments were irradiated in vacuum and the X-rays produced were collected by a 8 µm thick Be windowed Si(Li) detector with a crystal active area of 80 mm$^2$ and 145 eV resolution. The system configuration used allowed efficient detection of low energy X-rays such as the ones from Na. Operation and basic data manipulation, including elemental distribution mapping, was achieved through the OMDAQ software code, and quantitative analysis done with the GUPIX software. The quantification was performed in a representative area of the four glaze cross-sections with an area of analysis of ca. 500×500µm.

Consistency and comparability of µ-PIXE results were monitored by measuring glass standard CMOG C (The Corning Museum of Glass). The relative standard deviation for $SiO_2$, $K_2O$, CaO, and PbO is below 11% and for the remaining elements or oxides, $Na_2O$, $Al_2O_3$, $Fe_2O_3$, and Cl, is below 35%, except for Cl. The relative differences between the measured average value and the certified composition were below 20% for $Na_2O$, below 15% MgO, $Al_2O_3$, $K_2O$ and CaO, and below 5% for $SiO_2$, $Fe_2O_3$ and PbO as can be seen in Table 3.1. Values close to limit of detection presented high relative difference (e.g. Cl). The content of $SnO_2$ of the reference glass was bellow detection limit, thus was not quantified.

**Table 3.1.** Reference composition and analytical results (wt.%) for CMOG C reference glass (n=5).

| Oxides[1] | Na$_2$O | MgO | Al$_2$O$_3$ | SiO$_2$ | Cl | K$_2$O | CaO | TiO$_2$ | Fe$_2$O$_3$ | SnO$_2$ | PbO |
|---|---|---|---|---|---|---|---|---|---|---|---|
| CMOGC Certified (wt.%) | 1.1 | 2.8 | 0.9 | 34.9 | 0.1 | 2.8 | 5.1 | 0.8 | 0.3 | 0.2 | 36.7 |
| CMOGC Meas. (wt.%) | 1.3 | 2.4 | 0.8 | 33.3 | 0.3 | 2.5 | 4.5 | 0.5 | 0.3 | 0.0 | 36.0 |
| RSD (%) (n=4) | 25 | 14 | 20 | 6 | 32 | 4 | 4 | 69 | 16 | - | 11 |
| LOD (ppm) | 236 | 105 | 101 | 81 | 411 | 403 | 708 | 88 | 88 | 797 | 1620 |

[1] RSD – Relative Standard desviation; LOD – Average Limit of detection

### 3.2.2.2 Variable Pressure Scanning Electron Microscopy with energy dispersive spectrometer (VP-SEM-EDS)

Observation under VP-SEM with an energy dispersive spectrometer (EDS) was performed on white glaze cross-section using a HITACHI 3700N scanning electron microscope interfaced with a Quantax EDS microanalysis system. The Quantax system was equipped with a Bruker AXS XFlash® Silicon Drift Detector (129 eV Spectral Resolution at FWHM - Mn Ka). The operating conditions for EDS analysis were in backscattered electron mode, 20 kV accelerating voltage, 10 mm working distance and 120 mA emission current. VP-SEM allowed the analysis without coating, which enables posterior analysis by other techniques.

### 3.2.2.3 Micro-Raman spectroscopy (μ-Raman)

μ-Raman analyses were performed on the glaze surface and cross-sections, allowing mineralogical characterization of the glaze crystalline compounds. Raman spectroscopy analyses molecular and crystal lattice vibrations, being affected by the composition, bonding, chemical environment, phase, and crystalline structure of the material (Smith and Clark, 2004). Therefore unambiguous identification of materials can be achieved through this technique. The non-destructive and non-invasive characteristics of μ-Raman made its application widely used for characterization of inorganic crystalline compounds present in glazes (Coentro et al., 2012; Vieira Ferreira et al., 2013). For the analysis a Labram 300 Jobin Yvon spectrometer, equipped with a He-Ne laser of 17 mW power operating at 632.8 nm was used, as well as a solid state external laser of 50 mW power operating at 514.5 nm. Spectra were recorded as extended scans and the laser beam was focused either with a 50x or a 100x Olympus objective lenses or with a 50x Olympus ultra-long working distance (ULWD) objective for depth probing. The laser power at the surface of the samples was varied with the aid of a set of neutral density filters (optical densities 0.3, 0.6, 1 and 2).

### 3.2.3   Biomass estimation of photosynthetic microorganisms

Samples for the determination of chlorophyll *a* concentration were collected from four distinct tiles from north and south sides of the passageway. The sampling area was the entire tile and each tile had an area of 15 × 15 cm (225 cm$^2$). Samples were scraped with sterilized scalpels into centrifuge tubes and biomass was measured by extracting chlorophyll with dimethyl sulfoxide (Shoaf and Lium, 1976) with subsequent determination by spectrophotometry, as described by Burnison (1980). The chlorophyll *a* concentration was determined on the same day of sampling.

### 3.2.4   Biofilm covered area determined by digital image analysis

The areas covered by the biofilms were estimated by digital image analysis. Digital images of different colonized glazed tiles from walls exposed to the North (panels E and H) were recorded and the images submitted to Principal Components Analysis for the enhancement of the colonized area, following the protocols of Miller et al. (2010, 2011) and Rogerio-Candelera et al. (2011). The selected bands were then scaled, segmented into binary by a thresholding algorithm, and the selected pixels finally counted for area estimation. HyperCube (Army Geospatial Centre, USA) and ImageJ (National Institutes of Health, USA) were the software packages used for digital image analyses.

### 3.2.5   Identification of phototrophic microorganisms by culture techniques

Phototrophic microorganisms were collected by scraping the biofilm with a sterile scalpel into sterile Eppendorf tubes. Samples were then inoculated in Petri plates containing solid M7 culture medium (Elendt and Bias, 1990) and into flasks with liquid S2T2 culture medium (Lichtlé, 1979). Cultures were kept at 18–20ºC, under a 12:12h light:dark cycles (30–40 μmol m$^{-2}$ s$^{-1}$). The development of photothrophic strains was followed using a light microscope Leica DMLS and a Nikon TMS. Identifications were performed at the Coimbra collection of Algae (Algoteca de Coimbra - ACOI) (http://acoi.ci.uc.pt/) at the Department of Life Sciences, University of Coimbra, based on morphological characters determined by light microscopy. Taxonomic identification was carried out according to Bourrelly (1990) and Komárek and Anagnostidis (1999). Images were recorded with a Leica DFC420 camera.

In addition, four samples from the North side were directly examined for algae and lichens identification using a Leitz Diaplan microscope with differential interference contrast (DIC) optics and the photomicrographs were recorded with a DeltaPix Camera (InfinityX).

### 3.2.6   Isolation and identification of fungi

Biofilm samples for fungal identification by culture procedures were placed on PDA culture medium (samples from panels B, D and E) and other samples from the same panels were

suspended in sterile water and inoculated onto PDA culture medium (Scharlau, Spain). Cultures were incubated at room temperature with natural light cycles. Individual colonies were transferred to fresh PDA plates. Some fungal colonies were identified by morphological features. However, 5 pure cultures named PP1 to PP5 were characterized in terms of colony development, morphology, and were also identified by molecular biology techniques since identification by morphological features was not possible. Genomic DNA isolated from fungi by the following procedure. Fungal mycelium was collected from pure cultures PDA plates and placed inside 1.5 mL Eppendorf tube containing 500 µL of TNE buffer (10 mM Tris–HCl, 100 mM NaCl, 1 mM EDTA; pH 8) and glass beads. The mixture was shaken in a cell disrupter (Fast Prep-24, Solon, OH, USA) at full speed for 2 min. The DNA was purified by phenol/chloroform extraction and ethanol precipitation.

The internal transcribed spacer (ITS) regions, including ITS1, 5.8S rRNA gene and ITS2, were amplified using the universal primer pair ITS1 (5′-TCC GTA GGT GAA CCT GCG G-3′) and ITS4 (5′-TCC TCC GCT TAT TGA TAT GC-3′) (White et al., 1990). PCR reactions were performed in a BioRad iCycler thermal cycler (BioRad, Hercules, CA, USA) using the following thermocycling program: 2 min denaturing step at 95ºC, followed by 35 cycles of denaturing (95ºC for 30s), annealing (55ºC for 30s) and elongation (72ºC for 1 min), with an additional extension step at 72ºC for 10 min at the end. To evaluate the PCR results, products were separated on 1% (w/v) agarose gels, stained with SYBR Green I (Roche Diagnostics, Mannheim, Germany) and visualized under UV light. Positive PCR products were sent to Macrogen Europe (Amsterdam, The Netherlands) for purification and sequencing using the same primers that were used for ampification. In order to approximate the phylogenetic affiliations of fungal strains, the received sequences were compared, using BLASTn algorithm, to the non-redundant databases of sequences deposited at the National Center for Biotechnology Information (NCBI). Isolates PP1, P3, P4 and P5 due to the low similaty obtained with the ITS sequence amplification was performed using the ITS5 (5´-GGA AGT AAA AGT CGT AAC AAG G-3´) (White et al., 1990) and LR5 (5´-TCCTGAGGGAAACTTCG-3´) (Vilgalys and Hester, 1990) and sequences were submitted to the previously described procedure starting from the PCR reactions.

### 3.2.7  Identification of microbial communities by molecular methods

Since the thicker biofilms were found on glazed tiles from the North side of the tunnel, samples for the identification of microorganisms by molecular methods were collected from three panels on this side (B, D and E) by scraping the biofilm with a sterile scalpel into sterile Eppendorf tubes in a similar form to the samples collected for culture analysis. DNA was extracted using the FastDNA® 179 SPIN for Soil Kit (MP Biomedicals, France) in conjunction with the FastPrep® 180 instrument, following the manufacturer's protocol. PCR amplifications of bacterial 16S rRNA gene fragments were performed using the primers pair 616F (5'- AGAGTTTGATYMTGGCTCAG-3') (corresponding to position 27 of Escherichia coli 16S rRNA gene) and 907R (5'-CCCCGTCAATTCATTTGAGTTT-3') (Zimmermann et al., 2005), with PCR conditions comprising a denaturing step of 2 min at 95ºC, 35 cycles of denaturing (95ºC for 15 s), annealing (55ºC for 15 s), and elongation (72ºC for 2 min), following a terminal elongation step of 10 min at 72ºC.

Cyanobacterial 16S rRNA gene fragments were amplified using the primers Cya106F (5'-CGGACGGGTGAGTAACGCGTG A- 3') and Cya781R (5'- GACTACTGGGGTATCTAATCCCWTT-3'), and PCR conditions described by Nübel et al. (1997). Eukaryotic 18S rRNA genes were amplified using the primers EukA (5'-191 AACCTGGTTGATCCTGCCACT-3') and EukB (5'-TGATCC TTCTGCAGGACT-3') (Diez et al., 2001). The PCR amplification protocol consisted of denaturing step of 2 min at 95°C, followed by 35 cycles of denaturing at 95°C for 15 s, annealing of oligonucleotides at 50°C for 12 s, and elongation at 72°C for 2 min, following a terminal step of 10 min at 72°C, and ending at 4°C. For fungi the primers ITS1 (5'-TCCGTAGGTGAACCTGCGG-3') and ITS4 (5'-TCCTCC GCT TATTGATATGC-3') were used to amplify the internal transcribed spacers 1 and 2 flanking the 5.8s ribosomal RNA gene (ITS) as described by White et al. (1990). PCR amplifications were performed using ExTaq DNA polymerase (Takara, Tokyo, Japan). PCR products were inspected on 1% (w/v) agarose gels. Amplification products were purified with the JetQuick PCR Purification Spin Kit (Genomed, Löhne, Germany) and cloned with the TOPO TA Cloning Kit (Invitrogen, Carlsbad, CA). Clone representatives were sequenced by SECUGEN Sequencing Services (Madrid, Spain) to determine their phylogenetic affiliations. Sequence data were edited using the software BioEdit and submitted for homology search using the Blast algorithm (Altschul et al., 1990) on the NCBI database (http://www.ncbi.nlm.nih.org/ blast/). Low quality (short) sequences were removed from the dataset. Sequences were checked for chimera by BELLEROPHON server (Huber et al., 2004) using a variety of window sizes (200-400 bp) and corrections. Putative chimeric sequences were excluded from further analysis. Sequences were aligned using the program MUSCLE (Edgar, 2004). After this analysis, all sequences were compared to the non-redundant database of sequences deposited at the National Center for Biotechnology (NCBI) using BLASTN algorithm (Altschul et al., 1990). Aligned sequences were clustered into operational taxonomic units (OTUs) using the program DOTUR (Schloss and Handelsman, 2005) and based on a 97% sequence identity cutoff.

### 3.2.8  Confocal Laser Scanning Microscopy (CLSM)

Two fragments of biofilms from North side were collected (where the biofilm was thicker) together with small pieces of their supporting surface. The samples were placed onto Nunc Lab-TekTM chambered coverglass and were observed live. Images were captured with a Leica TCS-SP5 AOBS CLSM using a Plan-Apochromatic 63 6 (NA 1.4, oil) objective. The biofilms were observed with multi-channel detection. The reflection mode (excitation at 488 nm, 224 and emission at 480 to 495 nm), which allowed recording of reflective signals originating from inorganic solid material (viewed in the grey channel) was used to visualize the external surfaces and mineral particles. The 488 nm line of an Ar laser was used for imaging the auto fluorescence of the photosynthetic pigments and the reflection. Extracellular polysaccharides (EPS), or mucilage, were labeled with the broad-spectrum carbohydrate-recognizing lectin Concanavalin-A-Alexa Fluor 488 (Molecular Probes, Inc., Eugene, OR, USA) (0.8 mM final concentration). Concanavalin-A (Con-A) was observed in the blue channel using the 488 nm line of an Ar laser in the emission range of 490

to 530 nm. Phycoerythrin and chlorophyll a fluorescences could be detected between 555–595 nm and 690–750 nm respectively (viewed in the red channel). Further details and single cell pigment identification were described elsewhere (Roldán et al., 2004).

### 3.2.9  Field emission scanning electron microscopy (FESEM)

FESEM analyses were also conducted to determine surface topography, microorganism morphology and distribution, as well as their relationship with the substrate. These analyses were carried out with a FESEM Jeol JSM-7001F microscope. Tile samples were previously sputter coated with a thin gold/palladium film.

## 3.3  Results

### 3.3.1  White glaze characterization

Optical microscopy and VP-SEM of the glaze section allowed the observation of the microstructure of the glaze which showed minerals with different shapes and sizes disperse in a glassy matrix (Fig. 3.3).
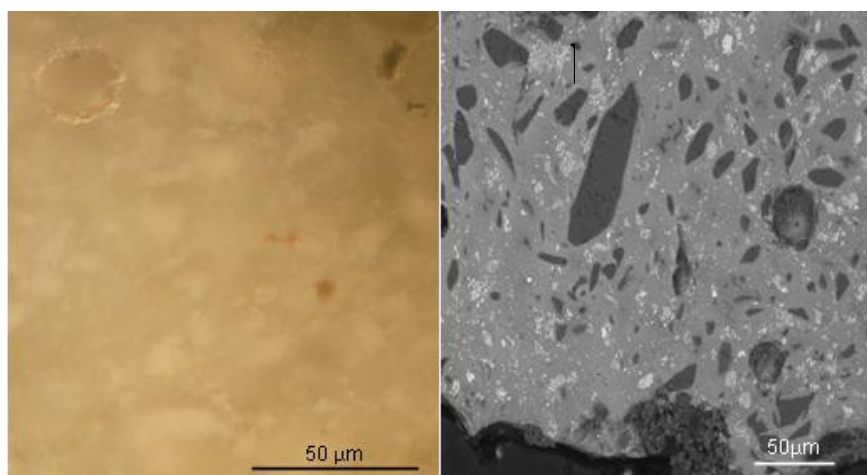


**Fig. 3.3** White glaze cross-section of sample W: (a) observed under optical microscope with white tin oxide crystals distributed on the glassy matrix and (b) backscattered electron image showing several mineral inclusions**.**

Chemical analyses of the white glaze indicated a lead- alkali type of glaze with lead contents in the range 19–43 wt. % PbO and 39-55wt. % $SiO_2$ with a total alkali ($Na_2O+K_2O$) contents in the range 5–8 wt. % (Table 3.2). The opacification was achieved by the addition of $SnO_2$ (9-13 wt %)(Table 3.2).

**Table 3.2.** Average chemical composition of the white glaze and standard deviation (Std) in wt. %.

| Oxides (wt. %) | $Na_2O$ | MgO | $Al_2O_3$ | $SiO_2$ | Cl | $K_2O$ | CaO | $TiO_2$ | $Fe_2O_3$ | $SnO_2$ | PbO |
|---|---|---|---|---|---|---|---|---|---|---|---|
| **Average** | 1.73 | 0.47 | 4.33 | 48 | 0.27 | 4.29 | 0.64 | 0.06 | 0.47 | 10.08 | 28.67 |

| Std | 0.7 | 0.1 | 0.7 | 7.4 | 0.1 | 1.1 | 0.3 | 0.1 | 0.4 | 3.7 | 12 |
| --- | --- | --- | --- | --- | --- | --- | --- | --- | --- | --- | --- |

The Raman signature of these inclusions showed that the recrystallization occurs in the form of cassiterite (635 cm$^{-1}$) (Coentro et al., 2012). Additional, µ-Raman analysis revealed that the silica rich inclusions were mainly quartz (460 cm$^{-1}$) and that the potassium rich inclusion were potassium feldspar (514 cm$^{-1}$) (Coentro et al., 2012).

### 3.3.2 Biomass estimation of photosynthetic organisms

On average, chlorophyll *a* concentration revealed a higher biomass of photosynthetic microorganisms on the North side (0.34 mg/cm$^2$), in agreement with visual observation (Fig. 3.2) than on the south side (0.25 mg/cm$^2$).

### 3.3.3 Biofilm covered area

The estimation of the areas covered by the phototrophic biofilm by means of digital image analysis techniques from North side resulted in a coverage ranging from 32.68% (panel E) to 38.40% (panel H). In the case of panel E the image analysis treatment was based in the binarization from false color images obtained from PCA bands. Panel H samples were more difficult to analyse as the central motif was originally green painted. Therefore, from a false-color image obtained with the three PCA bands we subtracted another false-color image originated from the minority PCA bands (Fig. 3.4).
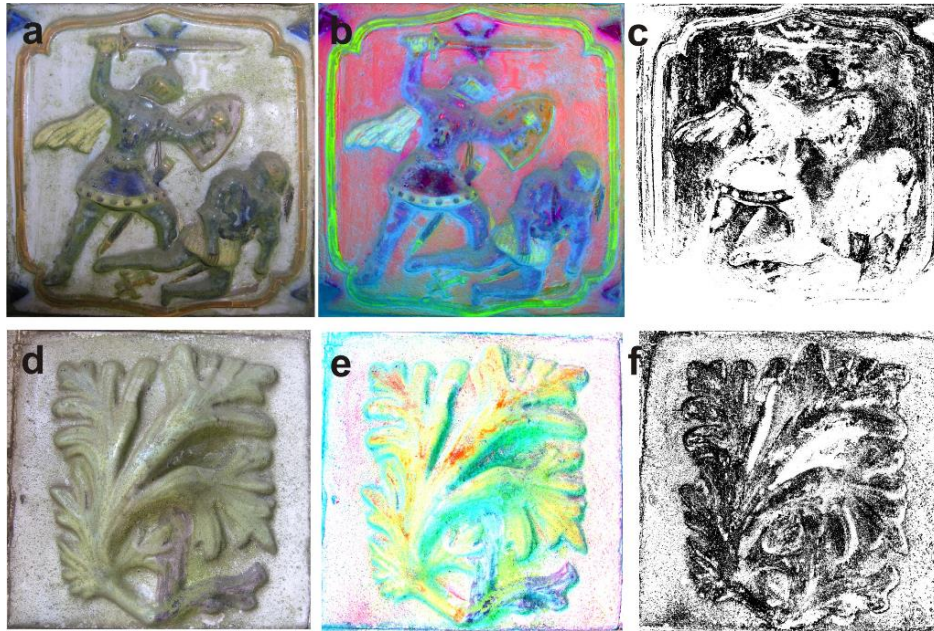
**Fig. 3.4.** Digital image analysis of tile from panel E and H. (a) Original image of one of the glazed tiles of panel E. (b) False-color image obtained from PCA bands. (c) Binary image showing the measured areas. (d) Original image of one glazed tile of panel H. (e) Result of the substraction of pixel values of two false-color images from PCA bands. (f) Binary image showing the measured areas.

### 3.3.4  Direct light microscopy observation of the collected biofilm

The observation of the four samples of biofilm collected from panel E allowed us to identify mainly two species of green algae, *Trebouxia* sp. and shorts filaments of *Trentepohlia* s.l. (including *Printzina*). *Trebouxia* cells were surrounded by hyaline fungal hyphae (Fig. 3.5a) as example of the lichen-forming process, and free-living (nonlichenized), short filaments of *Trentepohlia* s.l. (Fig. 3.5b). Among these green algae we found a dematiaceous fungi with brown hyphae, surrounding dead cells of green algae (Fig. 3.5c). The fungus produces 1-septate conidia (Fig. 3.5). No well-developed lichens were observed.
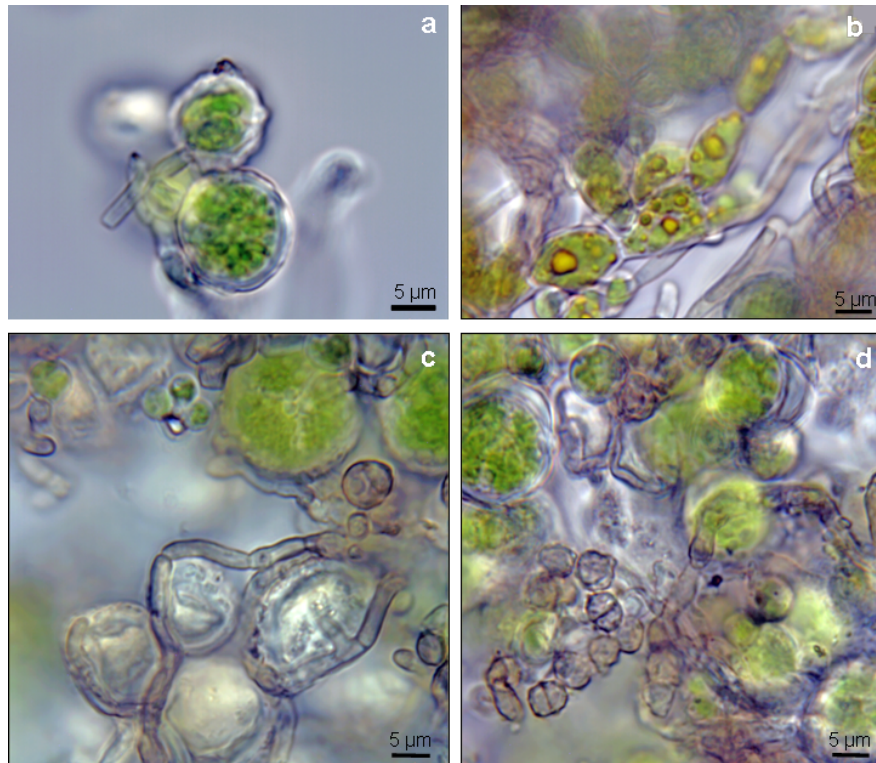
**Fig. 3.5** Micrographs of the biofilm samples observed by light microscope. (a) *Trebouxia* cells surrounding by hyaline hyphae of fungi. (b) Non lichenized short filaments of *Trentepohlia* sl. (c) Dematiaceous fungi with brown hyphae among green algae and surrounding dead cells of green algae. (d) 1-septate conidia**.**

## 3.3.5 Identification of photosynthetic microorganisms by culture techniques

Concerning the identification of photosynthetic microorganisms, three panels from the North side were analysed and a total of 22 taxa were identified (Table 3.3). Within the eukaryotic photosynthetic microorganisms, the phylum Chlorophyta was represented by nine different genera: *Apatococcus, Bracteacoccus, Desmococcus, Diaphragma, Dictyochloris, Jaagiella*, *Stichococcus*, *Trentepohlia* and *Ulothrix*

The phylum Charophyta was represented by the genus *Klebsormidium*. Among the prokaryotic photosynthetic microorganism seven different genera of Cyanobacteria were found: *Aphanocapsa*, *Calothrix, Nostoc*, *Tolypothrix*, *Gloeocapsa*, *Gloeothece* and *Plectonema*. The greatest Cyanobacteria biodiversity was found in panel F, while panel E presented the greatest biodiversity of Chlorophyta. Charophyta was found in both panels (E and F). Most of the Cyanobacteria and Chlorophyta found were reported to be photobionts in the lichen association (*Nostoc, Gloeocapsa, Calothrix, Trebouxia, Trentepohlia*) (Ahmadjian, 1993).

**Table 3.3** Phototrophic microorganisms identified by culture methods on glazed tiles from the North side of the Triton tunnel.

| Genera/Species | Sample | | |
| --- | --- | --- | --- |
| | B | E | F |
| **Chlorophyta** | | | |
| *Apatococcus lobatus* (Chodat) J. B. Petersen | * | * | * |
| *Bracteacoccus minutus* Schwarz | | | * |
| *Desmococcus olivaceus* (Pers. Ex. Ach.) Laundon | | * | |
| *Diaphragma radiosum* Geitler | | | |
| *Dictyochloris pulchra* Deason & Herndon | * | | |
| *Jaagiella alpicola* Vischer | * | * | |
| *Stichococcus bacillaris* Nägeli | | | * |
| *Trentepohlia monilia* Wildeman | | * | |
| *Trentepohlia* sp. | | * | |
| *Ulothrix* sp. | * | * | * |
| **Charophyta** | | | |
| *Klebsormidium flaccidum* (Kützing) P.C.Silva, K.R.Mattox & W.H.Blackwell var. *crissum* (R.Chodat) H.Ettl & Gärtn | | * | |
| *Klebsormidium flaccidum* (Kützing) P.C.Silva, K.R.Mattox & W.H.Blackwell var. *nitens* (Kützing) T.Mrozinska | | | * |
| *Klebsormidium pseudostichococcus* (Heering) H.Ettl & Gärtner | | * | * |
| **Cyanobacteria** | | | |
| *Aphanocapsa parietina* Nägeli | * | | |
| *Calothrix* sp. | | | * |
| *Gloeocapsa* sp. | * | | |
| *Gloeothece* sp. | | * | |
| *Nostoc commune* Vaucher ex Bornet & Flahault | | | * |
| *Nostoc paludosum* (Kützing) Bornet & Flahault | | * | |
| *Nostoc punctiforme* (Kützing) Hariot | | | * |
| *Plectonema edaphicum* (Elenkin) Vaulina | | | * |
| *Tolypothrix distorta* Kützing | * | | * |

### 3.3.6  Idenfication of the fungal isolates

Table 3.4 presents the fungi isolated by culture methods, a total of 11 filamentous fungal genera and yeast were identified from the biofilm samples placed directly in the culture media. In addition, 5 fungal strains were isolated by suspending the biofilm samples in water and placing them into half-strength PDA. Morphologically the 5 isolates resembled the dematiaceous fungi previously observed on the micrographs of the biofilm (Fig. 3.5).

**Table 3.4.** Fungi identified by culture methods on glazed tiles from the North side of the Triton tunnel.

| Genera | Sample | | |
|---|---|---|---|
| | B | D | E |
| *Isolated directly on PDA* | | | |
| *Arthrinium* sp. | | * | |
| *Alternaria* sp. | * | | * |
| *Cladosporium* sp. | * | | * |
| *Epicoccum sp.* | * | | * |
| *Fusarium* sp. | * | | |
| *Gliocladium* sp | * | | |
| *Neofusicoccum sp* | | | * |
| *Penicillium* sp. | * | * | |
| *Pestalotiopsis* sp. | | | |
| *Tricoderma* sp. | | | * |
| *Yeasts* | | | * |
| *Isolated after dilution in sterile water and grown on half-stregth PDA* | | | |
| PP1 | * | | |
| PP2 | * | | |
| PP3 | | | * |
| PP4 | * | | |
| PP5 | | | * |

The idenfication of dematiaceous fungi based solely on morphological traits cannot be achieved, therefore the 5 fungal strains (isolated PP1 to PP5) were selected for identification by molecular methods. The comparison of their nucleotide sequences with sequences in GenBank revealed two different fungal taxa from Ascomycota phylum belonging to the Chaetothyriales and Capnodiales order, respectively with similarities between 91 and 99 % (Table 3.5 ).

**Table 3.5** Phylogenetic affiliations of five fungal strains (isolates PP1 to 5) isolated from the tiles.

| Fungal strain[1] | Sequence | Closest relative (accession nr.)[2] | Similarity (%) |
|---|---|---|---|
| PP1, PP3, PP4 and PP5 | ITS | Teratosphaeria capensis (JN712501) / *Devriesia* sp.*(HQ914861)* | 93/91 |
| PP1, PP3, PP4 and PP5 | LSU | Devriesia hilliana (GU214414) | 99 |
| PP2 | ITS | *Phialophora sessilis* (EU514700) | 99 |

[1] Accession numbers of fungal strains
[2] Closest relative obtained by comparison with the NCBI database and corresponding accession number

The isolate PP2 revealed a good similarity (99%) with the closest relative *Phialophora sessilis.* However, sequences of isolates PP1, PP3, PP4 and PP5, showed a low similarity with the based solely on the comparison of the ITS region (Table 3.5) and even if a close match was

achived with the LSU region the morphological features were distict. Therefore, these sequences clearly represented previously unknown specie. The specie correspondent to those isolates were primarily distinguished based on DNA sequence comparisons and analysis of the macro- and micromorphological characteristics, being them described and classified in Crous et al (2012), as a new specie named *Devriesia imbrexigena* A.J.L. Phillips & M.L. Coutinho (Accession nr. JX915745-52) (Fig. 3.6).



**Fig. 3.6.** Microscopic detail of *Deveresia imbrexigena* Branched chain of arthroconidia, buds developing on the chain of arthroconidia Scale bars = 5 μm (Crous et al., 2012)**.**

### 3.3.7 Identification of microbial communities by molecular methods

Prokaryotic and eukaryotic microorganisms within the samples from the North side of the tunnel were characterized by DNA-based molecular analyses. A total of 75 clones were analyzed (Table 3.6). Sequence analyses revealed the presence of a variety of microorganisms belonging to Bacteria, Fungi, and Chlorophyta. Microorganisms belonging to all the three groups were found only in samples from panel E, which showed the greatest diversity within Bacteria and Fungi. The tiles showed the presence of Alphaproteobacteria, Chloroflexi and Actinobacteria. Among Alphaproteobacteria, *Sphingomonas* sp. and *Rhodovastum atsumiense* were identified on panel E, and *Aurantimonas* sp. on panel D. *Modestobacter* sp. and *Anaerolinea thermophila* were the only genera detected belonging to Actinobacteria and Chloroflexi, respectively. However, most of these bacteria show very low similarity with their closest relatives, which suggest that even affiliation to a genus could be questionable. Within Cyanobacteria, *Nostoc* sp., *Tolypothrix* sp. and *Chroococcidiopsis* sp. were found, all in samples from panel D.

**Table 3.6** Phylogenetic affiliations of microorganisms identified by molecular biology methods on glazed tiles from the North side of the Triton tunnel.

| Representative clone | No. of clones | Similarity(%) | Closest relative (accession nr.)[1] | Panels B | D | E |
|---|---|---|---|---|---|---|
| **Domain Bacteria** | | | | | | |
| TE-K23 | 3 | 80 | *Oocystis solitaria* chloroplast (FJ968739) | | | * |
| TE-K7 | 1 | 91 | *Chlorella saccharophila* chloroplast (D11349) | | | * |
| TE-K34 | 10 | 88 | *Chlorella ellipsoidea* chloroplast (X12742) | | | * |
| TE-K33 | 4 | 79 | *Anaerolinea thermophila* (NR_036818) | | | * |
| TE-K41 | 1 | 97 | *Modestobacter* sp. (FR682686) | | | * |
| TE-K2 | 2 | 91 | *Rhodovastum atsumiense* (AB381935) | | | * |
| TE-K15 | 1 | 97 | *Sphingomonas* sp. (EU337119) | | | * |
| TD-K6 | 1 | 99 | *Aurantimonas* sp. (AB600133) | * | | |
| TE-K47 | 1 | 92 | *Beijerinckia fluminensis* (EU401905) | | | * |
| **Cyanobacteria** | | | | | | |
| TE-K14 | 1 | 91 | *Chlorella saccharophila* chloroplast (D11348) | | | * |
| TE-K40 | 1 | 83 | *Oocystis solitaria* chloroplast (FJ968739) | | | * |
| TB-K42 | 4 | 83 | *Oocystis solitaria* chloroplast (FJ968739) | * | | |
| TD-K2 | 22 | 91 | *Oocystis solitaria* chloroplast (FJ968739) | | * | |
| TD-K4 | 1 | 94 | *Tolypothrix* sp. (HM751846) | | * | |
| TD-K19 | 1 | 94 | *Chroococcidiopsis* sp. (DQ914863) | | * | |
| TD-K3 | 1 | 93 | *Nostoc* sp. (AM711549) | | * | |
| TD-K6 | 1 | 96 | *Chroococcidiopsis* sp. (AM711549) | | * | |
| **Domain Eukaryota** | | | | | | |
| **Chlorophyta** | | | | | | |
| TB-K43 | 3 | 99 | *Apatococcus lobatus* (FR693368) | * | | |
| TE-K9 | 1 | 99 | *Trentepohlia* sp. (JQ617947) | | | * |
| **Fungi** | | | | | | |
| TB-K37 | 1 | 96 | *Capnobotryella* sp. (AJ972857) | * | | |
| TB-K9 | 4 | 98 | *Capnobotryella* sp. (AJ972857) | * | | |
| TB-K13 | 1 | 98 | *Stigmina* sp. (GU214700) | * | | |
| TB-K14 | 2 | 98 | *Capnobotryella* sp. (AJ972857) | * | | |
| TE-K1 | 1 | 83 | *Capronia* sp. (EU139148) | | | * |
| TE-K10 | 1 | 95 | *Fellomyces sichuanensis* strain (AF444461) | | | * |
| TE-K7 | 1 | 92 | *Kockovaella schimae* strain (AF444479) | | | * |
| TE-K12 | 2 | 100 | *Umbilicaria calvescens* (HM161484) | | | * |
| TE-K4 | 1 | 100 | *Hortaea thailandica* (CU214637) | | | * |
| TE-K11 | 1 | 97 | *Saccharata* sp. (JN225922) | | | * |

[1] Closest relative obtained by comparison with the NCBI database and corresponding accession number.

The fungi present on the artistic tiles were found on panels B and E, and were represented by the phyla Ascomycota (*Capnobotryella* sp.*, Stigmina* sp.*, Capronia* sp.*, Umbilicaria calvescens, Hortaea thailandica* and *Saccharata* sp.) and Basidiomycota (*Fellomyces sichuanensis* and *Kockovaella schimae*). The highest number of fungal clones belonged to *Capnobotryella* sp. which was found on panel B. Within Chlorophyta, 5 different species were identified: *Oocystis solitaria*, *Chlorella saccharophila*, *Chlorella ellipsoidea*, *Apatococcus lobatus* and *Trentepohlia* sp. (Table 3.6). The highest number of clones was obtained for *Oocystis solitaria* (panel D), and for the genus *Chlorella*, which was mainly found in samples from panel E.

### 3.3.8  Confocal Laser Scanning Microscopy

CLSM was used in the reflection and in the fluorescence mode. The reflection mode revealed inorganic material and was shown in the grey channel. The fluorescence mode revealed the fluorescence from photosynthetic pigments in the red channel. Small spots of EPS labeled with

con-A, were visualized in the blue channel. The biofilms from the semi-circle on the North side were primarily composed of *Trebouxia* sp., but also included *Trentepohlia* sp., moss protonemata, fungal hyphae and actinobacteria. *Trebouxia* sp. was present as single cells and aggregates, formed by groups of cells and autospores (Fig. 3.7a). Moss protonemata pigment fluorescence was hardly visible, when compared with the fluorescence intensity of *Trebouxia* sp. On the tile surface, a green layer of microorganisms was observed. Their thickness was variable and could be measured only in samples collected together with the substrate. In these cases the side views of the 3D reconstructed images were used to determine biofilm architecture and to measure their thickness, which ranged from 20 to 45 µm. Cells fluorescence was intermixed with the irregular or cracked tile inorganic material that was the basis of the biofilm. If the cells were not penetrating the substrate the red would be displayed in an even layer over the gray layer corresponding to the inorganic surface, not mixed with it, as is the case (Fig. 3.7b).
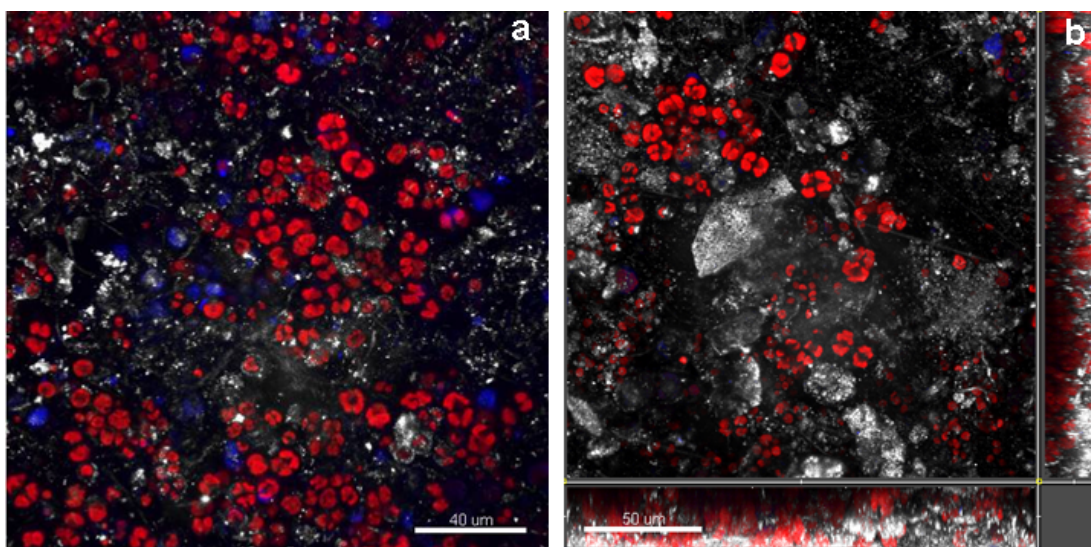


**Fig. 3.7** Confocal micrographs of biofilm-forming microorganisms collected from Pena National Palace (Sample semi-circle North side). (a) Maximum intensity projection of a biofilm scraped from tiles showing small quantity of inorganic materials. It was mainly composed by clusters of the green alga Trebouxia sp. Note the single, stellate chloroplasts showing red fluorescence due to the fluorescence of chlorophylls a and b. Cells showed internal division or were filled with autospores. Some autospores were free. Small amounts of EPS were scattered among on the substrate. Neither the cells nor the autospores were surrounded by EPS. (b) 3D extended focus projections in x-y, x-z and x-z views of a Trebouxia sp. biofilm with substrate showing the 3D view into microstructure of tiles. Cells were scattered among the irregularities of the substrate. Biofilm thickness =26 µm. Color allocation: white = reflection from inorganic materials; red = autofluorescence of chlorophylls; blue = extracellular polymeric substances (EPS) dyed with Con A-Alexa 488.

Lambda scans of pigments from *Trebouxia* sp., at 488 nm excitation wavelength (Fig. 3.7a), showed a broad emission peak at ca. 690 nm from the overlaping of chlorophylls *a* and *b* emission spectrum and a small shoulder around 740 nm, in the range of wavelengths of near infrared. Spectrum of adult cells (Fig. 3.8b) had no differences compared with the spectrum of spores (Fig. 3.8c).
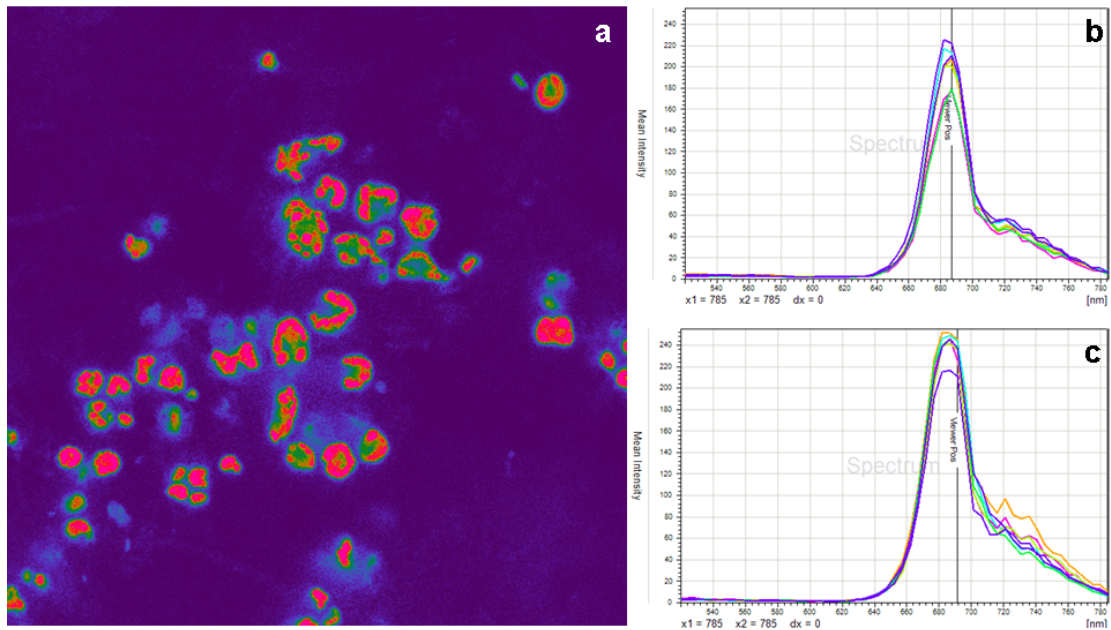
**Fig. 3.8** Fluorescence properties of *Trebouxia* sp. from a biofilm from Pena National Palace (North side). Pseudocolor confocal x-y-λ single section corresponding to the emission peak of chlorophylls *a* and *b*. Light colors represented the maximum fluorescence. (a) 2D plots of in vivo spectral profiles from lambda scans (Excitation wavelength = 488 nm. Steps = 50, band-width = 20 nm) (b, c). Mean fluorescence intensity of single vegetative cells (b) and spores (c) present in the biofilm of *Trebouxia* sp.

### 3.3.9 Field emission scanning electron microscopy (FESEM)

FESEM images showed a dense microbial colonization over the glazed surface, in fissures and pores (Fig. 3.9). The preferential growth of microorganisms in the fissures (Fig. 3.9 a and c) and also within pores (Fig. 3.9e) was evidenced. Diverse unicellular and filament morphologies were observed over the glaze (Fig. 3.9 b, d and f). A filamentous *Nostoc*-like cyanobacterium is shown in Fig. 3.9d. The adhesion of the filamentous organisms by EPS to the glaze is notorious in Fig. 3.9f.
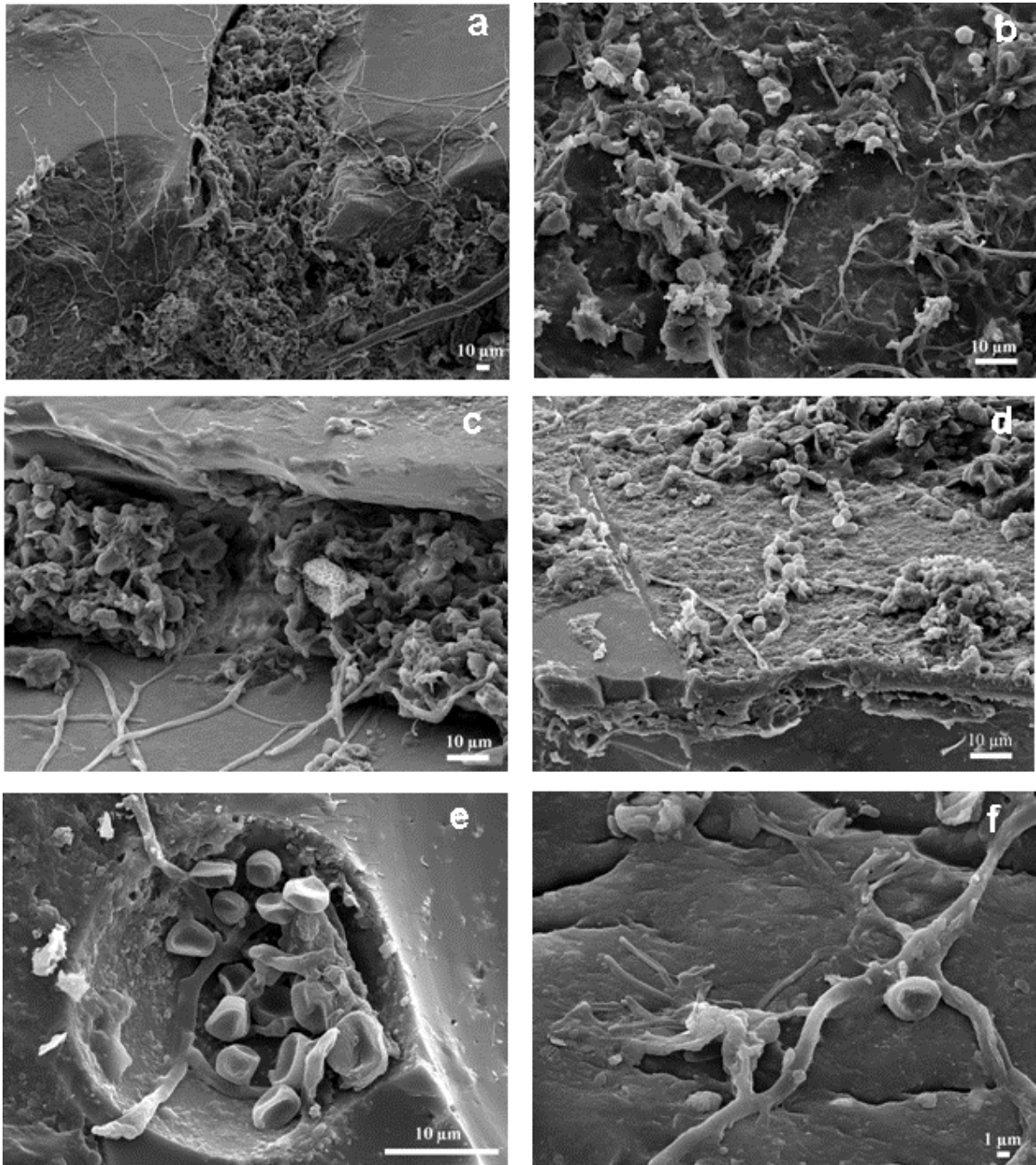
**Fig. 3.9.** FESEM images of biofilm over glaze fragments at different magnifications. (a) Filamentous and unicellular microorganisms can be observed growing on a fracture of the glaze. (b) Surface of the glaze densely colonized. (c) Colonization on a fracture of the glaze. (d) Filaments of moniliform cells compatible with Nostoc sp. (e) Filamentous and unicellular microorganisms growing inside a pore or bubble. (f) Microorganisms growing in contact with the substrate**.**

## 3.4    Discussion

The dense biological colonization on tile glazed surfaces is not a common phenomenon in this type of materials when exposed outdoor, because usually are washed out by rain. However, when the tiles are located in a rain-protected niche like the Triton tunnel, favorable microclimatic conditions can promote it. Pena National Palace is located on top of a hill, surrounded by a forest, with mildly cold temperatures and high humidity environment. This together with the sheltered

location, with a wind channel created by the passageway, and the high density of visitors and organic and inorganic airborne particles, might explain the high microbial colonization found on these tiles. This is supported by the high values of photosynthetic biomass, the high biodiversity of microorganisms (Table 3.3 and Table 3.6), and also the results of biofilm coverage determined by digital image analysis (Fig. 3.4). Direct observation and biomass quantification indicated that the North side showed a more dense microbial colonization than the south side, and therefore the study was mainly focused on the North side. Using CLSM it was possible to obtain the *in vivo* three-dimensional localization from biofilm thick samples without isolation. With the lambda-scan function it was possible to discriminate cells with particular fluorescence signatures within the biofilm (Fig. 3.7). Besides *Trebouxia* sp. and *Trentepohlia* sp. the observations on the biofilms obtained from the semi-circle in North side (panel E) indicate a complex community where hyaline and dematiaceous fungi were the most common microbial components (Fig. 3.5). Despite the presence of potential phycobionts and mycobionts, no well-developed lichen could be found, probably due to the pre-lichenization stage. Differences between culture-based and molecular methods are commonly reported in the literature (Bougoure and Cairney, 2005; Rastogi and Sani, 2011), but our data suggest that a combination of culturing and culture-independent approaches, as used in this work, can provide complementary and useful information. In fact, the Chlorophyta *Trentepohlia* was previously identified by Fonseca et al. (2010), who used molecular techniques to study the composition of the biofilms found on mortars at the Pena National Palace. Microscopy revealed the presence of *Trentepohlia* and *Trebouxia* on the tiles. These two genera can be frequently found as phycobionts of lichens. In addition, *Trentepohlia* sp. was identified by molecular methods on panel E.

Dematiaceous fungi were present in the biofilm samples observed at the light microscope, which is in agreement with the culture-independent results. Direct examination by light microscopy revealed that there is a considerable abundance of this type of fungi in the biofilm and some of the fungi were involved in pre-lichenization processes (Fig. 3.5c, d). The identification of a lichenized fungi (*Umbilicaria calvescens*) (Hestmark, 2009), and two yeasts associated to lichens (*Fellomyces sichuanensis*, *Kockovaella schimae*) (Prillinger et al., 1997) supports this hypothesis. In addition, the genera *Capnobotryella, Capronia and Phialophora* contain species that opportunistically colonize lichens (Hoog and Pavia, 2006, Harutyunyan et al., 2008; Halici et al., 2010), although some species of *Capnobotryella and Phialophora sessilis* were isolated from marble monuments and marble powder (Hoog and Pavia, 2006, Sert et al. 2007a,b, 2011). The low similarity verified for some fungi identfied directly by DNA-analysis of the biofilm were indicative that some unknown species could be part of the biofilm. This result was later confirmed with the characterization of the cultured isolates that allowed the identification of the new specie *Deveresia imbrexigena* described in Crous et al. (2012).

The Chlorophyta identified using culture methods (Table 3.3) presented a higher diversity than those identified with molecular biology methods (Table 3.6). Only *Apatococcus lobatus* and *Trentepohlia* sp. were identified by both methods. All the genera identified in culture media were previously found colonizing stone (Macedo et al. 2009), with the exception of *Diaphragma*,

*Dictyochloris* and *Jaagiella*, aerophytic and soil algae, which grow in mucilage of cyanobacteria and mosses. This can explain its appearance on the Pena National Palace tiles since these were coated by a biofilm containing large amounts of dust and sand. Regarding the identification of Chlorophyta by molecular methods, *Oocystis solitaria* and *Chlorella ellipsoidea* were the most common species, found in panels D and E, respectively (Table 3.6). Two clones were identified as *Chlorella saccharophila* chloroplasts. This latter species had been previously identified on artistic tiles from Venice (Giacomucci et al., 2011). According to Macedo et al. (2009), *Chlorella* is the most widespread genus found on stone monuments in the Mediterranean Basin, whereas *Oocystis* species (including *O. solitaria*) appeared in the travertine substrate from Fontana dei Quattro Fiumi, Rome, Italy (Ricci and Pietrini 1994). The cyanobacteria genera *Nostoc* and *Tolypothrix*, which are nitrogen-fixing cyanobacteria, were identified using culture-dependent and independent techniques. The presence on buildings of nitrogen-fixing cyanobacteria has been considered as possibly relevant for the establishment and development of other organisms, such as heterotrophic bacteria (Grant, 1982). Concerning the bacterial communities, panel D solely revealed the presence of *Aurantimonas* sp. In contrast, panel E showed the highest diversity among Bacteria. Ahmadjian (1993) reported that *Nostoc* and *Calothrix* are phycobiont of lichens. Büdel and Henssen (1983) found that *Chroococcidiopsis* occurred as a phycobiont in members of the Lichinaceae, a family of ascomycete fungi from which most species are lichenized, and have a distribution largely in temperate regions. Our data suggest that in the biofilm coating the tiles the first stages of binding between mycobionts and phycobionts are occurring (Fig. 3.5). The Cyanobacteria identified on the tiles (*Aphanocapsa*, *Calothrix, Nostoc*, *Tolypothrix*, *Gloeocapsa*, *Gloeothece* and *Plectonema*), are well known by their ability to produce EPS (Fig. 3.5 and Fig. 3.9). This allows their attachment and survival in this relatively inhospitable environment. FESEM images allowed us to observe the dense colonization over the glaze surface but especially in fissures, which suggests that they are the cause of the flaking, probably as a result of volume changes, penetration in the ceramic matrix and by release of metabolic substances, such as organic and inorganic acids as occur in stone materials (Gorbushina, 2007).

## 3.5    Conclusions

The high diversity of microorganisms on what seems to be an inhospitable substrate, a lead-based glazed tile, confirms the importance of understanding the relationship between substrate and microorganisms. The polyphasic approach, traditional culture methods and molecular biology methods applied for microbial characterization revealed a biological patina consisting of microalgae, cyanobacteria, bacteria, and fungi. Some of the fungi were involved in a lichenization process or close interaction with the photosynthetic community. A new fungal specie (*Deveresia imbrexigena*) was identified on these glazed tiles.

Some of the identified microorganisms penetrated within fissures and pores. Even though the penetration of hyphen and other biological structures on the glazed tiles were perceived in these colonized tile samples, the cause of the observed deterioration can be difficult to define. As mentioned in Chapter 2 the deterioration is a complex issue, resulting from many synergetic and

antagonistic factors. To understand the role of the main identified microorganisms (phototrophic microorganisms and fungi) in the deterioration of the majolica glazed tiles, laboratory biodeterioration experiments, under controlled conditions, have to be performed on tile models in order to assess solely the biodeteriogenic action of these microorganisms on the glazed tiles. Since historical tiles, like those analysed in this chapter, have undergone a process of ageing during the years, to study the ageing effect on the biodeterioration susceptibility and bioreceptivity also artificially weathered models should be used in the laboratory experiments.

# Evaluation of biodeterioration and bioreceptivity of majolica tiles by phototrophic microorganisms under laboratory conditions
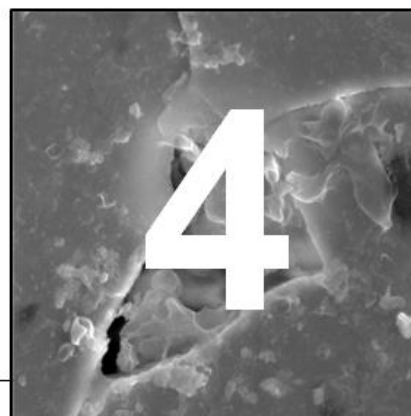
Biodeterioration of materials is a well-recognized matter; still the type and magnitude of damage produced by microorganisms on glazed tiles have not yet been established. The aim of this work was to evaluate the biodeterioration and bioreceptivity of pristine and artificially aged majolica glazed tile by a multi-species photoautotrophic culture (*Trentepohlia laginefera*, *Chlorella ellipsoideia*, *Apathococcus vulgaris*, *Nostoc microscopicum*). Intrinsic properties of tile models, including surface morphology, chemical composition and hydric properties (water absorption by capillarity and water vapour permeability), were assessed in order to relate them to tiles bioreceptivity. Biofilm growth and biomass quantification was performed by digital image analysis, colorimetry and *in vitro* chlorophyll *a* quantification for bioreceptivity assessment. Scanning electron microscopy (SEM), micro Raman spectroscopy (μ-Raman) and micro particle induced X-ray emission (μ-PIXE) were conducted to evaluate the effect of the microorganisms on the glazed tiles. Data showed that artificially aged tiles presented higher bioreceptivity than pristine tiles, due to their higher roughness, capillary kinetics and water vapor permeability. Biophysical deterioration, visible due to the unevenness of the micro-cracking network edges, caused by the chasmolithic growth of phototrophic microorganisms was also observed.

## 4.1 Introduction

As previously mentioned in Chapter 2, microbial communities colonizing glazed tiles have recently been reported by a few authors (Oliveira et al., 2001; Pedi et al., 2009; Giacomucci et al., 2011; Silva et al., 2011), providing a first insight on the biodiversity of bacteria, cyanobacteria, microalgae and fungi that colonize this substrate. Phototrophic microorganisms (cyanobacteria and microalgae) were identified as major components of the biocoenesis developing on glazed ceramic tiles (Chapter 3 and 6) (Oliveira et al., 2001). These microorganisms are known to be pioneer colonizers on monuments and historical buildings due to their photosynthetic ability and adaptation to growth on inhospitable environments through the formation of biofilms (Ortega-Calvo et al., 1991; Cuzman et al., 2011). It has been reported that the growth of photosynthetic-based biofilms over monuments, besides disfiguring them also results in more severe physico-chemical

deterioration, such as fractures, surface imprints and chemical depletion (Palmer and Hirsch, 1991; Brehm et al., 2005; Crispim and Gaylarde, 2005; Macedo et al., 2009; Coutinho et al., 2013). Therefore, the development of photosynthetic-based biofilms can cause severe damage and consequent irretrievable material loss, which is of particular concern in the case of cultural heritage assets. The deterioration and damage (considering the loss of value) caused by these alterations of a substrates induced by microorganisms is designated biodeterioration (Hueck, 1965).

In order to preserve a given material biodeterioration, it is essential to understand its deterioration mechanisms as well as the material's susceptibility to be colonized by organism. The direct analysis of colonized surfaces, for studying biodeterioration processes can be a problematic due to synergetic/antagonistic actions between different deterioration factors. For this reason, biodeterioration have often been evaluated by laboratory-based simulations, which rely on the artificial inoculation of microorganisms on a substrate under controlled environmental conditions. These procedures have been developed for different materials, such as stone, glass, unglazed ceramics and concrete materials providing important data on the mechanisms of deterioration and susceptibility of these materials (Ranogajec et al., 2008; Miller et al., 2009; Herisson et al., 2013; Rodrigues et al., 2014). The concept of the influence of intrinsic properties of the material on the degree of biological colonization was described in Chapter 2, being defined by the materials bioreceptivity. Several bioreceptivity studies have been performed on stone, which were reviewed by Miller et al. (2012), alsofew were made on modern ceramic materials (Gazulla et al., 2011; Gladis and Schumann, 2011a; Portillo et al., 2011; D'Orazio et al., 2014). These studies concerning ceramics were made on ceramic roofing tiles and bricks.

To the best of the author knowledge no laboratory study has been made to assess the bioreceptivity and biodeterioration caused by photoautotrophic microorganisms on majolica glazed tiles. Moreover, modern pristine industrial tiles differ greatly from historical tiles, due to their chemical and mineralogical composition and reduction of production flaws (e.g. crazing, pitting and fractures). In addition, most of the historical glazed tiles have undergone a process of ageing. Therefore, the aim of this study was to ascertain the difference between the bioreceptivity of pristine and artificially aged majolica glaze tiles and simultaneously analyze the biodeterioration potential of phototrophic microorganisms. In order to achieve this goal the following specific steps were performed: i) reproduction models of majolica glazed tiles based on the composition of the white glaze wall tiles from Pena National Palace, ii) artificial ageing of the reproduced model tiles to simulate the natural ageing processes, iii) chemical and physical characterization of the model tiles reproduced in this experiment, iv) inoculation and incubation of the reproduced majolica glazed tiles with a selected mixture of phototrophic microorganisms, and finally v) analyses of the growth and damage induced by the inoculated microorganisms on the glaze wall tile models.

## 4.2    Materials and methods

### 4.2.1   Manufacture of majolica glazed tile models

In the previous chapter, small white glaze samples collected from the nineteenth century tiles, located in the Triton tunnel at Pena National Palace (Sintra, Portugal), were chemically, mineralogical and morphologically characterized (Chapter 3). These tiles presented a biological patina growing over them. For this reason, their composition was selected for the reproduction of the majolica glazed tiles.

Glazed wall tile models were produced in laboratory according to traditional technology. A commercial ceramic paste (PF, SIO-2 CERÁMICA COLLET S.A., Spain) was kneaded manually, rolled-out and cut into squares (approximately 2.5x2.5 cm). At the centre of each square a concentric circular depression was made to better sustain the microbial suspension that would be inoculated. After air-drying under compression to avoid deformation during approximately two weeks, the ceramic body was fired at 950 ºC (100 ºC per hour and 1 h dwell). The lead–tin majolica model glaze was prepared by adjusting the composition with 100g of the commercial frit TR29 (Ferro) and pure raw laboratory materials: carbonates (3.4 g of $Na_2CO_3$, 1.5 g of $MgCO_3$, 13.23 g of $K_2CO_3$, 3.6 g of $CaCO_3$) and oxides (60 g of $SiO_2$, 15 g of $SnO_2$, 0.1 g of $TiO_2$ and 0.3 g of $Fe_2O_3$). The powders were ground in agate mortar during 15 min before put into suspension with deionized water. The glaze was applied by pouring the raw glaze suspension over the dry ceramic body according to traditional manufacturing. After 24 hours air-drying tiles were fired at 980 ˚C (at a heating rate of 100 ˚C/hour with 1 h dwell at 980˚C).

### 4.2.2   Artificial ageing

For studying the secondary bioreceptivity (Guillitte, 1995; Miller et al., 2012) and the effect of ageing of tiles on the biodeterioration by phototrophic microorganisms, 19 of the 38 tiles samples were subjected to artificial ageing. For this purpose, the reproduced tile models were chemically corroded by immersion into alkaline NaOH solution (pH 10) during 10 days. The reaction containers were sealed to prevent interactions with the atmosphere and made of inert material (polyethylene) in order to avoid any reactions between the electrolyte and container walls. Afterwards, the samples were rinsed with distilled water and air-dried. To simulate mechanical decay samples were submitted to thermal shock, though cycles (n=3) of heating (150 ˚C) during 20 min directly followed by immersion into ice-cold water. A set of 38 glazed tiles from each typology (19 pristine and 19 aged surfaces) were selected for the experiment.

### 4.2.3 Laboratory-based tiles biodeterioration experiment

#### 4.2.3.1 Tested microorganisms and tiles inoculation

The selection of photoautotrophic microorganisms used for the biodeterioration experiment was based on the microorganisms previously identified on the glazed wall tiles from Pena National Palace (Portugal) described in Chapter 3. The Chlorophyta *Trentepohlia laginefera* (strain ACOI 1067), *Chlorella elipsoideia* and *Apathococcus vulgaris* (strain ACOI 193) and one cyanobacterium *Nostoc microscopicum* (strain ACOI 578) from the Coimbra collection of Algae (*Algoteca de Coimbra* -ACOI) at the Department of Life Sciences, University of Coimbra, Portugal (http://acoi.ci.uc.pt/) of the Department of Life Sciences - University of Coimbra, were the components of the photoautotrophic inoculum used in this work. The inoculum was grown in BG11 liquid culture medium (Fluka Biochemika, Switzerland) for enrichment. At the inoculation day, each set of tiles were placed inside a glass Petri dish suspended over a net with distilled water at the bottom (Fig. 4.1).
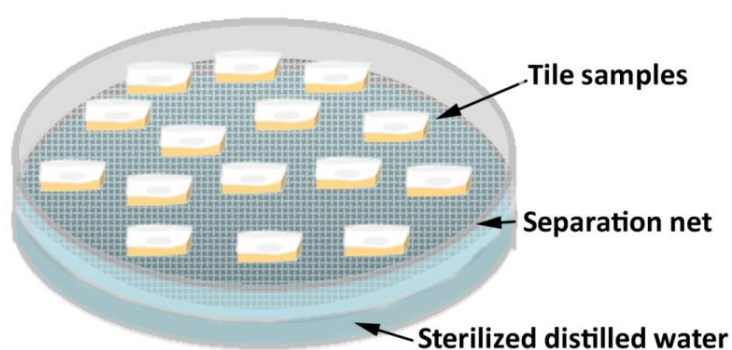


**Fig. 4.1.** Illustration of the experimental set-up. Glass Petri dish ($\varnothing$ = 9 cm) with distilled water at the bottom and a net to separate the water from the glazed tile samples.

Pristine and aged samples (16 of each) were placed inside separately petri dishes. A third petri dish was used to place the control samples: three pristine and three aged tile samples without the inoculum. The experimental design can be seen in Fig. 4.2. Prior to the inoculation with microorganisms, the three the Petri dishes, with the water at the bottom and the tiles on top of the net were autoclaved at 121 ºC at 100 kPa above atmospheric pressure for 20 min. After a slow cooling at room temperature, 150 µl of phototrophic culture was inoculated on the glazed surface of the tiles. All the tile samples (inoculated and control samples) were kept under the same conditions (22-23 ºC and 75-95% RH) close to a window, but sheltered from direct sunlight to provide optimal conditions for phototrophic microbial growth during the time span of the experiment, 12 months.

Samples with microorganisms were re-inoculated with 150 µl of the phototrophic culture every 3 months, in order to simulate constant reposition of cells that occurs in outdoor environments.
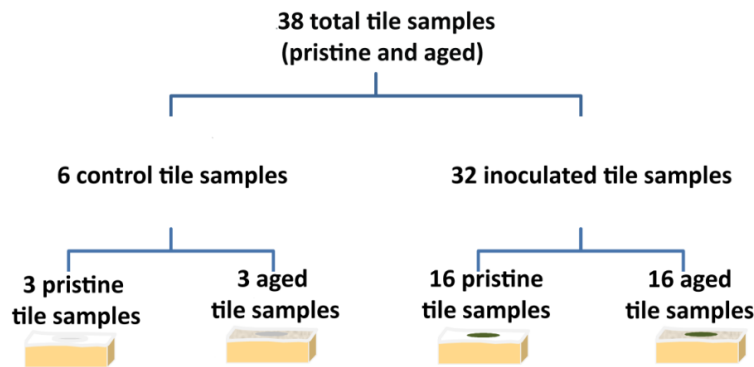


**Fig. 4.2** Scheme with experimental design with the number of replicates of pristine and aged control and inoculated samples

### 4.2.3.2 Quantification and characterization of phototrophic growth on the glazed tiles

*Photographic record.* Photographic records were made with a Olympus C-5060 digital camera every three months over the period of 12 months after the start of the biodeterioration experiment. A Kodak Color scale was included for light and color adjustment of the images.

*Digital image analysis.* The surface area covered by the green biofilms was estimated by digital image analysis at the end of the incubation time (12 months). Digital images of the colonized glazed tiles samples were individually recorded. Images were submitted to Principal Components Analysis (PCA) for the enhancement of the colonized area according to the protocols of Miller et al. (2010, 2011) and Rogerio-Candelera et al. (2011). Selected bands were then scaled and segmented into binary with a thresholding algorithm (Sezgin and Sankur, 2004), and pixels were finally counted for area estimation. HyperCube (Army Geospatial Centre, USA) and ImageJ (National Institutes of Health, USA) were the software packages applied for digital image analyses.

*Color measurement.* The biofilm color of pristine (n=3) and aged (n=3) tile samples was measured directly over the tile models surface by portable spectrophotometer (Minolta CM-508i). The CIELab color space was chosen for characterization of the biofilm color. This color space allows describing colors by means of the measurement of three parameters: L*, a* and b* (chromatic coordinates), as defined by CIE (Commission Internationale de l'Éclairage) (CIE, 1986). In this color space L* indicated lightness, which varies from 0 black to 100 white; the a* parameter run on a scale of -60 (green) to +60 (red); and the b* data run on a scale of -60 (blue) to +60 (yellow).

*Determination of Chlorophyll* a *(Chla) by fluorescence spectroscopy.* The biofilm of inoculated samples pristine (n=3) and aged (n=3) samples was scraped with sterile scalpels directly into seperate centrifuge tubes. Chlorophyll was extracted with dimethyl sulfoxide (Shoaf and Lium, 1976) and subsequent immediately determinated by fluorescence spectroscopy. Fluorescence spectroscopy was measured due to the very low concentrations of Chla in the

solution. Emission spectra of the Chl*a* solution were measured using a spectrofluorometer SPEX Fluorolog-3 FL3-22 performed with an excitation wavelength of 430 nm (optimum for Chl*a* molecules) (v), slits of 4.5 nm, an integration time of 0.3 s and an increment of 1.0 nm.

### 4.2.4  Characterization of pristine and aged majolica tile models before and after biodeterioration experiment

Prior to the biodeterioration experiment, pristine and aged tiles (t= 0 months) were characterized for ceramic body chemical and mineralogical composition by wavelength dispersive X-ray fluorescence (WD-XRF) and X-ray diffraction (XRD) analysis. The glaze was also chemical and mineralogically characterized by u-PIXE and μ-Raman. Morphological and microstructure of the glaze was evaluated for both pristine and aged tile samples by optical microscopy and SEM-EDS.

The intrinsic physical characteristics of the pristine (n=3) and aged (n=3) reproduction tiles prior to the incubation experiment were assessed through hydric properties by water absorption by capillarity and water vapour permeability. Water absorption by capillarity via the glaze layer was quantified by weighting the water uptake of the samples at increasing time intervals of 3 min, 10 min, 15 min, 30 min and hourly according to (Pereira and Mimoso, 2012). The capillary coefficient (Q) is defined as the coefficient between water suction mass and the square root of time, thus adopts the unit here noted in $g/m^2/s^{1/2}$. Water vapour permeability of the tiles was estimated by the dry method registering the weight uptake of water passing through the tile in which is mounted on the top of a recipient with dry $CaCl_2$ and positioned inside a chamber with controlled environment at 20 ºC and 75% relative humidity according to Pereira and Mimoso (2012) (Fig. 4.3).
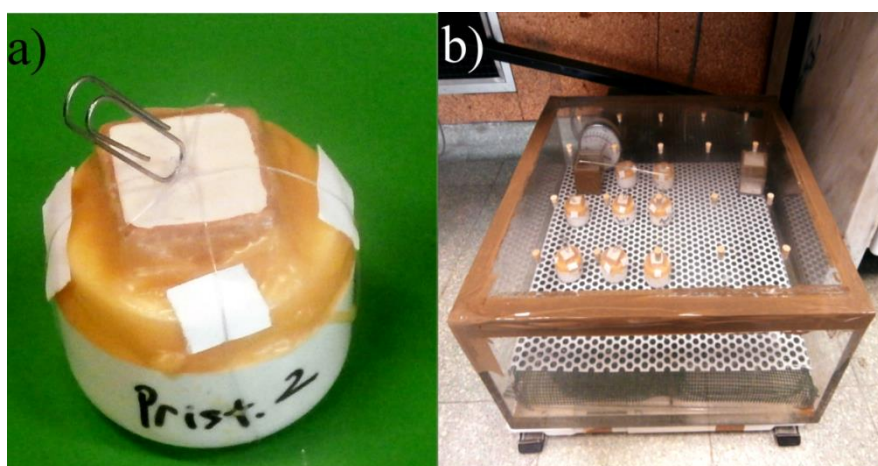


**Fig. 4.3.** Experimental set-up for determination of water vapor permeability, (a) tile sample embedded in wax over a plastic container and (b) chamber used for the experiment with the tile samples inside.

Surface roughness of the pristine (n=3) and aged (n=3) tiles glaze was also measured by an Ambios XP-Plus 200 Stylus profilomenter; three scan lines on each sample with 2mm length were performed at speed of 0.1 mm and stylus tracking force of 0.1 mg. The values of roughness parameters: Average Roughness (Ra), Root-Mean-Square Roughness (Rq) and Total Roughness Height (Ry) were calculated using the XP-Plus Software. After the biodeterioration experiment all the samples, pristine and aged control and inoculated samples (t=12m) were characterized for glaze chemical characterized by morphological evaluation of the glaze surface was evaluated by optical microscopy and Scanning Electron Microscopy with X-ray analysis (SEM-EDS), µ-PIXE for the detection of surface chemical alterations for both pristine and aged tile samples. In addition intrinsic physical characteristics through water absorption by capillarity by the glazed surface was assessed, using the procedure described above.

## 4.2.5  Analytical techniques

A multi-analytical approach was used to characterize the tile models before and after the biodeterioration experiment regarding morphological and chemical alterations; for some techniques the samples were analyzed at with the biofilm and after repeated cleaning of the surface with a cotton swab soaked in a 1:1 water ethanol solution to remove biofilm traces.

### 4.2.5.1  Wavelength dispersive X-ray fluorescence (WD-XRF)

Elemental analyses were conducted by WD-XRF spectrometry on finely grinded samples. The analyses were made with a PANalytical XRF-WDS 4 kW AXIOS (PANalytical B.V., Almelo, The Netherlands) sequential spectrometer using an Rh X-ray tube and samples were measured under a He flow. Spectra deconvolution by the iterative least squares method and standard less semi-quantitative analysis based on the fundamental parameter approach were performed with the SuperQ IQ+ software package (PANalytical B.V., Almelo, The Netherlands).

### 4.2.5.2  X-ray diffraction (XRD)

XRD analysis were performed for identification of crystalline phases (mineralogical characterization) present on the powdered ceramic body before and after artificial ageing The XRD patterns were recorded on a Rigaku Dmax III-C 3 kW diffractometer (Rigaku Corporation, Tokyo, Japan), using Cu Kα radiation at 40 kV and 30 mA settings in the 2θ range from 20° to 80°, and an acquisition time of 1s and 2θ increment of 0.08º. The resulting spectra were deconvoluted using a suitable software (EVA, Bruker AXS GmbH, Karlsruhe, Germany) and crystalline phases were identified by comparing the peak positions and intensities with those listed in the software standard files (ICDD, Newtown Square, PA, USA).

### 4.2.5.3  Micro particle induced X-ray emission ($\mu$-PIXE)

μ-PIXE analysis was made to determine the average composition of the glaze fragments from the Pena National Palace and of the glaze used to produce the glaze tile models (pristine and aged). The historical glaze fragments were analyzed in polished cross-sections, while the glaze from the produced tiles, both the pristine and aged were analyzed before and after the experiment directly on the surface of tile. Analysis performed following the biodeterioration experiment were made after repeated cleaning of the glaze tiles surface with a cotton swab soaked in a 1:1 water ethanol solution to remove biofilm traces as described in Section 4.2.5. An Oxford Microbeams OM150 type scanning microprobe was used for focusing down to 3 x 4 μm$^2$ at 1 MeV proton beam. The glaze sample were irradiated in vacuum, the produced X-rays were collected by a 8 μm thick Be windowed Si(Li) detector with a crystal active area of 80 mm$^2$ and 145 eV resolution. The system configuration used allowed efficient detection of low energy X-rays such as the ones from Na. Operation and basic data manipulation, including elemental distribution mapping, was achieved through the OMDAQ software code, and quantitative analysis done with the GUPIX software. The quantification was performed in a representative area of the glaze cross-sections with an area of analysis of ca. 500x500 μm. The accuracy of the analysis was based on analysis of the glass standard CMOG C (The Corning Museum of Glass) described in Chapter 3.

### 4.2.5.4  Micro Raman spectroscopy (μ-Raman)

μ-Raman was carried out on the glaze surface for mineralogical characterization of the glaze crystalline inclusions and on the crystals deposited on the glaze surface before biofilm removal (stage (i) section 4.2.5.). A Labram 300 Jobin Yvon spectrometer was used, equipped with a He-Ne laser of 17mW power operating at 632.8 nm and also a solid state external laser of 50 mW power operating at 514.5 nm. Spectra were recorded as an extended scan. The laser beam was focused either with a 10x, 50x or a 100x Olympus objective lens. The laser power at the surface of the samples varied with the aid of a set of neutral density filters (optical densities 0.3, 0.6, 1 and 2).

### 4.2.5.5  Optical microscopy

Microscopic observations and documentation were carried out using a Zeiss Axioplan 2 light microscope fitted with a Nikon DMX digital camera.

### 4.2.5.6  Scanning electron microscopy - energy dispersive X-ray spectrometry (SEM-EDS)

Pristine, aged and corresponding control model tiles were analysed by SEM to assess the microbe-substrate interactions with the biofilm and after repeated cleaning of the surface with a cotton swab soaked in a 1:1 water ethanol solution to remove biofilm traces. SEM-EDS analyses

were performed with a HITACHI 3700N scanning electron microscope interfaced with a Quantax EDS microanalysis system. The Quantax system was equipped with a Bruker AXS XFlash® Silicon Drift Detector (129 eV Spectral Resolution at FWHM - Mn Ka). The operating conditions for EDS analysis were in backscattered electron mode, 20 kV accelerating voltage, 10 mm working distance and 120 mA emission current. Samples were coated with Gold coating.

### 4.2.6  Statistical analysis

Statistical analysis were made to the results of oxide concentration; Chl*a* concentration ; colour measurments; digital image analysis and physical parameters determined on pristine and aged tile models. The aim of statistical analysis was to determine significant differences between the average values found for pristine and aged tile models and between control and inoculated samples regarding the above mentioned parameters. The experimental data were subjected to analysis of variance made with Microsoft Excel 2010 for Windows, and the averages were compared by the Turkey HDS Test at 5% level of significance.

### 4.3    Results

### 4.3.1   White glaze composition of the historical tiles

µ-PIXE analyses were performed on five white glaze fragments collected from the Pena National Palace´s historical tiles. The composition of the major and minor components in wt. % was 1.5 of $Na_2O$, 0.6 MgO, 5 $Al_2O_3$, 50 $SiO_2$, 4 $K_2O$, 1.2 CaO, 0.1 $TiO_2$, 0.5 $Fe_2O_3$, 9   $SnO_2$ and 30 PbO.

### 4.3.2.  Majolica tile models

### 4.3.2.2. Chemical and mineralogical composition

The manufactured model tiles presented a ceramic body with 60 of $SiO_2$, 20 of $Al_2O_3$, 13 of CaO, 3.4 of $K_2O$ and 1.3 of $TiO_2$ and 2.4 of $Fe_2O_3$, in wt. %, as major oxide components according to the WDXRF analysis. After firing the main mineralogical phases found by XRD on the ceramic body were quartz, gehlenite and anorthite (Fig. 4.4).
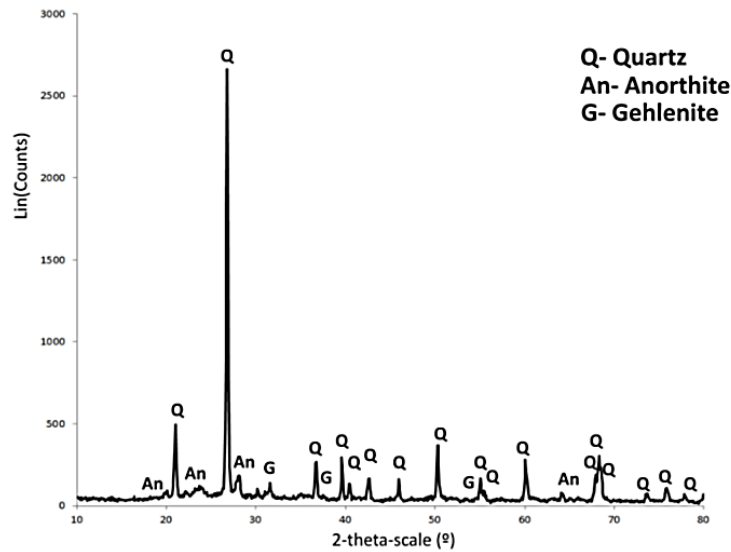
**Fig. 4.4.** Diffractogram obtained by XRD for the fired ceramic body with signalization of the main mineral phases of the tile models.

Table 4.1 shows the chemical composition obtained by µ-PIXE analyses of the produced glaze. $SiO_2$ (47 wt. %) and PbO (35 wt. %) were the main components of the pristine glaze; $SnO_2$ was the opacifier present in the majolica glazes, which was found in a considerable amount (10 wt. %). $Al_2O_3$ was also a major component of glazes present in approximately 3.4 wt. %. The proportions of alkalis ($Na_2O+K_2O$) were less than 2 wt. % of the total concentration of the glaze. Regarding the aged glazed tile samples composition is similar, only a slight increase in standard deviation of lead oxide and lower $SiO_2$ could be observed (Table 4.1). However, average composition of the pristine and aged tiles was not significantly different.

**Table 4.1** Composition of the pristine and aged glaze surfaces in oxide weight percentage (wt. %).

| Oxides (wt. %) | Pristine (mean±SD) | | | Aged (mean±SD) | | |
|---|---|---|---|---|---|---|
| $Na_2O$ | 0.3(a) | ± | 0.04 | 0.3(a) | ± | 0.06 |
| MgO | 0.4(a) | ± | 0.03 | 0.4(a) | ± | 0.01 |
| $Al_2O_3$ | 3.4(a) | ± | 0.3 | 3.2(a) | ± | 0.1 |
| $SiO_2$ | 47.0(a) | ± | 2.7 | 45.2(a) | ± | 5.2 |
| Cl | 0.1(a) | ± | 0.05 | 0.1(a) | ± | 0.1 |
| $K_2O$ | 1.5(a) | ± | 0.1 | 1.3(a) | ± | 0.01 |
| CaO | 1.0(a) | ± | 0.08 | 1.1(a) | ± | 0.1 |
| $TiO_2$ | 0.1(a) | ± | 0.02 | 0.1(a) | ± | 0.01 |
| $Fe_2O_3$ | 0.2(a) | ± | 0.01 | 0.2(a) | ± | 0.03 |
| $SnO_2$ | 10.2(a) | ± | 0.1 | 10.0(a) | ± | 1.0 |

| | | | | | | |
|---|---|---|---|---|---|---|
| **PbO** | 35.7(a) | ± | 2.5 | 38.0(a) | ± | 4.5 |

Mean ± SD;

Values followed by the same letters in brackets in the same line are not significantly different by the Tukey HDS test at p<0.05.

Regarding the mineralogical composition of the glazes´ crystalline inclusions, quartz and cassiterite were identified by micro Raman spectroscopy (μ-Raman) analysis (Fig. 4.5). Quartz Raman spectra showed the characteristic Raman bands at 125, 200 and the highest band at 460 cm$^{-1}$. Cassiterite was identified by focusing directly over the glaze with the most intense characteristic band at 633 cm$^{-1}$.
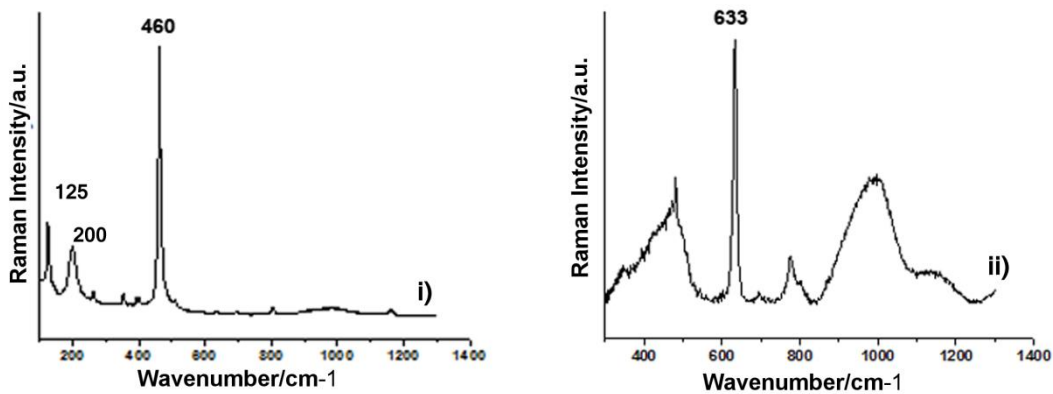


**Fig. 4.5.** μ-Raman spectra of (i) quartz and (ii) cassiterite identified on the white glaze of the tile models. Laser excitation 632.8 nm; 100× objective ULWD; laser power was kept at 1 mW.

### 4.3.2.3. Surface morphology and microstructure

Fig. 4.6 depicts the surface morphology and microstructure of the pristine and aged glazes before inoculation which were examined under optical microscopy and VP-SEM. Differences were perceived between the pristine and the aged tile models. The pristine glaze surfaces presented irregularities due to the mineral inclusions of tin and quartz dispersed though a smooth glassy phase matrix (Fig. 4.6 a and c). Along the surface micro-crack network could be observed by VP-SEM analysis (Fig. 4.6 c). At higher magnifications of these fissures pristine regular edges could be seen (Fig. 4.6 e). The ageing of the tile models resulted in the alteration of the glaze surface. Optical Microscope observations showed an irregular and rougher surface (Fig. 4.6 b). No well-defined hydrated corrosion layer was visible on the glaze surface (Fig. 4.6 d). The micro-crack network was significantly enhanced with the ageing process, and the edges showed corrosion and

had become irregular SEM-BSE-images showed areas richer in light elements in some fissures (Fig. 4.6 d and f).
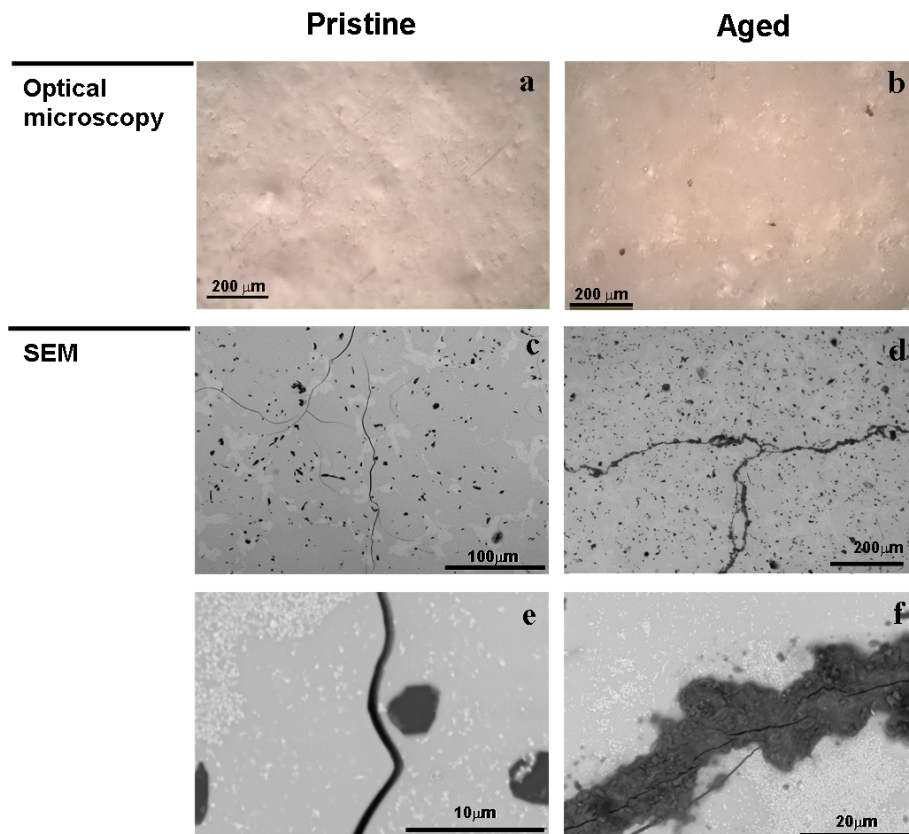


**Fig. 4.6** Microstructure and Surface morphology of representative samples of the pristine and aged glaze tile models before inoculation, observed under optical microscopy (a and b) and two BSE images, one general overview (c and d) and detail of the fissure (e and f).

### 4.3.2.4. Intrinsic physical characteristics of the pristine and aged tiles

The intrinsic physical characteristics measured in the pristine and aged model tiles, namely capillsrity coefficient and water vapour permeability corfficient presented significant differences between the two substrates (Table 4.2).

**Table 4.2.** Physical parameters analysed in pristine (n=3) and aged (n=3) samples. ANOVA average and standard deviation (±Std).

| Model tile | Q | δ | Ra | Rq | Ry |
|---|---|---|---|---|---|
| **Pristine** | 1.3±1.4(a) | $1.5 \times 10^{-10} \pm 4.6 \times 10^{-11}$ (a) | 12.58±3.3(a) | 14.87±3.3(a) | 57.95±14.0(a) |

| **Aged** | 10.8±6.1(a) | $3.9 \times 10^{-10} \pm 1.3 \times 10^{-10}$ (b) | 13.03±1.4(a) | 15.58±1.2(a) | 60.00±3.5(a) |

Q, capillarity coefficient (g.m-2.s-1/2); δ, water vapour permeability coefficient (Kg/m.h.Pa); Ra, average roughness (Å); Rq, root-mean-square roughness (Å); Ry, total roughness height (Å);

Mean ± SD;

Values followed by the same letters in brackets in the same column are not significantly different by the Tukey HDS test at p<0.05.

Capillary absorption refers to the water suction of glazed tile surface through crack network on the glazed surface and the open capillary pores of the ceramic body. Capillary coefficient of the aged samples showed a higher and more rapid water uptake (Q average 10.8), in comparison with the pristine samples (Q average 1.3) (Fig. 4.7.).
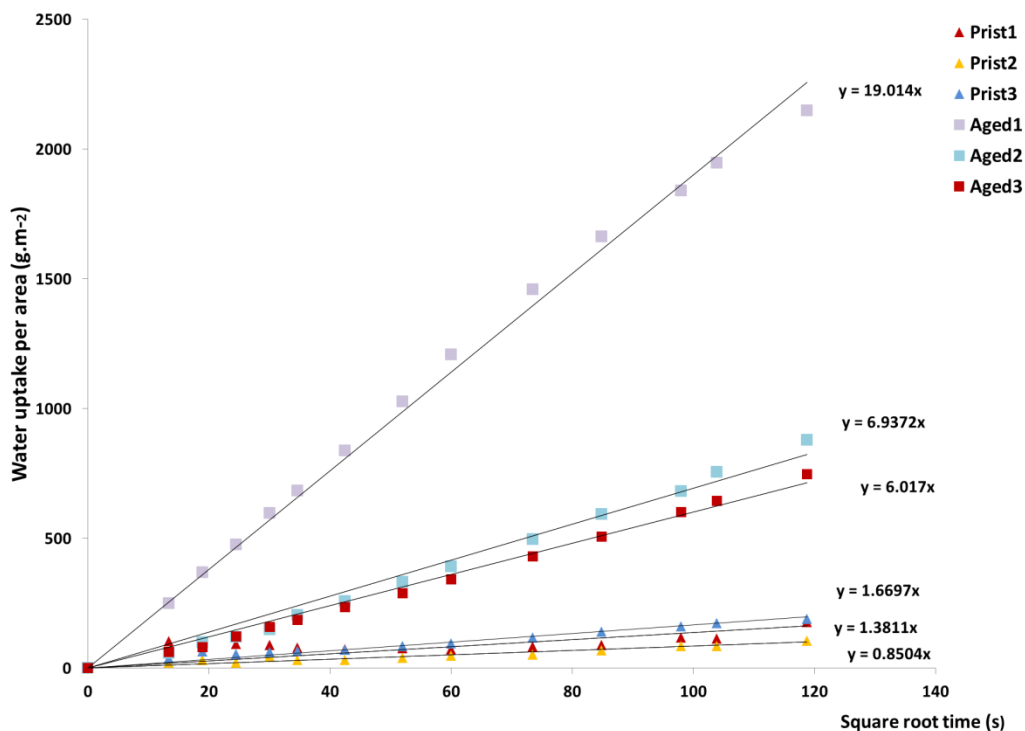


**Fig. 4.7.** Water uptake by capillarity of the pristine (Prist 1-3) and aged (Aged 1-3) tile models through the glaze with linear trendlines and equation with capillary coefficient value.

The pristine samples presented close values of capillary coefficient among the three replicates. Differing from the aged samples in which capillary coefficient values varied among the samples, indicating that the ageing process probably had not affected equally all tile samples (Table 4.2). Water vapor permeability was also assessed, as samples were not in direct contact with liquid water (Fig. 4.8). The permeability of the pristine samples was lower than the aged tiles, $1.5 \times 10^{-10}$ and $3.9 \times 10^{-10}$ respectively (Table 4.2 for ANOVA results).
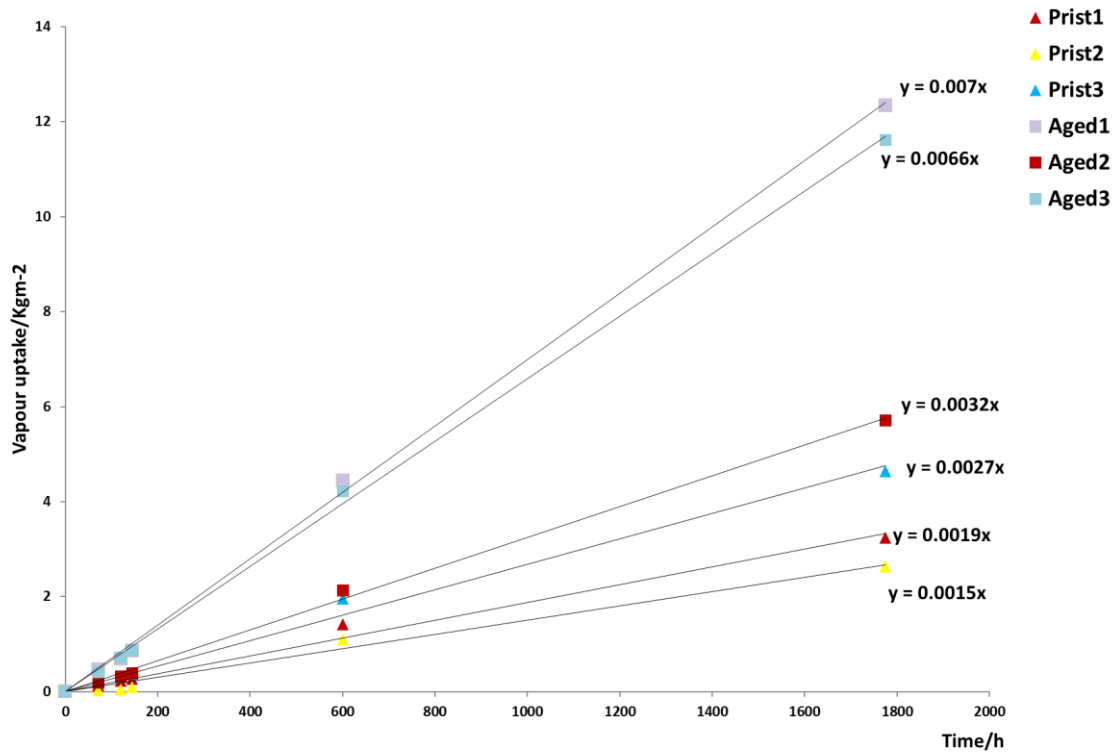
**Fig. 4.8.** Water vapor permeability of pristine (Prist 1-3) and aged(Aged 1-3) tile samples before inoculation with linear trendlines and equation with capillary coefficient values.

Table 4.2 also shows the results of the the roughness parameters of pristine and aged samples before the inoculation. The Average Roughness (Ra), Root-Mean-Square Roughness (Rq) and Total Roughness Height (Ry) parameter of the surface of the aged samples were greater than that of the pristine samples, but they were not significantly different ($p > 0.05$) (Table 4.2 for ANOVA results).

### 4.3.3. Characterization of the biofilm after the biodeterioration experiment

The biodeterioration experiment was made by the incubation of a phototrophic biofilm on the pristine and aged tile models. The phototrophic biofilm colonized the glaze surfaces slowly during the incubation time of 12 months. After the incubation period, pristine and aged set of samples showed visually detectable differences in terms of color and extent of surface coverage by the biofilm (Fig. 4.9).
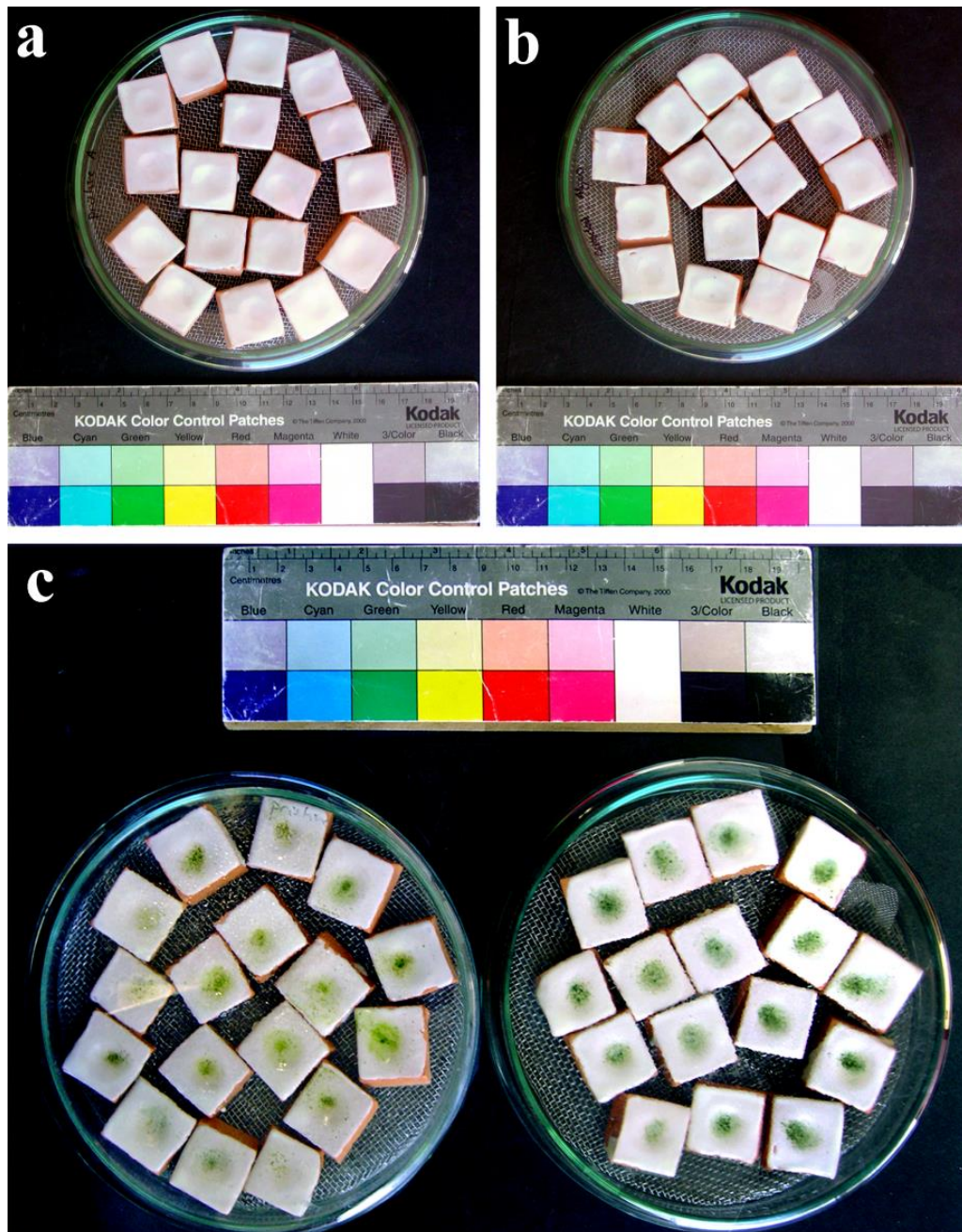
**Fig. 4.9** Images of the tile models before and after biodeterioration experiment. Petri dishes with (a) pristine tile samples before inoculation, (b) aged tile samples before inoculation and (c) inoculated pristine (left) and aged (right) tiles samples after 12 months incubation.

A polyphasic approach was conducted to quantify the visually detected differences in terms of extent of surface coverage of the biofilm, chromacity and biomass estimation. Table 4.3 summarizes the average values for the pristine and aged tiles obtained by these different methodological approaches, presenting the average values and standard deviation with the ANOVA results.

**Table 4.3.** Characteristics of the biofilm on the pristine and aged samples after 12 months of incubation. Biofilm covered area, obtained by Digital image analysis (n=16); colorimetric parameters (L*, a* and b*) (n=16) and intensity of Chla fluorescence measured at 684 nm (n=3) average values are presented together with the standard deviation and the ANOVA results**.**

| Sample | Covered area (mm$^2$)[1] | Colorimetry[1] | | | Intensity of Chla fluorescence at 684 nm (cps) [1] |
|---|---|---|---|---|---|
| | | L* | a* | b* | |
| **Pristine** | 24±9.7(a) | 64.3±7.9(a) | -0.61±2.5(a) | 22.1±7.4(a) | 2.45x10$^6$±4.8x10$^5$(a) |
| **Aged** | 43±13.4(b) | 55.0±4.8(b) | -4.4±1.1(b) | 18.3±2.1(a) | 7.21x10$^5$±6.4x10$^5$(b) |

[1] The values correspond to average ± SD. Values followed by the same letters in a column are not significantly different by the Tukey HDS test at p<0.05.

The quantification of extent of biofilm-covered areas was obtained by digital image analysis, a technique which allows isolating areas covered by the biofilm and quantifying the difference of the photosynthetic biofilms developed on surface of the samples. Fig. 4.10 shows one pristine tile and aged tile with the area covered by biofilm and the images treated for digital image analysis.
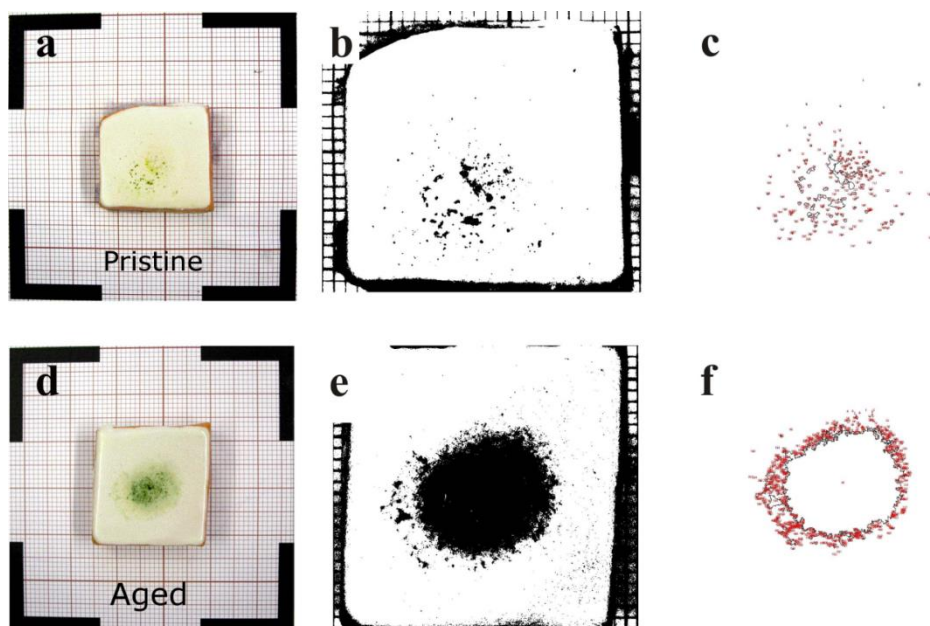


**Fig. 4.10.** Example of the application of digital image analysis in a pristine and an aged tile model covered by the green biofilm. (a) Original image of one of the pristine glazed tiles. (b) Segmented image (binary) of the first Principal Component. (c) Outlines of the areas selected for measuring of the first Principal Component of the pristine glazed tile. (d) Original image of one of the aged glazed tiles. (e) Segmented image (binary) of the first Principal Component. (f) Outlines of the areas selected for measuring of first Principal Component of the aged glazed tile.

The value of the areas covered by the phototrophic biofilms, were calculated from the segmentation of both the first and third Principal Components. After measuring the areas in every band, the outlines smaller than 0.001 mm$^2$ (1 pixel) were ignored for quantification and the average of the two measures (PC1 and PC3) were calculated. The tile surface area covered by biofilms ranged from 69 mm$^2$, in an aged sample, to 8 mm$^2$, in a pristine sample, of a total surface area per

tile of approximately 625 mm$^2$ (Fig. 4.11). Average covered area was higher on the aged samples (43 mm$^2$) than on the pristine model tiles (24 mm$^2$). Statistical analysis (Tukey HSD, p<0.05) revealed that the biofilm coverage area of the pristine and aged samples were significantly different (p<0.05) (Table 4.3).
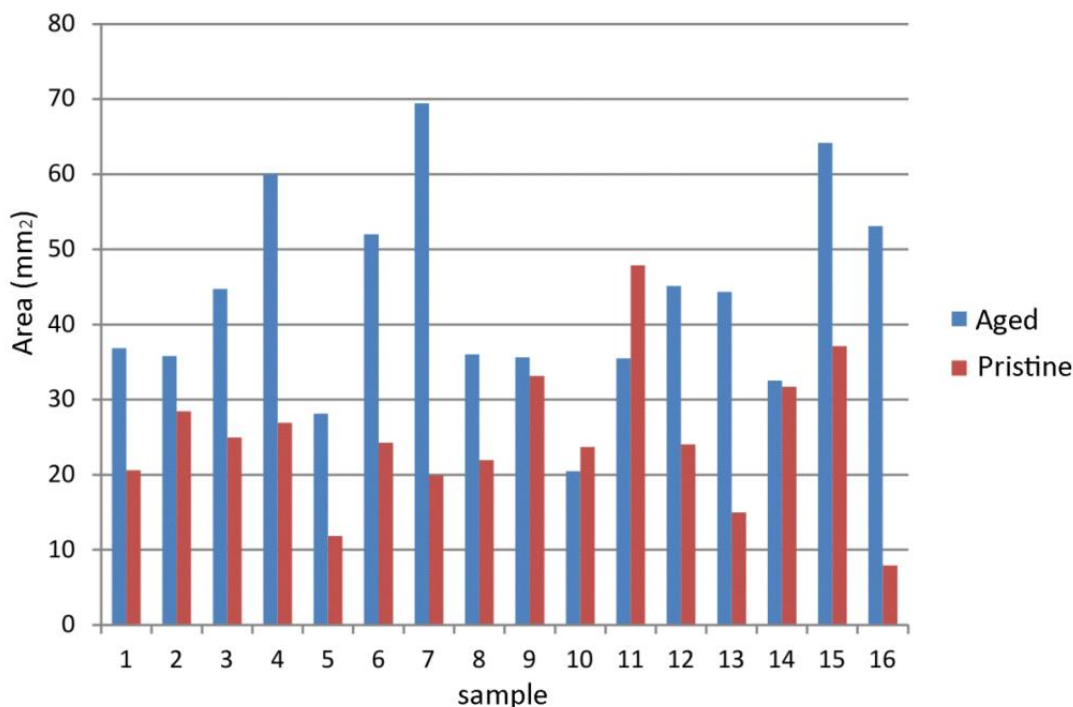


**Fig. 4.11.** Area (in mm$^2$) colonized by the phototrophic biofilms in aged (blue) and pristine (red) tiles obtained by digital image analysis.

The CIELab color parameters confirmed the differences in color and biomass, already verified by visual inspection and digital image analysis (Fig. 4.9 and Table 4.3). The L* parameter, which reflects the lightness-darkness, was significantly different for the pristine and the aged samples (Table 4.3). Lower L* values of the biofilm on the aged samples resulted in a darker green color. Concerning a* parameter, related to the redness-greenness, the biofilms of the aged samples was significantly greener than the pristine samples. This more intense green color can indicate a higher concentration of the green pigment Chl*a*. In terms of yellowness-blueness b* pristine and aged samples biofilms were not significantly different (Table 4.3).

The intensity of Chl*a pigments* fluorescence was estimated by chlorophyll extraction technique which also revealed a significant difference between pristine and aged tiles (Table 4.3). The aged tiles presented a higher fluorescence value and hence a higher Chl*a* pigment concentration, which indicates a higher photosynthetic biomass on the aged samples. This is in accordance with the results from the CIELab color analysis.

### 4.3.4. **Scanning Electron microscopy (SEM)**

SEM observations were made on inoculated samples after the biodeterioration experiment had ended. SEM results showed dense microbial colonization growing over the glazed surfaces on both pristine and aged tiles samples (Fig. 4.12). Cryptoendolithic growth of phototrophic microorganisms in glaze fissures was also observed in the both types of inoculated samples (Fig. 4.12 a and b). On the inoculated samples, particularly those with chasmolithic growth, the fissures seemed to present uneven levelling of the edges. The adhesion of microorganisms by EPS to the glaze and their penetration into fissures was noteworthy (Fig. 4.12 a, b, e). It was also interesting to observe that biofilm remains even after the surface cleaning with cotton swab soaked with an water-ethanol solution (Fig. 4.12a,b,e). After the removal of the biofilm, superficial deposits with imprints of the rod-shaped cells were observed (Fig. 4.12d), indicating etching of the substrate by the inoculated phototrophic microorganisms.
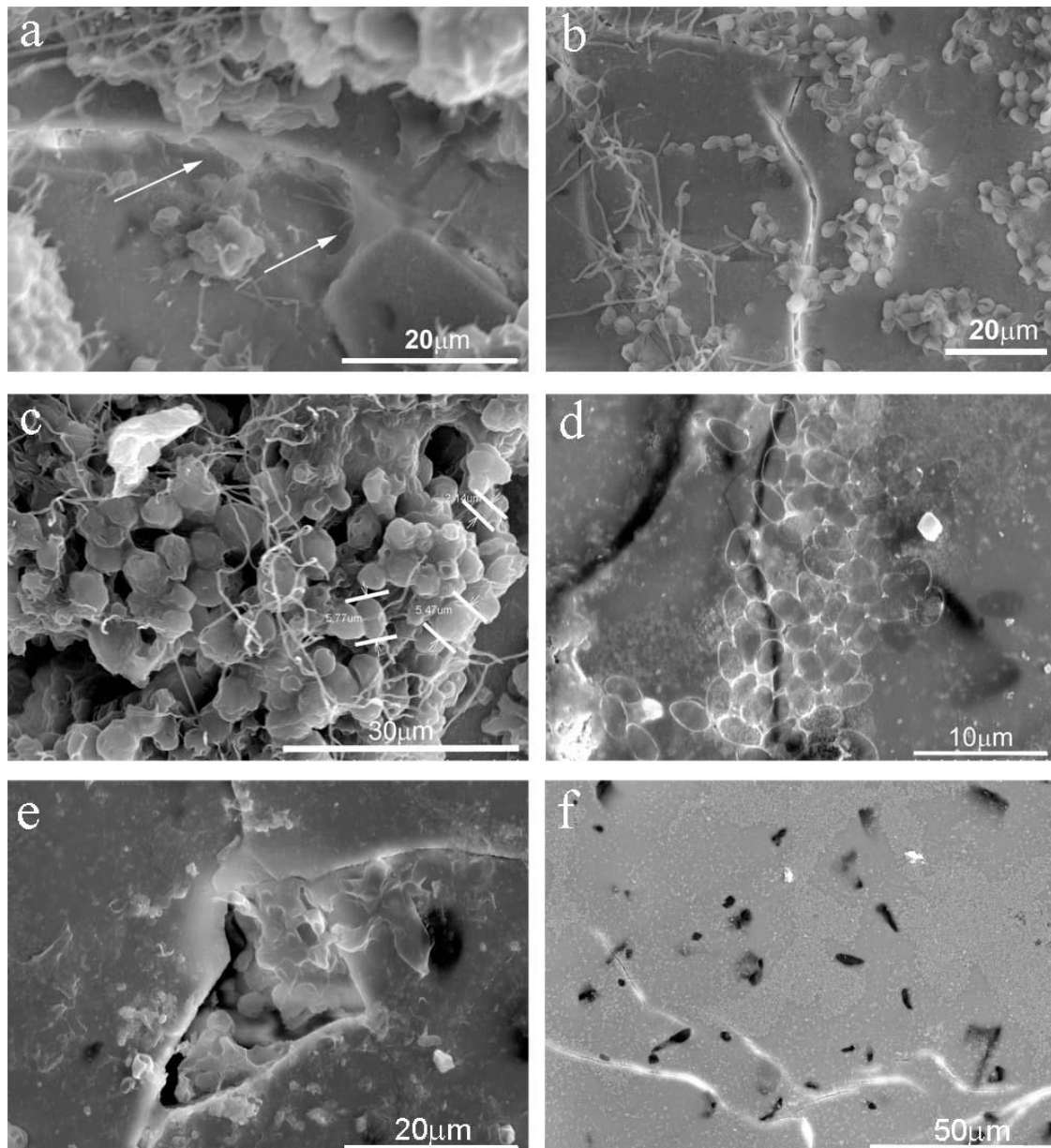
**Fig. 4.12.** SEM images of majolica tile models after inoculation experiments. (a) Growth of microorganisms within a fissure of a pristine model glaze with EPS indicated by arrows. (b) Colonization near a fracture of the aged glaze with penetration EPS into the fracture. (c) oval shapes phototrophic microorganism over a pristine glaze sample (d) and fingerprints of oval shaped cell after removal of the biofilm on the same pristine sample (e) Growth of microorganisms within a surface fracture of a pristine tile. (f) Surface of the control pristine glaze after experiment.

### 4.3.5. Post experimental capillary water absorption

Capillarity coefficient of the control and inoculated samples (pristine and aged) after the 12 months incubation experiment were also calculated in order to determine if the phototrophic colonization altered this particular hydric property (Fig. 4.13). As expected, Pristine control samples still showed a lower capillary coefficient (1.5-2.1 $g.m^{-2}.s^{-1/2}$) than aged control samples. These former samples also showed a higher variation range of capillary coefficient values (7.9-13.4 $g.m^{-2}.s^{-1/2}$) (Fig. 4.13).
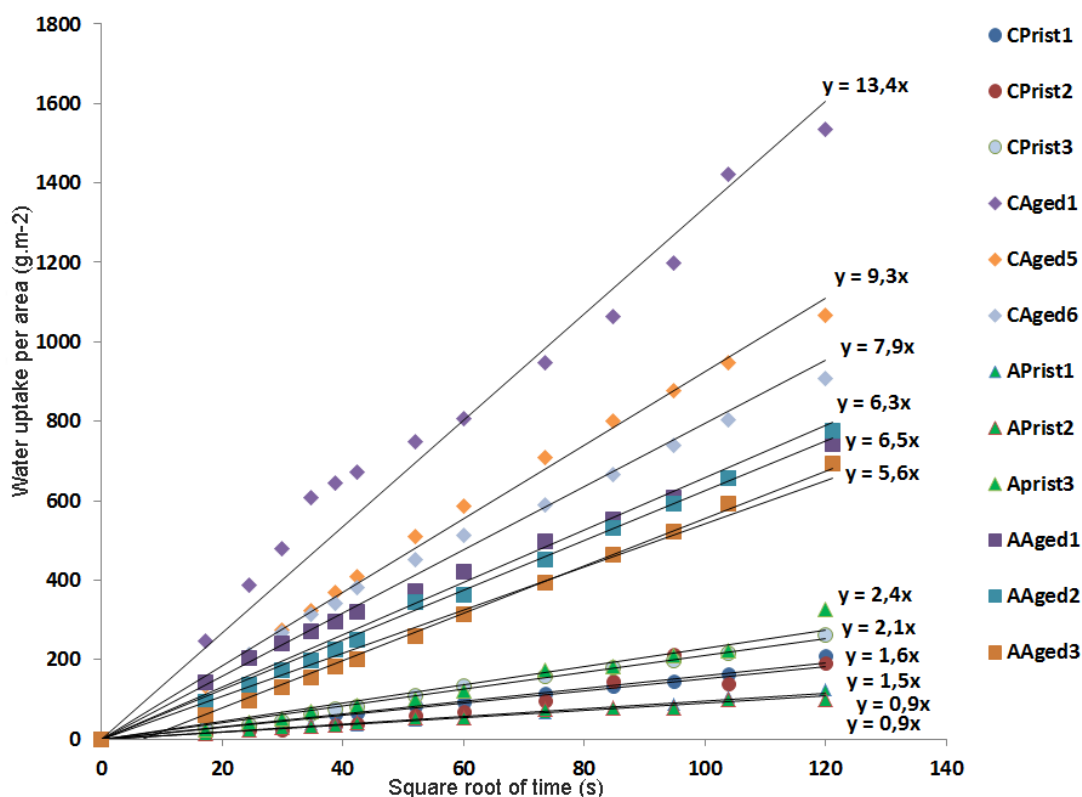
**Fig. 4.13.** Water uptake by capillarity of the pristine and aged inoculated samples (APrist and AAged) and control samples (CPrist and CAged) with linear trendlines and equation with capillary coefficient values.

After the removal of the biofilm from the glazed surfaces, water uptake of the inoculated pristine and aged tile samples after the 12 months of incubation was also measured. Aged inoculated samples showed a lower water uptake and thus a lower capillary coefficient (5.6-6.32 $g.m^{-2}.s^{-1/2}$) in comparison to the control samples (Fig. 4.13). Yet, capillary coefficient values of controls and inoculated samples were not significantly different ($p<0.05$). Pristine samples showed no particular tendency (0.9-2.4 $g.m^{-2}.s^{-1/2}$) in comparison to the pristine control samples (Fig. 4.13).

### 4.3.6.    Characterization of the corrosion products

Characterization of the corrosion products after the biodeterioration experiment was performed on both control and inoculated pristine and aged samples which presented corrosion products on the surface. These comprised mainly majorly crystalline compounds identified by µ-Raman as calcium carbonate and calcium sulphate. Raman spectra of the calcium compounds showed bands at 156, 286, 712 and 1088 $cm^{-1}$ (Maguregui et al., 2009) for the carbonate and bands at 412 and 1008 $cm^{-1}$ (Maguregui et al., 2009) for sulphate. However, due to fluorescence

interference caused by the biofilm, the identification of compounds on the inoculated samples was difficult.

### 4.3.7. Chemical characterization of the glaze surface

In order to understand if there was an uptake of elements by the microorganisms and/or depletion of elements from the glaze during the biodeterioration experiment, the glazed surface of control samples and inoculated samples after biofilm removal were analysed by u-PIXE (Table 4.4).

After the experiment, analysis of control samples showed no significant change regarding the major and minor components of the glaze, being the values in the range of variation of the pristine and aged samples before the experiment (Table 4.1). CaO seemed to be the only oxide that presented some variation in regard to values before the experiment, with an increment from 1 wt. % to 2-3 wt. %. Concerning the inoculated samples, although average values seemed to indicate an increase of PbO in relation to the control samples, these differences were not statistically significant.

**Table 4.4. Chemical composition of control and inoculated samples after 12 months incubation**

| Sample | Control | | Inoculated | |
|---|---|---|---|---|
| | Pristine (t=12m) | Aged (t=12m) | Pristine (t=12m) | Aged (t=12m) |
| $Na_2O$ | 0.3±0.1 | 0.3±0.1 | 0.3±0.1 | 0.3±0.1 |
| $MgO$ | 0.4±0.04 | 0.4±0.02 | 0.4±0.01 | 0.4±0.1 |
| $Al_2O_3$ | 3.1±0.15 | 3.0±0.07 | 3.0±0.2 | 3.1±0.4 |
| $SiO_2$ | 45.5±4.0 | 42.7±1.0 | 45.4±4.4 | 41.7±4.8 |
| $P_2O_5$[1] | n.d. | 0.1±0.2 | n.d. | 0.2±0.3 |
| $Cl$[1] | 0.1±0.09 | n.d. | 0.1±0.1 | 0.2±0.01 |
| $K_2O$ | 1.5±0.2 | 1.4±0.1 | 1.4±0.1 | 1.4±0.2 |
| $CaO$ | 2.1±1.8 | 2.9±3.2 | 1.3±0.2 | 1.5±0.8 |
| $TiO_2$ | 0.1±0.02 | 0.1±0.02 | 0.1±0.01 | 0.1±0.1 |
| $Fe_2O_3$ | 0.2±0.03 | 0.3±0.02 | 0.2±0.01 | 0.2±0.1 |
| $SnO_2$ | 9.9±0.48 | 10.0±0.72 | 10.3±1.6 | 10.8±1.0 |
| $PbO$ | 36.7±3.9 | 38.9±3.4 | 37.5±2.9 | 40.1±3.4 |

N.D. – not detected

For detecting chemical damage on the glazes surfaces, μ-PIXE mapping of Si and Pb were performed on colonized and non-colonized areas within the same sample (Fig. 4.14 and Table 4.5). The mapping confirmed that no significant alteration, on distribution of these two elements (Si and Pb) was observed and heterogeneity of their distribution was associated to the glaze microstructure (Fig. 4.14).
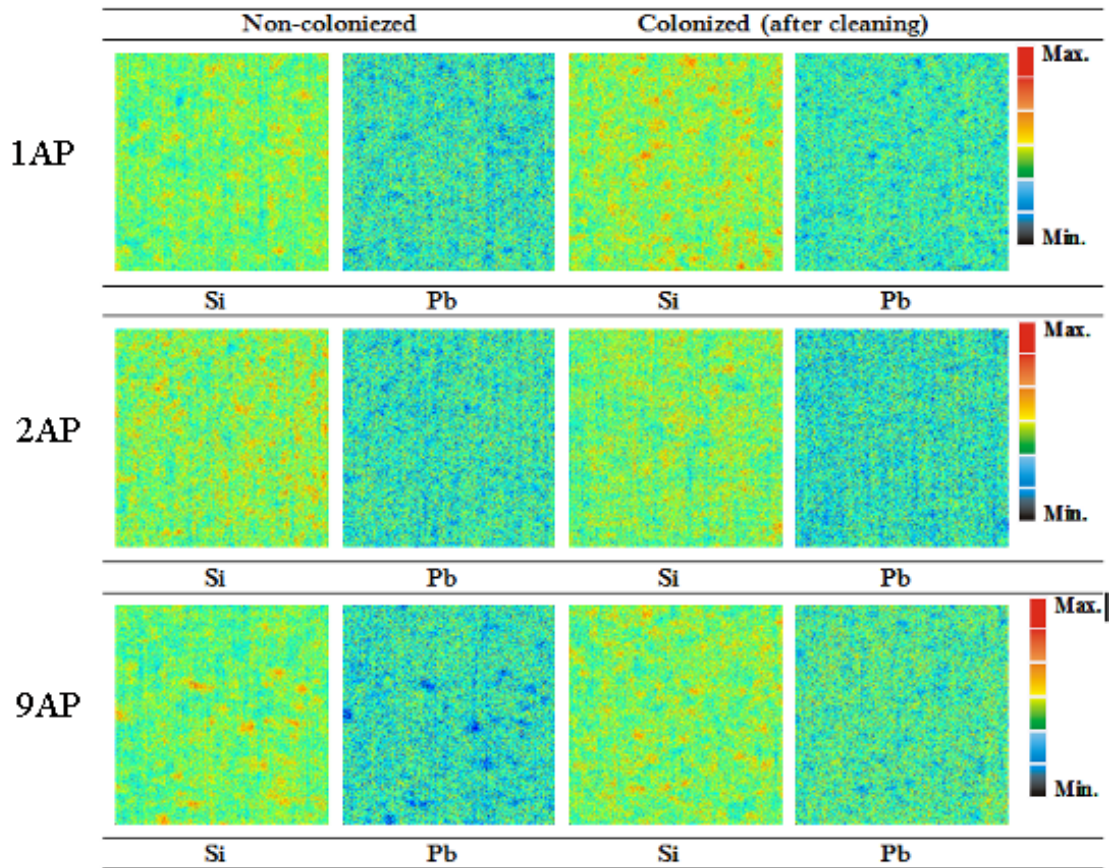
**Fig. 4.14.** PIXE mapping of the glaze surface on three pristine inoculated samples (1AP, 2AP and 9AP) on a non-colonized area and on a colonized area after biofilm removal.

The results of the analysis correcponding to each mapped area (Fig. 4.14), also confimed that no statictically significant and systematic alteration on the other elements of the glaze (Table 4.5)

**Table 4.5** Surface composition of the colonized samples on areas previously covered by biofilm and non-colonized areas.

| Sample | 1AP | | 2AP | | 9AP | |
|---|---|---|---|---|---|---|
| Area | NC | C | NC | C | NC | C |
| Na$_2$O | 0.36 ± 0.02 | 0.30±0.03 | 0.65±0.03 | 0.31±0.02 | 0.32±0.02 | 0.34±0.03 |
| MgO | 0.35±0.01 | 0.37±0.01 | 0.37±0.01 | 0.36±0.01 | 0.37±0.01 | 0.38±0.02 |
| Al$_2$O$_3$ | 3.08±0.02 | 2.99±0.02 | 3.03±0.02 | 3.07±0.02 | 3.03±0.02 | 3.17±0.02 |
| SiO$_2$ | 50.21±0.05 | 46.08±0.05 | 49.6±0.05 | 48.96±0.05 | 47.9±0.05 | 48.23±0.05 |
| Cl | 0.15±0.01 | 0.18±0.01 | 0.24±0.01 | 0.15±0.01 | 0.14±0.01 | 0.17±0.01 |
| K$_2$O | 1.65±0.02 | 1.47±0.02 | 1.79±0.02 | 1.52±0.02 | 1.62±0.02 | 1.42±0.02 |
| CaO | 1.06±0.02 | 1.71±0.03 | 1.33±0.02 | 1.15±0.02 | 1.21±0.02 | 0.97±0.02 |
| TiO$_2$ | 0.09±0.01 | 0.09±0.01 | 0.08±0.01 | 0.11±0.01 | 0.07±0.01 | 0.1±0.01 |
| Cr$_2$O$_3$ | N.D. | 0.08±0.01 | N.D. | N.D. | N.D. | 0.01±0.01 |
| Fe$_2$O$_3$ | 0.23±0.01 | 0.22±0.02 | 0.16±0.01 | 0.23±0.01 | 0.22±0.01 | 0.2±0.02 |
| SnO$_2$ | 9.28±0.09 | 10.14±0.09 | 9.33±0.09 | 9.16±0.09 | 9.78±0.09 | 9.39±0.09 |
| PbO | 33.54±0.5 | 36.39±0.055 | 33.43±0.5 | 34.99±0.54 | 35.34±0.51 | 35.63±0.53 |

NC, non colonized area; C, colonized area

N.D.,not detected

## 4.4 Discussion

### 4.4.1 Tile models

The characterization of tiles from Pena National Palace (Portugal) showed a glaze composition of an alkali-lead silicate glaze, commonly applied in the majolica production technique (Tite, 2009). The major oxide composition of these 19th century tiles was qualitatively similar to the earlier majolica glazes of the 17 and 18th century found in Portuguese tiles (Coentro et al., 2012; Silva et al., 2014). The main difference was related to the proportions of some oxides, namely Na$_2$O, K$_2$O and Al$_2$O$_3$. The production of ceramic tile models is complex, since the glaze and ceramic body have in their composition many mineral raw materials. Besides the materials, a variety of other factors can influence the final characteristics of ceramic products, such as granulometry and firing conditions (temperature, cycle and atmosphere). Therefore, a commercial ceramic paste was selected that would present the suitable characteristics to allow the firing of the glaze and being relatively porous. The produced glaze was an approximate composition of the glaze found in the Pena National Palace tiles (Table 3.2). The compounds selected for the glaze production in this work, solely comprised materials with known compositions and a commercial frit (powdered glass). However, in historic glazes other crystalline phases different from quartz and tin oxide can be found, such as potassium feldspars (Coentro et al., 2012). The absence of feldspar minerals probably was responsible for the slightly lower concentration of alkalis on the final composition of the tile models (Table 4.1). Apart from the surface composition, another surface feature evaluated was the microfissures network of the glaze. These cracks present also on the pristine model tiles were intentionally produced. Differential thermal properties of the glaze and ceramic body and tensions of glassy matrix with crystalline inclusions during cooling might result in

fissures (Eggert, 2006; Carter and Norton, 2013). Traditional firing is often accompanied by production faults, for instance the presence of microfissures network has been described as very common on historical glazed tiles (Mimoso et al., 2011; Personal observation).

The artificial ageing was traduced in changes in the microfissures network. More cracks were visible on the surface of the aged samples (Fig. 4.6). Although the glaze is an impermeable coating, the presence of surface flaws, such as pitting or fissure network results in a higher permeability of the glaze. Thus, the differences in water permeability of the pristine and aged tiles could be justified by the differences in the fissure network observed on the tile models. Since fissures were broader on the aged samples, the water uptake was consequently higher (Fig. 4.7). The relation between crack network and water transport properties has been analysed in concrete samples, denoting a strong correlation between crack network parameters and water transport properties (Zhou et al., 2012).

The properties related to water movement have been described as determinant on the primary bioreceptivity of a substrate, since water availability is the main limiting factor of microorganism's growth (Miller et al., 2009; Gazulla et al., 2011; Portillo et al., 2011).

The surface roughness of glazes, which is dependent on the micron-scaled irregularities in the surfaces caused by crystals, un-reacted raw materials and surface flaw (Fröberg and Hupa, 2008). The presence of mineral inclusions affects the glazes corrosion and its physical features such as roughness (Fröberg and Hupa, 2008). Based on these facts, the presence of quartz and cassiterite mineral inclusions was essential for the tile model glazes produced in order to be similar to historical glazes regarding surface microstructure and phase composition. The corrosion of glazes with mineral inclusions by alkaline attack have shown to be accompanied with the slight increase of roughness values due to differential corrosion of the glassy matrix and crystalline inclusions (Cannillo et al., 2009). The increase of roughness has been regarded as favourable surface feature for microbial colonization (Koestler et al., 1997). However, in this case no significant differences of surface roughness were observed for the pristine and aged samples. Bidimensional measurements of the surface texture by contact technique (mechanical stylus), might have some drawbacks in relation to the microstructure characterization (Santos and Júlio, 2013). Although the topography of the glaze was characterized, localized roughness alteration, such as observed by SEM (Fig. 4.6) and smaller scale roughness might not have been evaluated, which could explain why no significant differences between the pristine and aged samples roughness was observed, even if surface gloss and SEM observations seemed to suggest a difference.

The physical deterioration of glazed wall tiles occurs due to several factors, such as water movements, freeze-thaw cycles and salt crystallization (Borges et al., 1997). These factors lead to volume fluctuations due to different expansion properties of the glaze and the raw clay materials resulting in crack propagation and later in scaling of the glaze (Eggert, 2006). Such deterioration forms have been associated with an increase in water permeability and decrease of physical resistance of the substrate (Borges et al., 1997; Larbi, 2004; Figueiredo et al., 2009).

Based on the chemical and mineralogical composition of the produced glazed models and on the physical features (hygric properties) we can consider that the produced models were

suitable to represent majolica glazed tiles. In addition, the ageing process resulted in alterations similar (broadening and densification of fissures and higher permeability) to those observed on weathered tiles. Therefore, chemical and physical features representing the initial state of the pristine and aged tile models (see Table 4.1 and Table 4.2) seem to be suitable models for the biodeterioration experiment.

### 4.4.2  Bioreceptivity

Bioreceptivity assessment of a given material involves the quantification of the microbial growth (Guillitte, 1995; Miller et al., 2012). Therefore, after the biodeterioration experiment a set of techniques were applied for characterizing the photosynthetic-based biofilms developed on the glazed surfaces (image analysis, colorimetry and fluorescence spectroscopy). These techniques have been extensively used in the characterization of photosynthetic biofilms on inorganic surfaces (Miller et al., 2009; Sanmartín et al., 2010; Rogerio-Candelera et al., 2011). Moreover, Miller et al. (2012) claimed, in a literature review concerning the bioreceptivity of stone, that these methods appeared to be the most reliable for estimating epilithic biomass on stone surfaces.

The digital image analysis allowed the determination of the growth extent of the green biofilms covering the tiles surface. The collected data indicated that the growth of photoautotrophic microorganisms was higher on the aged tiles (Fig. 4.11). This fact was also supported by Chl *a* fluorescence, which revealed higher amounts of Chl*a* on the aged tile models.

In addition, CIELAB color parameters were used to quantify the differences verified by visual examination (Table 4.3). A lower L* parameter value of the aged samples covering-biofilm resulted from a darker color, and thus indicated higher concentration of Chl a pigment and therefore more phototrophic microorganism biomass (Sanmartín et al., 2010). Also a* parameter (redness-greenness), showed that the biofilm on aged samples was significantly greener than on the pristine samples. This color parameter, despite being less significant than L*parameter, has also been linked to the photosynthetic pigments concentration (Chl*a*, carotenoids, and phycocyanins) (Sanmartín et al., 2010) (Table 3). All this results indicated that the development of microorganisms was higher on the aged tiles, thus their bioreceptivity was higher than the pristine model tiles.

The main differences in bioreceptivity between pristine and aged tiles were related to the hydric properties (water absorption by capillarity and water vapor permeability). All values obtained for these features were higher on the aged samples and these could justify their higher bioreceptivity. In fact, studies that appraised the bioreceptivity of different clay roofing tiles substrates by phototrophic microorganisms also concluded that higher porosity lead to an increase of bioreceptivity of phototrophic microorganisms (Gazulla et al., 2011; Portillo et al., 2011). Water availability and surfaces with anchoring sites and micro-refuges are known to support the attachment and settlement of biological colonization (Scardino et al., 2008).

Artificially aged glaze surfaces were more susceptible to colonization by phototrophic microorganisms than pristine glaze surfaces. Based on these facts we can infer that the ageing

processes of glazed ceramics probably result in an increase of the features which increase bioreceptivity. Thus, the conservation condition of glazed ceramics substrates is an important issue in what concerns bioreceptivity and more deteriorated glaze tiles might be more rapidly colonized than sound or new glaze tiles.

### 4.4.3 Biodeterioration

Biodeterioration damage, particularly physical damage, caused by the inoculated phototrophic microorganisms were observed on the tile models after 12 months-incubation. Colonization within fissures of the glaze, as in other substrates causes physical stress damage and on glazed substrates could lead to the flaking of the glaze (Palmer and Hirsch, 1991; Mandal and Rath, 2013). This form of physical damage due to chasmolithic growth of biofilms on glazed ceramics has been reported in the literature indicating that the development of these microorganism on glazed ceramic tiles can seriously compromise their durability (Palmer and Hirsch, 1991; Coutinho et al., 2013). However, we could not detect a significant change of the hydric properties of the glazed tile models due to biological action (Fig. 4.13). Yet, all values obtained for the aged inoculated samples were lower in comparison to the aged control samples. The remains of EPS and other substances in the fissures of the glaze could explain these changes in the permeability of the aged samples. Nevertheless, we could observe biological imprints on the inoculated samples (Fig. 4.12d).

Regarding the biochemical attack on glaze, the corrosion products identified after the experiment were carbonates, which are common corrosion products of silicate glass (Rodrigues et al., 2014) and ceramic body (Maguregui et al., 2009). However, this compound was also present on control samples, which were kept under the same humid conditions during 12 months. This indicates that these carbonates are a natural product of the tiles ageing when in humid conditions.

The chelating action of EPS and other macromolecules produced by phototrophic microorganisms to capture divalent ions and other metal ions have been well described in the literature (e.g. Rossi et al., 2012; Suresh Kumar et al., 2014). In fact, some cyanobacterial strains have shown capacity to bind calcium ions, which is indicative of chemical and physical damage on the substrate (Rossi et al., 2012). However, in the present work results were inconclusiveconcerning the difference between the quantities of formed crystals on the controls and on the inoculated samples, partly because of the dense biofilm formed on the colonized surfaces that hindered the visualization of corrosion products.

Regarding the alteration of the surface composition we could observe that there was slight increase in lead composition. The corrosion of historical lead based glaze compositions has been described to occur with lead lixiviation and the formation of a lead rich layer that is detached when reaching a certain thickness (Bonnet, 2003). Some phototrophic microorganisms have been described as having acid EPS (Rossi et al., 2012), and the corrosion of lead glazed in acid media results in the increase of lead lixiviation rate (Wood and Blachere, 1978). However, the

obtained variation between inoculated areas and non-colonized areas were not significantly different.

## 4.5    Conclusions

In resume, the bioreceptivity of tile pristine samples was lower than aged tile samples indicating that the susceptibility to biological colonization is related to the intrinsic properties of the substrates.

The biodeterioration experiment have demonstrated the damaging potential of the tested phototrophic microorganisms on glazed wall tiles, through chasmolithic growth, that can lead to glaze detachment as observed on the tiles from Pena National Palace (Chapter 3). With this experiment it was possible to observe that this damage can occur without any other deterioration form, such as soluble salt decay or frost damage.

Glazed ceramic tiles are complex composite materials, which difficult the evaluation of the biochemical deterioration process. Therefore, further research will be necessary to effectively quantify the effect of the microorganisms on the chemical corrosion of glazed surfaces.

# Biodeterioration of majolica tiles by the fungus *Devriesia imbrexigena* under laboratory conditions
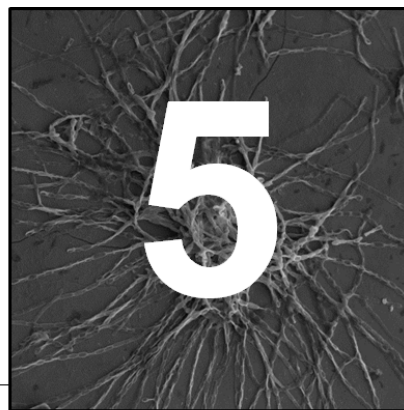
It is well known that fungi can be found on cultural heritage assets, promoting material´s biodeterioration. However, little is known on the biodeterioration damage of glazed tiles induced by these microorganisms, even though they constitute part of the microbial communities that colonize glazed wall tiles (Chapter 2 and 6). In this chapter biodeterioration of pristine and artificially aged majolica tile models caused by the fungus *Devriesia imbrexigena* was assessed under laboratory conditions. This fungal species was previously identified and isolated from biodeteriorated artistic tiles of the Pena National Palace, Portugal (Chapter 3). The extent of fungal growth was evaluated by digital image analysis after 12 months of incubation. Optical microscopy, SEM, µ-Raman and µ-PIXE analyses were also conducted to evaluate fungal biodeterioration on the majolica tile models. The results revealed that organic acids exuded by *D. imbrexigena* induced the precipitation of calcium oxalate crystals on the glaze surface.

## 5.1    Introduction

Outdoor assets are subjected to the development of biological patinas on their surfaces which can lead to undesirable alterations designated as biodeterioration (Hueck, 1965). On ceramic materials the main biodeteriogenic effects previously described in Chapter 2 are: (i) aesthetic biodeterioration due to the production of organic pigments and development of colored biofilms; (ii) physical biodeterioration resulting from mechanical forces produced by biofilms on pores, cracks, fissures and ceramic-glaze interface and (iii) chemical biodeterioration due to direct action of metabolic products excreted by microorganisms.

Some fungi, like black yeasts and meristematic fungi, are able to survive in adverse environmental conditions, such as low humidity and high sun irradiation due to the production of melanin and meristematic development, making them apt to develop on inorganic substrates (Sterflinger, 2010). Giacomucci et al. (2011) identified *Aureobasidium pullulans* and uncultured Dothioraceae, among other fungi on adhesive treated glazed wall tiles. These authors related the presence of *A. pullulans* to climatic conditions, particularly high relative humidity, as they were mainly on tiles from the lower part of the building.

The role of fungi on the biodeterioration of inorganic materials, such as stone wall paintings and glass, is well known (Saiz-Jimenez et al., 2012; Sterflinger and Piñar, 2013; Rodrigues et al., 2014, Leo and Urzi, 2015). Laboratory experiments with unglazed ceramics have shown that fungi were able to form bioprecipitates and penetrate into pores causing biodeterioration (Radeka et al., 2007a, 2008). Several studied on colonized glass from cultural heritage assets (Rolleke, 1999; C Schabereiter-Gurtner et al., 2001; Carmona et al., 2006) and laboratory experiments (Gorbushina and Palinska, 1999; Bartosik et al., 2010; Rodrigues et al., 2014) have provided an important insight on glass biodeterioration. However, studies regarding glazed tiles have only focused on the identification of microorganisms (Oliveira et al., 2001; Pedi et al., 2009; Giacomucci et al., 2011; Coutinho et al., 2013). To the best of our knowledge no laboratory experiments have been performed on fungal biodeterioration of glazed ceramic tiles. As previously mentioned in this work, to gain an insight on the biodeterioration of building materials both field sample analysis and laboratory studies should be conducted. Therefore, laboratory based biodeterioration experiment is essential to have a better understanding of the effects of fungal growth on glazed tiles. The fungus *Devriesia imbrexigena*, AJL Phillips & ML Coutinho, a dematiaceous fungus previously identified on majolica glaze tiles from Pena National Palace (Chapter 3) (Crous et al., 2012), was selected for this biodeterioration experiment . Since biodeterioration damage were observed on Pena National Palace tiles (Chapter 3), the biodeterioration produced by the fungus *D. imbrexigena* was studied in this chapter both on pristine and artificially aged majolica glaze tile models.

Tile models were produced with similar glaze composition as those of Pena National Palace glaze tiles. Half of the produced tile models were artificially aged to simulate weathering. The production and ageing processes of the glazed tile models were described in Chapter 4. In order to assess tile biodeterioration under laboratory conditions, tile models were inoculated with *D. imbrexigena* and incubated for 12 months. At the end of the incubation period, fungal growth was evaluated by digital image analysis on both pristine and aged tile models. Biodeterioration damage were assessed by optical microscopy (OM), scanning electron microscopy (SEM), micro Raman spectroscopy (μ-Raman) and micro particle induced X-ray emission analysis (μ-PIXE).

## 5.2    Materials and methods

### 5.2.1    Pristine and aged majolica glazed tile models

Glazed wall tiles were reproduced in the laboratory according to the manufacturing of ceramic tiles such as described in section 4.2.1 (Chapter 4). For studying the bioreceptivity of glazed tiles and subsequent biodeterioration, half of the tile models (19) were maintained pristine and the other half was subjected to accelerated ageing through a process described in section 4.2.2 (Chapter 4). The chemical composition of the pristine and aged tiles is presented in Table 4.1 (Chapter 4).

The main physical features of the pristine and aged tile models are summarized in Table 5.1. Experimental data were subject to analysis of variance (ANOVA) made with Microsoft Excel 2010 software for Windows, and the averages were compared by the Tukey HDS Test at the 5% level of significance.

**Table 5.1** Average and standard deviation (±Std) of pristine (n=3) and aged (n=3) samples with ANOVa results (adapted from Table 4.2, Chapter 4).

| Model tile | Q | δ | Ra |
|---|---|---|---|
| **Pristine** | 1.3±1.4(a) | $1.5\times10^{-10}\pm4.6\times10^{-11}$(a) | 12.6±3.2(a) |
| **Aged** | 10.8±6.1(a) | $3.9\times10^{-10}\pm1.3\times10^{-10}$ (b) | 13.0±1.4(a) |

Q, capillarity coefficient (g.m-2.s-1/2); δ, water vapour permeability coefficient (Kg/m.h.Pa); Ra, average roughness (Å)

Mean ± SD;

Values followed by the same letters in brackets in the same column are not significantly different by the Tukey HDS test at p<0.05.

### 5.2.2   Laboratory-based tiles biodeterioration experiment

An axenic culture of the fungus *D. imbrexigena,* previously isolated from glazed tiles from Pena National Palace (Chapter 3; Crous et al., 2012) was used for inoculating the glazed tile models. This fungus was a dominant species on the biofilm samples from Pena National Palace tiles (Chapter 3). The fungus was grown in half-strength PDA plates at room temperature. For preparing the inoculum, fungal biomass was scraped from the PDA plates with a sterile scalpel and suspended in diluted PDA liquid medium (2%) (Scharlau, Spain). Although the fungus was collected from nutrient-poor substrates (glazed tiles), it was part of a biofilm being surrounded by photosynthetic microorganisms that provided nutrients for its survival. Therefore nutrients at low concentration (diluted PDA liquid medium) were added in the inoculum suspension ($10^5$cells/mL) to simulate a nutrient poor substrate. At the inoculation day, each set of tiles was placed over a net inside a glass Petri dish ($\varnothing$ = 9 cm) with distilled water at the bottom to avoid direct contact with water (Fig. 4.1 in Chapter 4).

Pristine and aged tile samples were placed separately inside two Petri dishes (Fig. 5.1). A third Petri dish was used for control samples: three pristine and three aged tile samples. Prior to the inoculation, all Petri dishes were autoclaved at 121 ºC at 100 kPa above atmospheric pressure for 20 min. After slow cooling, 150 µl of fungal suspension was inoculated onto the glazed surface of the tile models. The six control samples were not inoculated (Fig. 5.1). The remaining samples were re-inoculated with 150 µl of the fungus suspension every 3 months, to simulate reposition of cell that occurs in natural environments. The fungal suspension was freshly prepared following the procedure described above. All tile samples (inoculated and control samples) were kept under the same conditions (22–23 ºC and 75–95% RH) during the incubation period (12 months).

**38 total tile samples**
**(pristine and aged)**

**6 control tile samples**

**32 inoculated tile samples**

**3 pristine tile samples**

**3 aged tile samples**

**16 pristine tile samples**

**16 aged tile samples**
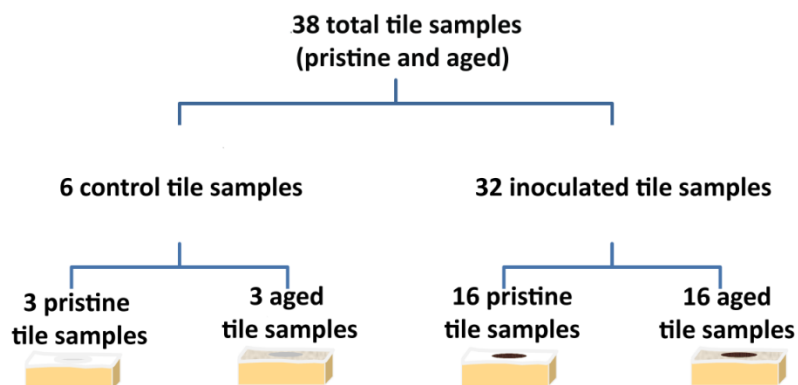
**Fig. 5.1.** Scheme of the experimental design showing the number of replicates of pristine and aged control and inoculated samples.

### 5.2.3    Post-experiment analyses of tile surface alterations

A multi-analytical approach was used to characterize morphological and chemical alterations on the glaze surfaces after 12 months of experiment.

### 5.2.3.1 Quantification and characterization of the fungal growth on the glazed tiles

Photographic records were made with an Olympus C-5060 digital camera every three months. A Kodak color scale was included in each record for light and color adjustment of the images. At the end of the incubation experiment, the surface area covered by the black fungus was estimated by digital image analysis. Digital images of the colonized glazed tile samples were individually recorded as described in section 4.2.3.2 (Chapter 4.)

### 5.2.3.2  Optical microscopy

Microscopic observations and documentation were carried out using a Zeiss Axioplan 2 light microscope fitted with a Nikon DMX digital camera.

### 5.2.3.3  SEM-EDS analysis

Pristine, corroded and control samples were analysed by SEM to assess the fungal proliferation and microbe-substrate interactions after 12 months of incubation. Tile models with the biofilm were first observed in VP-SEM mode with a HITACHI 3700N scanning electron microscope interfaced with a Quantax EDS microanalysis system. The Quantax system was equipped with a Bruker AXS XFlash® Silicon Drift Detector (129 eV Spectral Resolution at FWHM - Mn Ka). VP-SEM mode was performed for observation of fungal structure and EPS and sheath coverage in 10 kV accelerating voltage, 10mm working distance and 30Pa. The operating conditions for EDS analysis were in backscattered electron mode, 20 kV accelerating voltage, 10–12 mm working

distance and 120 mA emission current.

Then, samples were coated with gold and observations were performed under SEM with an energy dispersive spectrometer (EDS) were performed with the same equipment. In secondary electron mode conditions were 20 kV accelerating voltage and 10–12 mm working distance. In addition cleaned tile models were analysed under SEM to assess corrosion patterns, crystalline compounds and leached elements. Biofilm was removed from the samples with a cotton swab embedded in a 1:1 water-ethanol solution.

### 5.2.3.4 Water absorption by capillarity of the pristine and aged tile models

The intrinsic physical characteristics of the control, inoculated pristine (n=3) and aged (n=3) model tiles were assessed after the incubation experiment. Water absorption by capillarity through the glazed surface was measured after removal of the biofilms with a cotton swab embedded in a 1:1 water-ethanol solution. Water absorption by capillarity was quantified according to Pereira and Mimoso (2012) and as described in Section 4.2.4. (Chapter 4). Water capillary coefficient (Q) was noted in $g.m^2.s^{1/2}$.

### 5.2.3.5 µ-Raman

µ-Raman was carried out for characterizing crystals formed on the surface of the glaze using a Labram 300 Jobin Yvon spectrometer, equipped with a He-Ne laser of 17mWpower operating at 632.8 nm and also a solid state external laser of 50 mW power operating at 514.5 nm. Spectra were recorded as an extended scan. The laser beam was focused either with a 10×, 50× or a 100× Olympus objective lens. The laser power at the surface of the samples varied with the aid of a set of neutral density filters (optical densities 0.3, 0.6, 1 and 2). For comparison purposed spectra of the compound whellite ($CaC_2O_4.H_2O$) (Fluka) were also made.

### 5.2.3.6 $\mu$-PIXE

µ-PIXE was performed in order to study potential chemical biodeterioration effects on the glaze surface with an Oxford Microbeams OM150 type scanning microprobe for focusing down to 3 × 4 $\mu m^2$ a 1 MeV proton beam. The glaze samples were irradiated in vacuum and the produced X-rays were collected by an 8 µm thick Be windowed Si (Li) detector with a crystal active area of 80 $mm^2$ and 145 eV resolution. The system configuration used allowed the efficient detection of low energy X-rays such as the ones from Na. Operation and basic data manipulation, including elemental distribution mapping, was achieved through the OMDAQ software code, and quantitative analysis was done with the GUPIX software. The quantification was performed in a representative area of the glaze cross-sections with an area of analysis of ca. 500×500µm. The accuracy of the analysis was described in Chapter 3.

### 5.2.3.7 Statistical analysis

Statistical analysis were made to the results of digital image analysis and capillary coeficient determined on pristine and aged tile models after 12 months experiment. The aim of statistical analysis was to determine significant differences between the average values found for pristine and aged tile models and between control and inoculated samples regarding the above mentioned parameters. The experimental data were subjected to analysis of variance made with Microsoft Excel 2010 for Windows, and the averages were compared by the Turkey HDS Test at 5% level of significance.

## 5.3    Results
### 5.3.1    Evaluation of fungal growth: visual inspection and digital image analysis

Colonization of the glazed tile surfaces by *D. imbrexigena* occurred at a slow rate during the 12 months of the experiment. Fig. 5.2 shows the extent of surface coverage before and after inoculation. According to visual examination, no preferential growth was evident between pristine and aged tile samples.
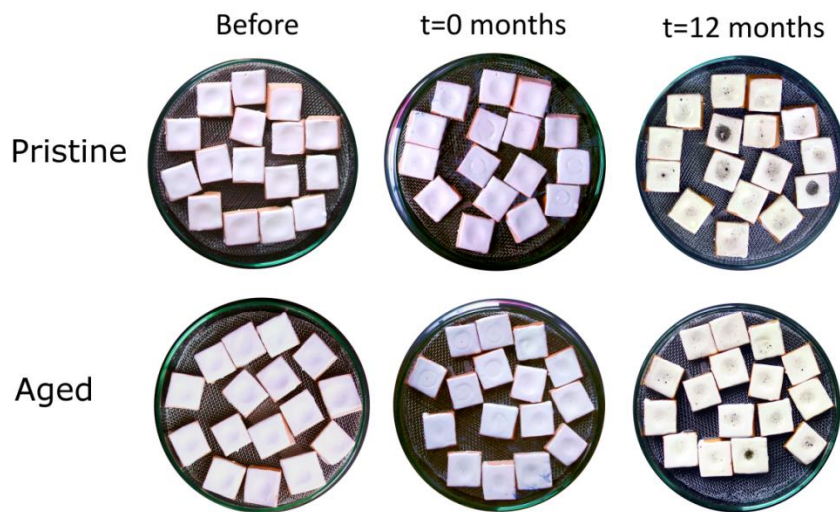


**Fig. 5.2.** Petri dishes with pristine and aged tile models, at three different stages: before inoculation (before), after inoculation (t=0) and after 12 months of incubation (t=12 months).

The quantification of tile areas covered by the fungus was obtained by digital image analysis. These procedures allowed quantifying areas covered by the fungus biofilms and the comparison the difference of the development on each sample (Fig. 5.3)
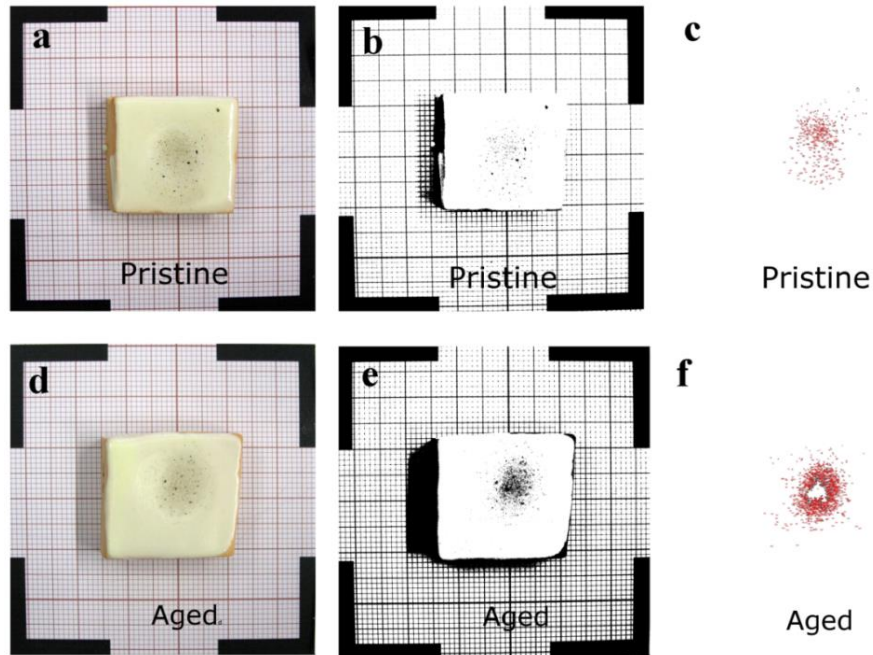
**Fig. 5.3.** Example of the application of digital image analysis in a pristine and an aged tile model covered by the fungus. (a) Original image of the pristine glazed tiles; (b) Segmented image (binary) of the first Principal Component of pristine glazed tile; (c) Outlines of the areas selected for measuring of the extent of fungal colonization from first Principal Component of the pristine glazed tile; (d) Original image of the aged glazed tiles; (e) Segmented image (binary) of the first Principal Component of the aged glazed tiles and (f) Outlines of the areas selected for measuring extent of fungal colonization from first Principal Component of the aged glazed tile.

The values of the areas covered by the fungus were calculated from the segmentation of both the first and third Principal Components. After measuring the areas in every band, the outlines with area below 0.001 mm$^2$ (1 pixel) were ignored for quantification and the average of the two measures (PC1 and PC3) calculated. The tile surface areas covered by fungus presented values with a high variance, ranging from 69 mm$^2$ to 2 mm$^2$ on the aged samples and from 83 mm$^2$ to 0.2 mm$^2$ on the pristine samples, from a total approximate surface area of 625 mm$^2$ per tile. Fig. 5.4 summarizes the valued of covered area obtained for each tile samples showing that dispersion of values was very high, since the extent of fungal proliferation on the samples was very variable. Although the average coverage area was slightly higher on the weathered (22±19 mm$^2$) than on the pristine model tiles (17±24 mm$^2$), due to the high standard deviation the difference in colonization between the pristine and aged samples was not statistically significant (p>0.05).
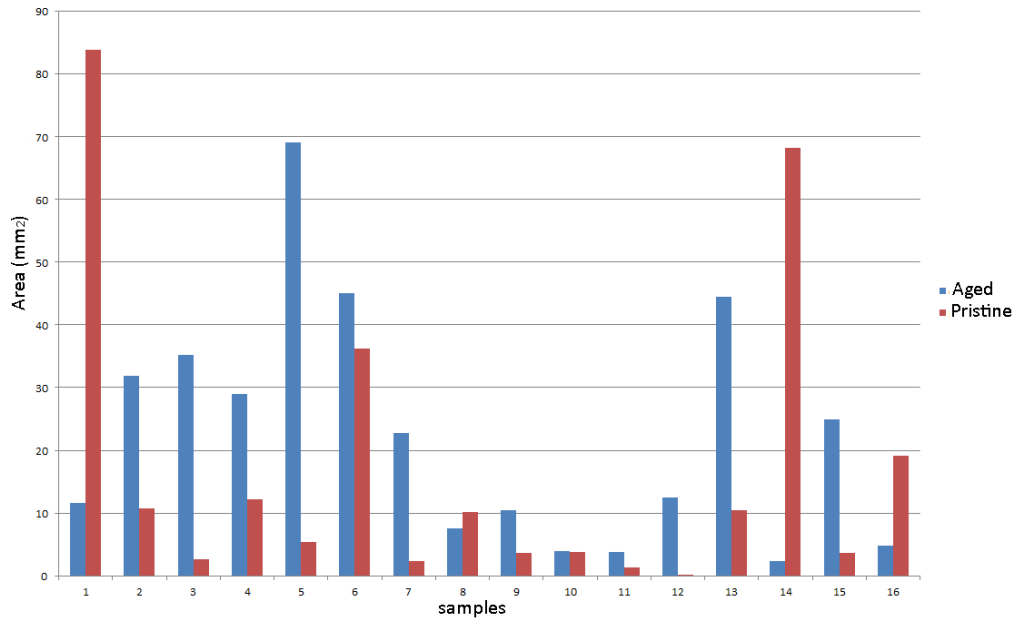
**Fig. 5.4.** Area (in mm$^2$) colonized by the fungus in aged (blue) and pristine (red) tiles obtained by digital image analysis.

### 5.3.2 Optical Microscopy

Pristine and aged glazed tiles were examined by optical microscopy after the incubation period of 12 months. Fig. 5.5 displays examples of control and inoculated samples at different magnifications. On control samples crystals with different sizes were observed over the glaze surface (Fig. 5.5 a, b). The morphology of the crystals at higher magnifications was difficult to evaluate due to the curved surface of the samples and three-dimensional structure of the crystals. Lower magnified images showed the difference between fissure (signed with letter F) network of the pristine and weathered samples (Fig. 5.5 a b), shown in detail in section 4.3.2.2 of Chapter 4 (Fig. 4.5). Regarding the inoculated samples, fungal microcolonies could be observed over the surface and white crystals were seen on the surface and close to the fungal structures (Fig. 5.5 c and d). The crystals on the inoculated samples were bigger than the crystals detected on the control samples. Howeverdue to of the glaze features (white, translucent, heterogeneous and irregular surface), it was difficult to achieve a general overview of the crystal distribution.
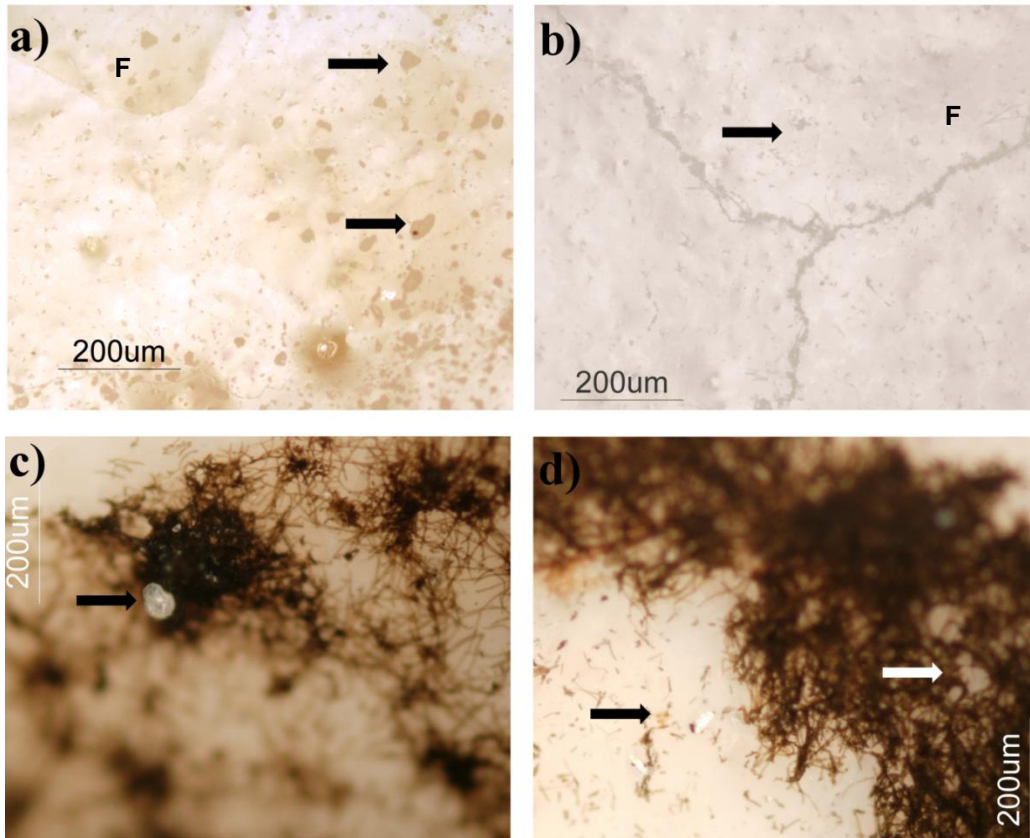
**Fig. 5.5.** Optical microscopy of glazed tile models after 12 months of incubation with crystals indicated by arrows. (a) crystals on the surface of the glaze of a pristine control sample and fissure marked with letter F; (b) crystals on the surface of the glaze of an aged control sample and fissure marked with letter F; (c) crystals and fungal microcolonies on the surface of the glaze of a pristine sample on top of fungi; and (d) crystals and fungal microcolonies on the surface of the glaze of an aged sample.

### 5.3.3  SEM-EDS analysis

SEM observations allowed higher resolution and greater depth of focus of the glaze surface of the control pristine and aged samples (Fig. 5.6). Crystals were found a heterogeneous distributed over the glassy surface of control pristine (Fig. 5.6 a) and aged glazed tile models (Fig. 5.6 c). Higher magnifed SEM images revealed the crystal morphology on both pristine and aged samples with irregular and rhombohedral-like shaped crystals (Fig. 5.6 c, d). EDS analysis allowed their elemental characterization as calcium rich crystals (Fig. 5.6 e, f).
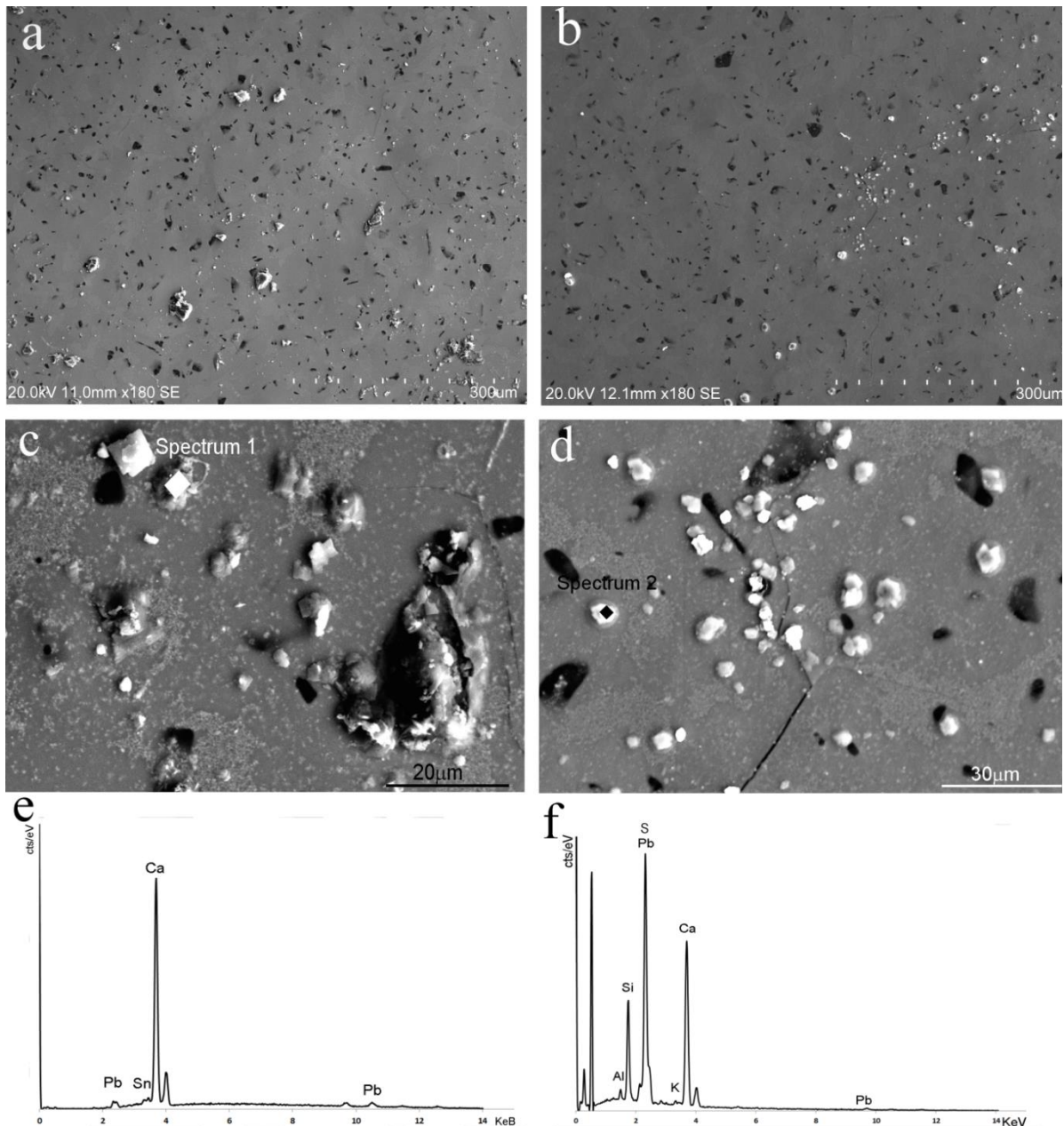
**Fig. 5.6.** SEM images of control glazed tiles after 12 months incubation. (a) crystals on the surface of the glaze of a pristine control sample; (b) crystals on the surface of the glaze of an aged control sample; (c) higher magnification of the crystals shown in (a); (d) higher magnification of the crystals shown in (b); (e) EDS of a crystal indicated as spectrum 1 in (c); and (f) EDS of a crystal indicated as spectrum 2 in (d).

SEM analysis showed the surface of the inoculated glazed tile models after 12 months of incubation (Fig. 5.7). VP-SEM images revealed Ca-rich crystalson the glaze surface with fungal hyphae covered by a mucilaginous matrix, probably EPS (Fig. 5.7a.b). EDS micro-analysis of the crystal revealed high concentration of Ca and C (Fig. 5.7b). On the inoculated samples, larger crystals could be observed and also smaller crystals near to the fungal hyphae (Fig. 5.7c). After removal of the biofilm, on both pristine (Fig. 5.7d) and aged (Fig. 5.7e) glazed tile samples, neither cell imprints were visible on the glazed surfaces nor penetration of hyphae in fissures. On both

pristine (Fig. 5.7c) and aged (Fig. 5.7d) samples *D. imbrexigena* seemed to have developed only on the surface without penetration.
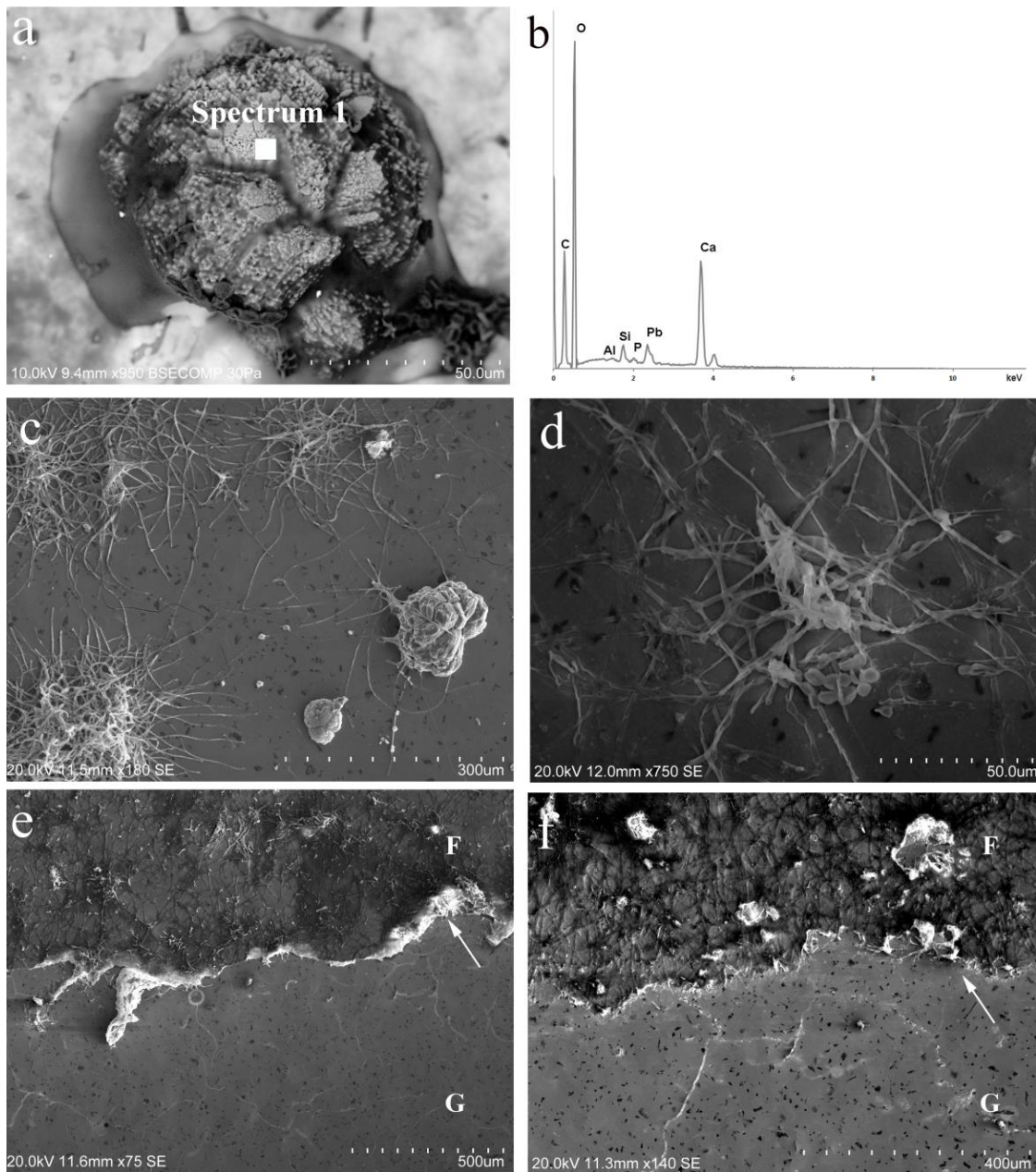


**Fig. 5.7.** SEM images of inoculated glazed tiles after 12 months incubation. (a) VP-SEM BSE image of a crystal on the surface of the glaze of a pristine sample with fungal hyphae covered by a mucilaginous matrix; (b) EDS spectrum of an area signed as Spectrum 1 in (a); (c) crystals on the surface of the glaze of an pristine sample close to fungal biomass; (d) Fungi on the glaze surface on an aged sample; (e) surface of a pristine tile sample with fungal hyphae (F) and clean glaze surface (G) with the interface signed with white arrow; and (f) surface of an aged tile sample with an area covered by fungal hyphae (F) and a cleaned glaze surface (G) with the interface signed with a white arrow.

### 5.3.4   Post-experiment water absorption by capillarity

Fig. 5.8 shows the linear part of the water uptake by capillary of the pristine (n=3) and aged (n=3) control samples (non-inoculated) plotted together with pristine (n=3) and aged (n=3) inoculated tile samples, after 12 months incubation. No significant differences in water uptake could be detected between the pristine control and inoculated samples (Fig. 5.8). Only one inoculated sample (FPrist2) showed a higher slope compared with all other pristine samples. Concerning the aged samples, the slope of the water uptake was higher compared to the pristine samples, in agreement with the initial stage of the pristine and aged tile models (Fig. 4.5 in Chapter 4). The water uptake of the aged control samples showed a slight increase in comparison to the inoculated samples (Fig. 5.8). To summarize, no statistical distinction of the water uptake behavior was obtained forthe control and inoculated tile samples.
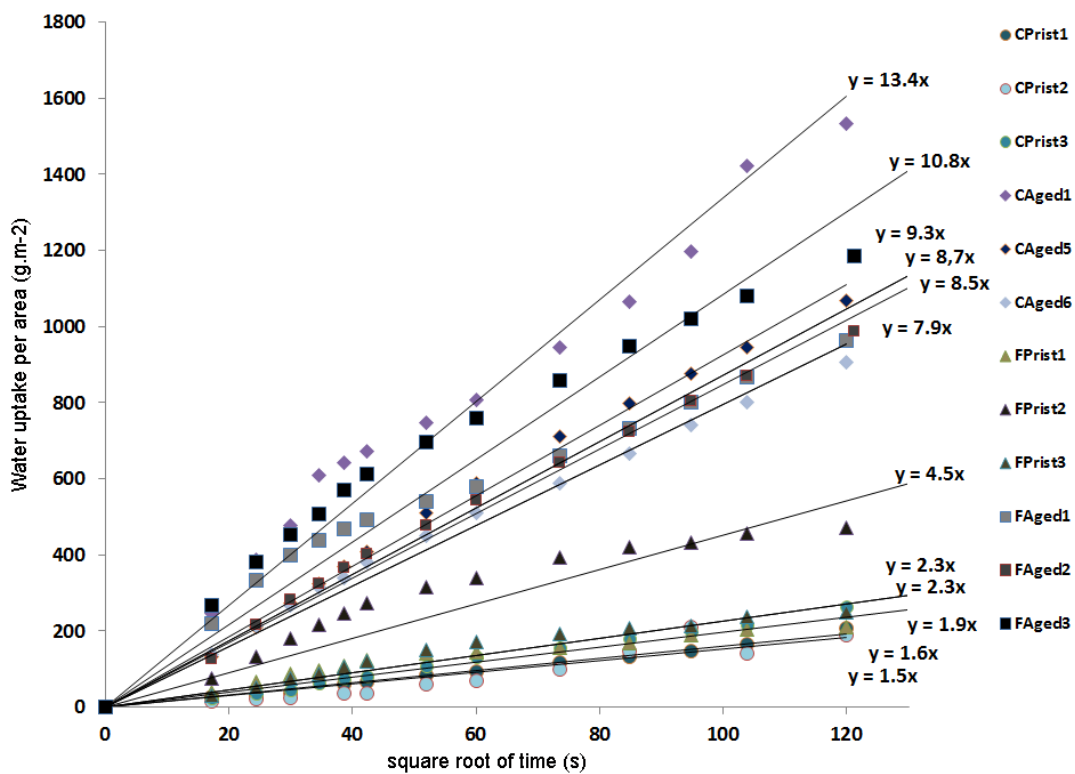


**Fig. 5.8.** Water uptake by capillarity of the pristine and aged inoculated samples (FPrist and FAged) and control samples (CPrist and CAged) with linear trendlines and equation with capillary coefficient values.

### 5.3.5 µ-Raman

The µ-Raman analysis allowed the identification of crystalline substances formed on the glazed tile surfaces (Table 5.2). All samples revealed calcium carbonate crystals over the glaze, which could be identified by the Raman spectra with bands at 156, 286, 712 and 1088 cm$^{-1}$ (Maguregui et al., 2009). Calcium sulphate was also present on the samples with most intense bands at 412 and 1008 cm$^{-1}$(Maguregui et al., 2009).

**Table 5.2.** Crystalline substances found over the glaze samples after 12 months incubation, identified by µ-Raman.

| Tile samples | Calcite (CaCO$_3$) | Gypsum (CaSO$_4$) | Oxalates |
|---|---|---|---|
| Inoculated pristine | * | * | * |
| Inoculated aged | * | * | * |
| Control pristine | * | * | |
| Control aged | * | | |

Regarding the inoculated pristine and aged tiles besides calcite and gypsum, some irregular shaped crystals assigned to oxalates could be detected (Table 5.2 and Fig. 5.9).
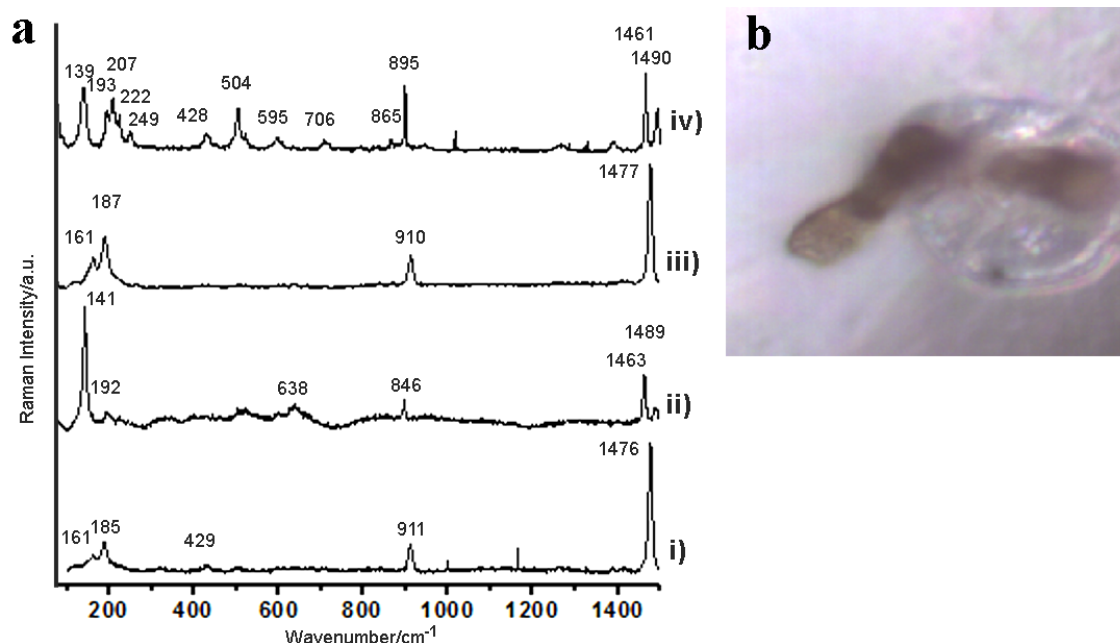


**Fig. 5.9.** Raman spectra and image of crystalline compounds identified over inoculated samples (a) Raman spectra of oxalate crystals over glaze tile samples. (i) Weddellite (CaC$_2$O$_4$.2H$_2$O) found on the surface of inoculated pristine glazes (ii) whellite detected on the surface of an inoculated sample (iii) Weddellite (CaC$_2$O$_4$.2H$_2$O) detected on the surface of an aged glazes and (iv) pure whellite (CaC$_2$O$_4$.H$_2$O) powder reference spectra was made in similar conditions to the tiles spectra. (b) microscopy image ofthe crystals identified in (a(ii)) with a brown fungal structure.

These oxalates may have a biological origin since they do not appear on control samples. Raman spectrum obtained from a crystal on a pristine sample showed characteristics bands at 161, 185, 429, 910 and 1476 cm$^{-1}$ (Fig. 5.9(i)), similar to the banding pattern described for Weddellite

(Frost, 2004). Similar crystals could be detected on the aged glazes (Fig. 5.9 (iii)), showing only a slight shift from the previously described bands. In the same sample, one spectrum was collected with bands at 161, 187, 638, 846, 1463 and 1489 cm$^{-1}$ that could be assigned to whellite (Frost, 2004).

### 5.3.6    µ-PIXE

µ-PIXE was used to analyze the surface of the pristine and aged samples, (controls and inoculated samples), after 12 months of incubation (Table 5.3). On control samples the surface composition did not seem to be significantly altered in comparison with the tile models before incubation (Table 4.1 in Chapter 4). The only exception was observed for calcium which showed a higher value and a higher standard deviation. On the inoculated samples (pristine and aged) no significant alterations in comparison with the respective control samples were noticed.

**Table 5.3.** Chemical composition in oxides of control (Table 4.4) and inoculated samples after 12 months experiment in wt.% (Average and Standard deviation).

| Sample | Control | | Inoculated | |
|---|---|---|---|---|
| | Pristine (t=12m) | Aged (t=12m) | Pristine (t=12m) | Aged (t=12m) |
| Na$_2$O | 0.3±0.1 | 0.3±0.07 | 0.3±0.05 | 0.3±0.1 |
| MgO | 0.4±0.04 | 0.4±0.02 | 0.4±0.05 | 0.4±0.1 |
| Al$_2$O$_3$ | 3.1±0.1 | 3.0±0.07 | 3.1±0.2 | 2.8±0.5 |
| SiO$_2$ | 45.5±4.0 | 42.7±1.0 | 44.6±4.4 | 43.8±4.6 |
| P$_2$O$_5$ | - | 0.1±0.2 | - | - |
| Cl | 0.1±0.09 | - | 0.1±0.07 | 0.1±0.1 |
| K$_2$O | 1.5±0.2 | 1.4±0.1 | 1.4±0.1 | 1.6±0.1 |
| CaO | 2.1±1.8 | 2.9±3.2 | 1.1±0.2 | 1.6±0.1 |
| TiO$_2$ | 0.1±0.02 | 0.1±0.02 | 0.1±0.02 | 0.1±0.1 |
| Fe$_2$O$_3$ | 0.2±0.03 | 0.3±0.02 | 0.2±0.01 | 0.3±0.1 |
| SnO$_2$ | 9.9±0.48 | 10.0±0.72 | 10.4±1.3 | 11.6±1.0 |
| PbO | 36.7±3.9 | 38.9±3.4 | 38.3±3.5 | 37.3±3.5 |

To verify if any significant alteration occured on the tile samples, three different glazed tiles were analysed in terms of surface composition on a non-colonized area and on a previously colonized area after removal of the biofilm (Table 5.4). The surface composition obtained by µ-PIXE analysis of three inoculated pristine sample is shown in Table 5.4.

**Table 5.4.** Composition of the colonized pristine samples on areas previously covered by the fungus and non-colonized areas in oxide weight percentage (wt. %) average of a 750x750 µm$^2$. Results are presented with error value.

| Sample | 14FP | 16FP | 9FP |
|---|---|---|---|

| Area | NC | C | NC | C | NC | C |
|---|---|---|---|---|---|---|
| $Na_2O$ | 0.27 ± 0.01 | 0.29±0.01 | 0.29±0.01 | 0.27±0.01 | 0.31±0.02 | 0.24±0.03 |
| $MgO$ | 0.34±0.03 | 0.35±0.03 | 0.35±0.03 | 0.38±0.04 | 0.34±0.02 | 0.34±0.03 |
| $Al_2O_3$ | 3.47±0.02 | 3.22±0.02 | 3.32±0.02 | 3.22±0.02 | 3.24±0.02 | 3.20±0.02 |
| $SiO_2$ | 51.79±0.05 | 47.44±0.04 | 46.39±0.05 | 48.66±0.05 | 51.48±0.04 | 47.01±0.04 |
| $Cl$ | - | 0.17±0.01 | 0.16±0.01 | 0.16±0.01 | 0.14±0.01 | 0.14±0.01 |
| $K_2O$ | 1.71±0.02 | 1.33±0.01 | 1.40±0.02 | 1.42±0.02 | 1.55±0.01 | 1.27±0.01 |
| $CaO$ | 1.34±0.02 | 0.95 ±0.03 | 0.95 ±0.02 | 1.05±0.03 | 0.92±0.02 | 0.94±0.02 |
| $TiO_2$ | 0.10±0.01 | 0.09±0.01 | 0.12±0.01 | 0.10±0.01 | 0.09±0.01 | 0.12±0.01 |
| $Fe_2O_3$ | 0.24±0.01 | 0.22±0.02 | 0.26±0.01 | 0.22±0.02 | 0.22±0.01 | 0.22±0.01 |
| $SnO_2$ | 10.25±0.09 | 10.09±0.09 | 10.31±0.09 | 9.96±0.10 | 9.96±0.07 | 9.88±0.07 |
| $PbO$ | 30.49±0.52 | 35.80±0.47 | 35.44±0.54 | 34.57±0.56 | 31.74±0.41 | 36.54±0.41 |

NC, non colonized area; C, colonized area

Differences in lead and silica oxides composition of colonized and non-colonized areas were observed for samples 14FP and 9 FP. In fact, silica was higher for colonized areas and lower for non-colonized areas, whereas calies were lower on colonized areas and higher on ono-colonized areas. These variations of lead and silica values were not observed for sample 16FP. PIXE mappings of lead and silica elemtns reinformed these observations (Fig. 5.10). The heterogeneous glaze with crystalline quartz and tin compounds at the surface are probably the cause for these differences. No changes on elemental distribution maps could be observed resulting from fungal growth. The distribution of elements was similar to the glaze microstructure observed by SEM in Fig. 4.6 (Chapter 4) and no fungal imprints were visible on the surface. Calcium was not mapped since the mapping of calcium was affected by the tin oxide.
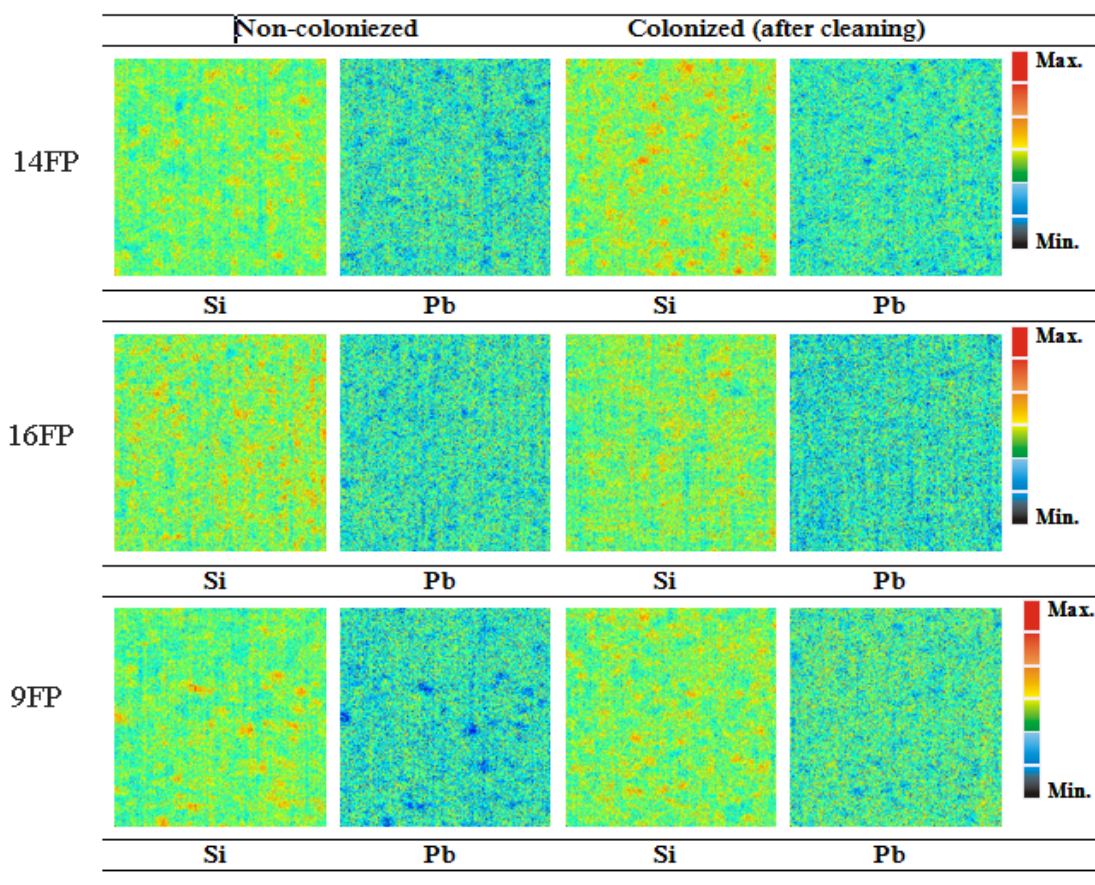
**Fig. 5.10.** PIXE mapping on the glaze surface of three pristine inoculated samples (14FP, 16FP and 9FP), both on a non-colonized and a colonized area after biofilm removal.

## 5.4    Discussion

The glazed ceramic tile models produced in the laboratory intended to represent historical majolica tiles in their pristine condition (pristine tiles) and after weathering (aged tiles). The production and artificial aging methods were described in Chapter 4. The glaze of both pristine and aged tiles showed similar chemical composition and the glaze layer showed a microfissures network. The artificial ageing promoted the broadening and densification of cracks of the microfissures network (Chapter 4). The correlation between fissure network and hydric properties was analysed as densification of crack network (number of cracks per area) and their broadening affect hydric properties (Zhou et al., 2012). In fact, the water absorption by capillary and the vapour permeability of the aged samples was higher on aged samples than on the pristine samples (Table 5.1). Several studies have shown that properties related to water movement are determinant on the primary bioreceptivity of a material (Miller et al., 2009; Gazulla et al., 2011; Portillo et al., 2011).

### 5.4.1    Fungal growth

The fungal strain selected for this experiment was isolated from a biofilm developing over historical and artistic glazed wall tiles and was described in this work as a new fungal species, namely *D. imbrexigena* (Chapter 3). The use of microorganisms isolated directly from a similar

substrate is of great relevance in order to properly evaluate the growth pattern and their damaging action on the substrate. Additionally, fungi from the same genus were found in other case studies concerning the microbial communities of glazed tiles. Therefore, we considered this microorganism as representative for other glazed tile assets (Chapter 6).

The *Teratosphaeriaceae* family , which includes the fungus used in this experiment, are characterized by slow growth (Egidi et al., 2014). This explains the slow development of *D. imbrexigena* over the substrates observed during the course of this experiment. The reason for choosing an axenic culture of this fungus relied on the fact that this organism is slow-growing and inoculation with multiple species might result in over-growth by other species that are not a major component of the biofilm found on the tiles from Pena National Palace (Chapter 3).

The characterization and evaluation of fungal proliferation on the pristine and aged tile samples showed no preferential growth (Fig. 5.2 and Fig. 5.4). Therefore, no difference in bioreceptivity of pristine and aged tile models could be detected. This is in contradiction to the results observed in Chapter 4, in which aged samples showed a higher bioreceptivity to photoautotrophic microorganisms than pristine tiles. However, in a study on biodeterioration of stained glass windows by fungi (*Penicillium* sp. and *Cladosporium* sp.), Rodrigues et al. (2014) observed no differences in glass biodeterioration between the initial non-corroded and corroded surfaces.

Bioreceptivity of a substrate to fungi is a complex issue, as they are heterotrophic microorganisms and thus dependent on a carbon source. The influence of the composition and physical features of the inorganic substrate might have been hidden by the effect of nutrient availability. The fungus *D. imbrexigena* was isolated from a complex multispecies biofilm growing over glazed wall tiles (nutrient poor substrate). However, in natural conditions the biofilm provides several nutrient sources, such as cell debris of bacteria, photosynthetic microorganisms and their organic exudates. In fact, other laboratory experiments on concrete with a fungal multispecies inoculum (*Alternaria*, *Cladosporium*, *Epicoccum*, *Fusarium*, *Mucor*, *Penicillium, Pestalotiopsis* and *Trichoderma*) showed that nutrient availability was a limiting factor when incubation on nutrient-poor media was tested (Giannantonio et al., 2009). Gadd et al., (2001) analysed the nutritional influence on fungal growth and biomass distribution in the presence of toxic metals (Cu, Cd and Zn). They concluded that when the amount of available carbon source increased the toxicity of the metals decreased. Therefore, possibly the use of higher nutritional culture media for laboratory assays might result in higher proliferation on the surfaces, which in short term experiments might result in more discernible growth. The same fact might also explain the heterogeneous growth among the samples observed in this work. To understand how the physical features, such as water permeability or roughness and chemical composition influence the bioreceptivity for fungi of a particular group of materials, the effect of these parameters on the nutrition availability must be analysed. For instance the permeability of the substrate will be traduced in the retention of medium (nutrients) on the surface or their absorption. Therefore, less permeable substrate may retain the nutrients on the surface and permit a higher fungal growth.

Finally, the quantification of fungal growth was solely based on digital image analysis, which might be limited for detecting differences between pristine and aged tiles with such reduced and heterogeneous fungal growth. Unlike the methods used for quantifying phototrophic biomass, the fungi-biomass estimation methods are still complex and many of the biomarkers are growth-phase dependent and have a weak correlation with biomass (Suberkropp et al., 1993; Miller et al., 1998). Therefore, probably a more accurate biomass quantitative method should be used, such as quantitative real-time PCR, which has been used to quantify fungi (Martin-Sanchez et al., 2013).

### 5.4.2   Biodeterioration by the fungus *D. imbrexigena*

Assessment of the detrimental effect of the fungus *D. imbrexigena* on the glaze was the main objective of this experiment. Regarding physical biodeterioration caused by fungal growth, no physical damaged caused by chasmolithic or cryptoendolithic growth or cell imprints were observed on the tile surface (Fig. 5.7). Moreover, no changes were evident between inoculated and control tile samples regarding capillary water absorption coefficient. However, based on the fact that no fungal penetration was observed, probably no precipitation or accumulation of EPS within the fissured occurred, contrary to what was observed for phototrophic microorganisms (Chapter 4).

Chemical alteration of the glaze surface during the experiment was evaluated by SEM-EDS analysis showing calcium rich minerals on all samples (Fig. 5.6 and Fig. 5.7). These were identified by μ-Raman, as calcium carbonate and calcium sulphate (Table 5.2). Carbonates and sulphates have been identified as common corrosion products of silicate glass and also of clay-based ceramic bodies (Fabbri et al., 2014; Rodrigues et al., 2014). In general, more crystals were observed on the inoculated samples compared to the control samples. Similar results were reported in other laboratory based experiments, in whichhigher amount of crystals were detected on inoculatedstained glass reproductions (Rodrigues et al., 2014).

Besides water corrosion products, some biogenic compounds were identified on the glaze surface of the inoculated samples, which presented the structure of the oxalate compounds (Table 5.2). Calcium oxalate, in the form of weddellite and whellite were identified on the glaze surface close to fungal structures. Oxalates have been considered biosignatures valuable for astrobiology on pre-existence of life in extreme environments, such as cultural heritage assets (Gorbushina et al., 2002; Frost et al., 2003; Rosado et al., 2013; Gadd et al., 2014). These metabolite compounds have a crucial role in many metal and mineral transformations intermediated by fungi (Gadd et al., 2014). In fact, the formation of calcium oxalate has been previously associated with the biochemical deterioration of the ceramic body by fungi and lichens, through the precipitation of this compound in the ceramic matrix (Ranogajec et al., 2005, 2008; Radeka et al., 2007b). Oxalic acid is used in industry for the sequestration of metal cations (Fomina et al., 2005; Wladimirsky et al., 2010), yet we could not detect the formation of any lead or tin oxalates, which would be expected due to high concentration of lead and tin of the glaze. Other studies have shown that some fungi can grow even in the presence of the most toxic chemical elements, such as Pb, Cd, Sn and Cu by producing several oxalates and acidic compounds that will easily chelate ions from insoluble complexes (Sayer et al., 1995, 1999; Fomina et al., 2005; Gadd et al., 2014).

The intrinsic heterogeneity of the crystalline glaze made the detection of compositional alterations difficult. Therefore, no significant chemical alterations of the glaze were noticed on the control nor on the inoculated samples (Table 5.3 and Table 5.4). The only exception was for calcium, which was slightly higher possibly due to the formation of calcium compounds over the glazed surface. Hence, no major compositional alterations could be associated with the fungal growth and/or high relative humidity

Although calcium oxalate formation has been considered protective in stone conservation (Doherty et al., 2007), the precipitation of compounds over glazes will alter their gloss and reflectance (Vendrell-Saz, 2003). Optical features such as gloss and reflectance are highly characterizing features of glazed tiles (Vendrell-Saz, 2003; Lobo and Pernão, 2010). Therefore the formation of calcium oxalates over the glaze has a detrimental effect on historical glazed tiles.

This experiment showed relevant results regarding the effect of the fungi in the deterioration, such as the chemical action on the glaze with the formation of calcium oxalate compound. In addition, this laboratory-based biodeterioration experiment provided information regarding the growth pattern of the fungus *D. imbrexigena*, which was less invasive than the phototrophic microorganisms tested in Chapter 4. However, more experiments need to be carried out to clarify the activity of fungi on the biochemical dissolution of glazes.

## 5.5    Conclusions

The laboratory-based biodeterioration experiment performed in this work allowed studying the development of the fungal biofilm over the tile surface and the detection of compounds with biological origin over the glaze surface. No significant differences could be detected regarding the bioreceptivity of the pristine and aged samples. Consequently glaze tile features could not be connected to fungal growth.

The limited growth of the fungus over the tested substrates confirmed that their development on these substrates is closely related to the presence of the photosynthetic microorganisms, bacteria and other nutritional sources deposited on tiles located outdoors. For bioreceptivity testing with fungi a preliminary step is needed in order to understand the effect of the surface features on the nutrition availability.

To summarize, the results obtained in this experiment indicated that *Devriesia imbrexigena* was able to mobilize elements present on the glaze and form oxalates. For the identification of these compounds, μ-Raman proved to be a useful tool in the investigation of biogenic compounds produced by fungi.

In order to effectively quantify the effect of fungi species on the biocorrosion of glazes, it would probably be necessary to simulate the corrosion in aqueous media without the presence of the ceramic body. The analysis of the lixiviation compounds with and without fungal colonization would allow the establishment of their effect of the lexivation rate of the glaze componenets. In order to analyse the lexivation rate of the glaze, probably a glass with similar composition of the

glaze tile should be analysed in order to avoid the contamination of the ceramic body, following the glass corrosion standart methologies.

Finally, Chapters 2, 3, 4 and 5 showed us that microbial communities growing over the glaze wall tiles produce several types of damage. Therefore, there is an urgent need to evaluate mitigation methods of biological colonization and also find more accurate solutions to eliminate those microbial communities and protect glazed wall tiles cultural heritage.

# An integrated approach to evaluate biocidal treatments on microbial community colonizing majolica glazed tiles
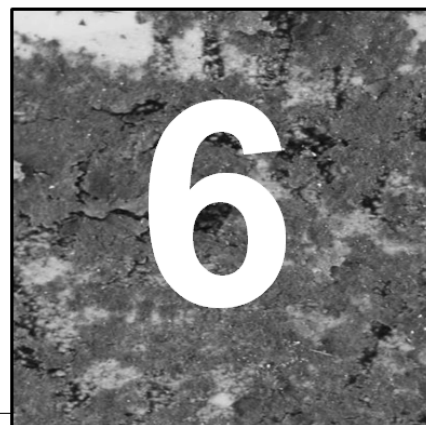
Gardens, such as the one surrounding *Casa da Pesca* located in the grounds of the Marquis of Pombal Palace, Portugal, were commonly ornamented with glazed tiles. Nowadays, some of these outdoor panels are deteriorated by the growth of a brown biofilm composed of green algae, cyanobacteria and dematiaceous fungi. Three commercial biocides (Biotin[®] T, Preventol[®] RI 80 and Albilex Biostat[®]) and titanium dioxide ($TiO_2$) nanoparticles were tested in situ. Their efficacy was monitored by visual examination, epifluorescence microscopy and DNA-based analysis. Preventol[®] RI 80 and Biotin[®] T showed a high biocidal efficacy, 4 months after the treatment, with changes in biodiversity. However, an initial stage of recolonization was detected 6 months after the application. The $TiO_2$ nanoparticles showed promising results by causing the detachment of the biofilm from the tile surface and no recolonization was detected after 6 months of monitoring.

## 6.1 Introduction

The *Marquês de Pombal* palace (palace of the Marquis of Pombal) was built during the 18th century in Oeiras, which is located in the western part of the nowadays Lisbon Metropolitan Area (Portugal). This Portuguese baroque manor house was connected to an estate. A cottage surrounded by a garden is located in the middle of the estate. This cottage has an artificial fish pond that was used for ludic activities, such as fishing, giving the name of *Casa da Pesca* (Fishing House).

The garden surrounding the *Casa da Pesca* is typical of baroque style decorated with a fountain, a cascade, terraces and stairs with several tile panels adorning the walls. During the 18th century glazed tiles were commmonly used as decorative elements in Portuguese baroque gardens. Many palaces and manor houses have their gardens decorated with these colorful ceramic elements, which can commonly be seen ornamenting fountains, stairs, benches and walls.

Nowadays, the *Marquês de Pombal* palace and estate are separated, since the estate is used as an agronomical station. Unfortunately, the *Casa da Pesca* and the surrounding garden were unkempt and are now extremely deteriorated. The tiles show several types of damage, such as salt damage, vandalism, accumulation of dirt and deterioration produced by living organism or

biodeterioration (Fig. 6.1). Microbial colonization of these tiles appears as a brownish biofilm covering the panels and causing severe aesthetic and physical-chemical biodeterioration. Biodeterioration is an important issue in the decay of building materials (Ortega-Calvo et al., 1991; Warscheid and Braams, 2000), as seen in the previous chapters of this thesis.



**Fig. 6.1.** Images damage and different pathologies found on the *Casa da Pesca* glazed wall tiles.(a) brown biological colonization, lacunar and detachment of the glaze; (b) severe biological colonization and lacunae of the glaze; and (c) biological colonization, lacunae of tiles and mechanical damage due to theft or vadalism.

As mentioned in Chapter 2, thebiodeterioration of glazed ceramic tiles, compared to other inorganic building materials, has been little studied. Only recently this topic has gained interest and

several articles have been published (Oliveira et al., 2001; Watanabe et al., 2006, 2009; Giacomucci et al., 2011; Coutinho et al., 2013). Any intervention to mitigate the damage produced by microorganisms on cultural heritage assets should begin with the characterization of the substrate and identification of microorganisms involved in  the biodeterioration (Alakomi et al., 2006). This enables us to understand the role played by microorganisms in the biodeterioration process and is crucial to design and select a mitigation strategy. An efficient mitigation should inactivate the organisms and prevent their re-growth for an acceptable period of time, causing no alteration to the substrate (Young et al., 2008).

In this study we characterized the *Casa da Pesca* glazed tiles and the microbial communities dwelling on them by culture and molecular biology methods. The eradication of microorganisms from inorganic building materials, usually involves mechanical and/or chemical methods. Regarding the removal of biofilms from glazed tiles and ceramics there are no general guidelines. John (1988), Mandal & Rath (2013), Oliveira et al. (2001) and Silva et al. (2011) were some of the authors that tested biofilm removal from ceramics. They tested diverse procedurest, such as chemical, thermal (heating) and gamma-radiation treatments. However, some methods produced undesirable results, on the substrate or had no long-term effect (Giacomucci et al., 2011; Silva et al., 2011; Mandal and Rath, 2013).

The removal of biological colonization from inorganic substrates, such as stone and mortars, is usually carried out with a brush and/or by the application of biocides. These are the most common procedures used as a conservation treatment on outdoor cultural heritage (Caneva et al., 1991, 2008; Berti et al., 2008). However, mechanical removal of biofilms is fastidious and has little effect, and can even spread the microorganisms resulting in a more severe colonization (Jurado et al., 2014). Moreover, if tiles are in fragile conservation condition and present areas in detachment, the mechanical removal can even enhance the risk of partial glaze loss.

Biocides, like Biotin[®] T and Preventol[®] RI 80, have been widely used to clean biofilms in cultural heritage assets on inorganic substrates, such as stone and mortars (Ascaso et al., 2002; Fonseca et al., 2010; de los Ríos et al., 2012). However, none of these studies monitored potential re-colonization after biocide application. The fact that biocides may not promote a long term protection has created some scepticism regarding their use. Therefore, in this study three different commercial biocides (Biotin[®] T, Preventol[®] RI 80 and Albilex Biostat[®]) and a heterogeneous photocatalysis biocide (in the form of nanocrystalline anatase $TiO_2$ nanoparticles) were tested *in situ*, and their effect was evaluated after 4 and 6 months of the application. Microbial community may development of resistance mechanisms (Morton et al. 1998). The resistance may result in colonization by new microbial communities due to biocide residues (Bastian et al., 2009, 2010) and also the need of several biocide applications due to lixiviation caused by rain water (Russel and Chopra, 1990; Mandal and Rath, 2013), as has been reported on several studies.

The efficacy of these biocides was monitored by photographic recording, epifluorescence microscopy of photoautotrophic microorganisms and denaturing gradient gel electrophoresis (DGGE). Finally, the effect of each treatment on the substrate was also evaluated using scanning electron microscopy (SEM) analysis.

## 6.2    Materials and Methods

### 6.2.1    Site description and sampling

This study was focused on the glazed ceramic wall tiles from the stair handrails that give assess to the artificial pound situated in the garden of *Casa da Pesca* (38º 41´52´´N; 9º 18´40´´W), located in Oeiras, Portugal. Oeiras has a temperate maritime climate characterized by mildly cold temperatures (average annual temperature 16 ºC) and high relative humidity levels (76%). Tiles facing north are covered with a brownish biofilm (Fig. 6.2). Besides the aesthetic damage that can be seen by comparison of a non-colonized tile and a colonized tile (Fig. 6.2 a,b), the tiles also show fissures and flacking of the glaze in the colonized areas. An area pf the glazed wall tiles completely covered with brownish biofilms was selected to test the biocide treatments (Fig. 6.2c).
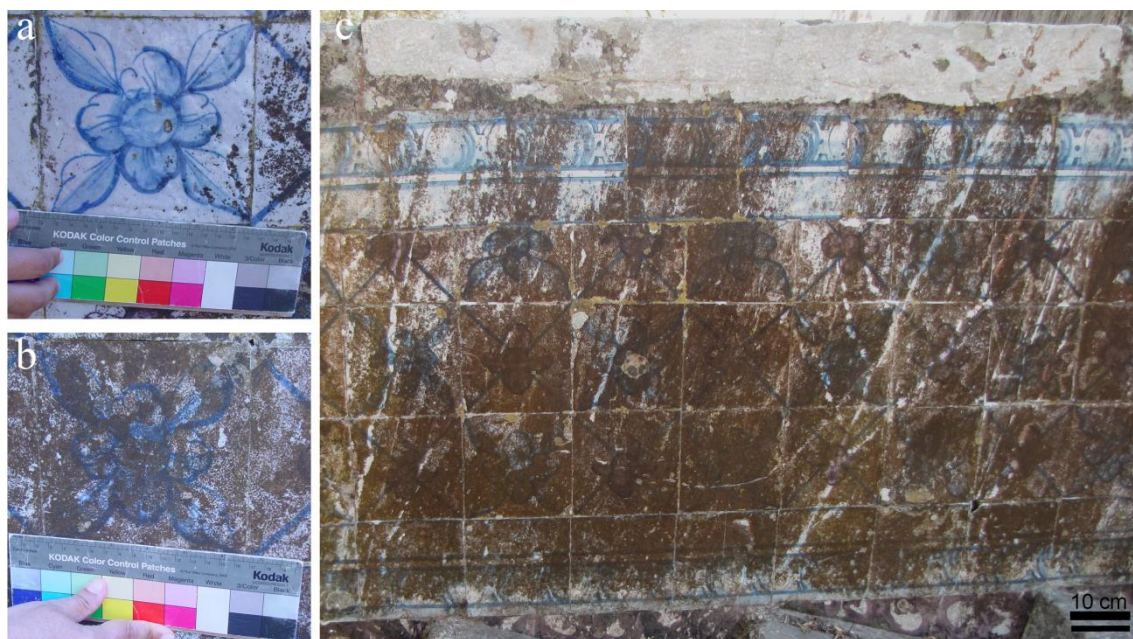


**Fig. 6.2.** Glazed wall tiles from the stairs handrails in the *Casa da Pesca* garden: (a) detail of a glazed tile almost without biofilm; (b) detail of a glazed tile covered by a brown biofilm; and (c) colonized tile area selected for the experiment before the treatments (August 2012).

Sampling surveys were conducted between August 2012 and March 2013. The biofilm samples were carefully scraped using a sterile scalpel and placed into sterile tubes for molecular biology analysis and culture techniques for the isolation of fungi. In addition, small glaze samples were collected from previously detached areas with a scalpel for chemical characterization and SEM-EDS. Samples for molecular biology analysis were taken before and 4 months after theapplication of biocidal treatments.

■

### 6.2.2  µ-Raman

µ-Raman analysis was performed on the glaze surface and cross-sections, allowing mineralogical characterization and the identification of the glaze crystalline compounds. A Labram 300 Jobin Yvon spectrometer, equipped with a He-Ne laser of 17 mW power operating at 632.8 nm was used, as well as a solid state external laser of 50 mW power operating at 514.5 nm. Spectra were recorded as extended scans and the laser beam was focused either with a 50x or a 100x Olympus objective lenses or with a 50x Olympus ultra-long working distance (ULWD) objective for depth probing. The laser power at the surface of the samples was varied with the aid of a set of neutral density filters (optical densities 0.3, 0.6, 1 and 2).

### 6.2.3  µ-PIXE

In order to determine the glaze chemical composition µ-PIXE analysis was performed using an Oxford Microbeams OM150 type scanning microprobe for focusing down to $3 \times 4$ µm$^2$ a 1 MeV proton beam. The glaze samples were irradiated in vacuum and the produced X-rays were collected by a 8 µm thick Be windowed Si(Li) detector with a crystal active area of 80 mm$^2$ and 145 eV resolution. The system configuration used allowed efficient detection of low energy X-rays such as the ones from Na. Operation and basic data manipulation, including elemental distribution mapping, was achieved through the OMDAQ software code, and quantitative analysis was done with the GUPIX software. The quantification was performed on a representative area of the glaze cross-section with an area of analysis of ca. 500×500µm. The accuracy of the analysis, based on analysis of CMOG C, was described in Chapter 3.

### 6.2.4  Morphological characterization of the biofilm
#### 6.2.4.1 Optical microscopy

Samples were directly examined with a Leitz Diaplan microscope with differential interference contrast (DIC) optics and images were recorded with a DeltaPix Camera (InfinityX).

#### 6.2.4.2 SEM –EDS analysis

SEM analyses were performed on three distinct samples: (i) polished-cross sections of the glaze for substrate characterization; (ii) samples of glaze with biofilm for evaluation of biofilm-substrate interactions and (iii) samples of the glaze treated with biocides (glaze surface). In this last case, the analysis were performed after cleaning the surface with a cotton swab soaked in a 1:1

water ethanol solution to remove the biofilm. Variable pressure (VP) mode was used for glazed sections and glaze surface after treatments to avoid carbon coating and preserve sample for other analytical techniques, such as µ-Raman. Observations under VP-SEM with an energy dispersive spectrometer (EDS) were performed with a HITACHI 3700N scanning electron microscope interfaced with a Quantax EDS microanalysis system. The Quantax system was equipped with a Bruker AXS XFlash® Silicon Drift Detector (129 eV Spectral Resolution at FWHM - Mn Ka). The operating conditions for EDS analysis: 20 kV accelerating voltage, 10 mm working distance and 120 mA emission current. For evaluation of biofilm-substrate interactions, samples of glaze were analysed with metallic coating Au and SEM observation was done in high vacuum, using secondary electron mode and a 10 kV accelerating voltage.

### 6.2.5  Isolation and identification of fungi from the biofilm

Biofilm samples for culture procedures were suspended in sterile water and inoculated onto PDA culture medium (Scharlau, Spain). Cultures were incubated at room temperature with natural light cycles. Individual colonies were transferred to fresh PDA plates. Eight pure cultures named CP1 to CP8 were characterized in terms of colony development, morphology, and identified by molecular biology techniques. Genomic DNA was isolated from fungi by the following procedure. Fungal mycelium was collected from pure cultures and placed into 1.5 mL Eppendorf tube containing 500 µL of TNE buffer (10 mM Tris–HCl, 100 mM NaCl, 1 mM EDTA; pH 8) and glass beads. The mixture was shaken in a cell disrupter (Fast Prep-24, Solon, OH, USA) at full speed for 2 min. The DNA was purified by phenol/chloroform extraction and ethanol precipitation.

The internal transcribed spacer (ITS) regions, including ITS1, 5.8S rRNA gene and ITS2, were amplified using the universal primer pair ITS1 (5′-TCC GTA GGT GAA CCT GCG G-3′) and ITS4 (5′-TCC TCC GCT TAT TGA TAT GC-3′) (White et al., 1990). PCR reactions were performed in a BioRad iCycler thermal cycler (BioRad, Hercules, CA, USA) using the following thermocycling program: 2 min denaturing step at 95ºC, followed by 35 cycles of denaturing (95ºC for 30s), annealing (55ºC for 30s) and elongation (72 ºC for 1 min), with an additional extension step at 72 ºC for 10 min at the end. To evaluate the PCR results, products were separated on 1% (w/v) agarose gels, stained with SYBR Green I (Roche Diagnostics, Mannheim, Germany) and visualized under UV light. Positive PCR products were sent to Macrogen Europe (Amsterdam, The Netherlands) for purification and sequencing using the same primers that were used for amplification. In order to approximate the phylogenetic affiliations of fungal strains, the received sequences were compared, using BLASTn algorithm, to the non-redundant databases of sequences deposited at the National Center for Biotechnology Information (NCBI).

### 6.2.6 *In situ* application of biocidal treatments on glazed wall tiles

Four different treatments were tested on the biofilms growing over the glazed wall tiles. A photocatalyst compound and three commercial biocides were applied on the colonized glazed tiles: i) Titanium dioxide P25 nanocrystalline anatase ($TiO_2$) with specific surface area of 50 $m^2$ $g^{-1}$ and a particle size of approximately 20 nm (Degussa, Germany); ii) Preventol[®] RI 80 (hereinafter Preventol), composed of alkyl-benzyl-dimethyl-ammonium chloride and isopropyl alcohol (Lanxess, Germany); iii) Biotin[®]T (hereinafter Biotin), which contains alkyl-benzyl-dimethyl-ammonium chloride, octyl-isothiazolone and 3-iodo-2propynyl-butylcarbamate (C.T.S., Spain), and iv) Albilex Biostat® (hereinafter Albilex), containing alkyl-benzyl-dimethyl-ammonium chloride and dihydroxide chromium ($H_2Cr_2O_7$) (2:1) (Albishausen & Co. Kg, Germany).

The $TiO_2$ treatment used in this study was prepared in an aqueous suspension 1% (w/v), which was previously tested on an outdoor cultural heritage asset (Fonseca et al., 2010). All commercial biocides were applied using the concentrations specified in the manufactures' instructions: 2% (v/v) for Biotin, 2% (v/v) for Preventol and 1% (v/v) for Albilex. Each of these four treatments was applied directly on 3 tiles with a paint-brush until soaking. This *in situ* experiment was performed in summer (August 2012) to guarantee no rain would occur immediately after treatments.

### 6.2.7 Monitoring of treatments efficacy

#### 6.2.7.1 Macroscopic observations

Macroscopic observations were performed by visual inspection and photographic documentation taken with a digital camera over a period of 6 months after the start of the experiment. Treated areas were photographed with a digital camera Olympus C-5060, and a Kodak Color scale was included for light and color adjustment of the images.

#### 6.2.7.2 Epifluorescence microscopy

The effect of the treatments on the phototrophic community of the biofilm was assessed 4 and 6 months after treatments application by qualitative evaluation of chlorophyll *a* (Chl*a*) autofluorescence through epifluorescence microscopy. The content of Chl*a* was qualitatively evaluated by red light emitted by the molecule when excited with blue light; if the molecule is degraded red fluorescence cannot be observed. Samples were taken from treated areas and from control area (non-treated biofilm) for comparison purposes. Samples were taken with a sterile scalpel and transferred to sterile Eppendorfs tubes. Biofilm samples were examined with a Zeiss Axioplan 2 optical microscope, equipped with a high resolution camera, Nikon DXM 1200F. Images

were captured under visible light and using a 40x Neofluar objective with a UV-2A filter cube (excitation 330-380 nm, DM 00 nm, BA 420 nm).

### 6.2.7.3 Molecular analysis of the microbial communities

*DNA extraction and PCR amplification* Biofilm samples were collected for the identification of cyanobacteria and eukaryotic communities. Samples were collected before (C0) and four months after the application of the treatments: T4 (TiO$_2$), B4 (Biotin), P4 (Preventol) and A4 (Albilex). For comparison purposes, one control sample of non-treated biofilm was also collected 4 months after the treatment application (C4). Total DNA was extracted using the FastDNA®SPIN for Soil Kit (MP Biomedicals, France) in conjunction with the FastPrep®instrument, following the manufacturer's protocol. PCR amplifications of cyanobacterial 16S rRNA gene fragments were performed using the primer pair Cya106F (5'- CGGACGGGTGAGTAACGCGTG A-3') and Cya781R (5'-GACTACTGGGGTATCTAATCCCWTT-3') as described by (Garcia-Pichel et al., 1997). Eukaryotic 18S rRNA genes were amplified using the primer pair EukA (5'-AACCTGGTTGATCCTGCCACT-3') and EukB (5'-TGATCC TTCTGCAGGACT-3') (Díez et al., 2001). Fungal ITS regions were amplified using the primers previously described in section 2.5.The PCR amplification protocol consisted of a denaturing step of 2 min at 95˚C, followed by 35 cycles of denaturing at 95˚C for 15 s, annealing of oligonucleotides at 60˚C for 12 s (55˚C for Eukarya-specific primers, 50˚C for ITS regions), and elongation at 72˚C for 2 min, following a terminal step of 10 min at 72˚C, and ending at 4˚C. PCR products were separated on 1% (w/v) agarose gels.

*Fingerprint analysis by DGGE* The PCR products of biofilm samples C0, C4, T4, B4, P4 and A4 were analysed by denaturing gradient gel electrophoresis (DGGE). Nested PCRs were performed using the amplification products obtained with the primer primers Cya106F-Cya781R, ITS1-ITS4 and EukA-EukB as DNA template. For the cyanobacterial 16S rRNA gene fragments, the primers 341F-GC (5'-CCTACGGGAGGCAGCAG-GC clamp-3') and 518R (5'ATTACCGCGGCTGCTGG-3') were used, as described by (Muyzer et al., 1993). For the eukaryotic 18S rRNA gene fragments, amplification was performed using the primer pair Euk1A (5'-CTGGTTGATCCTGCCAG-3') and Euk516r-GC (5'-ACCAGACTTGCCCTCC-GC clamp-3'), according to Díez et al., (2001). For the region ITS1, the primers ITS1-GC (5'-TCCGTAGGTGAACCTGCGG-GC clamp 3') and ITS2 (5'-GCTGCGTTCTTCATCGATGC-3') were used (Doaré-Lebrun et al., 2006). Amplified fragments were run in 6% polyacrylamide gels at 200V for 3.5h with denaturing gradients ranging from 30 to 50 % for cyanobacteria, and 20 to 45 % for fungi. The eukaryotic 18S rRNA gene fragments were run in a 6% polyacrylamide gel with denaturing gradient ranging from 20 to 50 %, at 100V for 16h. All runs were performed in a DCode Universal Mutation Detection System (Biorad), at 60ºC, in 0.5X TAE buffer. The 100% denaturing conditions correspond to 7M urea and 40% formamide. Gels were stained with ethidium bromide, and images were acquired using a UV transilluminator.

*Construction of 16S rDNA clone libraries and sequencing analysis.* Based on DGGE fingerprint analysis, the initial biofilm (C0) and the biofilm collected four months after the application of with Preventol (P4) were selected for construction of clone libraries and sequence analysis. PCR

products were purified using the JetQuick PCR Purification Spin Kit (Genomed, Löhne, Germany) and cloned with the TOPO TA Cloning Kit (Invitrogen, Carlsbad, CA). Representative clones were sequenced by MACROGEN Europe (Amsterdam, The Netherlands) to further determine their phylogenetic affiliations. DNA sequences were edited with Bioedit v7.0.4 software (Technelysium, Tewantin, Australia) and aligned with MUSCLE (Edgar, 2004). Aligned sequences were clustered into operational taxonomic units (OTUs) using the program DOTUR (Schloss and Handelsman, 2005), based on a 97% sequence identity cutoff. Homology search of the sequences was performed using the BLASTn algorithm (Altschul et al., 1990) of the NCBI database.

### 6.2.8   Phylogenetic analysis of fungal communities

Phylogenetic relationships between the fungal strains and representative clones detected in the initial biofilm, and the fungal representative clones obtained after Preventol treatment, were estimated. Preventol treated biofilm was selected for DNA sequencing analysis based on the DGGE analysis. The closest related sequences from GenBank were also included in order to approximate the identification of the initial fungal communities. The Neighbor-Joining analyses were conducted using MEGA 5.2.2. Gaps were treated as missing data, the Kimura 2 parameter substitution model was used, and bootstrap values were generated from 1000 replicates. The resulting topology was compared with results from other tree building algorithms, including Maximum-Likelihood and Minimum-Evolution methods.

### 6.2.9   Sequences accession numbers

Sequences resulting from this work were deposited in GenBank with accession numbers LN713987 to LN714021.

## 6.3   Results
### 6.3.1   Characterization of the glaze substrate

VP-SEM analysis of a glaze cross-section revealed a heterogeneous glaze with inclusions of different composition, form and size (Fig. 6.3). Element distribution mappings showed the distribution of these inclusions, which were rich in silica, potassium and tin (Fig. 6.3a-c). The chemical characterization of the white glaze by EDS revealed a silica lead glaze opacified with tin oxide crystals (Fig. 6.3d).
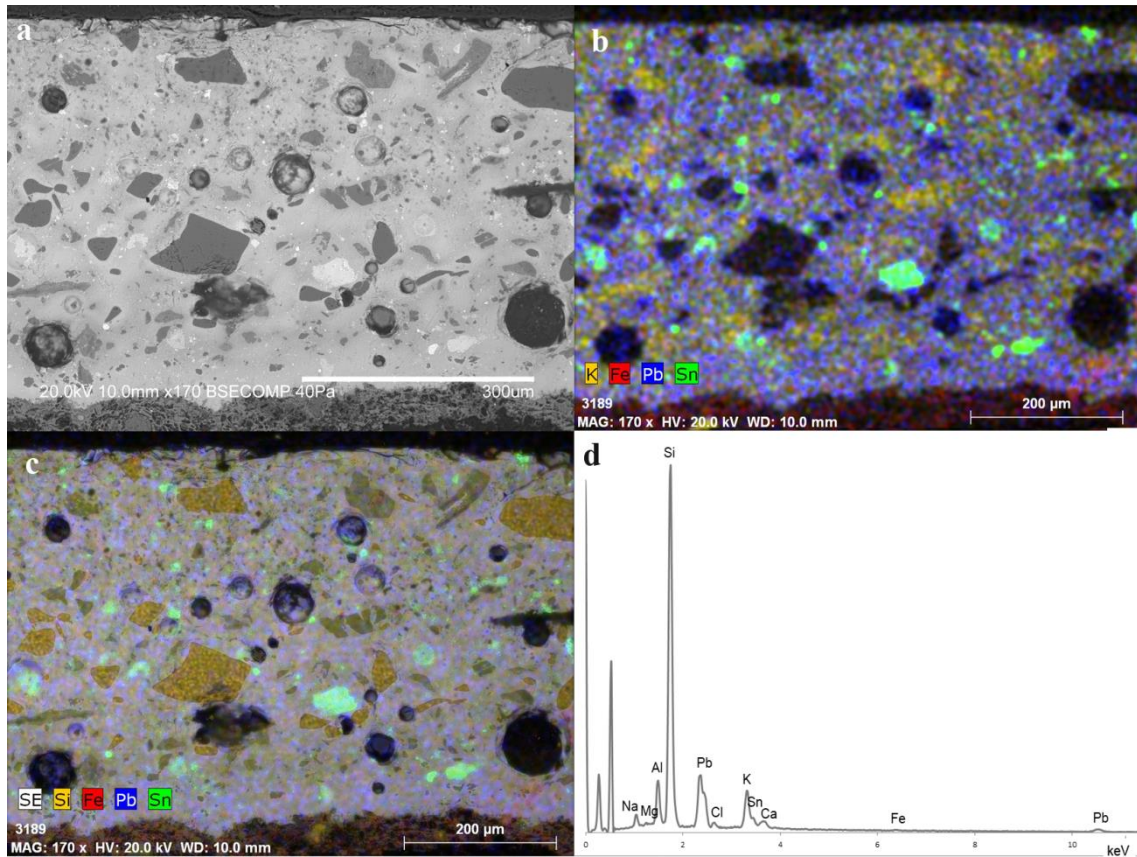
**Fig. 6.3.** VPSEM micrographs of the glaze: (a) SEM image of a glaze cross-section with inclusions; (b) false colored image showing the distribution of the elements K, Fe, Pb and Sn; (c) SE image with mapping of Si, Fe, Pb and Sn; (d) X-ray microanalysis spectrum obtained from a glaze section.

The mineralogical composition of the inclusions observed by VP-SEM (Fig. 6.3) was then determined by μ-Raman analysis. Quartz (Fig. 6.4 (i)), potassium feldspar (Fig. 6.4 (ii)) and cassiterite were identified (Fig. 6.4 (iii)).
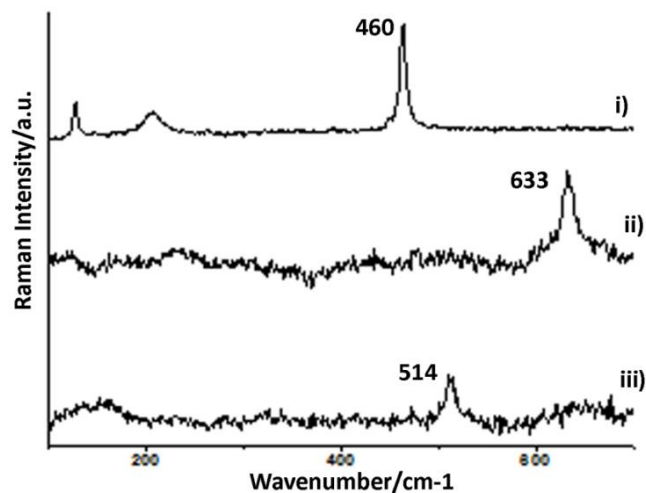


**Fig. 6.4.** Raman spectra of (i) quartz, (ii) cassiterite and (iii) potassium feldspar collected from the glaze cross-sections.

The average chemical composition of the four white glaze samples obtained by µ-PIXE is summarized in Table 6.1. According to the contents obtained, the glaze can be considered an alkali-lead silicate, being $SiO_2$ the major component (58 wt. %). Lead and potash were the main fluxing agents representing 22 and 5.7 wt. % of the glaze, respectively. In majolica glazes the main opacifier is tin oxide which was circa 4.9 wt. %.

**Table 6.1** Average chemical composition and standard deviation (Std) of the white glaze in wt. **%.**

| Oxides (wt. %) | $Na_2O$ | MgO | $Al_2O_3$ | $SiO_2$ | Cl | $K_2O$ | CaO | $TiO_2$ | $Fe_2O_3$ | $SnO_2$ | PbO |
|---|---|---|---|---|---|---|---|---|---|---|---|
| **Average** | 1.9 | 0.3 | 6 | 58 | 0.3 | 5.7 | 0.5 | 0.22 | 0.3 | 4.9 | 22 |
| **Std** | 0.2 | 0.1 | 1 | 1 | 0.1 | 0.9 | 0.1 | 0.02 | 0.1 | 0.5 | 2 |

### 6.3.2 Microbial community characterization by microscopy observations
#### 6.3.2.1 Optical microscopy

Direct optical microscopy observation of the biofilm samples collected from the surface of the tiles allowed us to identify the presence of a green alga, *Phycopeltis arundinacea* (Montage) De Toni, in large quantities. This microalgae presents green and orange brown coloration and the characteristic orange brown color and the dichotomous filaments radiating from the centre, which are more evident at the edge where the thalli show a more-or-less lobed margin (Fig. 6.5a) (F Rindi and Guiry, 2002; Rindi et al., 2004). The *Phycopeltis arundinacea* cells were surrounded by dematiaceous fungi with brown hyphae (Fig 6.5b). Although a close interaction between fungi and algae was observed, no lichens or lichenization process were identified on the biofilm.
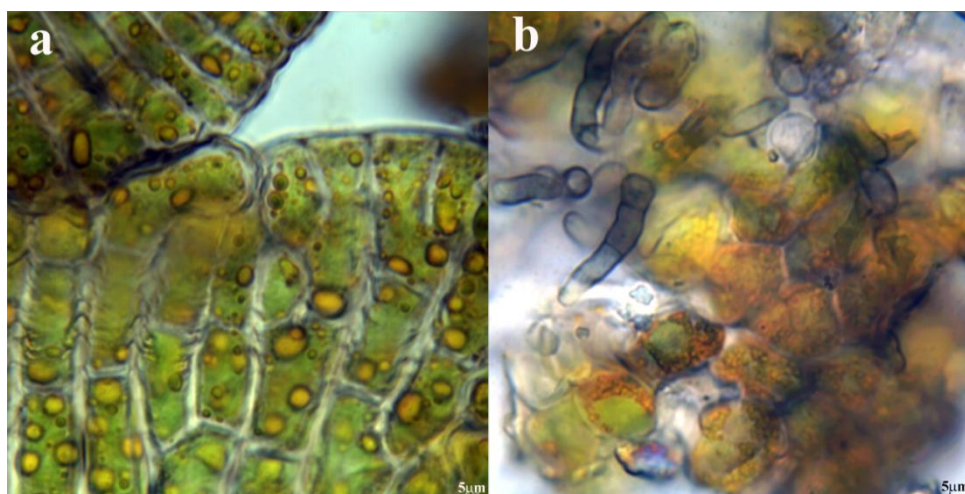


**Fig. 6.5.** Micrographs of the biofilm samples observed under the light microscope. (a) *Phycopeltis arundinacea*; and (b) *Phycopeltis arundinacea* cells surrounded by brown hyphae of a dematiaceous fungi.

#### 6.3.2.2 SEM analysis

Fig. 6.6 depicts SEM images of glaze fragments covered with biofilm showing a dense microbial colonization of microalgae and fungi over the glaze. In Fig. 6.6 (b) the algal thalli with the characteristic margin (arrow in Fig. 6.6b) surrounded and covered with filamentous fungi (Fig. 6.6a, b and c) can be seen.
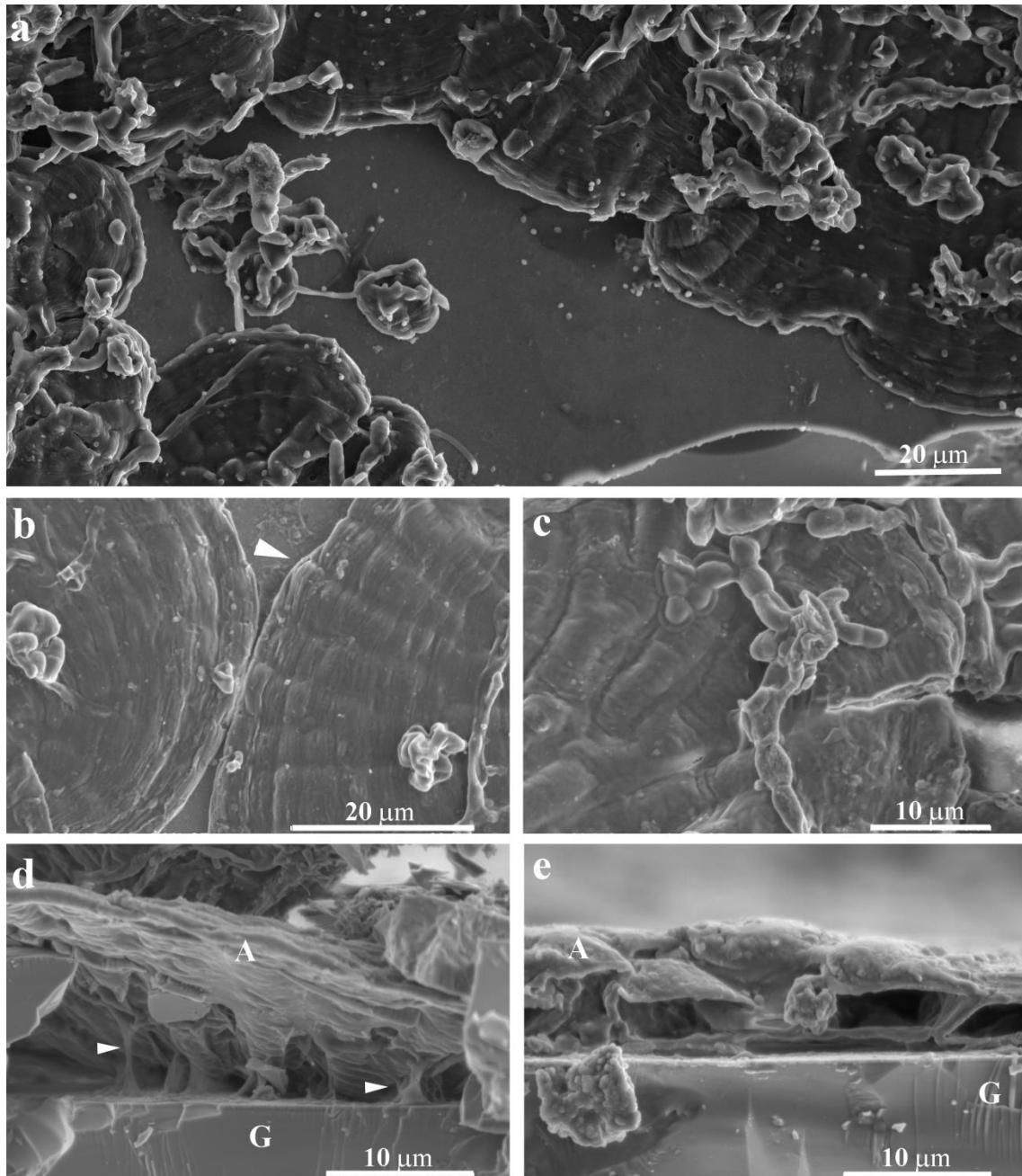


**Fig. 6.6.** SEM images of the biofilm over the glaze: (a) algae and fungal hyphae over the surface of the glaze; (b) algal thalli with the characteristic margin indicated with arrow over the glaze surface; (c) algae and fungal hyphae; (d) glaze section (G) with algae (A) and glaze fragments attached to EPS (arrows); and (e) section displaying algae (A) and glaze (G).

Fig. 6.6(d and e) shows glaze cross-sections where the algae-glaze interface can be appreciated. The strong adhesion of the organisms to the glaze by EPS can be clearly observed. In

addition fragments of the broken glaze that remained attached to the thallus (arrows in Fig. 6.6d) can also be observed. In Fig. 6.6e the unilayered thallus of *Phycopeltis* strongly adherent to the glaze by EPS can also be seen.

### 6.3.3 Fungal isolation and identification by molecular biology techniques

Eight fungal strains (isolated CP1 to CP8) were isolated and identified by molecular biology methods. The comparison of their nucleotide sequences with sequences in GenBank revealed three different fungal taxa belonging to the Capnodiales order of the Ascomycota phylum, with similarities between 94 and 99% (Table 6.2).

**Table 6.2**. Phylogenetic affiliations of eight fungal strains (isolates CP1 to 8) isolated from *Casa da Pesca* tiles.

| Fungal strain[1] | Closest relative (accession nr.)[2] | Similarity (%) |
|---|:---:|:---:|
| CP1, CP2, CP4, CP6 and CP7 | *Devriesia xanthorrhoeae* (HQ599605)[3] | 94 |
| CP3 and CP8 | *Devriesia modesta* (KF309984) | 99 |
| CP5 | *Neodevriesiaceae* sp. (KF309974) | 94 |

[1] Accession numbers of fungal strains are detailed in Fig. 6.12

2 Closest relative obtained by comparison with the NCBI database and corresponding accession number
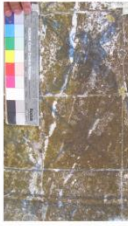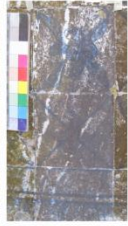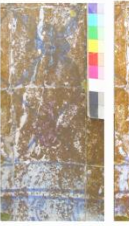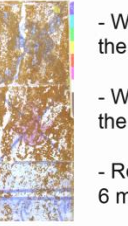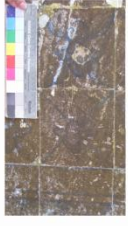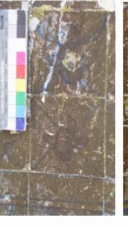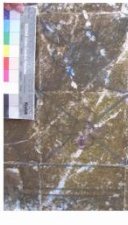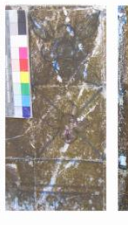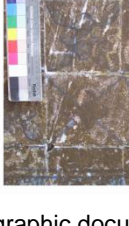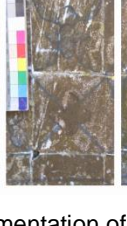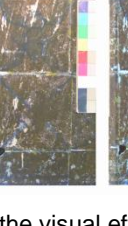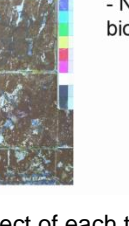
3 Recently described as *Neodevriesia xanthorrhoeae* (Quaedvlieg et al. 2014)

These taxa belong to the recently described *Neodevriesiaceae* family (Quaedvlieg et al., 2014), resulted from are-distribution of genera within the *Teratosphaeriaceae* family. Based on molecular analyses, these fungi were identified as: *Neodevriesiaceae* sp. 1 (close related to *Neodevriesia xanthorrhoeae*), *Devriesia modesta* and *Neodevriesiaceae* sp. 2. These identifications are also supported by the phylogenetic study detailed in section 6.3.4.4.

### 6.3.4 Efficacy of the biocidal treatments applied on the glazed wall tiles

#### 6.3.4.1 Visual inspections

Macroscopic observations revealed that the applied treatments induced changes in the biofilms through time, with the exception of the Albilex treatment, where no evident changes could be observed (Fig. 6.7).

| | Before | After | | Observations |
|---|---|---|---|---|
| | | 1 day / 4 months | 6 months | |
| TiO2 | | | | - White deposit is formed on the surface after the biocide application<br><br>- White deposit becomes less visible during the 6 months<br><br>- Reduction of biofilm-coveraged area at 6 months |
| BiotinT | | | | - No alteration of the biofilm right after the biocide application<br><br>- Biofilm changes colour during the 6 months<br><br>- Biofilm losses density |
| Preventol RI 80 | | | | - No alteration of the biofilm right after the biocide application<br><br>- Biofilm changes colour during the 6 months<br><br>- Biofilm losses density |
| Albilex Biostat | | | | - No alteration of the biofilm after the biocide application during the 6 months |

**Fig. 6.7.** Photographic documentation of the visual effect of each treatment applied on the brownish biofilms on glazed wall tiles from *Casa da Pesca* over 6 months.

The application of the photocatalytic biocide ($TiO_2$) resulted in a white layer deposited over the biofilm due to the white $TiO_2$ nanoparticles. These particles were lost through time, maybe due to the lixiviation of the particles by rain (Fig. 6.7). Although the variation of biofilm color and density was not evident, we could observe a decrease on biofilm coverage area (Fig. 6.7) and it clearly lost its adhesion to the substrate. Fig. 6.8 shows the biofilm flaking-off from the tile surface 6 months after the application of $TiO_2$ nanoparticles.
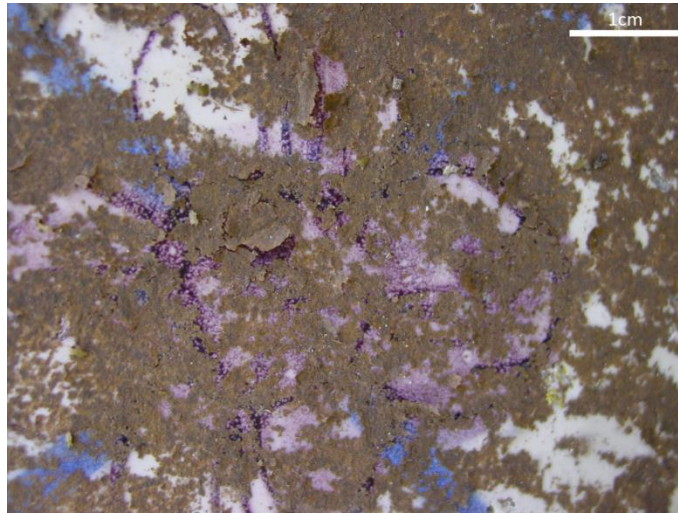
**Fig. 6.8.** Flacking-off and detached biofilm in the TiO2–treated area 6 months after treatment.

Biotin induced a slight color variation of the biofilm, but the most noticeable effect was the loss of density at the end of the experiment (Fig. 6.7). Preventol caused the most significant changes on the biofilm, altering its color, density and thickness (Fig. 6.7). These biocide effects on the biofilm were progressive after the treatment, but became significantly evident 4 months after biocide application (Fig. 6.7).Only Biotin and Preventol treatments allowed the visualization of the tile motifs; however, the degraded biofilm was still present over the glazed tiles.

### 6.3.4.2 Epifluorescence microscopy

The effect of the treatments on the photosynthetic community was analysed by epifluorescence observations, performed at two different times 4 and 6 months after biocide application (Fig. 6.9 and 6.10). After 4 months, an apparent decrease in the red light emission was observed for all treatments, except for the biofilm treated with Albilex, which indicates the degration of Chl*a* (Fig. 6.9).
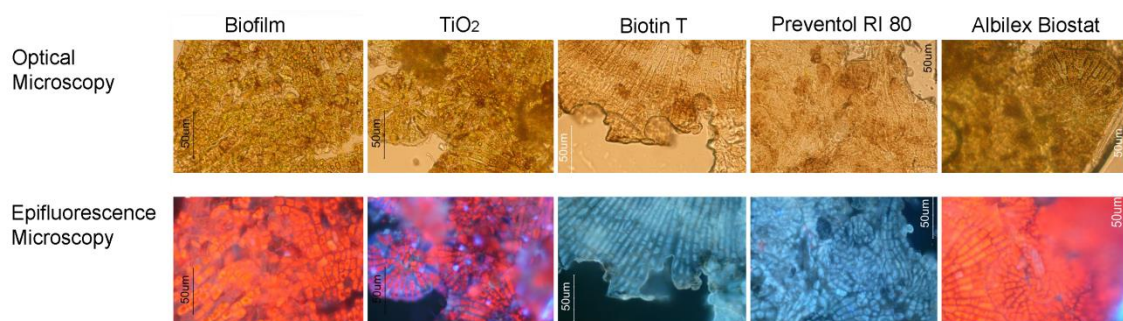


**Fig. 6.9.** Optical and fluorescence microscopy images of biofilm samples collected four months after the beginning of the experiment:biofilm without treatment, TiO$_2$-treated biofilm, Biotin-treated biofilm, Preventol-treated biofilm and Albilex-treated biofilm**.**

The non-treated biofilm (control) and those treated with Albilex showed similar Chl*a* fluorescence intensity (Fig. 6.9 Biofilm and Albilex Biostat). The absence of Chl*a* fluorescence for

samples treated with Biotin and Preventol was particularly evident, as well as the disruption of the algal structures which could be observed with optical microscopy (Fig. 6.9 Biotin T and Preventol RI 80). Regarding the samples treated with the photocatalytic biocide (TiO$_2$), punctual inactivation was observed in small areas displaying white-blue fluorescence which indicates that Chl$a$ has been altered (Fig. 6.9 TiO$_2$). After 4 months Preventol and Biotin appeared to be the most efficient treatments for the inactivation of photosynthetic community presented on these tiles, reducing the active Chl$a$ concentration.

Fig. 6.10 shows epifluorescence images of the biofilm samples collected six months after biocidal treatment.
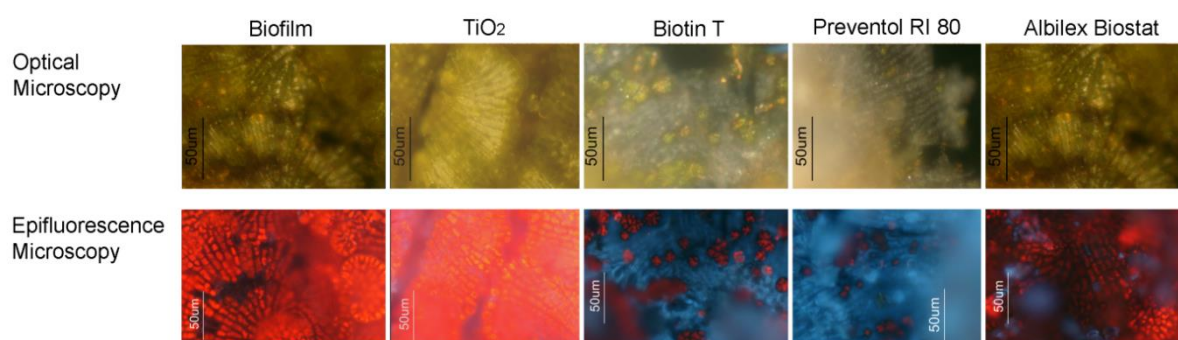


**Fig. 6.10.** Optical and fluorescence microscopy images of biofilm samples collected six months after the beginning of the experiment: biofilm without treatment, TiO$_2$-treated biofilm, Biotin-treated biofilm, Preventol-treated biofilm and Albilex-treated biofilm**.**

The comparison of the results obtained by optical microscopy and epifluorescence 4 months (Fig. 6.9) and 6 months (6.10 Biofilm) after the treatment application showed that the fluorescence of the non-treated biofilm (control) was preserved (Fig. 6.9 and 6.10 Biofilm).

The biofilm samples from the Biotin and Preventol treated areas did show small spots of red fluorescence after 6 months, which correspond to the green areas observed under visible light (Fig. 6.10 Biotion T and Preventol RI 80). TiO$_2$ and Albilex biofilm samples depicted red fluorescence similar to the non-treated biofilm (Fig. 6.10 TiO$_2$ and Albilex Biostat).

### 6.3.4.3 Molecular monitoring of microbial communities by DGGE

The DGGE profiles of the biofilm samples collected from *Casa da Pesca* glazed tiles before and four months after the application of the treatments are presented in Fig. 6.11. The DGGE profiles, derived from the cyanobacterial 16S rDNA (Fig. 6.11a), fungal ITS (Fig. 6.11b) and eukaryotic 18S rDNA (Fig. 6.11c) show the fragments of the non-treated biofilm collected before the experiment (lanes C0 in Fig. 6.11), the non-treated biofilm after 4 months (lanes C4 in Fig. 6.11) and the treated biofilm samples after 4 months (TiO$_2$ corresponds to lane T4, Biotin corresponds to lane B4, Preventol corresponds to lane P4, Albelix corresponds to lane A4 in Fig. 6.11).
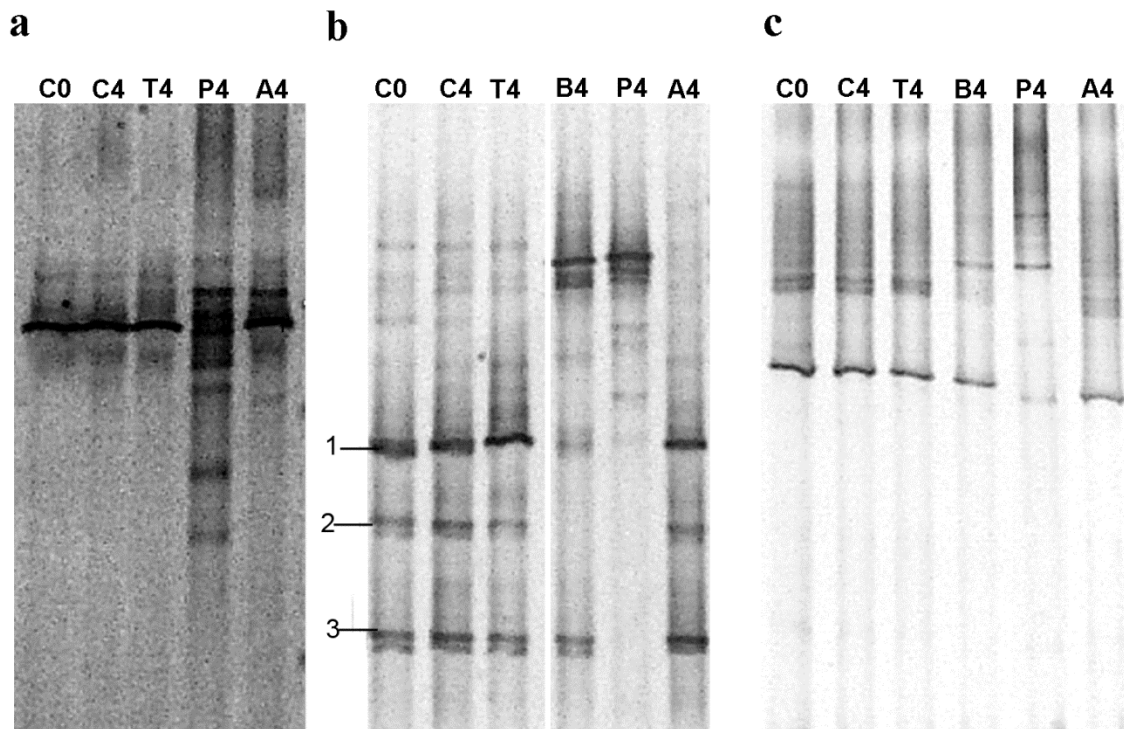
**Fig. 6.11.** DGGE profile of the biofilm samples collected from *Casa da Pesca* glazed tiles before and four months after the application of the biocides. (a) DGGE profiles for cyanobacterial 16S rDNA. (b) DGGE profiles for fungal ITS regions. Numbers 1-3 indicate bands corresponding to the identified fungal species *Devriesia modesta* (1), *Neodevriesiaceae sp.* 2 (2) and *Neodevriesiaceae sp.* 1 (3).(c) DGGE profiles for eukaryotic 18S rDNA. Lanes C0 and C4 correspond to samples of the biofilm without any treatment collected on the first day of the experiment and 4 months later, respectively. Lanes T4, B4, P4 and A4 correspond to samples collected 4 months afterbiocide application on areas treated with $TiO_2$, Biotin, Preventol and Albilex, respectively.

Regarding cyanobacteria, DGGE profiles of the non-treated biofilm samples were identical in composition during the four months of experiment (Fig. 6.11a, lanes C0 and C4). The biofilm samples treated with $TiO_2$ also showed similar DGGE pattern to the non-treated biofilms (Fig. 6.11a, lane T4). Noteworthy is the fact that no amplification was obtained for cyanobacterial 16S rDNA in the sample collected from the area treated with Biotin (B4), indicating that Biotin was able to damage the cyanobacteria present in the biofilm. In contrast, a visible change in the microbial community composition was observed for samples treated with Preventol (Fig. 6.11a, lane P4). Sample from the Albilex treated biofilm (A4) showed a DGGE profile similar to the non-treated samples (C0 and C4), depicting only one DGGE band in common with sample P4 (Fig. 6.11a, lane A4).

The fungal community profiles of the non-treated biofilms (Fig. 6.11b, lanes C0 and C4) showed a stable band pattern during the four months of experiment. In fact, the observed bands are coincident with the DGGE pattern of the fungal species described in section 3.3 (Fig. 6.11b): *Devriesia modesta* (band 1), *Neodevriesiaceae* sp. 2 (band 2) and *Neodevriesiaceae* sp. 1 closely related to *Neodevriesia xanthorrhoeae* (band 3). $TiO_2$ and Albilex seemed not to have caused changes in the fungal community composition, when comparing their DGGE patterns with the non-treated biofilms (Fig. 6.11b, lanes T4 and A4). On the contrary, a noticeable alteration occurred

after the application of Biotin and Preventol (Fig. 6.11b, lanes B4 and P4). The changes in the DGGE pattern were more drastic in samples treated with Preventol than in those treated with Biotin. Faded bands (numbers 1 and 3) positioned equally to the dominant bands of the non-treated samples are observed in the Biotin-treated sample. These bands corresponded to the fungi *Devriesia modesta* and *Neodevriesiaceae* sp. 1, respectively (Fig. 6.11b lane C0).

Similarly, the Eukaryotic 18S rDNA gene DGGE profiles did not show any variations in the banding patterns of the non-treated samples, and for biofilm samples treated with $TiO_2$ and Albilex (Fig. 6.11c, lanes C0, C4, T4, A4). DGGE profiles of the biofilm treated with Biotin (Fig. 6.11c, lane T4) and Preventol (Fig. 6.11c, lane P4) showed some changes comparatively to the DGGE profiles of the non-treated biofilm samples (Fig. 6.11c). Again, the DGGE banding pattern of the Biotin-treated sample showed faded bands corresponding to some of the dominant bands of the non-treated samples. Once again, the changes in the DGGE pattern were more drastic in samples treated with Preventol..

### 6.3.4.4 Phylogenetic identification of microbial communities before and after *in situ* application of Preventol

DNA-based molecular analyses of the non-treated biofilm samples revealed a microbial community mainly composed of photosynthetic microorganisms (chlorophyta and cyanobacteria) and fungi (Tables 6.3-6.5, sample C0). A total of 85 clones were retrieved from the 16S rDNA, 18S rDNA and ITS analysis of the non-treated sample (C0), with seven taxa identified (Tables 6.3-6.5). Regarding the biofilm treated with Preventol, four months after its application DNA-based molecular analyses show cyanobacteria and eukaryotes as the main components of the microbial community. A total of 60 clones were obtained from the 16S rDNA, 18S rDNA and ITS analysis of the Preventol-treated biofilm (Tables 6.3-6.5, sample P4). After this biocide treatment, DNA-based molecular analyses revealed a higher biodiversity with 20 taxa belonging to Chlorophyta, Ascomycota, Basidiomycota, Cyanobacteria, Verrucomicrobia and Proteobacteria. The similarity of the sequences retrieved varied between 94 and 99% for cyanobacteria, 98 and 100% for fungi and 96 and 99% for eukaryotes with their closest homologue sequences from GenBank (Tables 6.3-6.5).

Concerning Cyanobacterial 16S rDNA analysis, 37 clones were obtained from the non-treated biofilm (C0), showing similarities of 99% with their closest homologue sequences and between 91 and 97% with the closest cultured homologue sequences from the GenBank (Table 6.3, sample C0). Among them, Chlorophyta chloroplasts represented 97% of the obtained 16S rDNA sequences using primers specific for cyanobacteria, and only 3% of the sequences were related to cyanobacteria. These sequences were affiliated to uncultured eukaryote plastid (99% similarity) and reached a low similarity with its nearest cultured relative *Oocystis solitaria* (91% similarity). The identified uncultured cyanobacteria belonged to the *Iphinoe* genus from the

*Stigonematales* order and the closest cultured relative was from the species *Iphinoe spelaeobios* (97% similarity) (Table 6.3).

The cyanobacterial sequences obtained from the Preventol-treated sample showed higher biodiversity than the non-treated sample and were composed of Cyanobacteria, Verrucomicrobia and Proteobacteria (Table 6.3, sample P4). Cyanobacteria were the dominant phylum among the prokaryotic members of the treated biofilm (60%). The nearest cultured relatives were *Tolypothrix distorta* and *Anabaena sphaerica* representing each 30% of the total clones. Verrucomicrobia and Proteobacteria were represented by the species *Luteolibacter pohnpeiensis* (10%) and *Rhizobium* sp. (10%), respectively (Table 6.3). Chlorophyta chloroplasts were also obtained using primers specific for Cyanobacteria. *Oocystis solitaria* and *Coccomyxa subellipsoidea* were the closest cultured relatives, representing each 10% of the total clones (Table 6.3).

**Table 6.3.** Phylogenetic affiliations of the operational taxonomic units (OTUs) obtained from the 16S rDNA cyanobacterial sequences of the non-treated biofilm sample (C0) and Preventol-treated biofilm sample (P4) collected from *Casa da Pesca* glazed tiles.

**C0 CYA**

| Representative clone (accession nr.)[1] | Nr. of Clones | Closest relative (accession nr.)[2]/ Closest cultured relative (accession nr.)[3] | Similarity (%) |
|---|---|---|---|
| **Cyanobacteria** | | | |
| 10_E4 (LN713995) | 1 | Uncultured *Iphinoe* sp. partial 16S rRNA gene (LN615007) / *Iphinoe spelaeobios* LO2-B1 (HM748317) | 99/97 |
| **Chlorophyta chloroplasts** | | | |
| 10_E7 (LN713996) | 36 | Uncultured eukaryote clone, plastid (JX877651) / *Oocystis solitaria* chloroplast (FJ968739) | 99/91 |

**P4 CYA**

| Representative clone (accession nr.)[1] | Nr. of Clones | Closest relative (accession nr.)[2]/ Closest cultured relative (accession nr.)[3] | Similarity (%) |
|---|---|---|---|
| **Cyanobacteria** | | | |
| 09_E5 (LN713997) | 3 | *Tolypothrix distorta* SAG 93.79 (GQ287651)/ *Nostoc* cf. *verrucosum* (AB245144) | 99/96 |
| 09_D4 (LN713998) | 3 | Uncultured cyanobacterium clone (DQ471915) / *Anabaena sphaerica* RPAN12 (GQ466513) | 99/94 |
| **Verrucomicrobia** | | | |
| 09_D5 (LN713999) | 1 | Uncultured bacterium clone (GU444072) / *Luteolibacter pohnpeiensis* (AB331895) | 99/98 |
| **Proteobacteria** | | | |
| 09_F4 (LN714000) | 1 | Uncultured bacterium clone (FN421480) / *Rhizobium* sp. JC85 (FR714938) | 99/96 |
| **Chlorophyta chloroplasts** | | | |
| 09_G5 (LN714001) | 1 | Uncultured alga clone (FJ028695)/ *Oocystis solitaria* chloroplast (FJ968739) | 96/94 |
| 09_G4 (LN714002) | 1 | Uncultured eukaryote chloroplast (AB257629)/ *Coccomyxa subellipsoidea* C-169 plastid (HQ693844) | 96/96 |

1 Representative clones of OTUs at 97% identity for 16SrDNA analysis.
2 Closest relative obtained by comparison with the NCBI database and corresponding accession number.
3 Closest relative obtained by comparison with the EzTaxon database and corresponding accession number.

Regarding the *Ascomycota* present on the non-treated biofilm covering the glazed wall tiles, the same three isolated fungi belonging to the *Neodevriesiaceae* family were identified: *Neodevriesiaceae* sp. 2 (61% of clones), *Neodevriesiaceae* sp. 1 related to *N. xanthorrhoeae* (35%) and *D. modesta* (4%) (Table 6.4).

The ITS sequences obtained from the biofilm treated with Preventol belonged to Ascomycota and Basidiomycota (Table 6.4). The phylum Ascomycota was dominant, representing 80% of the total clones. Most of the sequences retrieved by this analysis belonged to the species *Aureobasidium pullulans* (68%). Two other members of the same phylum *Chalara* sp. (11%) and *Phoma pereupyrena* (5%), were also identified (Table 4)*.* Basidiomycota was represented by three species of the same genus*: Cryptococcus carnescens* (11%), *C. dimennae* (5%) and *C. foliicola* (5%) (Table 6.4).

Basidiomycota were represented by three species of the same genus*: Cryptococcus* sp., *C. magnus* and *C. psychrotolerans* (Table 6.4)*.* Two other Basidiomycota members, *Kondoa malvinella* and *Trichosporon mucoides*, were also related to the sequences retrieved from the Preventol treated-biofilm, each representing 3% of the analysed sequences(Table 6.4).

Among the Eukaryotes obtained from the 18S rDNA analysis of the non-treated biofilm, Chlorophyta represented 96% of the retrieved clones, which was represented solely by the genus *Phycopeltis* sp. A minor proportion of the sequences belonged to an unclassified *Ascomycota* from the *Capnodiales* order (4%) (Table 6.5).

The Eukaryotic analysis of the treated biofilm revealed organisms belonging to Chlorophyta, Ascomycota and Basidiomycota. The Chlorophyta *Phycopeltis* sp. was also present in Preventol-treated biofilm. However, this green alga represented only 7% of the clones retrieved from the treated sample, in relation to the 96% obtained from the non-treated biofilm (Table 6.5). The highest proportion of clones obtained for this eukaryotic marker from the treated biofilm belonged to the phyla Ascomycota and Basidiomycota, representing 33 and 60% of total clones, respectively. The species *Aureobasidium pullulans* (30%) represented a major part of the Ascomycota clones, while the remaining 3% were closer to an uncultured Ascomycota clone (Table 6.5).

Table 6.4. Phylogenetic affiliations of the OTUs obtained for fungal communities of the non-treated biofilm sample (C0) and Preventol-treated biofilm sample (P4) collected from *Casa da Pesca* glazed tiles.

**C0 ITS**

| Representative clone (accession nr.)[1] | Nr. of Clones | Closest relative (accession nr.)[2] | Similarity (%) |
|---|---|---|---|
| **Ascomycota** | | | |
| 10_A8 (LN714003) | 14 | *Neodevriesiaceae* sp. (KF309974) | 98 |
| 10_E10 (LN714004) | 8 | *Devriesia xanthorrhoeae*[3] CBS 128219 (HQ599605) | 95 |
| 10_B12 (LN714005) | 1 | *Devriesia modesta* strain CCFEE 5672 (KF309984) | 99 |

**P4 ITS**

| Representative clone (accession nr.)[1] | Nr. of Clones | Closest relative (accession nr.)[2] | Similarity (%) |
|---|---|---|---|
| **Ascomycota** | | | |
| 09_A3 (LN714006) | 13 | *Aureobasidium pullulans* strain 196B1 (HM849619) | 100 |
| 09_G2 (LN714007) | 2 | *Chalara* sp. LL-16.3 (AY188359) | 99 |
| 09_A2 (LN714008) | 1 | *Phoma pereupyrena* isolate A1S2-D31 (KJ767076) | 99 |
| **Basidiomycota** | | | |
| 09_A1 (LN714009) | 2 | *Cryptococcus carnescens* strain IWBT-Y815 (JQ993373) | 100 |
| 09_H2 (LN714010) | 1 | *Cryptococcus dimennae,* (AF410473) | 99 |
| 09_B3 (LN714011) | 1 | *Cryptococcus follicola* (AY557600) | 98 |

[1] Representative clones of OTUs at 97% identity for ITS analysis.
[2] Closest relative obtained by comparison with the NCBI database and corresponding accession number
[3] Recently described as *Neodevriesia xanthorrhoeae* (Quaedvlieg et al. 2014)

The fungal community of the non-treated biofilm growing over the glazed tiles from *Casa da Pesca* belonged to the *Neodevriesiaceae* family according to the taxonomic rearrangements introduced recently by Quaedvlieg et al. (2014). Currently this family continues to be the subject of taxonomic revision and several genera await definitive taxonomic placement. All isolated strains and representative clones of this study were classified into three different clades. One of them, supported by a 100% of bootstrap value, was identified as *Devriesia modesta*. The other two taxa (*Neodevriesiaceae* species 1 and 2), the most abundant in the biofilm, were independent clades supported by high bootstrap values (72–99%).

Table 6.5. Phylogenetic affiliations of the OTUs obtained from 18S rDNA sequences of the non-treated biofilm sample (C0) and Preventol-treated biofilm sample (P4) collected from Casa da Pesca glazed tiles.

| C0 EUK | | | | P4 EUK | | | |
|---|---|---|---|---|---|---|---|
| Representative clone (accession nr.)[1] | Nr. of clones | Closest relative (accession nr.)[2] | Similarity (%) | Representative clone (accession nr.)[1] | Nr. of Clones | Closest relative (accession nr.)[2] | Similarity (%) |
| **Chlorophyta** | | | | **Chlorophyta** | | | |
| 10_B2 (LN714012) | 24 | Phycopeltis sp. HBI HB-YN1202 (KC463792) | 98 | 09_D10 (LN714014) | 2 | Phycopeltis sp. HBI HB-YN1202 (KC463792) | 98 |
| **Ascomycota** | | | | **Ascomycota** | | | |
| 09_F12 (LN714013) | 1 | Capnodiales sp. CCFEE 5177 (KC315867) | 99 | 09_D7 (LN714015) | 9 | Aureobasidium pullulans isolate CMMB Ap1 (JN255732) | 99 |
| | | | | 09_B10 (LN714016) | 1 | Uncultured Ascomycota clone (JQ689427) | 99 |
| | | | | **Basidiomycota** | | | |
| | | | | 09_C7 (LN714017) | 13 | Cryptococcus sp. strain CBS 2993 (AB085800) | 99 |
| | | | | 09_A7 (LN714018) | 2 | Cryptococcus magnus strain JCM 9038 (AB032643) | 99 |
| | | | | 09_F6 (LN714019) | 1 | Cryptococcus psychrotolerans (AB085801) | 98 |
| | | | | 09_D9 (LN714020) | 1 | Kondoa malvinella isolate AFTOL-ID 859 (DQ667164) | 99 |
| | | | | 09_E9 (LN714021) | 1 | Trichosporon mucoides strain JCM 9939 (AB001763) | 96 |

[1] Representative clones of OTUs at 96% identity for 18SrDNA analysis.

[2] Closest relative obtained by comparison with the NCBI database and corresponding accession number.

They could be unknown species considering their low similarity percentages (93–94%) with the currently described species. Four months after the application of the biocide Preventol RI 80, the former dominant species of the *Neodevriesiaceae* family were no longer detected. The exposure to the biocide created a shift in phylogenetic community structure. A higher biodiversity of several lineages of fast growing Ascomycota and Basidiomycota were retrieved in the Preventol RI 80 treated biofilm (Table 6.4, Fig. 6.12).

Fig. 6.12 illustrates the phylogenetic study of the fungal community present on the biofilms before treatment and four month after Preventol RI 80 application.
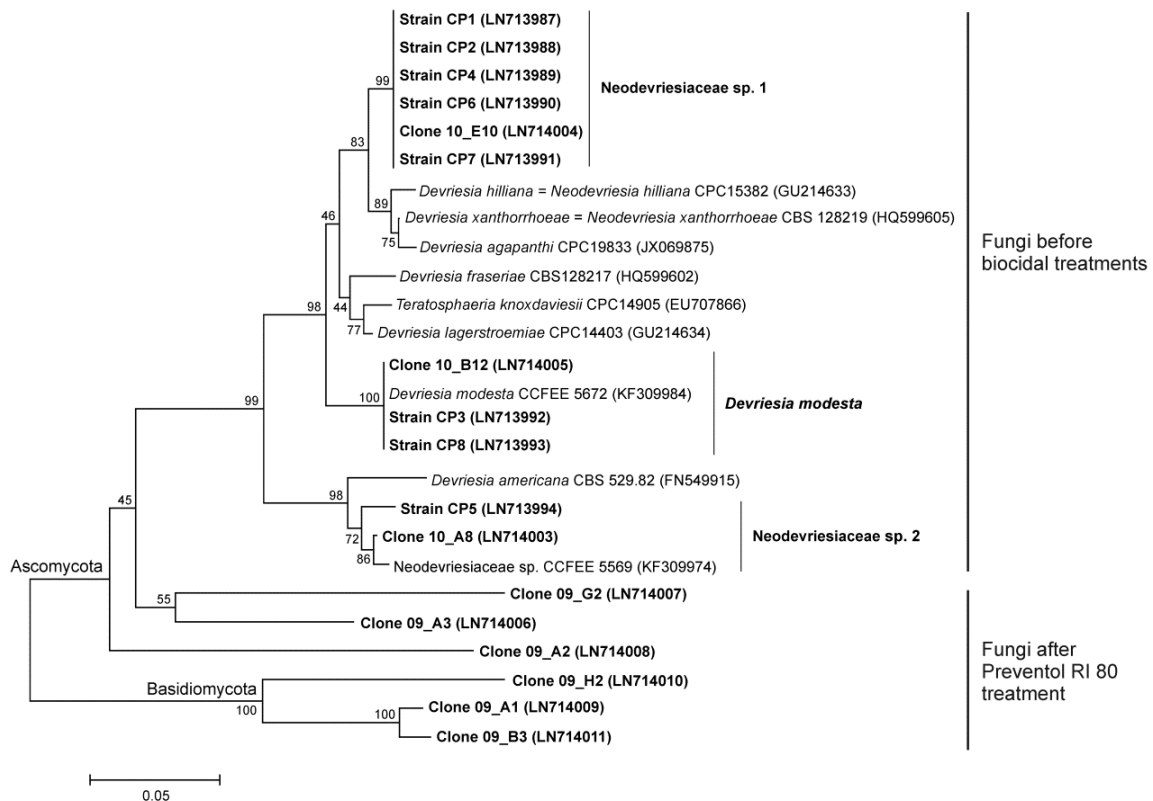


**Fig. 6.12.** Phylogenetic tree derived from ITS1-5.8S-ITS2 regions of rRNA gene sequences showing the relationships between isolated strains and OTU representative clones from biofilm samples collected on *Casa da Pesca* tiles (names in bold). The closest related sequences to the strains isolated before biocidal treatments were also included. All nodes of the tree were also recovered using Maximum-Likelihood and Minimum-Evolution treeing algorithms. Bar, 0.05 substitutions per nucleotide position**.**

### 6.3.4.5 Comparison of glaze surface before and after biocidal treatment

The potential alteration induced on the glaze substrates by the applied treatments was monitored by means of VP-SEM. Fig. 6.13 depicts the glaze surfaces showing no substantial changes between the treated and the non-treated colonized glaze. For all analyzed samples, fissures, pitting and accumulation of lead-rich corrosion products were observed (Fig. 6.13). Superficial deposits, were detected both on the non-treated and treated glazed tiles (Fig. 6.13).
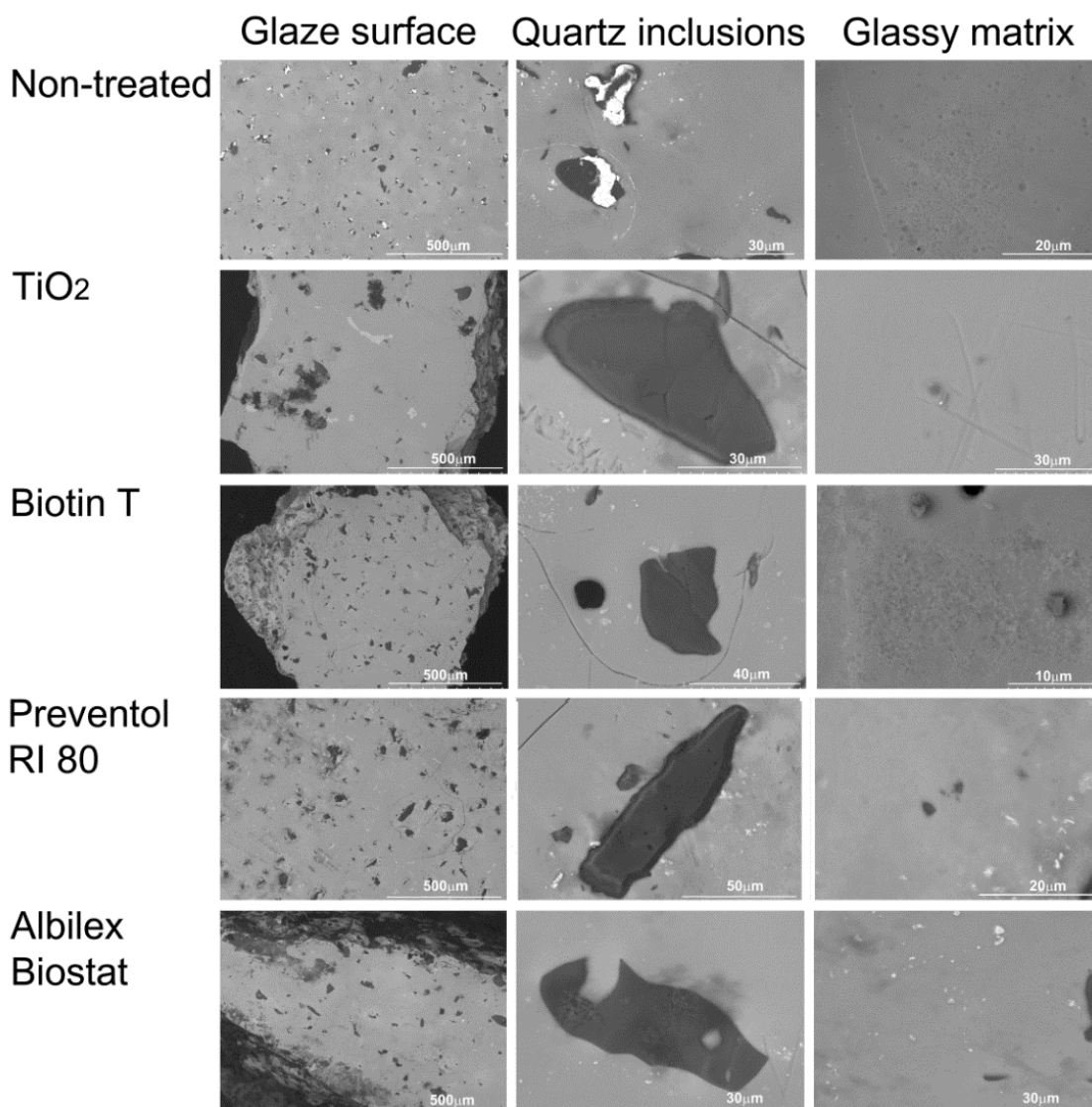
**Fig. 6.13.** VP-SEM image of the glazes after removal of the biofilms from a non-treated colonized glaze (Non-treated) and treated glazes (TiO$_2$, Biotin, Preventol and Albilex) Surface of morphology of the glaze and details in higher magnification of quartz inclusions can be observed.

## 6.4    Discussion

### 6.4.1    Microbial community growing on the glazed tiles

In this study, the microbial communities growing on glazed wall tiles from *Casa da Pesca* (Oeiras, Portugal) were characterized. Some authors have considered glazed substrates hostile for microbial colonization due to their reduced porosity and roughness which results in a low bioreceptivity (Gazulla et al., 2011).

The analysed tile panel from *Casa da Pesca* was manufactured according to the *majolica* production technique (Chapter 1) and therefore it contains significant amounts of lead oxide in its composition (Table 6.1) (Coentro et al., 2012). Lead is toxic to living organisms and lead can be lixiviated from the glassy matrix in acid media (Wood and Blachere, 1978). Microbial growth is often accompanied by acid excretion, such as the oxalic acid produced by fungi which could cause the release of lead from the substrates, thus their presence on lead-rich substrates could be

unexpected. However, the analysed tile panel was severely colonized. Some microorganism can develop in the presence of elements that are considered to be toxic, due to their survival strategies, such as formation of insoluble compounds or EPS protection (Sayer et al., 1995, 1999). Additionally, studies have shown that glazes can be colonized by dense biofilms whenever exposed to certain outdoor environments (Giacomucci et al., 2011; Coutinho et al., 2013). Specific environmental factors, such as mild cold temperatures, high relative humidity, moderate solar irradiance, shelter from direct rain and surrounding vegetation seem to allow the settlement of microorganisms on these substrates, as it was shown in Chapter 3 (Coutinho et al., 2013).

The aesthetic biodeterioration caused by the development of photosynthetic-based biofilms on the studied tile panel compromised its visual appreciation (Fig. 6.2). The growth of biofilms on glazed ceramic building materials has been associated with biodeterioration patterns, such as aesthetic damage, deepening of fractures or detachment of the glaze when chasmo- or/and endolithic growth occurs (Palmer and Hirsch, 1991; Giacomucci et al., 2011; Coutinho et al., 2013). Besides aesthetic and biophysical damage, some chemical damage on glazed surface have been reported, but little is still known on how microorganism affect the corrosion of historic glazes (Watanabe et al., 2009; Baricza et al., 2012).

The brown biofilm observed on the studied glazed tiles was mainly composed of Chlorophyta together with a minor proportion of fungi belonging to the *Neodevriesiaceae* family and a Cyanobacterium from the *Iphinoe* genus. Direct microscopy observation of the biofilm revealed the presence of the alga *Phycopeltis arundinacea*, which was corroborated by DNA-based analysis (Table 6.5). This subaerial green alga is mainly epiphytic on leaves of perennial terrestrial plants (John 2003; Rindi and Guiry 2002; Rindi et al. 2004), and to our knowledge, it has not been reported on cultural heritage assets nor on any inorganic building material. The natural substrate most frequently colonized by Phycopeltis arundinacea is the cuticule on the epidermis of leaves, normally impregnated by wax, like the surfaces of ivy leaves (*Hedera helix*) or *Eucalyptus* sp. (Rindi and Guiry 2002). In contrast, the chlorophyta *Oocystis solitaria* was previously identified on glazed tiles from Pena National Palace in Sintra, Portugal, but with very low similarity to the mentioned sequence (Coutinho et al., 2013)(Table 6.3). *Iphinoe* sp. the cyanobacterium identified on the non-treated biofilm was reported on mortars from Etruscan and Roman tombs (Diaz-Herraiz et al. 2014).

In general, the biodiversity of photoautotrophs in the biofilms collected from *Casa da Pesca* tiles was lower in comparison to the microbial diversity detected on the glazed tiles from Pena National Palace (Coutinho et al., 2013; Chapter 3). According to Macedo et al. (2009), environmental variables and site-specific characteristics have a strong influence on photosynthetic community development compared with the substrate properties.

Concerning the fungal community, DNA-based analysis and culture-dependent methods showed similar results. Ascomycota members of the *Capnodiales* order, especially from the *Neodevriesiaceae* family, were identified in the non-treated biofilm (Table 6.2, 6.4 and 6.5). Slow-growing species of rock-inhabiting fungi belonging to Capnodiales are resistant to harsh climatic conditions due to their strongly melanised dark colored cell walls (Ruibal et al., 2008; Egidi et al.,

2014). *Neodevriesiaceae* family was the most common fungal taxon detected in the *Casa da Pesca* biofilms. This novel family was recently described grouping members of the genera *Devriesia*, *Neodevriesia*, *Teratosphaeria* and *Tripospermum*. In addition several genera await taxonomic placement in this family (Quaedvlieg et al. 2014). The two most abundant fungi in the biofilm could be unknown species of the *Neodevriesiaceae* family. Further studies characterizing their morphology and other molecular markers should be conducted in order to describe them as novel species.

The first identified members of *Devriesia* were heat-resistant fungi isolated from heat treated soils (Seifert et al., 2004). Indeed, glazed surfaces exposed to direct sunlight during hot seasons can achieve relatively high surface temperatures. The heat and drought resistance of these organisms and other rock-inhabiting fungi that can develop in desert areas could explain their ability to colonize glazed wall tiles. A new species of this genus, *Devriesia imbrexigena* AJL Phillips & ML Coutinho was isolated from a similar substrate, the silica-lead glaze from the wall tiles of the Pena National Palace at Sintra, Portugal presented in Chapter 3 (Crous et al. 2012). The ecological relation between photosynthetic microorganisms and black slow-growing fungi is still not well understood. There is no certainty if the fungi are parasitizing the photosynthetic microorganisms or if there is a symbiotic relation between them, which enables survival in harsh substrate. Although biodeterioration damage caused by these fungi on ceramic substrates are still unknown, several authors have associated these fungi with aesthetical biodeterioration on stone substrates (Sert et al., 2007, 2010; Cutler et al., 2013; Egidi et al., 2014). Most of the retrieved sequences from the non-treated biofilms showed high similarity with microorganisms found on stone cultural heritage assets (e.g. Roman Necropolis of Carmona, Iranian archaeological heritage, Pena National Palace tiles) or soil (Bonazza et al., 2007; Benavente et al., 2011; Coutinho et al., 2013; Egidi et al., 2014). Such microorganisms have developed survival strategies to be able to grow in harsh conditions with limited water and nutrient availability and severe environmental conditions.

## 6.4.2 Efficacy evaluation of the tested biocides

Since microorganisms can damage the substrate they are living on, in a process known as biodeterioration, it is often necessary to eliminate or control their growth on cultural heritage assets. For this reason, the use of biocides is a common procedure in conservation and restoration interventions. Therefore, a group of commercial biocides that are frequently used on inorganic substrates, such as stone, together with a non-conventional $TiO_2$ nanoparticles biocide were tested on the colonized tiles from *Casa da Pesca*.

The assessment of the efficacy of biocides to be used on cultural heritage is always based on several variables, such as inactivation efficiency, alteration of coverage area of the biofilm, durability and effect on the substrate. Since multiple parameters, like biofilm macro- and microscopic morphological features, physiological characteristics and interaction with the substrate need to be analysed, we used a combination of different methods to provide a more complete set of data.

Photographic recording provided information regarding the area, color and density of the biofilm. In the case of photosynthetic biofilms several studies have proved that color is indicative of the physiological state of the microorganisms composing the biofilms (Prieto et al., 2002; Sanmartín et al., 2010). The density of the biofilm was also indicative of the physiological state of the microorganism. For instance, Chla fluorescence monitoring by epifluorescence microscopy clearly showed that when color had changes and density of the biofilm reduced the chlorophyll red fluorescence had decreased. The DGGE profile analysis of the non-treated biofilm samples (C0 and C4) confirmed the stability of the microbial population during the evaluation of the treatments, ensuring that the major changes were caused due to the effect of the treatment and not due to other environmental factors (Fig. 6.10). Moreover, DGGE profile analysis allowed us to monitor the changes in microbial diversity of the studied biofilms caused by the treatments. DGGE is a well-known tool for monitoring microbial populations on cultural heritage assets (e.g. (Miller et al., 2009; Qi-Wang et al., 2011; Piñar et al., 2013; Otlewska et al., 2014a)). However, DNA can persist undamaged after cell death; consequently DNA-based methods do not provide a differentiation between viable and non-viable cells. In addition, several drawbacks of this molecular fingerprint technique are known, including the fact that in complex microbial communities each band is not always associated with one organism and that co-migration can occur (Head et al., 1998; Marzorati et al., 2008). Thus, DNA-sequencing of a selected profile was necessary to give an insight into the biodiversity present on the altered biofilm. The results will be discussed for each biocide separately to provide a clear comprehension of the results obtained in this work focusing on the current knowledge of the mechanisms of biocidal action and through comparison with other case studies present in the literature.

### 6.4.2.1 Titanium dioxide

$TiO_2$ is a non-toxic substance that has been tested as an alternative product to conventional biocides on mortars and stones exposed outdoors (Fonseca et al., 2010; Pinho and Mosquera, 2011). The biocidal action of $TiO_2$ nanoparticles has been tested in many laboratory studies. Markowska-Szczupak et al., (2011) recently perfomed a literature review on this issue. $TiO_2$ nanoparticles (anatase phase based) when irradiated with UV light originates electrons in the conduction band and holes in the valence band, enabling catalytic reactions namely photocatalytisis (Kumar and Devi, 2011). Nanoparticles in contact with water react producing highly reactive hydroxyl radicals that are able of oxidizing most organic compounds, including cell components (Kiwi and Nadtochenko, 2005; Markowska-Szczupak et al., 2011).

Generally, several factors influence the antimicrobial activity of biocides, such as temperature, time of exposure, amount of organic material, growth conditions and growth phase of the microorganism on which they are tested (Russel, 1999). In addition, the efficiency regarding $TiO_2$ is also connected to the irradiation source and time of exposure. In fact the effectiveness of $TiO_2$ as a biocide has been variable according to the different irradiation sources(e.g. UV-lamps, solar irradiation and solar spectra lamps)  (Gazulla et al., 2011; Gladis and Schumann, 2011a;

Portillo et al., 2011). Hence, we decided to test its efficacy under natural environmental conditions where there is real need for a treatment for biofilm removal.

$TiO_2$ is a white solid and its application alone can caused color changes. Therefore, the analysis of the color parameter to monitor changes in the biofilm was difficult due to the interference of the biocides color. Neither macroscopic nor microscopic observations of the $TiO_2$-treated biofilm indicated alterations in biofilm density, chlorophyll fluorescence or cell structure (cell disruption).

The DGGE analysis of the $TiO_2$-treated biofilm sample after four months of application seemed to reinforce the macroscopic and microscopic observations and no changes on the genetic profile were observed.

The antimicrobial activity of $TiO_2$ nanoparticles through photocatalytic activity has been extensively studied and observed, as previously mentioned (Kiwi and Nadtochenko, 2005; Rajagopal et al., 2006). The effect of biocides on complex microbial communities could be inadequate due to the presence of extracellular polymeric substances (EPS) excreted by several microorganisms on the cell wall which protect them from environmental toxins (Russel, 1999; Stewart, 2002). In addition, surface properties of the microorganisms could influence the extent of membrane damage during the interactions with the nanoparticles and produced reactive oxygen species (ROS) (Hessler et al., 2012; Planchon et al., 2013).

Even if $TiO_2$ was not lethal for the microorganisms, it was the only biocide that caused significant changes in the biofilm-covered area. Self-cleaning properties of photocatalytic nanoparticles are well known, and the decrease in adherence of microorganisms has been previously reported on other ceramic substrates (Graziani et al., 2013). Therefore, the detachment of the biofilm visible six months after treatment is likely to have been caused by the self-cleaning effect induced by the $TiO_2$ nanoparticles (Fig. 6.8). In the field of cultural heritage, the removal of the microorganisms from the substrate is always a critical issue. Mechanical processes may result in material loss and surface alteration, which can cause irretrievable losses. Therefore, results obtained with $TiO_2$ causing the detachment of the biofilm is indeed promising for cleaning inorganic cultural heritage assets located outdoors.

### 6.4.2.2 Biotin

Biotion is a commercial broad-range biocide that has been tested with success on built cultural heritage (de los Ríos et al., 2012). This biocide has quaternary ammonium compounds in its composition (QACs) which are approved for conservation of cultural heritage monuments by the European Biocide Directive, which considers them to be relatively environmentally friendly (Cooke, 2002).

After the application of Biotin photographic recording showed color and density changes in the biofilm. Microscopic observations aided by epifluorescence corroborated the effect of Biotin on

the biological communities revealing an almost complete extinction of Chl*a* fluorescence accompanied by cell disruption (Fig. 6.8). Quaternary ammonium compounds, such as the compounds present in this biocide, are cationic surfactants that affect the permeability of the membrane causing its disruption and denaturation of structural proteins and enzymes (Buffet-Bataillon et al., 2012).

Regarding DGGE profiles of fungi and eukaryotic microorganisms some changes were observed. The amplification of the cyanobacterial 16S rRNA gene did not produced any positive PCR results probably due to the absence of cyanobacteria after biocide application. However, the most intense bands of the non-treated samples were still visible in the biofilm-treated sample (Fig. 6.10). We cannot conclude whether there was only a partial inactivation and some organisms remained viable or if these bands are the result of undamaged DNA from non-viable (or dead) microorganisms. Concerning the new bands, which are coincident in position to DGGE profile of the Preventol treated areas, these could indicate that a recolonization occurred in this area 6 months after the application. In addition, the reappearance of Chl *a* fluorescence on the biofilm six months after Biotin treatment seems to validate this view. This point is further discussed when analysing the Preventol results (section 6.4.2.3).

### 6.4.2.3 Preventol

Preventol is also a commercial quaternary ammonium based biocide that has been used for many years on cultural heritage assets, including stone monuments and mural paintings (e.g. Ascaso et al. 2002; Nugari et al. 2009). Photographic recording showed drastic changes of color and density of the biofilm in the treated area. However, no variation in the biofilm coverage area was observed. Similar to Biotin, four months after biocide application no Chl*a* fluorescence was observed. At this time, DGGE profile showed that most of the principal bands from the non-treated biofilm were no longer present on the Preventol-treated biofilm. These results indicate a successful activity of the biocide against the major components of the biofilm community. Indeed, several authors have mentioned the aggressive action of this biocide in the biological communities dwelling on stone (Ascaso et al., 2002; de los Ríos et al., 2012; Speranza et al., 2012).

Preventol-treated biofilm was selected for DNA-based sequencing based on the DGGE analysis since it resulted in the greatest variation in the DGGE banding pattern. The construction of clone libraries confirmed that most of the abundant members of the non-treated biofilm community could no longer be detected or the number of clones was significantly reduced (Tables 6.3–6.5). For instance, *Phycopeltis* sp. and *Oocysts solitarian* were still detected even after Preventol exposure, but resulted in a much lower number of clones. Furthermore, the fungal community of the non-treated biofilm was no longer detected.

Regarding the biodiversity after Preventol treatment, in general the microorganisms that were detected only on the treated biofilm are known to be able to grow in diverse climates and substrates, such as soil, sand, marine environment and some are even human (other animals) and plant as pathogens (Rosa e Silva et al., 2008; Yoon et al., 2008; Ramana et al., 2013; Curlevski et al., 2014). Some of the identified members belong to the following photoautotrophs genera

*Coccomyxa, Tolypothrix and Anabaena.* These have been identified on European stone monuments (Macedo et al., 2009; Cutler et al., 2013). Also, members of the genus *Cryptococcus* have also been identified in biofilms dwelling on stone buildings (Cutler et al., 2013). Pitzurra et al. (2001) identified *Cryptococcus* species, as well as other fungi that were acting synergistically with air pollution in the deterioration of calcareous rock. In terms of diversity the richest phylum present on the biofilm after the treatment with Preventol was *Basidiomycota* mainly represented by *Cryptococcus. Aureobasidium pullulans* was the most abundant *Ascomycota* after Preventol treatment. Giacomucci et al. (2011) found *A. pullulans* on a case of tertiary colonization of ceramic glazed panels in Venice (Italy). These, acrylic adhesive-treated tiles presented a biofilm growing between the ceramic body and the glaze. Other filamentous fungi found in the Preventol-treated biofilm, such as *Chalara* sp. and *Phoma* sp. have been found on diverse building materials (Piñar et al., 2009; Shirakawa et al., 2010). The phylogenetic tree of the fungal community before and after this treatment illustrates the overall change in the community composition (Fig. 6.12).

Prokaryotic biodiversity was also affected by the biocide. A higher prokaryotic biodiversity was retrieved on the treated biofilm four months after treatment with Preventol. Non-photosynthetic prokaryotes that were not identified in the non-treated community were found, such as one member of the *Verrucomicrobia* and another of the *Proteobacteria* phyla.

The interpretation of the changes in the microbial profile and the presence of "new" microorganisms (not detected in the non-treated biological community) raise one question: Were the "new" microorganisms present on the initial biofilm or not?The amplification by PCR-based methods, probably reflects only the major components of the biofilm, while the minor components are not amplified. However, the biocide treatments (Preventol and Biotin) could have caused DNA degradation of the major components allowing the amplification of the minor components. On the other side, a recolonization by foreign microorganisms using cell debris and biocide residues as nutrient source could also have occurred. In this case, probably an early development of photosynthetic microorganisms had already started at 4 month after the treatment when they were detected also by DNA-based analysis, but could not be detected at this time by epifluorescence. Later, six months after Preventol treatment the presence of the photosynthetic microorganisms was detected by epifluorescence. The recolonization after biocide treatments has been reported by other authors, maybe the most notorious case was the recolonization of microbial communities observed in the Lascaux Cave after several treatments with quaternary ammonium derivative (Bastian et al., 2010; Martin-Sanchez et al., 2012)

### 6.4.2.4 Albilex

Albilex is a commercial biocide that has been used successfully by the National Tile Museum in Lisbon to inactivate biological colonization of glazed wall tiles. Similar to the other tested commercial biocides (QAC based compounds), alkyl-benzyl-dimethyl-ammonium chloride is its main active compound. In addition it contains chromium dihydroxide ($H_2Cr_2O_7$) as an active

principle. Suresh Kumar et al. (2014) reported that this toxic metal ion can act as photosynthesis inhibitor, but results obtained in the present work do not provide any data corroborating this effect.

On the Albilex-treated biofilm area neither color nor density changes were observed, not even chlorophyll fluorescence alterations. In fact, this biocide seemed to have very little effect on the community profile as was observed by DGGE profile analysis. However, no conclusions can be drawn regarding the non-photosynthetic components of the non-treated biological community since no method was used to assess their viability after the application.

The procedure for the application of biocides on tiles used in the Portuguese Tile Museum usually involved submerging the tile in the biocide solution (personal communication). Hence, repeated applications or application with a poultice to ensure longer action might be necessary to improve its efficacy.

Concerning all tested treatments, at present no perceivable alteration of the glaze could be associated with them. The morphological characterization of the glaze surface by SEM analysis after exposure to tested biocide solutions is a common procedure to evaluate chemical resistance of glazes (Fröberg et al., 2007, 2009). The corrosion and fractures detected on the glazed surface were also visible on the colonized non-treated tiles, therefore the applied treatments did not affect the glaze surface.

## 6.5   Conclusions

The brownish biofilm growing over the glazed wall tiles from *Casa da Pesca* was composed of a complex community of fungi, microalgae and cyanobacteria. Microalgae community was mainly composed of Phycopeltis sp. Results of the evaluation of the commercial biocides in relation to the lethal efficacy against the identified microorganisms showed that at the tested concentration and application methods Preventol was the most effective biocide followed by Biotin. $TiO_2$ nanoparticles were not effective in the inactivation of the microorganisms. However, $TiO_2$ had a physical action on the biofilm causing its detachment from the substrates. Albilex seemed to have little or no effect on the microbial biofilm under the tested conditions. However, it must be highlighted that even the most efficient tested biocides showed no long term protection. These results are illustrative of the limited time scale effect of the tested biocides. Lixiviation by rain and consequent decrease in concentration might have allowed the recolonization of the treated substrates by microorganisms.

Concerning the monitoring methods used to evaluate biocides efficacy, they seemed to be suitable to provide information on their lethal efficacy against the photosynthetic community. However, for the non-photosynthetic community sometimes the data were sometimes inconclusive. Therefore, we propose that complementary methods which can provide information regarding the viability of the non-culturable microorganisms should be added to the monitoring of biocides, such as RNA-based analysis.

The results showed that Biotin and Preventol were the most efficient biocide regarding the inactivation of the initial microbial community. $TiO_2$ showed to be efficient in promoting biofilm

detachment from the tile surface. Therefore, further investigations should be performed regarding the combined use of QACs biocides followed by application of $TiO_2$ nanoparticles to promote detachment of biofilms from inorganic building materials.

.

# Preliminary tests of titanium dioxide thin film coatings on historical glazed tiles to prevent biological colonization
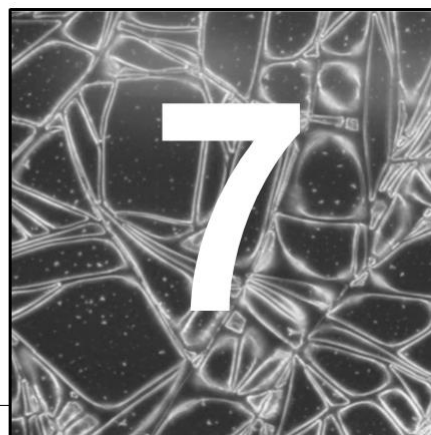
The control of biological colonization and biodeterioration is a major problem of outdoor cultural heritage assets, since microorganisms may damage their host substrates. Glazed wall tiles exposed outdoors are also prone to biological colonization (Chapter 2, 3 and 6) which may cause physical and/or chemical damage on the substrate (Chapter 3, 4, 5 and 6). Therefore, titanium dioxide ($TiO_2$) thin films obtained by sol-gel were tested on historical glazed wall tile samples in order to prevent biological colonization. The application of this type of coatings was tested on four different Portuguese glazed tiles. The chemical characterization was performed both for the tile glaze and ceramic body. In addition, the mineralogical composition of the ceramic body was characterized. The deposited thin film was characterized by micro Raman spectroscopy (μ-Raman) and field emission scanning electron microscopy (FE-SEM). Moreover, potential chromatic and mineralogical alterations of the ceramic paste were assessed by color measurements and X-ray diffraction (XRD), respectively. The efficiency of antimicrobial properties of the sol-gel films was assessed by inoculating the fungus *Cladosporium* sp. previously isolated from glazed wall tiles from Pena National Palace.

## 7.1    Introduction

Functionalization of surfaces is today a well-established field and glazed tiles are used as a support for several purposes (Berto, 2007). Among others, the self-cleaning and antimicrobial properties have been extensively studied through the deposition of photocatalytic $TiO_2$ coatings on diverse types of ceramic and glass substrates (Gazulla et al., 2011; Gladis and Schumann, 2011a; Graziani et al., 2013; Murugan et al., 2013; Radeka et al., 2014). The application of $TiO_2$ has also been used in the field of cultural heritage to prevent stone and mortars´ biological colonization (Fonseca et al., 2010; Pinho and Mosquera, 2011; La Russa et al., 2012, 2014; Quagliarini et al., 2012; Graziani et al., 2013; Franzoni et al., 2014). As described in Chapter 6 conventional procedures for controlling and preventing biodeterioration include mechanical, physical and chemical intervention methods, such as mechanical cleaning and biocide application (Caneva et al., 1991; Berti et al., 2008). However, the most common biocides do not offer long-lasting action

(Russel and Chopra 1990), as demonstrated in Chapter 6. The photo-stability and non-toxic characteristics of $TiO_2$ are an advantage, since the use of organic compounds outdoors is limited due to low resistance to temperature variations, UV aging and increase of substrate bioreceptivity.

The photocatalytic properties of $TiO_2$ have been extensively studied and reviewed since the 1970´s (Mills and Hunte, 2000; Kumar and Devi, 2011). Fig. 7.1 illustrates the $TiO_2$ electronic structure and the photocatalytic effect. $TiO_2$ in the form of anatase phase is characterized by an bandgap energy ($E_{bandgap}$) of 3.2 eV (circa $\lambda$=388 nm )(Mills and Hunte, 2000). The bandgap energy is equal to the amount of energy that needs to be given to the atom to be able to remove electron from the valence band into the conduction band. Therefore, when $TiO_2$ is exposed to ultraviolet (UV) light ($\lambda$ <400, $E \geq E_{anatase\ bandgap}$), holes ($h^+$) and excited electrons ($e^-$) are generated. The holes are capable of oxidizing water and electrons are able to reduce oxygen forming radicals (Fig. 7.1).
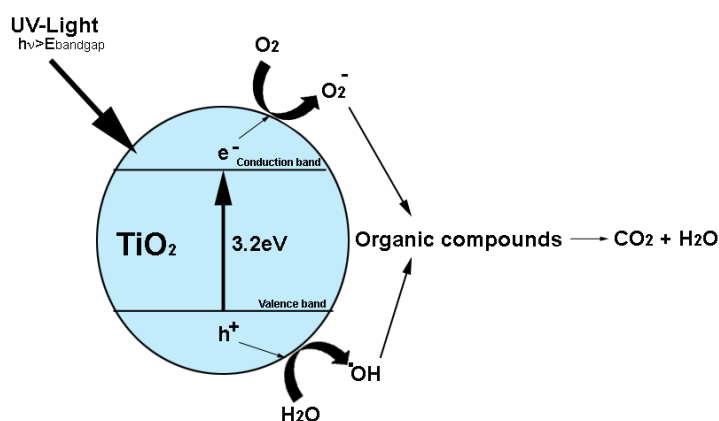


**Fig. 7.1.** Schematic illustration of TiO2 electronic structure characterized by its valence (VB) and conduction band (CB) energy positions and photocatalytic reactions.

The biocidal effect of $TiO_2$ is based on the formation of free-radicals and hydrogen peroxide through irradiation with UV-light, as showed above. Similar to other organic compounds, these radicals attack cell walls and cell structures resulting in the inactivation of the microorganisms (Markowska-Szczupak et al., 2011).

$TiO_2$ coated surfaces, also become super-hydrophilic when irradiated with UV-light. The formation of $OH^-$ ions layer on the photocatalyst´s surface leads to a water contact angle close to 0º (Fujishima and Zhang, 2006). This phenomenon is responsible for the self-cleaning effect through the creation of a thin water layer over the surface which avoids the accumulation of dirt and other particles, such as microorganisms' on the surface.

Although $TiO_2$ can be applied as nanoparticles such as tested in Chapter 6, a common procedure is the immobilization of this compound on surfaces through the deposition of thin-films. Photoactive, photo-stable and colorless $TiO_2$ thin-coatings can be produced by different methods, such as sol-gel, sputtering or chemical vapour deposition among others (Takeda et al., 2001; Pinho and Mosquera, 2011; Murugan et al., 2013). Sol-gel (also known as alkoxide route) is probably the simplest method in terms of required equipment. This method involves a two-step reaction:

hydrolysis and condensation; where metal alkoxides are used as precursors (Ti-OR in the case of $TiO_2$) due to their affinity in reacting with water (Fig. 7.2). Through this reaction with water the removal of the alkyl group occurs. The condensation either with water by oxolation or with alcohol by alcoxolation results in the formation of Ti-O-Ti bonds forming amorphous hydroxides (Fig. 7.2). Posterior heat treatment is necessary in order to obtain the crystalline titanium oxide phase.
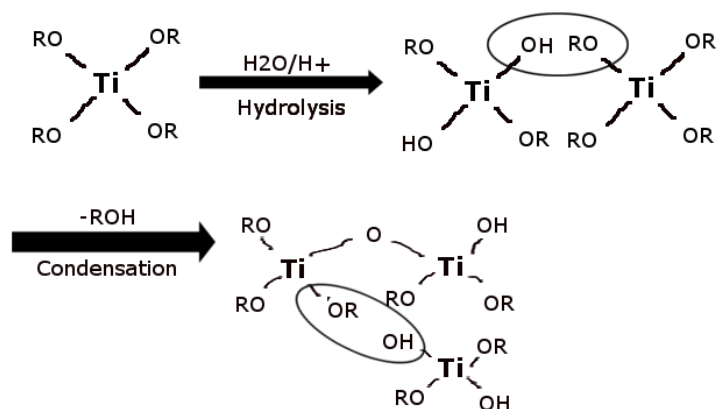


**Fig. 7.2.** Hydrolysis and condensation reactions of the sol-gel method.

$TiO_2$ coatings produced by the sol-gel method have been applied widely on glass and glaze substrates (Kemmitt et al., 2004; Aubry et al., 2007; Addamo et al., 2008; Medina-Valtierra et al., 2009). However, the application of any treatment on cultural heritage raises questions beyond their efficacy, durability and cost. Any intervention on cultural heritage assets must be harmless to the material, not cause significant alterations and also be retractable, in order not to interfere with future interventions. In this chapter the assessment of the efficacy of photocatalytic $TiO_2$ coatings applied on historical glazed tiles to protect them against biological colonization is presented. The deposited sol-gel thin-films were characterized by μ-Raman and FESEM. The efficacy of the $TiO_2$ coatings on glazed tiles for preventing microbial growth was evaluated by inoculating the fungus *Cladosporium* sp. and further evaluating fungal growth, chromatic variation and mineralogical composition.

## 7.2 . Materials and methods

### 7.2.1 Tile samples

A set of four different tile types were selected for sol-gel thin coatings deposition (samples 1BW, 2W, 3TS and 4MW). Table 7.1 summarizes the description of the sample tiles used in this work. Samples 1BW, 2W and 3TS were obtained from a deposit of construction materials from demolished buildings and 4MW is an industrial modern white tile. Samples were cut into pieces with circa 1,5 x 3 cm$^2$. Prior to coating application, glaze surfaces were cleaned with ethanol and rinsed with distilled water. Small samples of the ceramic body were cut into smaller pieces (10x10mm) for compositional analysis.

**Table 7.1.** Description of the tile samples selected for the experiment.

| Ref. | Description |
|---|---|
| **1BW** | Blue and white majolica tile. Possibly dating from the XVIII/XIX century |
| **2W** | Green and white tile. Green enamel applied with a stencil (only the white glaze selected) |
| **3TS** | Transparent glazed tile. Early 20th century tiles from the Sacavém ceramic factory |
| **4MW** | Modern industrial white tile |

### 7.2.2  Tile characterization

Elemental analysis of tiles´ ceramic body and glaze was conducted by wavelength dispersive X-ray fluorescence spectrometry. The analyses were performed with a PANalytical XRF-WDS 4 kW AXIOS (PANalytical B.V., Almelo, The Netherlands) sequential spectrometer using a Rh X-ray tube and an He flow. Spectra deconvolution by the iterative least squares method and standardless semi-quantitative analysis based on the fundamental parameter approach were carried out with the SuperQ IQ+ software package (PANalytical B.V., Almelo, The Netherlands). The glaze was analysed directly over the tile samples and the ceramic paste separated from the glaze and grinded into a fine powder. For accuracy purposes the lead-silicate reference glass Corning Museum of Glass C (CMOG C) was analysed simultaneously.

### 7.2.3  Synthesis and application of TiO$_2$ coatings

Sol-gel was prepared according to a previously described procedure (Yung et al. 2007 in Maver et al. (2009)) using the following reagents without further purification: Titanium (IV) isopropoxide (Aldrich, 99.9%) as precursor, ethanol (CH$_3$OH) (Sigma-Aldrich, puriss p.a.) and acid water (HNO$_3$). Sol was refluxed for 48h at 85ºC. The superficial liquid phase was collected and separated from the white deposit formed after the refluxing process. The sol was deposited on the tile samples through the Spincoat G3P – 8 (Special Coating Systems, SCS) device at a speed of 2500 rpm/s. Samples were air dried for 24 hours prior to thermal treatment. Tiles with air dried coatings were annealed on the furnace at 350 ºC for 4 hours. The thermal treatment was necessary in order to crystallize the amorphous TiO$_2$ thin film into the anatase phase.

### 7.2.4  Characterization of TiO$_2$ thin film

µ-Raman was performed to analyse the crystallinity of the thin film with a Labram 300 Jobin Yvon spectrometer, equipped with a He-Ne laser of 17 mW power operating at 632.8 nm and also a solid state external laser of 50 mW power operating at 514.5 nm. Spectra were recorded as an extended scan and the laser beam was focused with 100✕ Olympus objective lens. The laser power at the surface of the samples was varied with the aid of a set of neutral density filters of 0.6.

To analyse the surface morphology and thickness of the thin films treated samples were observed by FESEM carried out with a Jeol JSM-7001F microscope equipped with an Oxford EDS light elements detector for chemical analysis using secondary X-rays and standard ZAF corrections that allow semi-quantitative microanalysis. Tile samples were previously sputter coated with a thin gold/palladium film.

### 7.2.5 Tertiary bioreceptivity experiment

A set of non-treated tile samples and a set of samples treated with $TiO_2$ coating were selected for a tertiary bioreceptivity experiment (Fig.7.3). The selected fast growing fungus *Cladosporium* sp. was isolated from the biological patina growing over the *majolica* glazed tiles from Pena National Palace, Portugal (Coutinho et al., 2011). The fungus was grown in PDA plates at room temperature. For the inoculum the fungus was scraped from 1 $cm^2$ of the PDA plates with a sterile scalpel and suspended in dilute PDA liquid medium (10 g/l) (Scharlau, Spain). At the inoculation day, each set of tiles were placed inside a glass Petri dish suspended over a net with distilled water at the bottom. Samples with and without coating of the same tile sample where placed together. Prior to the inoculation with microorganisms, the Petri dishes, with the water at the bottom and the tiles on top of the net were autoclaved at 120 ˚C at 100 kPa above atmospheric pressure for 20 min. After slow cooling at room temperature, 150 µl of fungal suspension was inoculated on the glazed tile surfaces´. All tile samples (inoculated and control samples) were kept outdoors on the terrace of a building situated in Almada (Portugal) exposed to direct sunlight for 40 days (March to April). The climatic conditions are characterized by mild temperatures with average day temperature of circa 14-16 ºC. The water at the bottom of the Petri dishes was periodically re-filled.
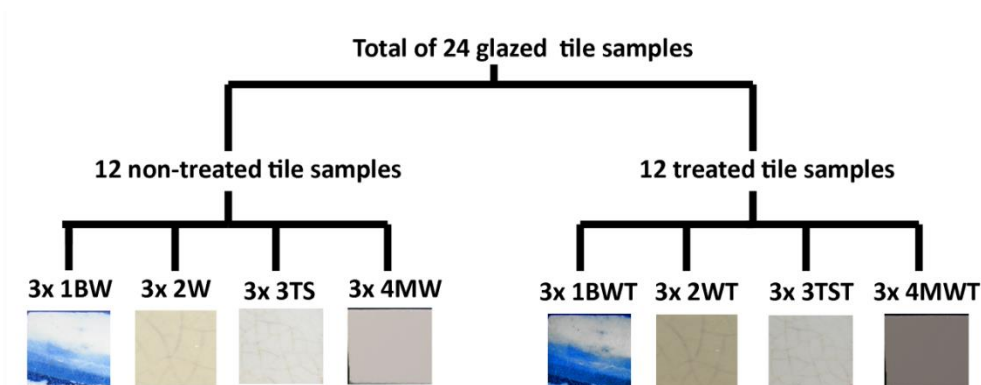


**Fig. 7.3.** Scheme with experimental design with the number of replicates of non-treated and $TiO_2$ treated samples.

### 7.2.6 Characterization of tiles before and after treatment

Macroscopic inspection was performed by visual inspection and photographic documentation before and after the coating application made with an Olympus C-5060 digital

camera. A Kodak Color scale was included in each record for light and color adjustment of the images.

The effect of the $TiO_2$ coating on the visual appearance of the tile samples was also evaluated by UV–Visible diffuse reflectance on a Shimadzu UV-2501PC spectrometer using $BaSO_4$ as a reference. The UV–Visible diffuse reflectance spectra were converted into chromaticity values defined by CIELab coordinates. The color was defined through three different parameters, L*(brightness), a*(red/green) and b*(yellow/blue). In order to assess the chromatic alteration caused by $TiO_2$ coating tile samples were analysed before and after coating deposition. Difference between each parameter was calculated, $\Delta$L*, $\Delta$a*and $\Delta$b* as well as total color difference ($\Delta$E$*$) with the following equation (Eq. 7.1):

$$\Delta E *= \sqrt{[(\Delta L *)^2 + (\Delta a *)^2 + (\Delta b *)^2]} \text{ (Eq. 7.1)}$$

X-ray diffraction (XRD) analysis was performed for identification of crystalline phases (mineralogical characterization) present on the powdered ceramic body. After coating deposition and thermal treatment, analysis was performed for detection of phase alteration of the ceramic body due to the thermal treatment. The XRD patterns were recorded on a Rigaku Dmax III-C 3 kW diffractometer (Rigaku Corporation, Tokyo, Japan), using Cu K$\alpha$ radiation at 40 kV and 30 mA settings in the 2$\theta$ range from 20° to 80°, and an acquisition time of 1s and 2$\theta$ increment of 0.08°. The resulting spectra were deconvoluted using a suitable software (EVA, Bruker AXS GmbH, Karlsruhe, Germany) and crystalline phases were identified by comparing the peak positions and intensities with those listed in the software standard files (ICDD, Newtown Square, PA, USA).

## 7.3    Results

### 7.3.1    Glaze and ceramic body chemical characterization

The chemical compositionthe glaze and ceramic body of the tile samples are shown in Table 7.2. The tile samples 1BW, 2W and 3TS showed a glaze with $SiO_2$ and PbO as main components. The content of alkalis ($Na_2O+K_2O$) was higher for sample 1BW, followed by sample 2W and 3TS. Glaze 1BW depicted the lowest content of $Al_2O_3$ of the three glazes and 3TS the highest content. On samples 1BW and 2W the calcium content was lower, while the glaze of the sample 3TS showed a higher amount (Table 7.2). Both tiles from sample 1BW and 2W are opaque white glazes with $SnO_2$ as the opacifier. In addition, sample 1BW was taken from a blue and white tile, therefore cobalt was also detected (Table 7.2).

The glaze of sample 4MW, taken from a modern industrial tile was totally different from the other tiles with $SiO_2$, $Al_2O_3$ and CaO as major components. The total alkalis content was low and ZrO was the opacifier used in this glaze (3 wt. %).

The ceramic body of samples 1BW and 2W was rich in $SiO_2$ and CaO (Table 7.2) with similar contents of $Al_2O_3$ and $Fe_2O_3$. The ceramic body of samples 3TS and 4MW showed lower contents of CaO and $Fe_2O_3$ and was richer in $Al_2O_3$ (Table 7.2).

**Table 7.2** Major and minor oxide components of the glaze and ceramic body of the tile samples in wt. %.

| Sample | 1BW | | 2W | | 3TS | | 4MW | | CMOG C | |
|---|---|---|---|---|---|---|---|---|---|---|
| Area | G | C | G | C | G | C | G | C | Meas | Ref |
| Na$_2$O | 4 | <1 | 1 | <1 | <1 | <1 | 1 | 1 | 1 | 1.07 |
| Al$_2$O$_3$ | 3 | 8 | 4 | 11 | 10 | 21 | 14 | 22 | 0.9 | 3 |
| SiO$_2$ | 60 | 39 | 71 | 57 | 66 | 73 | 67 | 62 | 45 | 34.8 |
| K$_2$O | 5 | 1 | 3 | 2 | 4 | 2 | 3 | 3 | 3 | 2.84 |
| CaO | 1 | 45 | 1 | 22 | 5 | <1 | 9 | 9 | 6 | 5.07 |
| TiO$_2$ | <1 | 1 | <1 | 1 | <1 | <1 | <1 | <1 | 0.9 | 0.79 |
| Fe$_2$O$_3$ | 1 | 5 | 1 | 5 | 1 | 1 | 1 | 1 | 0.6 | 0.34 |
| CoO | 2 | - | - | - | - | <1 | - | - | 0.2 | 0.18 |
| ZrO | | | | | | | 3 | <1 | - | - |
| SnO$_2$ | 5 | - | 5 | - | - | - | - | - | 0.4 | 0.19 |
| PbO | 17 | <1 | 14 | <1 | 15 | <1 | <1 | <1 | 27 | 36.7 |

G-Glaze; C-Ceramic body; Meas-Measured; Ref-Reference composition; <1 - <1wt. %

## 7.3.2  Characterization of TiO$_2$ thin film
### 7.3.2.1  µ-Raman analysis

Raman spectra obtained directly on the tiles surface revealed bands corresponding to the anatase polymorphic phase of TiO$_2$, at frequencies of 146 cm$^{-1}$ (B1g mode, very intense), 198 cm$^{-1}$ (Eg mode, very weak), 400 cm$^{-1}$ (B1g mode, intense), 516 cm$^{-1}$ (A1g, B1g modes, less intense) and 634 cm$^{-1}$ (Eg mode, less intense) with a slight shift from assignments made in the literature (Sekiya et al., 2001). Fig. 7.4 present a spectrum obtained on sample 3TS, showing the banding pattern of anatase.
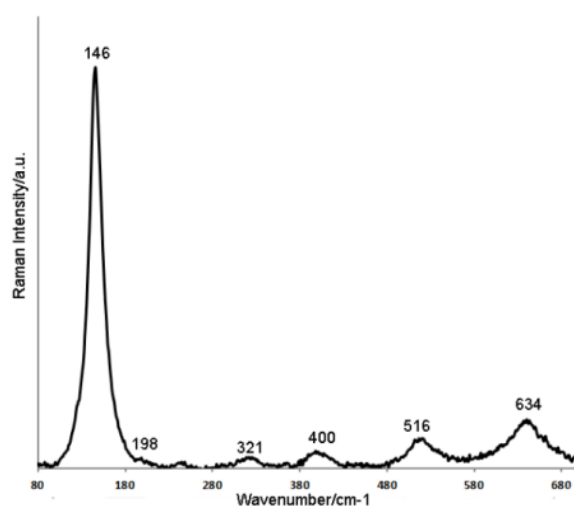


**Fig. 7.4.** Example of anatase Raman spectra collected from the thin film deposited on a 3TS sample.

### 7.3.2.2  Morphology of the TiO$_2$ coating

SEM investigations of the tile samples section allowed observing the thin film section and through the SEM software the range of thickness of the TiO$_2$ coating, which was 60-89 nm (Fig. 7.5).
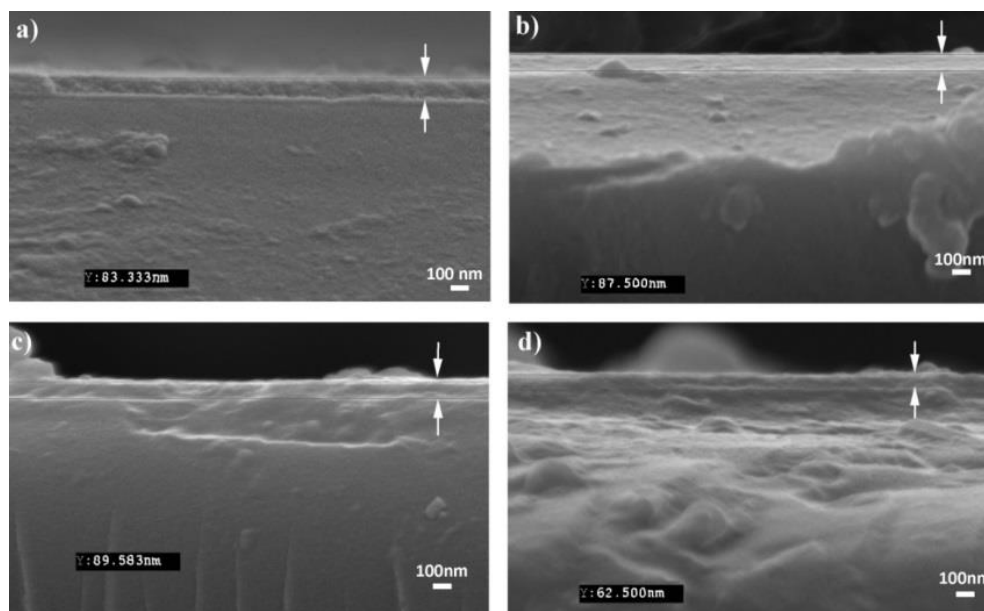
**Fig. 7.5.** SEM images of the cross-section of the coated surfaces with arrows indicating the TiO2 coating and Y value showing the measures thickness of the thin film. (a) sample 1BWT with Y= 83.33nm, (b) sample 2WT with Y= 87.500nm, (c) sample 3TST with Y= 89.583nm, and (d) sample 4WMT with Y= 62.500nm.

Surface morphology of the applied $TiO_2$ coatings was investigated by FESEM. The $TiO_2$ film seemed to have adhered to the tiles' glaze surface (Fig. 7.6). On the tile samples presenting microfissures, like samples 1BWT and 3TST the film showed a fissure situated over the pre-existing glaze fissure (Fig. 7.6 a, b). Some larger agglomerates could be observed scattered over the surface (Fig. 7.6 a, b). At higher magnification nanostructure of the thin film seemed to be similar on all tile samples small agglomerates (Fig. 7.6 c, d, e, f). Some pores were also observed (Fig. 7.6 c, e, f).
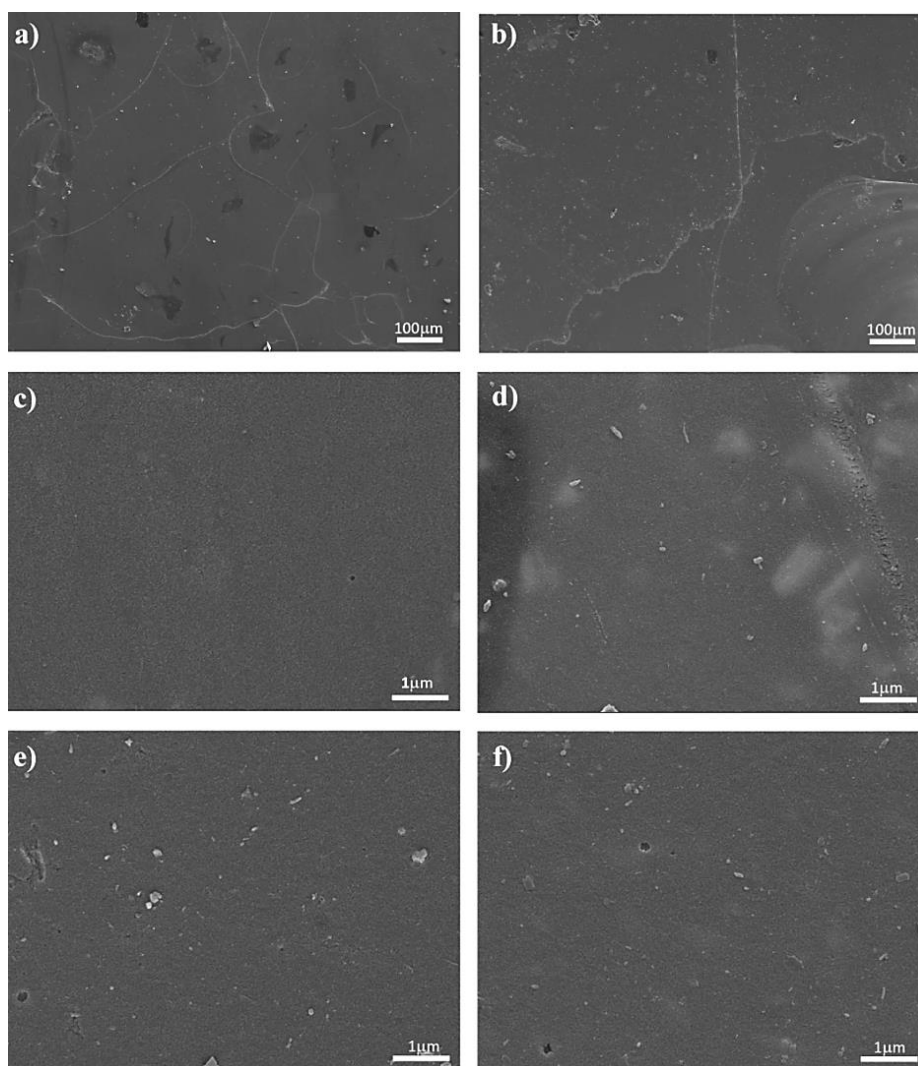
**Fig. 7.6.** Scanning electron microscopy images of the TiO2 coated glazed surfaces of the tile samples: (a) surface of 1BWT sample, (b) surface of 3TST sample. (c) higher magnification of surface of TiO2 on sample 1BWT sample, (d) higher magnification of surface of TiO2 on sample 2WT sample, (e) higher magnification of surface of TiO2 on sample 3TST sample and (f) higher magnification of surface of $TiO_2$ on sample 4MWT.

### 7.3.3  Tertiary bioreceptivity experiment

Photographic documentation throughout 40 days of incubation showed fungal growth on the non-treated and treated samples (Fig. 7.7). The results showed fungal growth rate was faster for the first 10 days of incubation. There was no significant growth between the 10th and the 20th days of incubation or between the 20th and 40th day, confirming the stagnation of the fungal growth (Fig. 7.7).

Fungal proliferation over the tile surface was most extensive on samples 1BWT and 4MV and least on samples 2W and 3TS. Regarding comparison between the non-treated and $TiO_2$-coated tiles, photographic documentation allows observing that proliferation of fungus was higher on the non-treated samples (Fig. 7.7). The only exception was sample 4MW were the treated tiles presented a higher proliferation (Fig. 7.7).
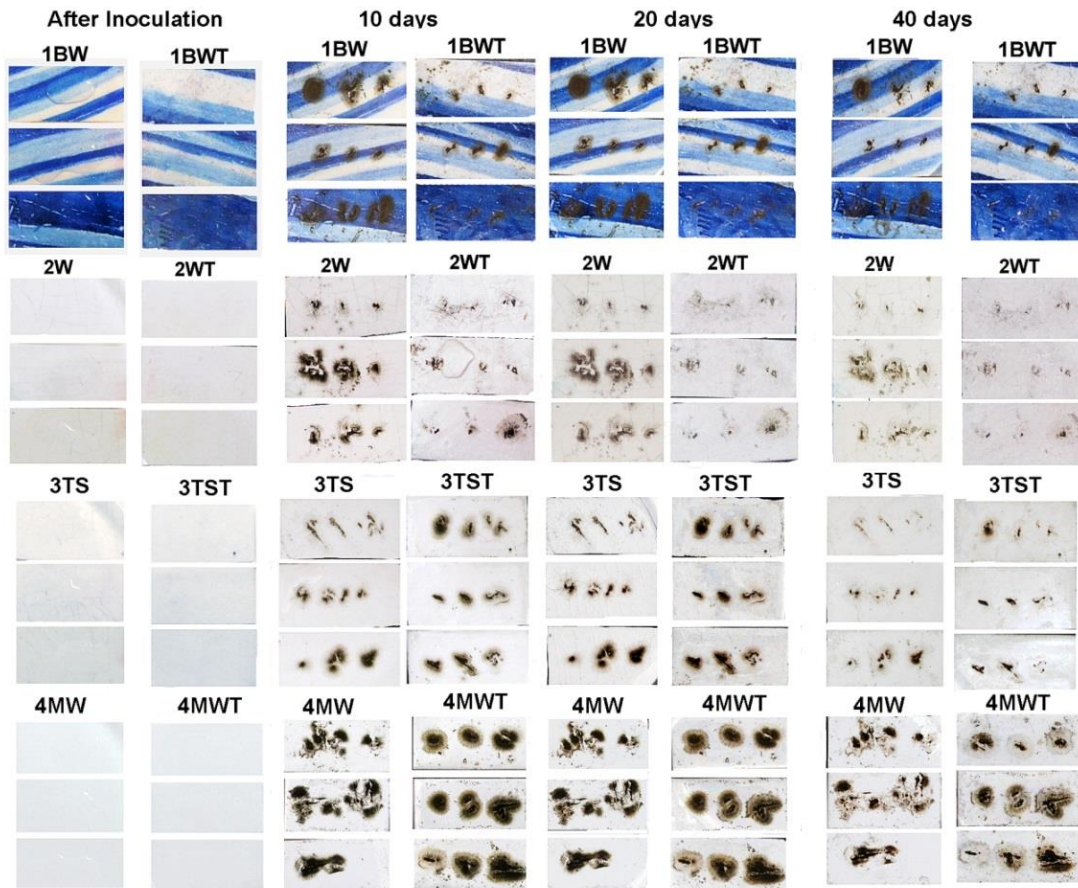
**Fig. 7.7.** Photographic documentation made during the experiment of the fungal growth on glaze tiles samples 1BW (uncoated); 1BWT ($TiO_2$ coated); 2W (uncoated); 2WT ($TiO_2$ coated); 3TS (uncoated); 3TST ($TiO_2$ coated); 4MW (uncoated) and 4MWT ($TiO_2$ coated).

### 7.3.4 Evaluation of the chromatic alteration caused by thin film deposition

Visual inspection and photographic recording were performed before and after the coating application. The major changes that occurred due to the application of the $TiO_2$ coating were related to the iridescent effect of the coating on the surface when observed under oblique angles (Fig. 7.8). Dispite this effect being similar on all tile surfaces, it was difficult to document by photographic recording.
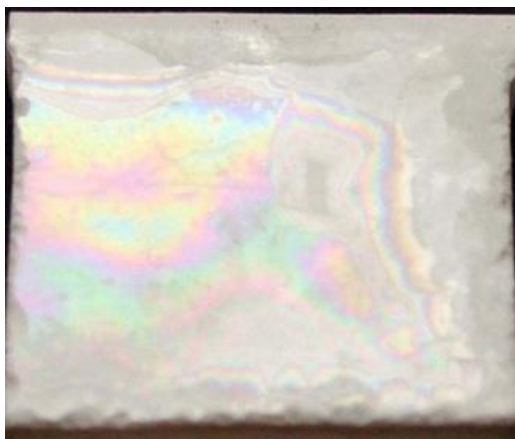
**Fig. 7.8.** Iridescent of the tile sample 4MW after the application of the $TiO_2$ coating photographed in an oblique angle.

On tile samples 1BW, the iridescent effect was accompanied with the formation of grey stains underneath the coating (Fig. 7.9). The stains were only visible on this particular tile type, none of the other samples showed this effect after the coating application and could not be identified by µ-Raman.
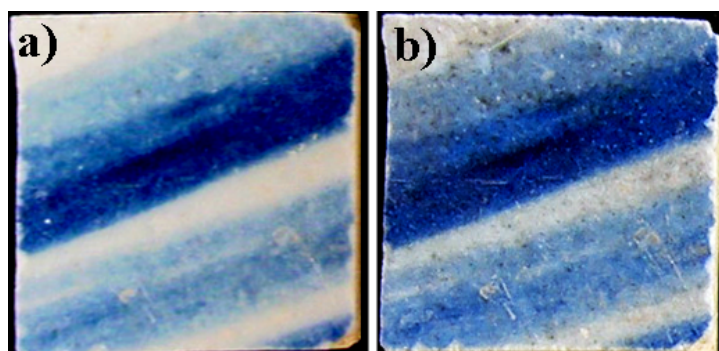


**Fig. 7.9**. Image of tile sample from tile 1BW (a) before and (b) after the coating.

Chromatic changes caused by the coating application and the thermal treatment and were analysed by color measurements using the CIELAB coordinates (Fig. 7.10). The $\Delta E^*$ of obtained before and after the application of the coating varied between 3.38 and 5.93. These values are the result of the variation of the luminosity parameter ($\Delta L^*$) which were considerably higher than the variation of the chromaticity expressed in $\Delta a^*$ and $\Delta b^*$ (Fig. 7.10).
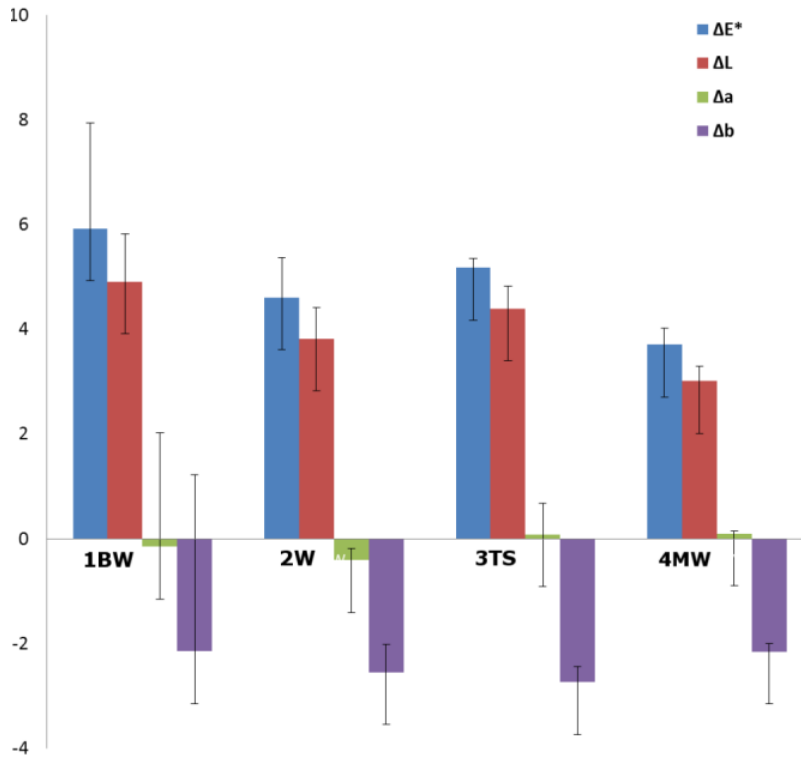
**Fig. 7.10.** Colorimetric variation before and after the application of the coating expressed in $\Delta E^*$, $\Delta L^*$, $\Delta a^*$ and $\Delta b^*$.

### 7.3.5 XRD analysis

Fig. 7.11 shows the diffractograms of the ceramic body before and after $TiO_2$ coating and thermal treatment. XRD results revealed that the ceramic body of sample 1BW contained quartz ($SiO_2$), calcite ($CaCO_3$), gehlenite ($Ca_2Al_2SiO_7$), äkermanite ($Ca_2Mg.Si_2O_7$) and wollastonite ($CaSiO_3$) (Fig. 7.11a). The mineralogical composition of sample 2W was similar regarding the detected mineral phases, but the Ca-bearing phases presented less intense bands (Fig. 7.11a). Quartz was the most prominent peak on sample 2W (Fig. 7.11b), instead of calcite and gehlenite that were the main phases in sample 1BW (Fig. 11a). Quartz ($SiO_2$) and mullite ($3Al_2O_32SiO_2$) were the mineral phases detected in sample 3TS (Fig. 7.11c). XRD revealed quartz ($SiO_2$) as the most prominent phase, as well as albite ($NaAlSi_3O_8$) in sample 4MW (Fig. 7.11d). The analysis performed on the paste after thermal treatment to evaluate the effect of the application of the film, suggested that no significant changes occurred in the crystalline phases of the tiles.

.
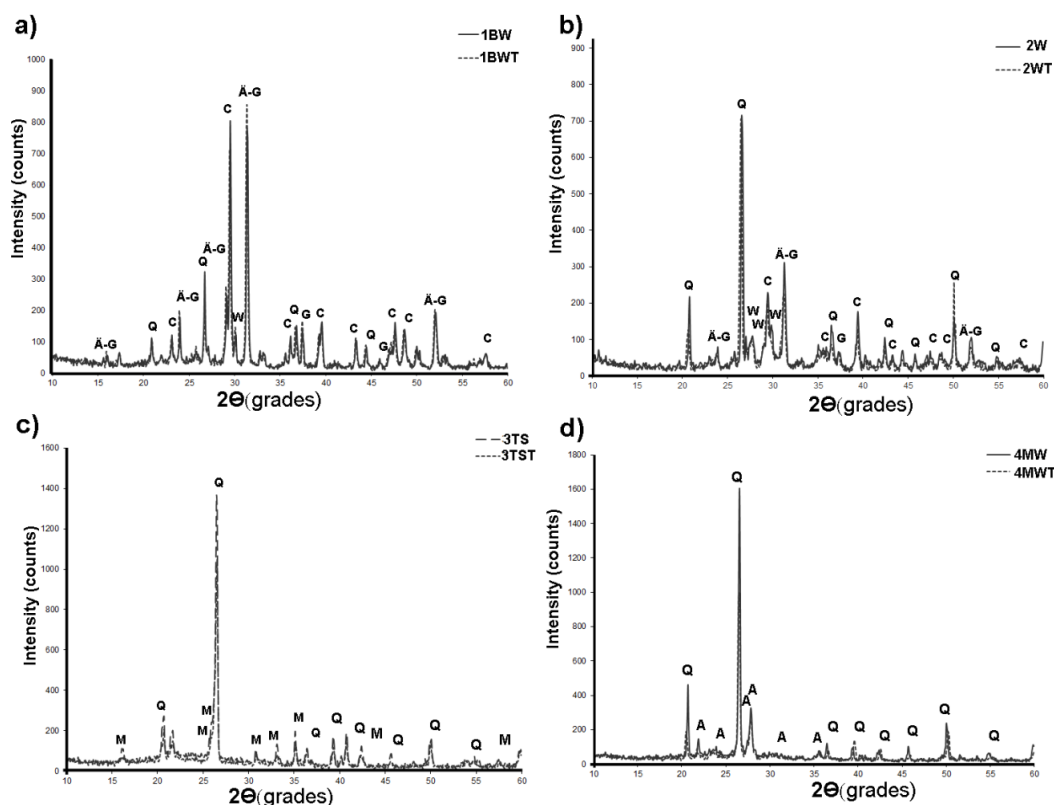
**Fig. 7.11**. X-ray diffraction patterns of the ceramic body before (1-1BW, 2- 2GW, 3 -3TS, 4-4WM) and afterheat-treatment at 450ºC. (1-1BWT, 2-2GWT, 3-3TST, 4 - 4WMT): A – Albite, C- Calcite, G- Gehlenite, Q-Quartz, M – Mulite, W – Wollastonite and Ä – Äkermanite.

## 7.4 Discussion

The reproduction of tiles can be a difficult issue due to the innumerous variables involved the production of ceramic, such as granulometry, nature of raw materials and firing (cycle and temperature). In addition, $TiO_2$ coated tiles are already a marked product with good results in modern tiles (Berto, 2007). Therefore, the preliminary test was performed on real tiles samples in order to evaluate the effect on weathered samples and to be able to teste the coating in several compositions. The use of old materials for testing conservation treatments can be controversial, yet many studies have adopted this approach due to the the aforementioned difficulties (Vaz et al., 2008; Pereira et al., 2012; Prudêncio et al., 2012; Ottosen et al., 2014).

### 7.4.1 Tile samples

The composition of the ceramic body was analysed in order to determine the major and minor components of the glaze and ceramic body. The chemical characterization confirmated the type of glaze and ceramic body through comparison based on the stylistic features and previously published characterization.

The glaze sample 1BW taken from a blue and white majolica tile, was a lead-alkaline silicate glaze opacified with $SnO_2$ (Table 7.2). Other studied tiles presenting similar stylistic features

showed comparable composition (Pereira et al., 2011). The ceramic body of sample 1BW showed a Ca-rich composition (Table 7.2) and mineral phases commonly found on ceramic bodies with high content of Ca, such as gehlenite, wollastonite and anorthitic plagioclases which are formed when fired above 950ºC (Jordan et al., 2008). The presence of calcite after firing has been associated with lower firing temperature, high rates of Ca/Si ratio or degradation of calcium phases (Fabbri et al., 2014). Regarding the morphology of the glaze some fissures were observed on the glaze, but no well-developed micro crack network was visible at naked eye.

Sample 2W presented a lead-tin silicate glaze and a ceramic body with a lower content of CaO and higher $Al_2O_3$ content than sample 1BW (Table 7.2). The glaze of sample 2W was also a lead-tin silicate glaze, used in the majolica technique. Based on stylistic features the tile presented the decoration of the tiles used for building cladding during the 1840-1920 (RTEACJMSS, n.d.). The composition of the ceramic body also showed still a relatively high Ca content therefore Ca-bearing phases were still detected by XRD, such as calcite, gehlenite, äkermanite and wollastonite. These phases were similar to the blue and white tile´s ceramic body (1BW). The glaze presented a microcracks network, that can occur due to the ageing process or be formed during the production process (Eggert, 2006).

Samples 3TS was taken from a tile produced in *Sacavém's* factory in the beginning of the 20th century. This presented a lead silicate glaze rich in CaO without any opacifying compound. The glaze was applied over a white ceramic body rich in $SiO_2$ and $Al_2O_3$, probably fired at high temperatures, since quartz and mullite were the main mineral phases detected. Mullite is formed on ceramic bodies with low content in CaO (González-García et al., 1990). The results of the ceramic body characterization are in agreement with the notes on ceramic paste recipes presented in the catalogue of the *Museu da Cerâmica de Sacavém* which described the use of kaolin, ball clays, feldspars and small amount of cobalt oxide (Assunção et al., 2003). In fact, cobalt was detected as a minor element (Table 7.2). The glaze layer showed a well-defined crack network, due to the porosity of the ceramic body and tendency to expand by hydration developing a crack network with ageing, typical of this type of ceramic.

The modern industrial tile 4MW showed a ZrO opacified glaze which is today the most commonly used opacifier. The composition of the ceramic body comprised a modern ceramic paste with lower content of calcium oxide and with a high content of alumina and silica described for modern tile compositions (Dondi et al., 2014). The glaze was smooth and no surface flaws were visually detected on the surface.

In conclusion, the four ceramic tiles showed different compositions and physical features. The three historical tiles had considerable amounts of lead in their composition; only the modern tile did not present lead in its glaze composition. Nowadays, lead oxide can no longer be used in high amounts due to its toxicity (Belgaied, 2003). Also, their physical features were different due to different extents of crack network.

### 7.4.2 Characterization of the TiO$_2$ coatings

The µ-Raman analysis confirmed the presence of the the polymorphic anatase on all samples. This crystalline phase of TiO$_2$ is the most widely used for photocatalytic purposes (Kemmitt et al., 2004; Awitor et al., 2008). Morphological and structural characterization of the coating showed a good surface coverage and few surface flaws, like pores and agglomerate (Fig. 7.6). The micro fissures detected on the coating of some tiles samples seemed to result from pre-existing fissures. The nanostructure of the TiO$_2$ film was similar to other sol-gel produced coatings, described in the literature (Alzamani et al., 2013).

### 7.4.3 Effect of TiO$_2$ coatings on tiles bioreceptivity

In order to test the efficacy of the deposited coatings, a tertiary biodeterioration laboratory experiment was performedI was observed that the fungus *Cladosporium sp*. was able to proliferate on all tile samples, both on the coated and non-treated ones. Nevertheless,fungal proliferation was lower on the TiO$_2$-treated samples; suggesting that the coating reduced the tiles bioreceptivity (Fig. 7.7). However, on one of the coated samples (4MW) the fungal proliferation seemed to be higher than on the non-coated sample.

A regression of fungal growth could be observed on the samples due to the total consumption of the available nutrient. However, due to the photocatalytic effect this seemed to be more extensive on the TiO$_2$-coated samples.

The results obtained in Chapter 5 showed that the bioreceptivity of tiles to fungal colonization was in general reduced and seemed to indicate that fungal growth was strongly dependent on the presence of nutrients (Gadd et al., 2001; Giannantonio et al., 2009). Thus, the use of a fast growing fungus and higher nutrient concentration in the inoculum resulted in a faster and more extensive growth, in comparison with the results from Chapter 5. Regarding the relation between growth and sample physical features, the samples with less fissures on the surface (1BW and 4MW) showed a higher fungal proliferation. A lower fungal proliferation occurred on samples with microfissures network on the glaze. These results suggest that the amount of nutrients retained on samples without surface fissures was higher, promoting a higher fungal proliferation. Further research needs to address this issue.

Although in most cases the deposited TiO$_2$-coating reduced tiles bioreceptivity, it did not avoid the fungal proliferation on the surface. In fact, other studies have also reported the inability of TiO$_2$ coating to completely prevent biological colonization (Graziani et al., 2013 and Chapter 6).

### 7.4.4 Applicability evaluation of TiO$_2$ coatings on historical glazed tiles

The application of the TiO$_2$ coating induced aesthetic changes on all tile samples. Even though it is frequently claimed in the literature that the application of this coatings is not accompanied by visual alteration of the substrates (Bertoncello et al., 2006; Murugan et al., 2013). However, the deposition of the thin TiO$_2$ coating over the tiles glaze caused the iridescence of the

surface and an increase in reflectivity due to optical interference (Fig. 7.8). In fact, the reflection between parallel surfaces (in this case $TiO_2$ coating and translucent glaze) generates optical interferences, like the ones described for self-cleaning glass (Tilley, 2010). These colored effects result in reflection amplitudes that depend on the light´s wavelength, which in reflectance cause interference like iridescence and color. In fact, the color of the films is related to the thickness of the thin-film. The increase of reflectivity observed on the coated samples has been described on glass samples (Tilley, 2010). This increase may be related to the difference between the refraction index of anatase and glass.

Adding to the aesthetical alterations on sample 1BW some grey stains were observed. Bertoncello et al. (2006) studied the application of silica sol-gel coatings on lead glass adding small amounts of $Pb(NO_3)_2$ on lead glass to avoid lixiviation of lead into the sol-gel layer. Further investigations should be performed to understand the formation of these stains.

Regarding the effect of the coating application process (thermal treatment) on the ceramic body, XRD revealed no drastic changes on the mineral phase composition. However, small changes might not be detected by XRD. According to thermal analysis of pottery the main reactions that can be observed until 350 ºC in calcareous ceramics are related to water loss by the dehydration and the beginning of de-hydroxylation of clay minerals (Fabbri et al., 2014). In fact, descarbonation reaction that could affect the high calcite content of samples 1BW and 2W only occurs at temperatures around 750 ºC (Fabbri et al., 2014). However, further analysis should involve the characterization of the thermal expansibility in order to understand the tension created by the expansion of the glaze and ceramic body during thermal treatment.

Based on the fact that the use of glazed tiles in architecture is strongly related to the aesthetical intension, the optical properties are extremely important features (Lobo and Pernão, 2010). These optical properties of tiles, such as color, gloss and reflection comprise the unique aesthetical effect associated with the use of tiles. Therefore, the alterations observed on the tiles surface after the application of $TiO_2$ coating suggest that this methodology is not suitable for glazed tiles from cultural heritage.

## 7.5     Conclusions

Results showed that despite the deposited $TiO_2$-coating presenting the intended characteristics with good adherence, anatase crystalline structure and a small decrease in bioreceptivity, their application was not suitable for application on cultural heritage. $TiO_2$ thin coatings induced alteration of the aesthetic and optical properties of the glazed tiles.

In addition, this experiment showed that the fungal growth was closely dependent on nutrients availability. The micro-cracks on the surface of the glaze seemed to be linked to to the fungal growth, probably due to the different amounts of nutrients that remain on the surface.

# Notes on the conservation of glazed wall tiles exposed to biological colonization
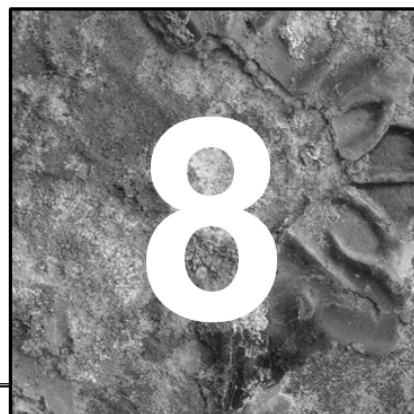


## 8.1 Introduction

The analysis of the two cases studies of biological colonization of glazed wall tiles exposed outdoors (Chapter 3 and 6) makes it opportune to comment on the conservation of glazed tiles regarding the protection against biological colonization.

According to the ICOM-CC preventive conservation is defined as "all measures and actions aimed at avoiding and minimizing future deterioration or loss. They are carried out within the context or on the surroundings of an item, but more often a group of items, whatever their age and condition. These measures and actions are indirect – they do not interfere with the materials and structures of the items. They do not modify their appearance." (ICOM-CC, 2009). However, whenever tiles biological colonization has already occurred invasive methods are needed, these were designated as remedial conservation actions which were defined by the ICOM-CC as "all actions directly applied to an item or a group of items aimed at arresting current damaging processes or reinforcing their structure. These actions are only carried out when the items are in such a fragile condition or deteriorating at such a rate, that they could be lost in a relatively short time. These actions sometimes modify the appearance of the items" (ICOM-CC, 2009). In this chapter the causes that favor biological colonization of glazed wall tiles are discussed and conservation measures to avoid or mitigate the biological colonization are proposed. Some of these observations have previously been described for stone monuments and outdoor collections (Lloyd, 2011; Salvadori and Charola, 2011), but others are specific for glazed tiles.

## 8.2 Environmental factors influencing biological colonization of glazed wall tiles

Biological growth is highly dependent on environmental conditions (e.g. wind, sunlight, temperature, rain, relative humidity), microclimatic conditions (e.g. local urban geometry, building design or adjacent materials) and atmospheric pollution (Warscheid and Braams, 2000). The creation of controlled environmental conditions to inhibit the growth of microorganisms cannot be achieved in outdoor environments. However, the identification of the conditions that can lead to biological colonization is a central aspect for the establishment of monitoring and maintenance measures. Fig. 8.1 shows several examples illustrating the above mentioned conditions that can enhance biological colonization.

According to the case studies analysed in Chapter 3 and 6, the tile panels depicting severe biological growth were facing north. For instance, in *Casa da Pesca* there was a remarkable difference between the north and south façades (Fig. 8.1 a, b). The spatial orientation seems to be an important factor regarding the formation of biofilms and several authors have described the preferential colonization of north-facing façades (Herrera and Videla, 2004; Macedo et al., 2009).

Shelter due to building characteristics or surrounding vegetation apart from creating particular environmental conditions, like protection from direct rain and solar irradiation, can also influence the biological colonization due to accumulation of particulate matter (Salvadori and Charola, 2011). The tiles from Pena National Palace (Sintra) were located in a tunnel (semi-sheltered) and the lack of lixiviation of the deposited particulate matter also seemed to enhance biological colonization (Chapter 3). The deposition of airborne particles (e.g. dust, pollen, spores, oil- and coal-fired carbonaceous particles) on the surface of the inorganic substrates, provides nutrients for specific microorganisms (Bastian et al., 2009). Also, the deposition of biological airborne particles on a surface is a influent factor (Salvadori and Charola, 2011). Pioneer microorganisms on glaze tiles, may then serve as nutrients to other microorganisms the secondary colonizers like previously described. Moreover, the first colonizers of inorganic substrates located outdoors are usually phototrophic microorganisms that can modify the glaze tile surface making it more bioreceptive to other organisms and also more able to retain water and particulate matter due to the production of extracellular polymeric substances.
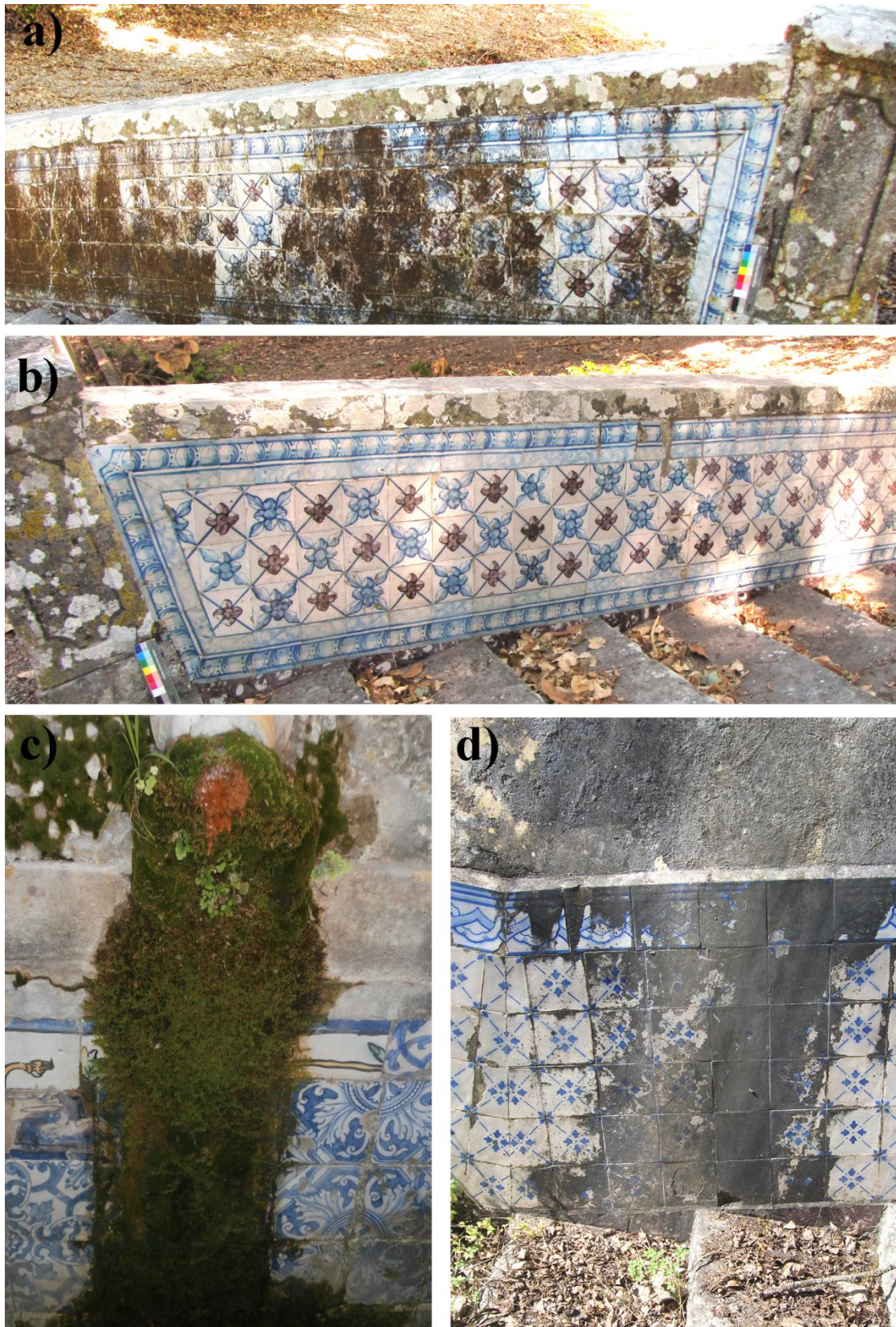
**Fig. 8.1** Examples of environmental factors influencing tiles biological colonization (a) North-facing tile panel from *Casa da Pesca* covered with a brown biofilm; (b) south-facing tile panel panels from *Casa da Pesca* without visible biofilm.(c) Tiles from fountain located in the garden of *Marquês de Fronteira* Palace with phototrophic microorganisms, mosses and vascular plants and (d) tile panel from *Casa da Pesca* located under a rain gutter showing a black patina.

Surrounding vegetation, particularly higher vegetation, increases relative humidity and decreases the temperature (Salvadori and Charola, 2011). Thus, tiles located in gardens with higher vegetation are also exposed to a higher risk of biological colonization. The tiles studied in Chapter 3 and 6 were both surrounded by vast vegetation. Some of the identified species, namely *Phycopeltis* sp., are known to be epiphytic on leaves (Chapter 6). Thus, the close presence of vegetation might enhance the colonization by these species.

Building design is also a relevant feature, since it can determine the micro environmental conditions and exposure of the tiles. Additionally, the location under eaves, rain- or fountain-spouts might enhance biological colonization. Fig. 8.1c shows the tiles applied in a fountain, which were covered with a dense biofilm with bryophytes, vascular plants and phototrophic microorganisms. Microbial biofilms are common in fountains due to the water availability and humid conditions. In *Casa da Pesca* dark particulate and biofilm developed over tiles located under a rain-spout (Fig. 8.1d).

## 8.3    Physical features of glazed wall tiles influencing biological colonization

Particular physical features such as surface design and surface roughness of the tiles or their arrangement might also favor microbial colonization. The tiles from the Triton tunnel in Pena National Palace were moulded high relief tiles (Chapter 3). The dense colonization of these tiles seemed to start from the depression areas close to the relief (Fig. 8.2a). Another example of physical features which can enhance biological colonization is the presence of unglazed areas on the tiles front face (Fig. 8.2b). These features can be due to physical or mechanical decay, but may also depend on the production techniques such as *cuerda-seca* and arista tiles. In these techniques tiles are made by separating the different colored glazes with a depression or relief, respectively. Hence, these tiles have areas without glaze which are more easily colonized, as could be seen in the lichen colonization of the tiles from Sintra National Palace (Sintra, Portugal) (Fig. 2.6a in Chapter 2).

According to the experimental results shown in Chapter 4 photosynthetic-based colonization seemed to be affected by the conservation condition of the tile surface. Artificially aged tiles showed a higher bioreceptivity compared to pristine tiles. Therefore, we expect higher risk of colonization by photossintethic microorganisms on weathered tiles. Additionally, as mentioned areas without glaze, where weathering has caused detachment, lacunae or fissures can readily be colonized by lichens and other organisms (Fig. 8.2b).
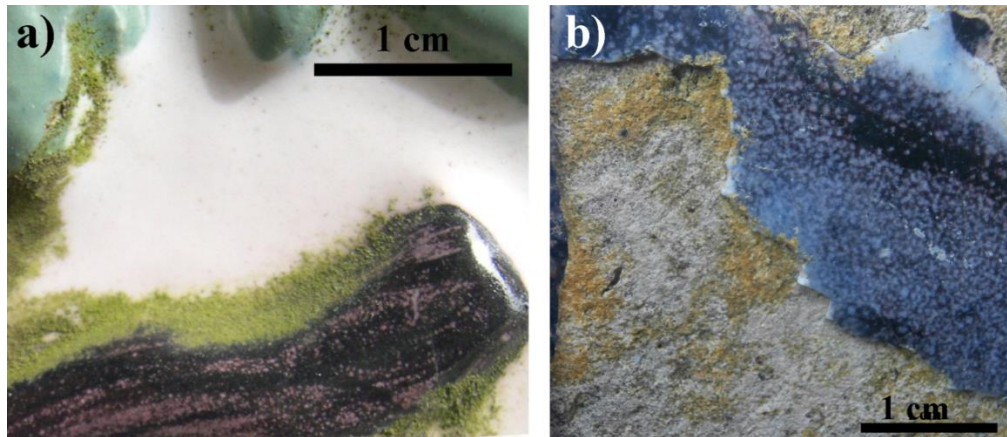
**Fig. 8.2** Tiles with different biological colonization due to physical features of the tiles. (a) Tile from Pena National Palace with dense colonization near the relief; (b) tile from Marques de Fronteira Palace showing biological colonization in areas where the glaze has fallen.

## 8.4    Influence of restoration treatments

Finally the restoration treatments and the presence of restoration materials on tiles can sometimes alter tile bioreceptivity or become a source of contamination. The use of organic-based materials for the integration of lacunae, such as organic based filling pastes or adhesive resins can sometimes lead to contamination of tiles by microorganisms. Although the presence of areas without glaze can readily be colonized, the application of materials with high bioreceptivity might also result in a risk of colonization for the substrate. Fig. 8.3 was taken at *Marquês de Fronteira* Palace (Lisbon) and shows colonization of the filling paste. Therefore, the application of treatment should always take into account the bioreceptivity of the material and the environmental conditions in which it will be used. Giacomucci et al., (2011) reported microbial colonization of tiles by microorganisms after a treatment with involved the application of an acrylic resin over the glaze surface.



**Fig. 8.3** Microbial colonization on the filling paste of glazed tilesfrom *Marques de Fronteira* Palace (Lisbon, Portugal).

## 8.5 Conservation strategies to control biological colonization of glaze wall tiles

Any preventive conservation plan should begin with the identification of the factors by making a risk analysis. Thus, tiles exposed to the above described factors or with certain physical features should be signalized in order to be more frequently submitted to monitoring and maintenance actions. The frequency of these actions is always specific for each case and can only be defined by the monitoring of biological colonization or recolonization phenomena (Lega et al., 2004; Salvadori and Charola, 2011).

Cleaning actions to remove the particulate deposits are particularly relevant in the case of cultural heritage assets, such as historical or/and artistic glazed wall tiles. These should be performed according to a maintenance plan that defines the periodicity of these cleaning actions. The control of surrounding vegetation, avoiding growth of vegetation over the tiles or cutting tree branches to avoid direct dripping might significantly reduce tiles biological colonization. In addition, the presence of eaves or a rain or fountain spouts, might be controlled by periodical cleaning of these structures. Therefore, suitable maintenance actions might not prevent biological colonization, but may minimize it and thus, reduce tiles biodeterioration.

In the case of the tiles from Pena National Palace, two cleaning campaigns were necessary during this working period (2010-2014). According to staff from the Palace, periodical cleaning occurred whenever the tiles were colonized by a dense biofilm. The first cleaning intervention was made in April 2011, and only water and a brush were used to remove the biofilm (Fig. 2.7 section of Chapter 2). However, in the subsequent years recolonization could be observed and a new intervention was conducted in 2014. The location of these tiles - sheltered from direct rain, strong wind, high relative humidity and their physical features (Chapter 3) - makes them very susceptible to biological colonization. Probably an earlier cleaning could avoid the dense settlement of these biofilms. However, the adopted cleaning procedured must be performed with the least abrasive method and the minimum times as possible. Even cleaning procedures might themselves also on long term be damaging (Lloyd and Lithgow, 2011).

Whenever restoration actions are needed, particular attention should be given to the bioreceptivity when selecting the materials to be used. Outdoor environmental conditions might cause the materials degradation and may become optimal for the growth of microorganisms. Other actions such as the application of protective coatings, like the coating tested in Chapter 7 may seem tempting; these have too many drawbacks and pose many ethical questions. According tothe results obtained in the present work it did not seem to be a good practice. Therefore future research is necessary to provide suitable materials to be used in outdoor conditions.

# Final remarks and future perspectives

9
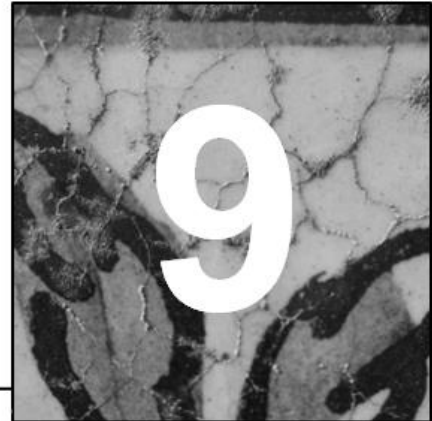
The results of the present work provided a first insight on the biodeterioration of majolica glazed tiles, particularly on the microbial communities growing over the glazes. Some of the existing gaps in knowledge concerning the biodeterioration of tiles were overcome with the findings described in this thesis. First, the characterization of microbial communities found on glazed tiles from Pena National Palace (Sintra) and *Casa da Pesca* (Oeiras) were performed by culture-independent and conventional microbiological methods. Simultaneously, characterization of the glaze was achieved together with the observation of biodeterioration patterns. The laboratory based experiments allowed to assess the bioreceptivity and biodeterioration of pristine and aged glazed models to phototrophic microorganisms and fungi. Additionally, mitigation strategies based on chemical methods were tested *in situ* on colonized tiles from *Casa da Pesca*. Finally, a preliminary approach on the application of a protective treatment based on titanium dioxide thin films, to prevent biological colonization on cultural heritage glazed tiles was carried out.

The main findings achieved in this work led to the following general conclusions:

1. The literature review on biodiversity, biodeterioration and bioreceptivity of architectural ceramic materials provided a comprehensive overview of biological colonization and biodeterioration of these materials. The most common ceramic elements used worldwide in architectural Cultural Heritage were analysed: bricks, architectural sculptures, roofing tiles and glazed wall tiles. Results gathered in this chapter did not allow a statistical analysis to establish any relation between a given organism and a ceramic typology, probably because there are not enough studies on this subject. For instance, studies on biodeterioration of glaze wall tiles are rare. In addition, the main biochemical and biophysical damage of both unglazed and glazed ceramic substrates were described. The exhaustive literature revision also helped to highlight the significant gaps in knowledge regarding biodeterioration of architectural ceramic materials.

2. The selected methodological approach for the identification of microbial communities provided an accurate identification of the tile colonizing microorganisms. An integrated approach of the complex microbial communities found on glazed wall tiles was achieved by analysing biofilms as a whole through the direct microscopic observation of photosynthetic microorganisms and fungi, achieving the recognition of lichenization processes, interactions among microorganisms and an estimate of the organism proportion on the biofilm. Additionally, culture and molecular methods

allowed the individual identification of the members of the biofilm. The biofilm from Pena National Palace wall tiles was composed of microalgae, cyanobacteria, bacteria, and some dematiaceous fungi. The methodological approach used in this work allowed the identification of a new fungal specie (*Devriesia imbrexigena*) growing over these glazed wall tiles. Some of the identified microorganisms were selected for laboratory based experiment. Regarding the microbial community found on glazed wall tiles from *Casa da Pesca* microalgae, cyanobacteria, and dematiaceous fungi were identified.

3. The analysed case studies (glaze wall tiles from Pena National Palace and *Casa da Pesca*) demonstrated that the development of biofilms over glazed surfaces are connected to specific environmental conditions, such as surrounding vegetation, shelter from rain, low solar irradiance (facing north) and surface relief. On both analysed studies the walls facing south showed less colonization or even no colonization on the glazed tile surface. Therefore, some notes on conservation measures to prevent or control microbiological growth were recommended.

4. Concerning the characterization of the white glaze, the combined use of µ-PIXE, µ-Raman and SEM-EDS proved to be suitable for the chemical, mineralogical and textural description of the glaze. µ-PIXE and SEM-EDS were the most suitable methods to provide an average composition and elemental distribution of the glaze, since majolica glazes are heterogeneous due to crystalline inclusions.

5. The primary bioreceptivity of tiles to phototrophic microorganism and fungi was evaluated on tile models produced in laboratory by inoculating them with a culture of phototrophic microorganism and other separately with an axenic fungal culture. Inoculated tile models were incubated during 12 months. Secondary bioreceptivity was also studied by submitting half of the produced tile models to an accelerated ageing process. Concerning photoautotrophic colonization data revealed that aged tile samples had higher bioreceptivity compared to pristine tiles, which was mainly due to the physical properties of the aged tile models, such as higher capillary coefficient and water vapour permeability coefficients. The evaluation of the primary and secondary bioreceptivity of glazed ties to fungi, showed no significant differences.

6. The laboratory based biodeterioration experiments have demonstrated the damaging potential of phototrophic microorganisms on glazed wall tiles. The most evident change of the tested photosynthetic microorganisms was physical due to the chasmoendolithic growth on fissures. This might led to physical damage on the substrate, like the deterioration patterns observed in Pena National Palace. In contrast, fungi were not able to provoke physical damage on the substrate, but their exudates, particularly oxalic acid was able to react with calcium leading to formation of calcium oxalate.

7. The cleaning and inactivation of a biofilm is a complex issue, since the inactivation of microorganisms depends on several factors. Our data on the in situ application of biocides on colonized wall tiles from *Casa da Pesca* revealed that the most efficient tested biocide (Preventol RI 80 and Biotin T) showed no long term protection. These results are illustrative of the limited time scale of most of the tested biocides. Lixiviation by rain and consequent decrease in concentration might have allowed the recolonization of organisms on the treated substrates. Results concerning

$TiO_2$ showed that this compound was not effective as a biocide, but caused biofilm detachment without the aid of any mechanical method. Concerning the monitoring methods used to evaluate the biocides, they showed to be suitable for providing information on the efficacy of the biocides.

8. The preliminary tests with $TiO_2$ nanoparticles revealed promising results due to the detachment of the biofilm. However, the application of $TiO_2$ thin coating based did not demonstrate evidences of being a good solution for historical glazes tiles, as their application altered important aesthetical features of the glaze, such as color and particularly the gloss.

9. The results of this thesis provided a first global overview on biodeterioration of majolica tiles by a multidisciplinary approach combining analyses of field surveys (case studies) together with laboratory based experiments. Glazed tile biodeteriogens were identified and tile biodeterioration patterns observed in colonized samples were reproduced under laboratory conditions.

Nowadays we are aware of the impact that microbial colonization has on the deterioration of cultural heritage. The diversity of materials that constitute the tangible cultural heritage is vast, from natural materials, such as stone, to man-made materials, like ceramics and synthetic polymers. Therefore, biodeterioration of many materials are still little studied, particularly for materials which´s use might be considered more seldom. In addition, the complex and multidisciplinary approaches needed to study materials biodeterioration make the knowledge concerning this issue to appear at a slow rate compared with the speed of microbial development. The results of this thesis although innovative and relevant for the preservation of glazed wall tiles are indeed very specific when considering the diversity of organisms, diversity of glazed ceramic typologies and mitigation strategies. In this perspective the following issues can be pointed out for further research:

- Microbial biodiversity found on glazed wall tiles should be further analysed. The identification of biodeteriogens is of great importance for the knowledge on biodeterioration mechanisms, as well as for drawing suitable conservation and mitigation strategies. Therefore, other cases of biologically colonized glazed wall tiles should be studied to achieve the taxonomic identification of the organisms composing these communities. There is also need of studies regarding the physiological features and ecological relations of the organisms that comprise glaze wall tile biofilms. For the identification of microorganisms, this thesis showed that polyphasic approaches with culture and culture-independent methods provide more complete and reliable results. In addition, only the combination of several identification methods allows the identification of novel species, and in the case of glazed wall tiles in both case studies microorganisms with low similarity to known microorganisms were detected and one novel fungal species was characterized, *Devriesia imbrexigena.* Since microbial biodiversity of glazed wall tiles is poorly known there is an urgent need of research in this area.

- The microbial communities studied in this work were mainly found developing over the glaze, but other type of colonizers should also be analysed. Based on observations

performed during this thesis some other cases were observed on tiles, namely endolithic microorganisms and ceramic body colonizers. Lichens were also frequently observed colonizing the areas were the glaze had fallen-off; therefore taxonomic identification should also be performed. Bacteria are another group of microorganism, whose role in the biodeterioration is probably underestimated,were not particularly explored in this thesis.

- On the biodeterioration of glazed wall tiles further colonized tiles (case studies) should be performed. Glazes can be produced with a variety of compositions and also with many different colorants, therefore further research is needed studying other types of glazed wall tiles.

- Laboratory tests should be performed using more glazed wall tile typologies and other microorganisms collected from this substrate. Other microorganisms and microorganism assemblages should be tested in diverse laboratorial conditions.

- Microorganism's mitigation and conservation strategies are still an urgent need in the field of conservation, particularly in the case of outdoor environments were the presence of microorganisms cannot be controlled. This is a transversal conservation problem affecting all kinds of materials found on outdoors cultural heritage. The investigation of novel methods, even when positive results are not achieved is always important to enhance our knowledge. The application of methodologies from other fields during the last decade's has significantly enhanced our understanding on the materialsand has also have provided important conservation methodologies. Therefore, investigation regarding the control of microorganisms used in other fields such as medical or pharmaceutical and  food industry, ought be performed and its application to glaze wall tiles should be tested

-  Finally, after further knowledge on this subject is achieved specific and standard guidelines should be developed for glazed wall tiles exposed to biological colonization in outdoor conditions. These guidelines would provide clear mitigation strategies to control glaze tiles biodeterioration and should be useful for institutions that have under their care outdoors glazed wall tiles.

# References

Addamo, M., Augugliaro, V., Di Paola, a., García-López, E., Loddo, V., Marcì, G., Palmisano, L., 2008. Photocatalytic thin films of TiO2 formed by a sol-gel process using titanium tetraisopropoxide as the precursor. Thin Solid Films 516, 3802–3807.

Ahmadjian, V., 1993. The Lichen Symbiosis. Wiley, New York.

Alakomi, H., Arrien, N., Gorbushina, A., Krumbein, W., Maxwell, I., McCullagh, C., 2004. Inhibitors of biofilm damage on mineral materials (Biodam), in: Proceedings of the 10th International Congress on Deterioration and Conservation of Stone. ICOMOS, Stockholm, pp. 399–406.

Alakomi, H.L., Paananen, A., Suihko, M.-L., Helander, I.M., Saarela, M., 2006. Weakening effect of cell permeabilizers on gram-negative bacteria causing biodeterioration. Appl. Environ. Microbiol. 72, 4695–703.

Al-Awadhi, H., Dashti, N., Khanafer, M., Al-Mailem, D., Ali, N., Radwan, S., 2013. Bias problems in culture-independent analysis of environmental bacterial communities: a representative study on hydrocarbonoclastic bacteria. Springerplus 2, 369.

Albertano, P., Bruno, L., Belleza, S., Paradossi, G., 2000. Polysaccharides as a key step in stone bio-erosion, in: Fassina, V. (Ed.), Proceedings of the 9th International Congress on Deterioration and Conservation of Stone, Volume 1. Elsevier, Venice, p. 1644.

Altschul, S.F., Gish, W., Miller, W., Myers, E.W., Lipman, D.J., 1990. Basic local alignment search tool. J. Mol. Biol. 215, 403–410.

Alzamani, M., Shokuhfar, A., Eghdam, E., Mastali, S., 2013. Influence of catalyst on structural and morphological properties of TiO2 nanostructured films prepared by sol–gel on glass. Prog. Nat. Sci. Mater. Int. 23, 77–84.

Andrade, F. a., Al-Qureshi, H. a., Hotza, D., 2011. Measuring the plasticity of clays: A review. Appl. Clay Sci. 51, 1–7. doi:10.1016/j.clay.2010.10.028

Andrés, A., Díaz, M.C., Coz, A., Abellán, M.J., Viguri, J.R., 2009. Physico-chemical characterisation of bricks all through the manufacture process in relation to efflorescence salts. J. Eur. Ceram. Soc. 29, 1869–1877.

APHA/AWWA/WEF, 2005. Standard Methods for the Examination of Water and Wastewater 21st ed. American Public Health Association, Washington, D.C.

Ascaso, C., Wierzchos, J., Souza-Egipsy, V., de los Rios, A., Rodrigues, J., 2002. In situ evaluation of the biodeteriorating action of microorganisms and the effects of biocides on carbonate rock of the Jeronimos Monastery (Lisbon). Int. Biodeterior. Biodegradation 49, 1–12.

Assunção, A.P., Pereira, C., Correia, E., 2003. Primeiras peças da produção da fábrica de loiça de Sacavém - o papel do coleccionador, Camara Municipal de Loures, Loures.

Aubry, E., Ghazzal, M.N., Demange, V., Chaoui, N., Robert, D., Billard, a., 2007. Poisoning prevention of TiO2 photocatalyst coatings sputtered on soda-lime glass by intercalation of SiNx diffusion barriers. Surf. Coatings Technol. 201, 7706–7712.

Awitor, K.O., Rivaton, A., Gardette, J.L., Down, a. J., Johnson, M.B., 2008. Photo-protection and photo-catalytic activity of crystalline anatase titanium dioxide sputter-coated on polymer films. Thin Solid Films 516, 2286–2291.

Bakar, B., Ibrahim, M., Johari, M., 2009. A Review: Durability of Fired Clay Brick Masonry Wall due to Salt Attack. Int. J. Integr. Eng. 1, 111–127.

Balderrama, A., Vidal, A.A., Cardiel, I.B. (Eds.), 2003. El Estudio y la Conservación de la Cerámica Decorada en Arquitectura, in: El Estudio Y La Conservación de La Cerámica Decorada En Arquitectura. ICCROM, Rome, pp. 1–45.

Bandini, G., Le Breton, J.-M., Rossillon, P., Meco, J., Balanda, É., Uribe Echeverría, A., 2002. Les metamorphoses de l´azur, l´art de l´azulejo dans le monde latin, 2nd ed. ars latina, Paris.

Baricza, A., Baknóczi, B., Tóth, M., Szabó, C., 2012. Deterioration of building ceramics by environmental factor - A case study on Zsolnay ceramics from the museum of applied arts (Budapest), in: Deterioration of Building Ceramics by Environmental Factors. Miskolc - Egyetemváros.

Bartosik, M., Zakowska, Z., Cedzińska, K., Rozniakowski, K., 2010. Biodeterioration of optical glass induced by lubricants used in optical instruments technology. Pol. J. Microbiol. 59, 295–300.

Bass, D., Richards, T. A., 2011. Three reasons to re-evaluate fungal diversity "on Earth and in the ocean." Fungal Biol. Rev. 25, 159–164.

Bastian, F., Alabouvette, C., Jurado, V., Saiz-Jimenez, C., 2009. Impact of biocide treatments on the bacterial communities of the Lascaux Cave. Naturwissenschaften 96, 863–8.

Bastian, F., Jurado, V., Nováková, a., Alabouvette, C., Saiz-Jimenez, C., 2010. The microbiology of Lascaux Cave. Microbiology 156, 644–652. doi:10.1099/mic.0.036160-0

Belgaied, J., 2003. Release of heavy metals from Tunisian traditional earthenware 41, 95–98.

Benavente, D., Sanchez-Moral, S., Fernandez-Cortes, A. Cañaveras, J., Elez, J., Saiz- Jimenez, C., 2011. Salt damage and microclimate in the Postumius Tomb, Roman Necropolis of Carmona, Spain. Environ. Earth Sci. 63, 1529–1543.

Berdahl, P., Akbari, H., Levinson, R., Miller, W. a., 2008. Weathering of roofing materials – An overview. Constr. Build. Mater. 22, 423–433.

Berendse, A., Keezer, M.B., Schoubye, S., Santos Simões, J.M., Tichelaar, J., 1967. Tiles a general history. Faber and Faber, London.

Berti, S., Pinzari, F., Tiano, P., 2008. Control of biodeterioration and bioremediation techniques. Physical methods, in: Caneva G, Nugari MP, S.O. (Ed.), Plant Biology for Cultural Heritage. Biodeterioration and Conservation. Los Angelos, pp. 317–8.

Bertoncello, R., Milanese, L., Dran, J.C., Bouquillon, A., Sada, C., 2006. Sol-gel deposition of silica films on silicate glasses: Influence of the presence of lead in the glass or in precursor solutions. J. Non. Cryst. Solids 352, 315–321.

Blachere, R., Procedure, E., 1976. Corrosion of Lead Glasses in Acid Media II, Concentration Profile Measurements. Physics 61, 292–294.

Bonazza, A., Sabbioni, C., Ghedini, N., Hermosin, B., Jurado, V., Gonzalez, J.M., Saiz-Jimenez, C., 2007. Did Smoke from the Kuwait Oil Well Fires Affect Iranian Archaeological Heritage? Environ. Sci. Technol. 41, 2378–2386.

Bonnet, C., 2003. Alteration of lead silicate glasses due to leaching in heated acid solutions 323, 214–220.

Borges, C., Caetano, C., Costa Pessoa, J., Figueiredo, M.O., Lourenço, A., Malhoa Gomes, M., Silva, T.P., Veiga, J.P., 1997. Monitoring the removal soluble salts from ancient tiles by ion chromatography. J Chromatogr. A 195–201.

Bougoure, D.S., Cairney, J.W.G., 2005. Fungi associated with hair roots of Rhodo- dendron lochiae (Ericaceae) in an Australian tropical cloud forest revealed by culturing and culture-independent molecular methods. Environmental Micro- biology 7, 1743-1754.

Bourrelly, P., 1990. Les algues d'eau douce e Initiation à la systématique, I: Les Algues Vertes. N. Boubée, Paris, 572 pp.

Brehm, U., Gorbushina, A., Mottershead, D., 2005. The role of microorganisms and biofilms in the breakdown and dissolution of quartz and glass. Palaeogeogr. Palaeoclimatol. Palaeoecol. 219, 117–129.

Büdel, B., Henssen, A., 1983. Chroococcidiopsis (Cyanophyceae), a phycobiont in the lichen family Lichinaceae. Phycol. 22, 367-375.

Buffet-Bataillon, S., Tattevin, P., Bonnaure-Mallet, M., Jolivet-Gougeon, A., 2012. Emergence of resistance to antibacterial agents: the role of quaternary ammonium compounds—a critical review. Int. J. Antimicrob. Agents 39, 381–389.

Burlamaqui, S., 1996. Cerâmica mural Portuguesa contemporânea. Quetzal Editores, Lisboa.

Burnison, B.K., 1980. Modified dimethyl sulfoxide (DMSO) extraction for chlorophyll analysis of phytoplankton. Canadian Journal of Fisheries and Aquatic Sciences 37, 729-733.

Buys, S., Oakley, V., 1996. The Conservation and Restoration of Ceramics, Butterworth-Heinemann series in conservation and museology. Butterworth-Heinemann.

Calligaro, T., Dran, J.C., Salomon, J., Walter, P., 2004. Review of accelerator gadgets for art and archaeology. Nucl. Instruments Methods Phys. Res. Sect. B Beam Interact. with Mater. Atoms 226, 29–37.

Camuffo, D., 1995. Physical weathering of stones. Sci. Total Environ. 167, 1–14.

Caneva, G., Nugari, M.P., Salvadori, O., 2008. Plant Biology for Cultural Heritage: Biodeterioration and Conservation, Getty Publ. ed. Getty Publications, Los Angeles.

Caneva, G., Nugari, M.P., Salvadori, O., 1991. Biology in the Conservation of Works of Art.

Cannillo, V., Esposito, L., Rambaldi, E., Sola, A., Tucci, A., 2009. Microstructural and mechanical changes by chemical ageing of glazed ceramic surfaces. J. Eur. Ceram. Soc. 29, 1561–1569.

Carmona, N., Laiz, L., Gonzalez, J.M., Garcia-Heras, M., Villegas, M.A., Saiz-Jimenez, C., 2006. Biodeterioration of historic stained glasses from the Cartuja de Miraflores (Spain). Int. Biodeterior. Biodegradation 58, 155–161.

Carneiro, J.M., 2009. O imaginário romântico da Pena. Chaves Ferreira Publicações, Porto.

Carter, C.B., Norton, M.G., 2013. Ceramic Materials: Science and Engineering, Springe. ed. New York.

Carter, N.E.A., Viles, H.A., 2004. Lichen hotspots: raised rock temperatures beneath Verrucaria nigrescens on limestone. Geomorphology 62, 1–16. doi:10.1016/j.geomorph.2004.02.001

Carvalho, A.P., Vaz, M.F., Samora, M.J., Pires, J., 2006. Characterisation of Ceramic Pastes of Portuguese Ancient Tiles. Mater. Sci. Forum 514-516, 1648–1652.

Cecchi, G., Pantani, L., Raimondi, V., Tomaselli, L., Lamenti, G., Tiano, P., Chiari, R., 2000. Fluorescence lidar technique for the remote sensing of stone monuments. J. Cult. Herit. 1, 29–36.

Chen, J., Blume, H.-P., Beyer, L., 2000. Weathering of rocks induced by lichen colonization — a review. Catena 39, 121–146.

Cheng, M.-D., Pfiffner, S.M., Miller, W. a., Berdahl, P., 2011. Chemical and microbial effects of atmospheric particles on the performance of steep-slope roofing materials. Build. Environ. 46, 999–1010.

Chua, N.K., Kwok, S.W., Tan, K.K., Teo, S.P., Wong, H.A., 1972. Growth on concrete and other similar surfaces in Singapore. J. Singapore Inst. Archit. 51, 13–15.

Clauzade, G., Roux, C., 1985. Likenoj de okcidenta Europo:ilustrita determinlibro. Bull. la Soc. Bot. Centre.Ouest 7, 1–893.

Coentro, S., Mimoso, J.M., Lima, A.M., Silva, A.S., Pais, A.N., Muralha, V.S.F., 2012. Multi-analytical identification of pigments and pigment mixtures used in 17th century Portuguese azulejos. J. Eur. Ceram. Soc. 32, 37–48.

Coentro, S., Trindade, R.A.A., Mirão, J., Candeias, A., Alves, L.C., Silva, R.M.C., Muralha, V.S.F., 2014. Hispano-Moresque ceramic tiles from the Monastery of Santa Clara-a-Velha (Coimbra, Portugal). J. Archaeol. Sci. 41, 21–28.

Cooke, M., 2002. European review of biocides. PharmaChem 48–50.

Correia de Carvalho, M., 2012. A pintura do azulejo em Portugal [1675-1725].Autorias e biografias - um novo paradigma. Universidade de Lisboa Faculdade de Letras.

Costa, M.L. da, Sanjad, T.A.B.C.T., Paiva, R.S., 2013. The mineralogy and chemistry of the German and Portuguese tiles used to face a historic building in the Amazon region and their natural susceptibility to tropical weathering. Acta Amaz. 43, 323–330.

Costerton, J.W., 1999. Introduction to biofilm. Int. J. Antimicrob. Agents 11, 217–21.

Costerton, J.W., Lewandowski, Z., Caldwell, D.E., Korber, D.R., Lappin-Scott, H.M., 1995. Microbial biofilms. Annu. Rev. Microbiol. 49, 711–45.

Coutinho, M.L., Miller, A.Z., Gutierrez-Patricio, S., Hernandez-Marine, M., Gomez-Bolea, A., Rogerio-Candelera, M.A., Philips, A.J.L., Jurado, V., Saiz-Jimenez, C., Macedo, M.F., 2013. Microbial communities on deteriorated artistic tiles from Pena National Palace (Sintra, Portugal). Int. Biodeterior. Biodegradation 84, 322–332.

Coutinho, M.L., Miller, A.Z., Macedo, M.F., Miller, A.Z., 2015. Biological colonization and biodeterioration of architectural ceramic materials: An overview. J. Cult. Herit. (In Press)

Coutinho, M.L., Pinheiro, C., Phillips, A., Macedo, M., 2011. Biodeterioration of tiles from Pena National Palace (Portugal). First step: identification of fungal community. Prepr. ICOM-CCs 16th Trienn. Conf. Int. Counc. Museums 82.(digital support)

Crispim, C.A., Gaylarde, C.C., 2005. Cyanobacteria and biodeterioration of cultural heritage: a review. Microb. Ecol. 49, 1–9.

Crous, P.W., Shivas, R.G., Wingfield, M.J., Summerell, B.A., Rossman, A.Y., Alves, J.L., Adams, et al., Fungal Planet description sheets: 128-153, Persoonia. 29 (2012) 146–201.Curlevski, N.J.A., Drigo, B., Cairney, J.W.G., Anderson, I.C., 2014. Influence of elevated atmospheric CO2 and water availability on soil fungal communities under Eucalyptus saligna. Soil Biol. Biochem. 70, 263–271.

Cutler, N.A., Oliver, A.E., Viles, H.A., Ahmad, S., Whiteley, A.S., 2013. The characterisation of eukaryotic microbial communities on sandstone buildings in Belfast, UK, using TRFLP and 454 pyrosequencing. Int Biodeter Biodegrad. 82, 124–133.

Cuzman, O.A., Tiano, P., Ventura, S., Frediani, P., 2011. Biodiversity on Stone Artifacts, in: J, L.-P. (Ed.), The Importance of Biological Interactions in the Study of Biodiversity. InTech Europe, pp. 367–390.

D'Orazio, M., Cursio, G., Graziani, L., Aquilanti, L., Osimani, A., Clementi, F., Yéprémian, C., Lariccia, V., Amoroso, S., 2014. Effects of water absorption and surface roughness on the bioreceptivity of ETICS compared to clay bricks. Build. Environ. 77, 20–28.

Dan, T.K., Shreedharan, V.P., Patel, M., Rohtagi, P.K., 1981. Mechanism of blackening of tile surface Ceramic. Ind J India.

De Freitas, V.P., Corvacho, H., Quintela, M., Delgado, J.M.P.Q., 2014. Assessing the durability of mortars tiles – A contribution for a prediction model. Eng. Fail. Anal. 44, 36–45.

De los Ríos, A., Pérez-Ortega, S., Wierzchos, J., Ascaso, C., 2012. Differential effects of biocide treatments on saxicolous communities: Case study of the Segovia cathedral cloister (Spain). Int. Biodeterior. Biodegradation 67, 64–72.

Del Campo, J., Sieracki, M.E., Molestina, R., Keeling, P., Massana, R., Ruiz-Trillo, I., 2014. The others: our biased perspective of eukaryotic genomes. Trends Ecol. Evol. 29, 252–9.

Diaz-Herraiz, M., 2014. Characterization of microbial communities in Etruscan and Roman tombs. The Institute for Natural Resources and Agrobiology, CSIC.

Díez, B., Pedrós-Alió, C., Marsh, T.L., Massana, R., 2001. Application of Denaturing Gradient Gel Electrophoresis (DGGE) To Study the Diversity of Marine Picoeukaryotic Assemblages and Comparison of DGGE with Other Molecular Techniques. Appl. Environ. Microbiol. 67, 2942–2951.

Doaré-Lebrun, E., El Arbi, a, Charlet, M., Guérin, L., Pernelle, J.-J., Ogier, J.-C., Bouix, M., 2006. Analysis of fungal diversity of grapes by application of temporal temperature gradient gel electrophoresis - potentialities and limits of the method. J. Appl. Microbiol. 101, 1340–50.

Doğan, N., Beril Tuğrul, A., 2001. Dosimetric evaluation of gamma doses using irradiated lead–alkali–silicate glass. Radiat. Meas. 33, 211–216.

Doherty, B., Pamplona, M., Miliani, C., Matteini, M., Sgamellotti, A., Brunetti, B., 2007. Durability of the artificial calcium oxalate protective on two Florentine monuments. J. Cult. Herit. 8, 186–192.

Doménech-Carbó, a., Doménech-Carbó, M.T., 2005. Electrochemical Characterization of Archaeological Tin-Opacified Lead-Alkali Glazes and Their Corrosion Processes. Electroanalysis 17, 1959–1969.

Dondi, M., Raimondo, M., Zanelli, C., 2014. Clays and bodies for ceramic tiles: Reappraisal and technological classification. Appl. Clay Sci. 96, 91–109.

Durbin, L., 2005. Architectural tiles : conservation and restoration : from the medieval period to the twentieth century, Butterwort. ed. Boston.

Edgar, R.C., 2004. MUSCLE: multiple sequence alignment with high accuracy and high throughput. Nucleic Acids Res. 32, 1792–1797.

Eggert, G., 2006. To whom cracks tell: a closer look at craquelure in glass and glaze. Stud. Conserv. 51, 69–75.

Egidi, E., Hoog, G.S., Isola, D., Onofri, S., Quaedvlieg, W., Vries, M., Verkley, G.J.M., Stielow, J.B., Zucconi, L., Selbmann, L., 2014. Phylogeny and taxonomy of meristematic rock-inhabiting black fungi in the Dothideomycetes based on multi-locus phylogenies. Fungal Divers. 65, 127–165.

References

El Nouhy, H.A., 2013. Assessment of some locally produced Egyptian ceramic wall tiles. HBRC J. 9, 201–209.

Elendt, B.P., Bias, W.R., 1990. Trace nutrient deficiency in Daphnia magna cultured in standard medium for toxicity testing: effects of the optimiza- tion of culture conditions on life history parameters of D. magna.Water Res 24, 1157-1167.

Eppler, R., 1992. Corrosion of Glazes and Enamels, in: Clark, D., Zoitos, B. (Eds.), Corrosion of Glass, Ceramics and Ceramic Superconductors. Noyes Publications, Park Ridge, Illinois.

Ettenauer, J.D., Piñar, G., Lopandic, K., Spangl, B., Ellersdorfer, G., Voitl, C., Sterflinger, K., 2012. Microbes on building materials - Evaluation of DNA extraction protocols as common basis for molecular analysis. Sci. Total Environ. 439C, 44–53.

Fabbri, B., 2003. La caratterizzazione dei materiali nel restauro di ceramica invetriata in contesto archittetonico, in: Balderrama, A., Vidal, A.A., Cardiel, I.B. (Eds.), El Estudio Y La Conservación de La Cerámica Decorada En Arquitectura. ICCROM, Rome, pp. 15–20.

Fabbri, B., Gualtieri, S., Shoval, S., 2014. The presence of calcite in archeological ceramics. J. Eur. Ceram. Soc. 34, 1899–1911.

Farinha, J.L.A., Tavares, D.S., 2003. The removal and replacing of architectural glazed tiles - azulejos, in: Balderrama, A., Vidal, A.A., Cardiel, I.B. (Eds.), El Estudio Y La Conservación de La Cerámica Decorada En Arquitectura. ICCROM, Rome, pp. 22–27.

Favero-Longo, S.E., Castelli, D., Fubini, B., Piervittori, R., 2009. Lichens on asbestos-cement roofs: bioweathering and biocovering effects. J. Hazard. Mater. 162, 1300–8.

Fernandes, P., 2006. Applied microbiology and biotechnology in the conservation of stone cultural heritage materials. Appl. Microbiol. Biotechnol. 73, 291–6.

Figueiredo, M., Silva, T., Veiga, J., 2009. Ancient glazed ceramic tiles: a long-term, study from the remediation of environmental impacts to the non-destructive characterization of materials, in: Proceedings of the Interntional Seminar on Conservation of Glazed Ceramic Tiles: Research and Practice. LNEC, Lisbon, p. 10.

Figueiredo, M.O., Veiga, J.P., Silva, T.P., Mira, J.P., Pascarelli, S., 2005. Chemistry versus phase constitution of yellow ancient tile glazes : A non-destructive insight through XAS. Nucl. Instruments Methods Phys. Res. Sect. B Beam Interact. with Mater. Atoms 238, 134–137.

Fomina, M., Hillier, S., Charnock, J.M., Melville, K., Gadd, G.M., Alexander, I.J., 2005. Role of Oxalic Acid Overexcretion in Transformations of Toxic Metal Minerals by Beauveria caledonica Role of Oxalic Acid Overexcretion in Transformations of Toxic Metal Minerals by Beauveria caledonica.

Fonseca, A.J., Pina, F., Macedo, M.F., Leal, N., Romanowska-Deskins, A., Laiz, L., Gómez-Bolea, A., Saiz-Jimenez, C., 2010. Anatase as an alternative application for preventing biodeterioration of mortars: Evaluation and comparison with other biocides. Int. Biodeterior. Biodegradation 64, 388–396.

Franzoni, E., Fregni, A., Gabrielli, R., Graziani, G., Sassoni, E., 2014. Compatibility of photocatalytic $TiO_2$ -based fi nishing for renders in architectural restoration : A preliminary study 80, 125–135.

Fröberg, L., Hupa, L., 2008. Topographic characterization of glazed surfaces. Appl. Surf. Sci. 254, 1622–1629. doi:10.1016/j.apsusc.2007.07.173

Fröberg, L., Hupa, L., Hupa, M., 2009. Corrosion of the crystalline phases of matte glazes in aqueous solutions. J. Eur. Ceram. Soc. 29, 7–14.

References

Fröberg, L., Kronberg, T., Törnblom, S., Hupa, L., 2007. Chemical durability of glazed surfaces. J. Eur. Ceram. Soc. 27, 1811–1816.

Frost, R.L., Jing, Y., Ding, Z., 2003. Raman and FTIR spectroscopy of natural oxalates: Implications for the evidence of life on Mars. Chinese Sci. Bull. 48, 1844.

Frost, R., 2004. Raman spectroscopy of natural oxalates. Anal. Chim. Acta 517, 207–214.

Fujishima, A., Zhang, X., 2006. Titanium dioxide photocatalysis: present situation and future approaches. Comptes Rendus Chim. 9, 750–760. doi:10.1016/j.crci.2005.02.055

Gadd, G.M., 2010. Metals, minerals and microbes: geomicrobiology and bioremediation. Microbiology 156, 609–43.

Gadd, G.M., 2007. Geomycology: biogeochemical transformations of rocks, minerals, metals and radionuclides by fungi, bioweathering and bioremediation. Mycol. Res. 111, 3–49.

Gadd, G.M., Bahri-Esfahani, J., Li, Q., Rhee, Y.J., Wei, Z., Fomina, M., Liang, X., 2014. Oxalate production by fungi: significance in geomycology, biodeterioration and bioremediation. Fungal Biol. Rev. 28, 36–55.

Gadd, G.M., Ramsay, L., Crawford, J.W., Ritz, K., 2001. Nutritional influence on fungal colony growth and biomass distribution in response to toxic metals. FEMS Microbiol. Lett. 204, 311–316.

Garcez, N., Lopes, N., de Brito, J., Sá, G., 2012. Pathology, diagnosis and repair of pitched roofs with ceramic tiles: Statistical characterisation and lessons learned from inspections. Constr. Build. Mater. 36, 807–819.

Garcia-Pichel, F., López-Cortés, A., Nübel, U., 2001. Phylogenetic and morphological diversity of cyanobacteria in soil desert crusts from the Colorado plateau. Appl. Environ. Microbiol. 67, 1902–10.

Garcia-Pichel, F., Nu, U., Muyzer, G., Nübel, U., Garcia-Pichel, F., Muyzer, G., 1997. PCR primers to amplify 16S rRNA genes from cyanobacteria. Appl. Environ. Microbiol. 63, 3327–3332.

Garcia-Rowe, J., Saiz-Jimenez, C., 1991. Lichens and bryophytes as agents of deterioration of building materials in Spanish cathedrals. Int. Biodeterior. 28, 151–163.

Gaylarde, C.C., Morton, L.H.G., Loh, K., Shirakawa, M. A., 2011. Biodeterioration of external architectural paint films – A review. Int. Biodeterior. Biodegradation 65, 1189–1198.

Gazulla, M.F., Sánchez, E., González, J.M., Portillo, M.C., Orduña, M., 2011. Relationship between certain ceramic roofing tile characteristics and biodeterioration. J. Eur. Ceram. Soc. 31, 2753–2761.

Gerard, L., 2007. The History of Gauged Brickwork. Butterworth-Heinemann, Oxford.

Giacomucci, L., Bertoncello, R., Salvadori, O., Martini, I., Favaro, M., Villa, F., Sorlini, C., Cappitelli, F., 2011. Microbial deterioration of artistic tiles from the façade of the Grande Albergo Ausonia & Hungaria (Venice, Italy). Microb. Ecol. 62, 287–98.

Giannantonio, D.J., Kurth, J.C., Kurtis, K.E., Sobecky, P., 2009. Effects of concrete properties and nutrients on fungal colonization and fouling. Int. Biodeterior. Biodegrad. 63, 252–259.

Gill, M.S., Rehren, T., Freestone, I., 2014. Tradition and indigeneity in Mughal architectural glazed tiles. J. Archaeol. Sci. 49, 546–555.

References

Giovannacci, D., Leclaire, C., Horgnies, M., Ellmer, M., Mertz, J.D., Orial, G., Chen, J., Bousta, F., 2013. Algal colonization kinetics on roofing and façade tiles: Influence of physical parameters. Constr. Build. Mater. 48, 670–676.

Gladis, F., Schumann, R., 2011a. Influence of material properties and photocatalysis on phototrophic growth in multi-year roof weathering. Int. Biodeterior. Biodegradation 65, 36–44.

Gladis, F., Schumann, R., 2011b. A suggested standardised method for testing photocatalytic inactivation of aeroterrestrial algal growth on TiO2-coated glass. Int. Biodeterior. Biodegradation 65, 415–422.

Golubic, S., Friedmann, E.I., Schneider, J., 1981. The Lithobiontic Ecological Niche, with Special Reference to Microorganisms. SEPM J. Sediment. Res. Vol. 51, 475–478.

Gómez-Alarcón, G., Cilleros, B., 1995. Microbial communities and alteration processes in monuments at Alcala de Henares, Spain. Sci. Total Environ. 167, 231–239.

González-García, F., Romero-Acosta, V., García-Ramos, G., González-Rodríguez, M., 1990. Firing transformations of mixtures of clays containing illite, kaolinite and calcium carbonate used by ornamental tile industries. Appl. Clay Sci. 5, 361–375.

Gorbushina, A.A., 2007. Life on the rocks. Environ. Microbiol. 9, 1613–31.

Gorbushina, A.A., Krumbein, W.E., Volkmann, M., 2002. Rock surfaces as life indicators: new ways to demonstrate life and traces of former life. Astrobiology 2, 203–13.

Gorbushina, A.A., Palinska, K.A., 1999. Biodeteriorative processes on glass : experimental proof of the role of fungi and cyanobacteria 183–191.

Görs, S., Schumann, R., Häubner, N., Karsten, U., 2007. Fungal and algal biomass in biofilms on artificial surfaces quantified by ergosterol and chlorophyll a as biomarkers. Int. Biodeterior. Biodegradation 60, 50–59.

Grant, C., 1982. Fouling of terrestrial substrates by algae and implications for control e a review. International Biodeterioration Bulletin 18, 57e65.

Graziani, L., Quagliarini, E., Osimani, A., Aquilanti, L., Clementi, F., Yéprémian, C., Lariccia, V., Amoroso, S., D'Orazio, M., 2013. Evaluation of inhibitory effect of TiO2 nanocoatings against microalgal growth on clay brick façades under weak UV exposure conditions. Build. Environ. 64, 38–45.

Green, T., Lange, O., 1994. Photosyntesis in Poikilohydric Plants: A Comparision of Lichens and Bryophytes, in: Schulze, E.-D., Caldwell, M.M. (Eds.), Ecophysiology of Photosynthesis. Springer Berlin Heidelberg, Berlin, Heidelberg, pp. 319–341.

Guillitte, O., 1995. Bioreceptivity: a new concept for building ecology studies. Sci. Total Environ. 167, 215–220.

Guillitte, O., Dreesen, R., 1995. Laboratory chamber studies and petrographical analysis as bioreceptivity assessment tools of building materials. Sci. Total Environ. 9697, 365–374.

Gulzar, S., Wörle, M., Burg, J.-P., Chaudhry, M.N., Joseph, E., Reusser, E., 2012. Characterization of 17th Century Mughal tile glazes from Shahdara Complex, Lahore-Pakistan. J. Cult. Herit. 3–8.

Halici, M.G., Hawksworth, D.L., Candan, M., Türk, A.O., 2010. A new lichenicolous species of Capronia (Ascomycota, Herpotrichiellaceae), with a key to the known lichenicolous species of the genus. Fungal Diversity 40, 37-40.

References

Hallmann, C., Stannek, L., Fritzlar, D., Hause-Reitner, D., Friedl, T., Hoppert, M., 2013. Molecular diversity of phototrophic biofilms on building stone. FEMS Microbiol. Ecol. 84, 355–72.

Hamilton, D., 1978. The Thames & Hudson Manual of Architectural Ceramics, Thames & H. ed. London.

Harutyunyan, S., Muggia, L., Grube, M., 2008. Black fungi in lichens from seasonally arid habitats. Stud. Mycol. 61, 83-90

Hassan, Z., Harun, S., 2013. Preservation of Malay Singgora Roof. Procedia Environ. Sci. 17, 729–738.

Hauck, M., Dulamsuren, C., Mühlenberg, M., 2007. Lichen diversity on steppe slopes in the northern Mongolian mountain taiga and its dependence on microclimate. Flora - Morphol. Distrib. Funct. Ecol. Plants 202, 530–546.

Head, I.M., Saunders, J.R., Pickup, R.W., 1998. Microbial evolution, diversity, and ecology: a decade of ribosomal RNA analysis of uncultivated microorganisms. Microb. Ecol. 35, 1–21.

Heikkilä, P., Salmi, T., Kotimaa, M., 1988. Identification and counting of fungal spores by scanning electron microscopy. Scand. J. Work. Environ. Health 14 Suppl 1, 66–7.

Herisson, J., van Hullebusch, E.D., Moletta-Denat, M., Taquet, P., Chaussadent, T., Hullebusch, E.D. Van, Moletta-Denat, M., Taquet, P., Chaussadent, T., van Hullebusch, E.D., Moletta-Denat, M., Taquet, P., Chaussadent, T., 2013. Toward an accelerated biodeterioration test to understand the behavior of Portland and calcium aluminate cementitious materials in sewer networks. Int. Biodeterior. Biodegradation 84, 236–243.

Herrera, L.K., Videla, H., 2004. The importance of atmospheric effects on biodeterioration of cultural heritage constructional materials. Int. Biodeterior. Biodegradation 54, 125–134.

Hessler, C.M., Wu, M.-Y., Xue, Z., Choi, H., Seo, Y., 2012. The influence of capsular extracellular polymeric substances on the interaction between $TiO_2$ nanoparticles and planktonic bacteria. Water Res. 46, 4687–96.

Hestmark, G., 2009. Newobservations and records for Umbilicaria (Umbilicariaceae) in Bolivia. The Bryologist 112, 833-838.

Hoffland, E., Giesler, R., Breemen, N. van, Jongmans, A.G., 2003. Feldspar Tunneling by Fungi along Natural Productivity Gradients. Ecosystems 6, 739–746.

Hoog, G.S. De, Pavia, U., 2006. Phialophora sessilis, 95, 281–284.

Huber, T., Faulkner, G., Hugenholtz, P., 2004. Bellerophon: a program to detect chimeric sequences in multiple sequence alignments. Bioinformatics 20, 2317-2319.

Hueck, H., 1965. The biodeterioration of materials as part of hylobiology. MaterOrg 1, 5–34.

Hughes, J., 1982. Penetration by rhizoids of the moss Tortula muralis Hedw. into well cemented oolitic limestone. Int. Biodeterior. Bull. 18, 43–46.

Hupa, L., Bergman, R., Fröberg, L., Vane-Tempest, S., Hupa, M., Kronberg, T., Pesonen-Leinonen, E., Sjöberg, A.-M., 2005. Chemical resistance and cleanability of glazed surfaces. Surf. Sci. 584, 113–118.

ICOM-CC, 2009. Terminology - ICOM-CC [WWW Document]. URL http://www.icom-cc.org/242/#.VP8ucHysVHU (accessed 3.10.15).

ICOMOS, 2008. ICOMOS-ISCS: Illustrated glossary on stone deterioration patterns. ICOMOS International Scientific Committee for Stone.

IHA-FLUL, n.d. Rede Temática em Estudos de Azulejaria e Cerâmica João Miguel dos Santos Simões [WWW Document]. URL http://redeazulejo.fl.ul.pt/ (accessed 4.7.15).

John, D., 2003. Filamentous and Plantlike green algae, in: Wehr, J.D., Sheath, R.G. (Eds.), Freshwater Algae of North America: Ecology and Classification. Academic Press, San Diego, pp. 311–352.

John, D., 1988. Algal growth on buildings: a review and methods of treatment. Biodeterior. Abstr. 2, 81–102.

Jones, A.S., 2002. El biodeterioro en el patrimonio arquitectónico de Antioquia, in: Videla, H.A., Herrera, L.K. (Eds.), Prevencion on Y Proteccion on Proteccion on Del Patrimonio Prevencion on Cultural Iberoamericano de Los Efectos Del Biodeterioro Ambiental,. Medellen, Colombia, pp. 143–153.

Jongmans, A.G., van Breemen, N., Lundstrom, U., van Hees, P.A.W., Finlay, R.D., Srinivasan, M., Unestam, T., Giesler, R., Melkerud, P.A., Olsson, M., 1997. Rock-eating fungi. Nature 389, 682–683.

Jordan, M.M., Montero, M. A., Meseguer, S., Sanfeliu, T., 2008. Influence of firing temperature and mineralogical composition on bending strength and porosity of ceramic tile bodies. Appl. Clay Sci. 42, 266–271.

Jurado, V., Miller, A.Z., Cuezva, S., Fernandez-Cortes, A., Benavente, D., Rogerio-Candelera, M., Reyes, J., Cañaveras, J., Sanchez-Moral, S., Saiz-Jimenez, C., 2014. Recolonization of mortars by endolithic organisms on the walls of San Roque church in Campeche (Mexico): A case of tertiary bioreceptivity. Constr. Build. Mater. 53, 348–359.

Karoglou, M., Moropoulou, A., Giakoumaki, A., Krokida, M.K., 2005. Capillary rise kinetics of some building materials. J. Colloid Interface Sci. 284, 260–4.

Kemmitt, T., Al-Salim, N.I., Waterland, M., Kennedy, V.J., Markwitz, a., 2004. Photocatalytic titania coatings. Curr. Appl. Phys. 4, 189–192.

Kiurski, J.S., Ranogajec, J.G., Ujhelji, A.L., Radeka, M.M., Bokorov, M.T., 2005. Evaluation of the effect of lichens on ceramic roofing tiles by scanning electron microscopy and energy-dispersive spectroscopy analyses. Scanning 27, 113–9.

Kiwi, J., Nadtochenko, V., 2005. Evidence for the Mechanism of Photocatalytic Degradation of the Bacterial Wall Membrane at the $TiO_2$ Interface by ATR-FTIR and Laser Kinetic Spectroscopy. Langmuir 21, 4631–4641.

Knapp, R.G., 2000. China's Old Dwellings. University of Hawaii Press.

Koestler, R.J., Warscheid, T., Nieto, F., Baer, N., Snethlage, R., 1997. Biodeterioration: Risk Factors and their Management. Environ. Sci. reasearch Rep. es 20, 52–36.

Komárek, J., Anagnostidis, K., 1999. Cyanoprocaryota I. In: Ettl, H., Gerloff, J., Heynig, H., Mollenhauer, D. (Eds.), Süßwasserflora von Mitteleuropa, Band 19/1. Gustav Fischer Verlag, p. 548

Konta, J., 1995. Clay and man: clay raw materials in the service of man. Appl. Clay Sci. 10, 275–335.

Kopar, T., Ducman, V., 2007. Low-vacuum SEM analyses of ceramic tiles with emphasis on glaze defects characterisation. Mater. Charact. 58, 1133–1137.

Krumbein, W.E., Urzì, C.E., Gehrmann, C., 1991. Biocorrosion and biodeterioration of antique and medieval glass. Geomicrobiol. J. 9, 139–160.

Kühnel, R.A., 2004. Cause and consequence: volume changes behind building material deterioration. Mater. Charact. 53, 171–180.

Kumar, R., Kumar, A., 1999. Biodeteriogens: Characteristics and Biodeterioration Mechanisms, in: Agnew N, Berland D, S.-A.S. (Ed.), Biodeterioration of Stone in Tropical Environments an Overview. The getty conservation institute, Los Angelos, pp. 12–32.

Kumar, S.G., Devi, L.G., 2011. Review on modified TiO2 photocatalysis under UV/visible light: selected results and related mechanisms on interfacial charge carrier transfer dynamics. J. Phys. Chem. A 115, 13211–41.

La Russa, M.F., Macchia, A., Ruffolo, S.A., De Leo, F., Barberio, M., Barone, P., Crisci, G.M., Urzì, C., 2014. Testing the antibacterial activity of doped TiO2 for preventing biodeterioration of cultural heritage building materials. Int. Biodeterior. Biodegradation 96, 87–96.

La Russa, M.F., Ruffolo, S.A., Rovella, N., Belfiore, C.M., Palermo, A.M., Guzzi, M.T., Crisci, G.M., 2012. Multifunctional TiO2 coatings for Cultural Heritage. Prog. Org. Coatings 74, 186–191.

Laiz, L., Piñar, G., Lubitz, W., Saiz-jimenez, C., 2003. Monitoring the colonization of monuments by bacteria : cultivation versus molecular methods. Environ. Microbiol. 5, 72–74.

Laiz, L.L., Gonzalez, J.M.J., Saiz-Jimenez, C.C., Portillo, M.C.M., Gazulla, M.F., Sanchez, E., 2006. Microbial assessment of the biological colonization on roofing tiles, in: Heritage,weathering and Conservation. London:; Taylor & Francis ; c2006, pp. 349–353.

Larbi, J.A., 2004. Microscopy applied to the diagnosis of the deterioration of brick masonry. Constr. Build. Mater. 18, 299–307.

Larsen, E.S., Nielsen, C.B., 1990. Decay of bricks due to salt. Mater. Struct. 23, 16–25.

Lega, A.M., Mazzotti, V., Fabbri, B., Pinna, D., 2004. Progetto di conservazione programmata di ceramiche del novecento esposte all'aperto nel centro storico di Faenza 503–512, tables, pl. 15.

Lemmen, H. van, 1993. Tiles 1,000 Years of Architectural Decoration. Harry N. Abrams, New York.

Leo, F., Urzi, C. 2015. Microfungi from deteriorated materials of cultural heritage. In: Fungi from different substrates. Misra, J.K, Tewari, J.P., Deshmukh, S.K., Vágvölgyi C., eds. New York: CRCPress Taylor and Francis.

Lichtlé, C., 1979. Effects of nitrogen deficiency and light of high intensity on *Cryptomonas rufescens* (Cryptophyceae). I. Cell and photosynthetic apparatus transformations and encystment. Protoplasma 101, 283e299.

Linnow, K., Halsberghe, L., Steiger, M., 2007. Analysis of calcium acetate efflorescences formed on ceramic tiles in a museum environment. J. Cult. Herit. 8, 44–52.

Lisci, M., Monte, M., Pacini, E., 2003. Lichens and higher plants on stone: a review. Int. Biodeterior. Biodegradation 51, 1–17.

Lloyd, H., Lithgow, K., 2011. Physical agents of deterioration, in: The National Trust Manual of Housekeeping: The Care of Collections in Historic Houses Open to the Public. The National Trust, p. 64.

Lloyd, H., 2011. Collections outdoors, in: The National Trust Manual of Housekeeping: The Care of Collections in Historic Houses Open to the Public. The National Trust, p. 579.

Lobo, C., Pernão, J., 2010. Glazed tiles as an improving element for environmental quality in Urban Landscape. Colour  Des. Creat. 9, 1–12.

References

López-Arce, P., Garcia-Guinea, J., 2005. Weathering traces in ancient bricks from historic buildings. Build. Environ. 40, 929–941.

López-Arce, P., García-Guinea, J., Fierro, J.L.G., 2003. Manganese micro-nodules on ancient brick walls. Sci. Total Environ. 302, 267–74.

Lurdes Esteves, 2003. Os grandes problemas de conservação e restauro do azulejo, in: Campos T, M.J. (Ed.), Azulejo 8/11. Lisbon, pp. 21–38.

Lynch, G., 2007. The History of Gauged Brickwork: Conservation, Repair and Modern Application, Butterwort. ed. Oxford.

Macedo, M.F., Miller, A.Z., Dionísio, A., Saiz-Jimenez, C., 2009. Biodiversity of cyanobacteria and green algae on monuments in the Mediterranean Basin: an overview. Microbiology 155, 3476–90.

Maguregui, M., Sarmiento, a., Escribano, R., Martinez-Arkarazo, I., Castro, K., Madariaga, J.M., 2009. Raman spectroscopy after accelerated ageing tests to assess the origin of some decayed products found in real historical bricks affected by urban polluted atmospheres. Anal. Bioanal. Chem. 395, 2119–2129.

Mandal, S., Rath, J., 2013. Algal colonization and its ecophysiology on the fine sculptures of terracotta monuments of Bishnupur, West Bengal, India. Int. Biodeterior. Biodegradation 84, 291–299.

Markowska-Szczupak, A., Ulfig, A.K., Morawski, A.W., 2011. The application of titanium dioxide for deactivation of bioparticulates: An overview. Catalysis 169, 249–257.

Martin-Sanchez, P.M., Bastian, F., Alabouvette, C., Saiz-Jimenez, C., 2013. Real-time PCR detection of Ochroconis lascauxensis involved in the formation of black stains in the Lascaux Cave, France. Sci. Total Environ. 443, 478–84.

Martin-Sanchez, P.M., Nováková, A., Bastian, F., Alabouvette, C., Saiz-Jimenez, C., 2012. Two new species of the genus Ochroconis, O. lascauxensis and O. anomala isolated from black stains in Lascaux Cave, France. Fungal Biol. 116, 574–89.

Marzorati, M., Wittebolle, L., Boon, N., Daffonchio, D., Verstraete, W., 2008. How to get more out of molecular fingerprints: practical tools for microbial ecology. Environ. Microbiol. 10, 1571–1581.

Maver, K., Stangar, U.L., Cernigoj, U., Gross, S., Cerc Korosec, R., 2009. Low-temperature synthesis and characterization of $TiO_2$ and $TiO_2$-$ZrO_2$ photocatalytically active thin films. Photochem. Photobiol. Sci. 8, 657–662.

Mazzotti, V., 2003. Progetto di conservazione preventiva di beni culturali in ceramica esposti all´aperto nel centro storico di Faenza. Alma Mater Studiorum Universitá di Bologna.

McNamara, C., Mitchell, R., 2005. Microbial deterioration of historic stone. Front Ecol Env. 3, 445–451.

Medina-Valtierra, J., Frausto-Reyes, C., Ramirez-Ortiz, J., Camarillo-Martínez, G., 2009. Self-cleaning test of doped TiO2-coated glass plates under solar exposure. Ind. Eng. Chem. Res. 48, 598–606.

Miller, A.Z., Laiz, L., Dionísio, A., Macedo, M.F., Saiz-Jimenez, C., 2009. Growth of phototrophic biofilms from limestone monuments under laboratory conditions. Int. Biodeterior. Biodegradation 63, 860–867.

Miller, A.Z., Rogerio-Candelera, M.A., Laiz, L., Wierzchos, J., Ascaso, C., Sequeira Braga, M.A., Hernández-Mariné, M., Maurício, A., Dionísio, A., Macedo, M.F., Saiz-Jimenez, C., 2010.

Laboratory-induced endolithic growth in calcarenites: biodeteriorating potential assessment. Microb. Ecol. 60, 55–68.

Miller, A.Z., Rogerio-Candelera, M.A., Dionísio, A., Macedo, M.F., Saiz-Jimenez, C., 2011. Microalgae as biodeteriogens of stone cultural heritage: qualitative and quantitative research by non-contact techniques. In: Johanssen, M.N. (Ed.), Microalgae: Biotechnology, Microbiology and Energy. Nova Science Publishers, New York, pp. 345-358.

Miller, A.Z., Sanmartín, P., Pereira-Pardo, L., Dionísio, A., Saiz-Jimenez, C., Macedo, M.F.F., Prieto, B., 2012. Bioreceptivity of building stones: A review. Sci. Total Environ. 426, 1–12.

Miller, M., Palojärvi, A., Rangger, A., Reeslev, M., Kjøller, A., Paloja, A., 1998. The Use of Fluorogenic Substrates To Measure Fungal Presence and Activity in Soil The Use of Fluorogenic Substrates To Measure Fungal Presence and Activity in Soil 64.

Mills, A., Hunte, S. Le, 2000. An overview of semiconductor photocatalysis 108, 1–35.

Mimoso, J.M., Silva, A.S., Costa, D.R., Gonçalves, T.D., Coentro, S.X., 2011. Decay of historic azulejos in Portugal : an assessment of research needs. LNEC, Lisbon.

Morton, L.H.G., Greenway, D.L.A., Gaylarde, C.C., Surman, S.B., 1998. Consideration of some implications of the resistance of biofilms to biocides. Int. Biodeterior. Biodegradation 41, 247–259.

Motti, R., Stinca, A., 2011. Analysis of the biodeteriogenic vascular flora at the Royal Palace of Portici in southern Italy. Int. Biodeterior. Biodegradation 65, 1256–1265.

Murugan, K., Subasri, R., Rao, T.N., Gandhi, A.S., Murty, B.S., 2013. Synthesis, characterization and demonstration of self-cleaning TiO2 coatings on glass and glazed ceramic tiles. Prog. Org. Coatings 76, 1756–1760.

Muyzer, G., de Waal, E.C., Uitterlinden, a G., 1993. Profiling of complex microbial populations by denaturing gradient gel electrophoresis analysis of polymerase chain reaction-amplified genes coding for 16S rRNA. Appl. Environ. Microbiol. 59, 695–700.

Nimis, P.L., 1993. The lichens of Italy: an annotated catalogue, Museo Regi. ed. Museu Ragiomale di Scienze Naturali, Torino.

Nimis, P.L., Monte, M., Tretiach, M., 1987. Flora e Vegetazione lichenica di aree archeologiche del Lazio. Stud. Geobot. 7, 153–161.

Nowicka-Krawczyk, P., Żelazna-Wieczorek, J., Otlewska, A., Koziróg, A., Rajkowska, K., Piotrowska, M., Gutarowska, B., Żydzik-Białek, A., 2014. Diversity of an aerial phototrophic coating of historic buildings in the former Auschwitz II-Birkenau concentration camp. Sci. Total Environ. 493, 116–23.

Nübel,U.,Garcia-Pichel, F.,Muyzer, G.,1997.PCRprimers toamplify62316S rRNAgenes from cyanobacteria. Applied and Environ. Microbiol. 63, 3327-3332

Nugari, M.P., Pietrini, A.M., Caneva, G., Imperi, F., Visca, P., 2009. Biodeterioration of mural paintings in a rocky habitat: The Crypt of the Original Sin (Matera, Italy). Int. Biodeterior. Biodegradation 63, 705–711.

Oakley, V.L., Jain, K.K., 2002. Essentials in the Care and Conservation of Historical Ceramic Objects. Archetype Publications.

Oliveira, M.M., Sanjad, T.B.C., Bastos, C.J.P., 2001. Biological degradation of glazed ceramic tiles 337–342.

Ordonez, S., Fort, R., Garcia del Cura, M.A., 1997. Pore size distribution and the durability of a porous limestone. Q. J. Eng. Geol. Hydrogeol. 30, 221–230.

Ortega-Calvo, J.J., Ariño, X., Hernandez-Marine, M., Saiz-Jimenez, C., 1995. Factors affecting the weathering and colonization of monuments by phototrophic microorganisms. Sci. Total Environ. 167, 329–341.

Ortega-Calvo, J.J., Hernandez-Marine, M., Saiz-Jimenez, C., 1991. Biodeterioration of building materials by cyanobacteria and algae. Int. Biodeterior. 28, 165–185.

Ortega-Calvo, J.J., Sanchez-Castillo, P.M., Saiz-Jimenez, C., Hernandez-Marine, M., 1993. Isolation and characterization of epilithic chlorophytes and cyanobacteria from two spanish cathedrals (Salamanca and Toledo). Nov. Hedwigia 57, 239–253.

Otlewska, A., Adamiak, J., Gutarowska, B., 2014a. Application of molecular techniques for the assessment of microorganism diversity on cultural heritage objects. Acta Biochim. Pol. 61, 217–225.

Otlewska, A., Adamiak, J., Gutarowska, B., 2014b. Clone-based comparative sequence analysis of 16S rRNA genes retrieved from biodeteriorating brick buildings of the former Auschwitz II-Birkenau concentration and extermination camp. Syst. Appl. Microbiol. (*In Press*)

Ottosen, L.M., Dias-Ferreira, C., Ribeiro, A.B., 2014. Electrochemical desalination of historic Portuguese tiles–Removal of chlorides, nitrates and sulfates. J. Cult. Herit. (*In Press*)

Palmer, J.R., Hirsch, P., 1991. Photosynthesis-• based microbial communities on two churches in northern Germany: Weathering of granite and glazed brick. Geomicrobiol. J. 37–41.

Papida, S., Murphy, W., May, E., 2000. Enhancement of physical weathering of building stones by microbial populations. Int. Biodeterior. Biodegradation 46, 305–317.

Patrick, R., 1977. Ecology of freshwater diatoms and diatom communities, in: Werner, D. (Ed.), The Biology of Diatoms. Blackwell Scientific Publications, Oxford, pp. 284–332.

Pattanaik, B., Adhikary, S.P., 2002. Blue-green algal flora at some archaeological sites and monuments of India. Feddes Repert. 113, 289–300.

Pedi, N., Conceição, E., Fernandes, M.J., Massa, D., Nogeira, E., Ribeiro, P., Arcoverde, J.H., Lemos, S., Marsden, A., Neves, R., 2009. Fungos isolados em azulejos do convento de Santo António, Recife, Pernambuco. IX Jorn. Ensino, Pesqui. e Extensão. [WWW Document]. URL http://www.eventosufrpe.com.br/jepex2009/cd/resumos/R0550-1.pdf

Pepe, O., Sannino, L., Palomba, S., Anastasio, M., Blaiotta, G., Villani, F., Moschetti, G., 2010. Heterotrophic microorganisms in deteriorated medieval wall paintings in southern Italian churches. Microbiol. Res. 165, 21–32.

Pereira, M., de Lacerda-Arôso, T., Gomes, M.J.M., Mata, a., Alves, L.C., Colomban, P., 2009. Ancient Portuguese Ceramic Wall Tiles ("Azulejos"): Characterization of the Glaze and Ceramic Pigments. J. Nano Res. 8, 79–88.

Pereira, S., Mimoso, J.M., Santos Silva, A., 2011. Physical-chemical characterization of historic portuguese tiles. LNEC, Lisbon.

Pereira, S.R.M., Esteves, L., Mendes, M.T., Musacchi, J., Rodrigues, J.D., Mimoso, J.M., 2012. Degradation forms of historical Portuguese tiles under accelerated salt ageing, in: Azulejar, 10-12 October., Aveiro.

Pereira, S.R.M., Mimoso, J.M., 2012. Salt Degradation of Historic Portuguese Azulejos, in: Azulejar 2012. Aveiro, pp. 1–10.

References

Pérez-Rodríguez, J.L., Maqueda, C., Jiménez de Haro, M.C., Rodriguez-Rubio, P., 1998. Effect of pollution on polychromed ceramic statues. Atmos. Environ. 32, 993–998.

Pharo, E.J., Zartman, C.E., 2007. Bryophytes in a changing landscape: The hierarchical effects of habitat fragmentation on ecological and evolutionary processes. Biol. Conserv. 135, 315–325.

Piñar, G., Piombino-Mascali, D., Maixner, F., Zink, A., Sterflinger, K., 2013. Microbial survey of the mummies from the Capuchin Catacombs of Palermo, Italy: biodeterioration risk and contamination of the indoor air. FEMS Microbiol. Ecol. 86, 341–56.

Piñar, G., Ripka, K., Weber, J., Sterflinger, K., 2009. The micro-biota of a sub-surface monument the medieval chapel of St. Virgil (Vienna, Austria). Int. Biodeterior. Biodegradation 63, 851–859.

Pinho, L., Mosquera, M.J., 2011. Titania-Silica Nanocomposite Photocatalysts with Application in Stone Self-Cleaning. J. Phys. Chem. C 115, 22851–22862.

Pinna, D., 2002. Le indagini biologiche per il restauro dei materiali ceramici Diagnostica per il restauro e la conzervazione dei materiali ceramici, in: Corso Di Aggiornamento. Museo Internazionale della Ceramiche, Faenza.

Pinna, D., Salvadori, O., 2008. Processes of biodeterioration general mechanisms, in: Caneva, G., Nugari, M.P., Salvadori, O. (Eds.), Plant Biology for Cultural Heritage. Biodeterioration and Conservation. The getty conservation institute, Los Angeles, pp. 15–34.

Pitzurra, L., Moroni, B., Iurlo, A., Di Cesare, A.M., Sbaraglia, G., Poli, G., Bistoni, F., 2001. Microbial growth and air pollution in carbonate rock weathering. Preliminary results of a in situ experimental study. Ann. Chim. 91, 785–93.

Planchon, M., Jittawuttipoka, T., Cassier-Chauvat, C., Guyot, F., Gelabert, A., Benedetti, M.F., Chauvat, F., Spalla, O., 2013. Exopolysaccharides protect Synechocystis against the deleterious effects of titanium dioxide nanoparticles in natural and artificial waters. J. Colloid Interface Sci. 405, 35–43.

Portillo, M.C., Gazulla, M.F., Sanchez, E., Gonzalez, J.M., 2011. A procedure to evaluate the resistance to biological colonization as a characteristic for product quality of ceramic roofing tiles. J. Eur. Ceram. Soc. 31, 351–359.

Portillo, M.C., Gonzalez, J.M., Saiz-Jimenez, C., 2008. Metabolically active microbial communities of yellow and grey colonizations on the walls of Altamira Cave, Spain. J. Appl. Microbiol. 104, 681–91.

Prakash, B., Veeregowda, B., Krishnappa, G., 2003. Biofilms: a survival strategy of bacteria. Curr. Sci. 85, 1299–1307.

Prieto, B., Rivas, T., Silva, B., 2002. Rapid Quantification of Phototrophic Microorganisms and their Physiological State through their Color. Biofouling 18, 237–245.

Prudêncio, M.I., Pereira, M.A.S., Marques, J.G., Dias, M.I., Esteves, L., Burbidge, C.I., Trindade, M.J., Albuquerque, M.B., 2012. Neutron tomography for the assessment of consolidant impregnation ef fi ciency in Portuguese glazed tiles (16th and 18th centuries). J. Archaeol. Sci. 39, 964–969.

Qi-Wang, Ma, G.-Y., He, L.-Y., Sheng, X.-F., 2011. Characterization of bacterial community inhabiting the surfaces of weathered bricks of Nanjing Ming city walls. Sci. Total Environ. 409, 756–62.

Quaedvlieg, W., Binder, M., Groenewald, J.Z., Summerell, B. a, Carnegie, a J., 2014. Introducing the Consolidated Species Concept to resolve species in the Teratosphaeriaceae. Persoonia 33, 1–40.

# References

Quagliarini, E., Bondioli, F., Goffredo, G.B., Licciulli, A., Munafò, P., 2012. Smart surfaces for architectural heritage: Preliminary results about the application of TiO2-based coatings on travertine. J. Cult. Herit. 13, 204–209.

Radeka, M., Bačkalić, Z., Vrebalov, M., 2008. The effect of firing temperature of clay roofing tiles on the mechanisms of frost action. Ind. Ceram. 20, 97–104.

Radeka, M., Kiurski, J., Markov, S., Marinković-Nedučin, R., Ranogajec, J., 2007a. Microbial deterioration of clay roofing tiles, in: Brebbia, C.A. (Ed.), Structural Studies, Repairs and Maintenance of Heritage Architecture XMaintenance of Heritage Architecture X, WIT Transactions on The Built Environment, Vol 95. WIT Press, Southampton, UK, pp. 567–575.

Radeka, M., Markov, S., Lončar, E., Rudić, O., Vučetić, S., Ranogajec, J., 2014. Photocatalytic effects of TiO2 mesoporous coating immobilized on clay roofing tiles. J. Eur. Ceram. Soc. 34, 127–136.

Radeka, M., Ranogajec, J., Kiurski, J., Markov, S., Marinković-Nedučin, R., 2007b. Influence of lichen biocorrosion on the quality of ceramic roofing tiles. J. Eur. Ceram. Soc. 27, 1763–1766.

Raimondi, V., Cecchi, G., Lognoli, D., Palombi, L., Grönlund, R., Johansson, a., Svanberg, S., Barup, K., Hällström, J., 2009. The fluorescence lidar technique for the remote sensing of photoautotrophic biodeteriogens in the outdoor cultural heritage: A decade of in situ experiments. Int. Biodeterior. Biodegradation 63, 823–835.

Raimondo, M., Ceroni, C., Dondi, M., Guarini, G., Marsigli, M., Venturi, I., Zanelli, C., 2009. Durability of clay roofing tiles: the influence of microstructural and compositional variables. J. Eur. Ceram. Soc. 29, 3121–3128.

Rajagopal, G., Maruthamuthu, S., Mohanan, S., Palaniswamy, N., 2006. Biocidal effects of photocatalytic semiconductor TiO2. Colloids Surf. B. Biointerfaces 51, 107–11.

Rajkowska, K., Otlewska, A., Koziróg, A., Piotrowska, M., Nowicka-Krawczyk, P., Hachułka, M., Wolski, G.J., Kunicka-Styczyńska, A., Gutarowska, B., Zydzik-Białek, A., 2014. Assessment of biological colonization of historic buildings in the former Auschwitz II-Birkenau concentration camp. Ann. Microbiol. 64, 799–808.

Ramana, C. V, Parag, B., Girija, K.R., Ram, B.R., Ramana, V.V., Sasikala, C., 2013. Rhizobium subbaraonis sp. nov., an endolithic bacterium isolated from beach sand. Int. J. Syst. Evol. Microbiol. 63, 581–5.

Ranogajec, J., Markov, S., Kiurski, J., Radeka, M., Ducman, V., 2008. Microbial Deterioration of Clay Roofing Tiles as a Function of the Firing Temperature. J. Am. Ceram. Soc. 91, 3762–3767.

Ranogajec, J., Radosavljević, S., Marinković-Nedućin, R., Živanović, B., 1997. Chemical corrosion phenomena of roofing tiles. Ceram. Int. 23, 99–103.

Ranogajec, J.G., Kiurski, J.S., Ujhelji, A.L., Radeka, M.M., Bokorov, M.T., Balint, J., Borbelj-Mesaros, A., 2005. Biochemical corrosion of ceramic roofing tiles by lichen actions. Interceram 54, 340–343.

Rastogi, G., Sani, R.K., 2011. Molecular techniques to assess microbial community structure, function, and dynamics in the environment. In: Ahmad, I., Ahmad, F., Pichtel, J. (Eds.), Microbes and Microbial Technology: Agricultural and Environ- mental Applications. Springer ScienceþBusiness Media, New York, pp. 29-57.

Ravaglioli, A., Krajewski, A., 1989. Chimica fisica tecnica e scienza dei materiali antichi ceramici e vetrosi. Museo Internazionale delle Ceramiche, Faenza.

Rede Temática em Estudos de Azulejaria e Cerâmica João Miguel dos Santos Simões (RTEACJMSS), n.d. Cronologia do azulejo português [WWW Document]. URL http://redeazulejo.fl.ul.pt/timeline/timeline-pt.html (accessed 3.28.15).

Rhodes, D., Hopper, R., 2000. Clay and Glazes for the Potter. Krause Publications.

Ricci, S., Pietrini, A.M., 1994. Caratterizzazione della microflora algale presente sulla Fontana dei Quattro Fiumi, Roma. In: Fassina, V., Ott, H., Zezza, F. (Eds.), Proceedings of the 3rd International Symposium on the Conservation of Monuments in the Mediterranean Basin. Soprintendenza ai Beni Artistici e Storici di Venezia, Venice, pp. 353-357.

Rindi, F., Guiry, M., 2002. The marine and terrestrial Prasiolales (Chlorophyta) of Galway City, Ireland: a morphological and ecological study. J. Phycol. 482, 469–482.

Rindi, F., Guiry, M., 2002. The genus Phycopeltis (Trentepohliaceae, Chlorophyta) in Ireland: a taxonomic and distributional reassessment. Phycologia 41, 421–431.

Rindi, F., Menéndez, J.L., Guiry, M.D., Rico, J.M., Menendez, J.L., Guiry, M.D., Rico, J.M., 2004. The taxonomy and distribution of Phycopeltis (Trentepohliaceae, Chlorophyta) in Europe. Cryptogam. Algol. 25, 3–17.

Rodrigues, A., Gutierrez-Patricio, S., Miller, A.Z., Saiz-Jimenez, C., Wiley, R., Nunes, D., Vilarigues, M., Macedo, M.F., 2014. Fungal biodeterioration of stained-glass windows. Int. Biodeterior. Biodegradation 90, 152–160.

Roeselers, G., Zippel, B., Staal, M., van Loosdrecht, M., Muyzer, G., 2006. On the reproducibility of microcosm experiments - different community composition in parallel phototrophic biofilm microcosms. FEMS Microbiol. Ecol. 58, 169–78.

Rogerio-Candelera, M.A., Jurado, V., Laiz, L., Saiz-Jimenez, C., 2011. Laboratory and in situ assays of digital image analysis based protocols for biodeteriorated rock and mural paintings recording. J. Archaeol. Sci. 38, 2571–2578.

Roldán, M., Thomas, F., Castel, S., Quesada, A., Hernández-Mariné, M., 2004. Non invasive pigment identification in living phototrophic biofilms by confocal imaging spectrophotometry. Applied and Environl. Microbiol. 70, 3745-3750.

Rolleke, S., 1999. Methods Analysis of bacterial communities on historical glass by denaturing gradient gel electrophoresis of PCR-amplified gene fragments coding for 16S rRNA 36, 107–114.

Rosa e Silva, L.K., Staats, C.C., Goulart, L.S., Morello, L.G., Pelegrinelli Fungaro, M.H., Schrank, A., Vainstein, M.H., 2008. Identification of novel temperature-regulated genes in the human pathogen Cryptococcus neoformans using representational difference analysis. Res. Microbiol. 159, 221–9.

Rosado, T., Gil, M., Mirão, J., Candeias, A., Caldeira, A.T., 2013. Oxalate biofilm formation in mural paintings due to microorganisms – A comprehensive study. Int. Biodeterior. Biodegradation 85, 1–7.

Rossi, F., Micheletti, E., Bruno, L., Adhikary, S.P., Albertano, P., Philippis, R. De, 2012. Characteristics and role of the exocellular polysaccharides produced by five cyanobacteria isolated from phototrophic biofilms growing on stone monuments. Biofouling 28, 215–24.

Ruibal, C., Platas, G., Bills, G.F., 2008. High diversity and morphological convergence among melanised fungi from rock formations in the Central Mountain System of Spain. Persoonia 21, 93–110.

References

Russel, A.D., 1999. Factors influencing the afficacy of antimicrobial agents, in: Russel, A.D., Hugo, W.B., Ayliffe, G.A.J. (Eds.), Princcipples and Practice of Disinfection, Preservation and Sterilization. Blackwell Science, Oxford, pp. 95–123.

Russel, A.D., Chopra, I., 1990. Undesrtanding antibacterial action and resistance. J. Med. Microbiol. 33, 421–423.

Sá, L., 2014. "Projecto SOS Azulejo": Da Prevenção Crimical à Salvaguarda Global do Patrimonio do Azulejo de Lisboa, in: Susana, V.F. (Ed.), A Herança de Santos Simões Novas Perspectivas Para O Estudo Da Azulejaria E Da Cerâmica. Colibri, Lisboa, pp. 57–70.

Sabo, R., Falcato, J., 1998. Portuguese decorative tiles: Azulejos. Abbeville Press, New York.

Saiz-Jimenez, C., 1995. Deposition of anthropogenic compounds on monuments and their effect on airborne microorganisms. Aerobiologia (Bologna). 11, 161–175.

Saiz-Jiménez, C., Laiz, L., 2000. Occurrence of halotolerant/halophilic bacterial communities in deteriorated monuments. Int. Biodeterior. Biodegradation 46, 319–326.

Saiz-Jimenez, C., Miller, A.Z., Martin-Sanchez, P.M., Hernandez-Marine, M., 2012. Uncovering the origin of the black stains in Lascaux Cave in France. Environ. Microbiol. 14, 3220–31.

Salvadori, O., Charola, E.A., 2011. Methods to prevent biocolonization and recolonization: An overview of current research for archietctural and archeological heritage, in: Charola, E.A., McNamara, C.J., Koestler, R. (Eds.), Biological Colonization of Stone Control and Prevention Methods. Smithsoneam Institution Scholarly Press, Washington, pp. 37–50.

Samad, L., Adhikary, S., 2008. Diversity of micro-algae and cyanobacteria on building facades and monuments in India. Algae 23, 91–114.

Sánchez de Rojas, M.I., Marín, F.P., Frías, M., Valenzuela, E., Rodríguez, O., 2011. Influence of freezing test methods, composition and microstructure on frost durability assessment of clay roofing tiles. Constr. Build. Mater. 25, 2888–2897.

Sand, W., 1997. Microbial Mechanisms of Deterioration of Inorganic Substrates_A general Mechanistic Overview. Int. Biodeterior. Biodegrad. 40, 183–190.

Sand, W., Jozsa, P., Mansch, R., 2002. Weathering, Microbiol, in: Encyclopedia of Environmental Microbiology. John Wiley & Sons, Inc., pp. 3364 – 3375.

Sanmartín, P., Aira, N., Devesa-Rey, R., Silva, B., Prieto, B., 2010. Relationship between color and pigment production in two stone biofilm-forming cyanobacteria (Nostoc sp. PCC 9104 and Nostoc sp. PCC 9025). Biofouling 26, 499–509.

Santos, P.M.D., Júlio, E.N.B.S., 2013. A state-of-the-art review on roughness quantification methods for concrete surfaces. Constr. Build. Mater. 38, 912–923.

Santos, T.P., Fátima Vaz, M., Pinto, M.L., Carvalho, A.P., 2012. Porosity characterization of old Portuguese ceramic tiles. Constr. Build. Mater. 28, 104–110.

Saporiti, T., 1992. Azulejos de Lisboa no século XX. Edições Afrontamento, OPorto.

Saxena, S., Upreti, D.K., Singh, A., Singh, K.P., 2004. Observations on Lichens Growing on Artifacts in the Indian Subcontinent, in: St.Clair, L.L., Seaward, M.R.D. (Eds.), Biodeterioration of Stone Surfaces. Springer Netherlands, Dordrecht, pp. 181–193.

Sayer, J. a, Cotter-Howells, J.D., Watson, C., Hillier, S., Gadd, G.M., 1999. Lead mineral transformation by fungi. Curr. Biol. 9, 691–4.

References

Sayer, J.A., Raggett, S.L., Gadd, G.M., 1995. Solubilization of insoluble metal compounds by soil fungi: development of a screening method for solubilizing ability and metal tolerance. Mycol. Res. 99, 987–993.

Scardino, A.J., Guenther, J., de Nys, R., 2008. Attachment point theory revisited: the fouling response to a microtextured matrix. Biofouling 24, 45–53.

Schabereiter-Gurtner, C., Piñar, G., Lubitz, W., Rölleke, S., 2001. Analysis of fungal communities on historical church window glass by denaturing gradient gel electrophoresis and phylogenetic 18S rDNA sequence analysis. J. Microbiol. Methods 47, 345–54.

Schabereiter-Gurtner, C., Piñar, G., Lubitz, W., Rölleke, S., 2001. An advanced molecular strategy to identify bacterial communities on art objects. J. Microbiol. Methods 45, 77–87.

Schloss, P.D., Handelsman, J., 2005. Introducing species richness DOTUR, a computer program for defining operational taxonomic units and estimating. Appl. Environ. Microbiol. 71, 1501–1506.

Seifert, K.A., Ickerson, N.L., Corlett, M., Jackson, E.D., Louis-Seize, G., 2004. Devriesia, a new hyphomycete genus to accommodate heat-resistant, cladosporium-like fungi. Can. J. Bot. 82, 914–926.

Sekiya, T., Ohta, S., Kamei, S., Hanakawa, M., Kurita, S., 2001. Raman spectroscopy and phase transition of anatase TiO2 under high pressure. J. Phys. Chemisrty Solids 62, 717–721.

Sert, H.B., Sümbül, H., Sterflinger, K., 2007b. A new species of Capnobotryella from monument surfaces. Mycol. Res. 3, 1235-1241.

Sert, H.B., Sümbül, H., Sterflinger, K., 2010. Two new species of Capnobotryella from historical monuments. Mycol. Prog. 10, 333–339.

Sert, H.B., Sümbül, H., Sterflinger, K., 2007a. Microcolonial fungi from antique marbles in Perge/Side/Termessos (Antalya/Turkey). Antonie Van Leeuwenhoek 91, 217–27.

Sezgin, M., Sankur, B., 2004. Survey over image thresholding techniques and quantitative performance evaluation. J. Electron. Imaging 13, 146–165.

Shirakawa, M.A., Tavares, R.G., Gaylarde, C.C., Taqueda, M.E.S., Loh, K., John, V.M., 2010. Climate as the most important factor determining anti-fungal biocide performance in paint films. Sci. Total Environ. 408, 5878–86.

Shirakawa, M.A., Werle, A.P., Gaylarde, C.C., Loh, K., John, V.M., 2014. Fungal and phototroph growth on fiber cement roofs and its influence on solar reflectance in a tropical climate. Int. Biodeterior. Biodegradation.

Shoaf,W.T., Lium, B.W., 1976. Improved extraction of chlorophyll a and b from algae using dimethyl sulfoxide. Limnol. Oceanogr. 21, 926-928.

Silva, T., Cabo Verde, S., Burbidge, C., Fernandes, A., Botelho, M., Dias, M., Burbison, C., Fernandes, A., Botelho, M., Dias, M., 2011. Perfis de contaminação e inactivação microbiana em azulejos, in: IX Congresso Ibérico de Arqueometria (CIA). Fundação Caloust Gulbenkian, Lisbon.

Silva, T.P., Figueiredo, M.-O., Prudêncio, M., 2013. Ascertaining the degradation state of ceramic tiles: A preliminary non-destructive step in view of conservation treatments. Appl. Clay Sci. 82, 101–105.

Silva, T.P., Figueiredo, Maria Ondina, Barreiros, M.A., Prudêncio, M.I., 2014. Diagnosis of pathologies in ancient (seventeenth-eighteenth centuries) decorative blue-and-white ceramic

tiles: Green stains in the glazes of a panel depicting Lisbon prior to the 1755 earthquake. Stud. Conserv. 59, 63–68.

Silvestre, J.D., de Brito, J., 2011. Ceramic tiling in building façades: Inspection and pathological characterization using an expert system. Constr. Build. Mater. 25, 1560–1571.

Silvestre, J.D., de Brito, J., 2009. Ceramic tiling inspection system. Constr. Build. Mater. 23, 653–668.

Šimonovičová, A., Gódyová, M., Ševc, J., 2004. Airborne and soil microfungi as contaminants of stone in a hypogean cemetery. Int. Biodeterior. Biodegradation 54, 7–11.

Smith, C., Aptroot, A., Coppins, B., Fletcher, A., Gilbert, O., James, P. (Eds.), 1992. The Lichens of Great Britain and Ireland. British Lichen Society.

Smith, G.D., Clark, R.J.., 2004. Raman microscopy in archaeological science. J. Archaeol. Sci. 31, 1137–1160.

Souffreau, C., Vanormelingen, P., Verleyen, E., Sabbe, K., Vyverman, W., 2010. Tolerance of benthic diatoms from temperate aquatic and terrestrial habitats to experimental desiccation and temperature stress. Phycol 49, 309–324.

Speranza, M., Sanz, M., Oujja, M., de los Rios, A., Wierzchos, J., Pérez-Ortega, S., Castillejo, M., Ascaso, C., 2013. Nd-YAG laser irradiation damages to Verrucaria nigrescens. Int. Biodeterior. Biodegradation 84, 281–290.

Speranza, M., Wierzchos, J., De Los Rios, A., Perez-Ortega, S., Souza-Egipsy, V., Ascaso, C., 2012. Towards a more realistic picture of in situ biocide actions: combining physiological and microscopy techniques. Sci. Total Environ. 439, 114–22.

Sterflinger, K., 2010. Fungi: their role in deterioration of cultural heritage. Fungal Biol. Rev. 24, 47–55.

Sterflinger, K., Piñar, G., 2013. Microbial deterioration of cultural heritage and works of art-tilting at windmills? Appl. Microbiol. Biotechnol. 97, 9637–46.

Stewart, P.S., 2002. Mechanisms of antibiotic resistance in bacterial biofilms. Int. J. Med. Microbiol. 292, 107–113.

Stupar, M., Grbić, M.L., Džamić, A., Unković, N., Ristić, M., Jelikić, A., Vukojević, J., 2014. Antifungal activity of selected essential oils and biocide benzalkonium chloride against the fungi isolated from cultural heritage objects. South African J. Bot. 93, 118–124.

Suberkropp, K., Gessner, M.O., Chauvet, E., 1993. Comparison of ATP and ergosterol as indicators of fungal biomass associated with decomposing leaves in streams. Appl. Environ. Microbiol. 59, 3367–3372.

Suihko, M.L., Alakomi, H.-L., Gorbushina, A., Fortune, I., Marquardt, J., Saarela, M., 2007. Characterization of aerobic bacterial and fungal microbiota on surfaces of historic Scottish monuments. Syst. Appl. Microbiol. 30, 494–508.

Suresh Kumar, K., Dahms, H.-U., Lee, J.-S., Kim, H.C., Lee, W.C., Shin, K.-H., 2014. Algal photosynthetic responses to toxic metals and herbicides assessed by chlorophyll a fluorescence. Ecotoxicol. Environ. Saf. 104C, 51–71.

Sylvestre, M., Urzl, C., Videla, H.A., Herrera, L.K., 2009. Understanding microbial inhibition of corrosion. A comprehensive overview. Int. Biodeterior. Biodegradation 63, 896–900.

Takeda, S., Suzuki, S., Odaka, H., Hosono, H., 2001. Photocatalytic TiO 2 thin film deposited onto glass by DC magnetron sputtering 338–344.

References

Tennent, N.H., 2013. The treatment of blackned archeological Delftware from Anaerobic Sites., in: Roemich, H., van Lookeren Campagne, K. (Eds.), Recent Advances in Glass, Stained-Glass and Cearamics Conservation: Preprints of the Interim Meeting of the ICOM-CC Woriking Group Glass and Ceramics and Forum of the International Scientific Commitee for the Conservation of Stained-Glass (Corpus Vitrearum). SPA Uitgevers, Zwolle, pp. 351–353.

Tennent, N.H., Baird, T., Gibson, L.T., 1996. The technical examination and conservation of blackened Delftware from anaerobic sites. Stud. Conserv. 41, 182–187.

Tiano, P., Accolla, P., Tomaselli, L., 1995. Phototrophic biodeteriogens on lithoid surfaces: an ecological study. Microb. Ecol. 29, 299–309.

Tilley, R.J.D., 2010. Color and The Optical Properties of Materials. John Wiley & Sons, New Jersey.

Tite, M., Freestone, I., Mason, R., Molera, J., Vendrell-Saz, M., Wood, N., 1998. Lead glazes in antiquity - Methods of Production and reasons for use. Archeometry 40, 241–260.

Tite, M., Watson, O., Pradell, T., Matin, M., Molina, G., Domoney, K., Bouquillon, A., 2015. Revisiting the beginnings of tin-opacified Islamic glazes. J. Archaeol. Sci. 57, 80–91.

Tite, M.S., 2009. The production technology of Italian maiolica: a reassessment. J. Archaeol. Sci. 36, 2065–2080.

Titze, A., de Hoog, G.S., 1990. Capnobotryella renispora on roof tiles. Antonie van Leeuwenhoek 58, 265-269.

Tomaselli, L., Lamenti, G., Bosco, M., Tiano, P., 2000. Biodiversity of photosynthetic micro-organisms dwelling on stone monuments. Int. Biodeterior. Biodegradation 46, 251–258.

Tourney, J., Ngwenya, B.T., 2014. The role of bacterial extracellular polymeric substances in geomicrobiology. Chem. Geol. 386, 115–132.

Trindade, M.J., Dias, M.I., Coroado, J., Rocha, F., 2009. Mineralogical transformations of calcareous rich clays with firing: A comparative study between calcite and dolomite rich clays from Algarve, Portugal. Appl. Clay Sci. 42, 345–355.

Uher, B; Aboal, M; Kovacik, L., 2005. Epilithic and chasmoendlithic phycoplora of monuments and buildings in South-Eastern Spain. Cryptogame 26, 275–358.

Uroz, S., Calvaruso, C., Turpault, M.-P., Frey-Klett, P., 2009. Mineral weathering by bacteria: ecology, actors and mechanisms. Trends Microbiol. 17, 378–87.

Urzì, C., Realini, M., 1998. Color changes of Notos calcareous sandstone as related to its colonization by microorganisms. Int. Biodeterior. Biodegradation 42, 45–54.

Vaz, M.F., Pires, J., Carvalho, A.P., 2008. Effect of the impregnation treatment with Paraloid B-72 on the properties of old Portuguese ceramic tiles 9, 269–276.

Velosa, A.L., Veiga, R., Martins, G., 2001. Water Behaviour of Old and New Tiles – A Contribution Towards the Conservation of Ceramic Façades, in: Freitas, V.P., Corvacho, M.H., Lacasse, M. (Eds.), XII DBMC - International Conference on Durability of Building Materials and Components. April 12th-15th Porto, pp. 1–7.

Vendrell-Saz, M., 2003. Ceramica aplicada en la arquitectura, in: Balderrama, A., Vidal, A.A., Cardiel, I.B. (Eds.), El Estudio Y La Conservación de La Cerámica Decorada En Arquitectura. ICCROM, Rome, pp. 10–14.

Ventolà, L., Cordoba, A., Vendrell-Saz, M., Giraldez, P., Vilardell, R., Saline, M., 2014. Decorated ceramic tiles used in Catalan Modernist Architecture (c.1870 to c.1925): Composition, decay and conservation. Constr. Build. Mater. 51, 249–257.

Videla, H.A., 2002. La Catedral de la Plata. Obras de conservación, puesta en valor y completamiento. Biodeterioro: su prevención, in: Videla, H.A., Herrera, L.K. (Eds.), Prevencion on Y Proteccion on Proteccion on Del Patrimonio Prevencion on Cultural Iberoamericano de Los Efectos Del Biodeterioro Ambiental,. Medellen, Colombia, pp. 111–123.

Vieira Ferreira, L.F., Casimiro, T.M., Colomban, P., 2013. Portuguese tin-glazed earthenware from the 17th century. Part 1: Pigments and glazes characterization. Spectrochim. Acta. A. Mol. Biomol. Spectrosc. 104, 437–44.

Ward, D.M., Weller, R., Bateson, M.M., 1990. 16S rRNA sequences reveal numerous uncultured microorganisms in a natural community. Nature 345, 63–5.

Warren, J., 1999. Conservation of Brick. Butterworth Heinemann.

Warscheid, T., 2000. Integrated concepts for the protection of cultural artifacts against biodeterioration, in: Ciferri, O., Tiano, P., Mastromei, G. (Eds.), Of Microbes and Art. Springer US, Boston, MA, pp. 185–201.

Warscheid, T., Braams, J., 2000. Biodeterioration of stone: a review. Int. Biodeterior. Biodegradation 46, 343–368.

Watanabe, K., Ohfuji, H., Ando, J., Kitagawa, R., 2006. Elemental behaviour during the process of corrosion of sekishu glazed roof-tiles affected by <I>Lecidea</I> s.lat. sp. (crustose lichen). Clay Miner. 41, 819–826.

Watanabe, K., Ohfuji, H., Kitagawa, R., Matsui, Y., 2009. Nanoscale pseudobrookite layer in the surface glaze of a Japanese <I>sekishu</I> roof tile. Clay Miner. 44, 177–180.

White, T.J., Bruns, T., Lee, S., Taylor, J., 1990. Amplification and direct sequencing of fungi ribosomal RNA genes for phylogenetics, in: Innis, M.A., Gelfand, D.H., Sninsky, J.J., White, T.J. (Eds.), PCR Protocols. A Guide to Methods and Applications. Academic Press, San Diego, pp. 315–322.

White, W.B., 1992. Theory of Corrosion of Glass and Ceramics, Corrosion of Glass, Ceramics and Ceramic Superconductors. William Andrew, Norwich.

Wimpenny, J., Manz, W., Szewzyk, U., 2000. Heterogeneity in biofilms. FEMS Microbiol. Rev. 24, 661–71.

Wirth, V., Dull, R., Llimona, X., Ros, R., Werner, O., 2004. Guía de campo de los líquenes, musgos y hepáticas. Omega, Barcelona.

Wladimirsky, A., Palacios, D., D'Antonio, M.C., González-Baró, A.C., Baran, E.J., 2010. Vibrational spectra of tin(II) oxalate. Spectrochim. Acta. A. Mol. Biomol. Spectrosc. 77, 334–335.

Wood, S., Blachere, J.., 1978. Corrosion of Lead Glasses in Acid Media 1, Leaching Kinetics. J. Am. Ceram. Soc. 61, 278–283.Yiu, C.Y., Ho, D.C.W., Lo, S.M., 2007. Weathering effects on external wall tiling systems. Constr. Build. Mater. 21, 594–600.

Yoon, J., Matsuo, Y., Adachi, K., Nozawa, M., Matsuda, S., Kasai, H., Yokota, A., 2008. Description of Persicirhabdus sediminis gen. nov., sp. nov., Roseibacillus ishigakijimensis gen. nov., sp. nov., Roseibacillus ponti sp. nov., Roseibacillus persicicus sp. nov., Luteolibacter pohnpeiensis gen. nov., sp. nov. and Luteolibacter algae sp. no. Int. J. Syst. Evol. Microbiol. 58, 998–1007.

References

Young, M., Alakomi, H., Fortune, I., Gorbushina, A.A., Krumbein, W.E., Maxwell, I., 2008. Development of a biocidal treatment regime to inhibit biological growths on cultural heritage: BIODAM. Environ. Geol. 56, 631–641.

Zhou, C., Li, K., Pang, X., 2012. Geometry of crack network and its impact on transport properties of concrete. Cem. Concr. Res. 42, 1261–1272.

Zucchiatti, A., Bouquillon, A., Giancarlo Lanterna, Lucarelli, F., Andrea Mandò, P., Paolo Prati, Salomon, J., Grazia Vaccari, M., 2002. PIXE and µ-PIXE analysis of glazes from terracotta sculptures of the della Robbia workshop. Nucl. Instruments Methods Phys. Res. Sect. B Beam Interact. with Mater. Atoms 189, 358–363.

Zucconi, L., Gagliardi, M., Isola, D., Onofri, S., Andaloro, M.C., Pelosi, C., Pogliani, P., Selbmann, L., 2012. Biodeterioration agents dwelling in or on the wall paintings of the Holy Saviour's cave (Vallerano, Italy). Int. Biodeterior. Biodegradation 70, 40–46.